THE UNIVERSITY
of EDINBURGH

Manipulating transcription factors in human induced pluripotent cell-derived cells to enhance the production and the maturation of red blood cells

CHENG-TAO YANG

THESIS PRESENTED FOR THE DEGREE OF DOCTOR OF PHILOSOPHY

THE UNIVERSITY OF EDINBURGH

2017

Declaration

I declare that all work presented here is my own and this thesis was composed by myself, unless otherwise stated in the text.

Cheng-Tao Yang

2017

Abstract

The most widely transfused blood component is red blood cells (RBCs), and voluntary donation is the main resource for RBC transfusion. In the UK, 7,000 units of RBCs are transfused daily but this life-saving cell therapy is completely dependent on donors and there are persistent problems associated with transfusion transmitted infections and in blood group compatibility. Furthermore, the quality, safety and efficiency of donated RBCs gradually decrease with storage time. A number of novel sources of RBCs are being explored including the production of RBCs from adult haematopoietic progenitor cells, erythroid progenitor cell lines and induced pluripotent stem cells (iPSCs). The iPSC source could essentially provide a limitless supply and a route to producing cells that are matched to the recipient. A number of protocols have been described to produce mature RBCs from human pluripotent stem cells but they are relatively inefficient and would be difficult to scale up to the levels required for clinical translation.

We tested and evaluated a defined feeder- and serum-free differentiation protocol for deriving erythroid cells from hiPSCs. RBC production was not efficient, the cells that were produced did not enucleate efficiently and they expressed embryonic rather than adult globin. We hypothesised that the production of RBCs from iPSCs could be enhanced by enforced expression of erythroid-specific transcription factors (TFs). Previous studies had demonstrated that Krüppel-like factor 1 (KLF1) plays an important role in RBC development and maturation so we generated iPSC lines expressing a tamoxifen-inducible KLF1-ER^{T2} fusion protein. Using zinc finger nuclease technology, we targeted the expression cassette to the *AAVS1* locus to ensure consistent expression levels and to avoid integration site specific effects and/or silencing. These iKLF1 iPSCs were applied to our defined RBC differentiation protocol and the activity of KLF1 was induced by adding tamoxifen. Activation of KLF1 from day 10 accelerated erythroid differentiation and maturation with an increase in the proportion of erythroblasts, a higher level of expression of erythroid

genes associated with maturation and an apparently more robust morphology. However, KLF1 activation had an anti-proliferation effect resulting in significantly less cell generated overall and HPLC analysis demonstrated that KLF1-activated cells expressed higher levels of embryonic globin compared to control iPSCs-derived cells. Many of the effects that were observed when KLF1 was activated from day 10 were not observed when activated from day 18. We therefore concluded that activation of exogenous KLF1 is able to promote erythroid cell production and maturation in progenitors (day 10) but not at the later stage of erythropoiesis (day 18). We hypothesised that KLF1 might require a co-factor to regulate RBC maturation and adult globin expression at the later stage of erythropoiesis.

The TF, B-cell lymphoma/leukaemia 11a (BCL11A), plays a key role in the suppression of foetal globin expression, thereby completing globin switching to adult globin. Preliminary data showed that iPSC-derived erythroid cells were able to express adult globin when transduced with a BCL11A-expressing lentiviral-vector. Based on that finding we then generated an iPSC line expressing tamoxifen-inducible BCL11A-ER^{T2} and KLF1-ER^{T2} fusion proteins, applied this iBK iPSC line to our differentiation protocol. Activation of both TFs from day 18 slightly increased the expression of genes associated with RBC maturation and the inclusion of BCL11A appeared to eliminate the anti-proliferation effect of KLF1. Most importantly, activation of both BCL11A and KLF1 from day 18 of the differentiation protocol increased the production of α-globin (foetal / adult globin) indicating that some definitive-like erythroid cells might be generated by activation of both TFs at the later stage of erythroid differentiation.

Collectively, these findings demonstrate that enforced expression of erythroid TFs could be a useful strategy to enhance RBC maturation from iPSCs.

Lay summary

The most widely transfused blood component is red blood cells. However, red blood cell transfusion is completely dependent on donors and there are persistent problems associated with blood type matching, transfusion-transmitted infections and blood storage. The aim of my study was to assess an alternative source to provide a limitless supply and replace the voluntary blood donation. My initial results showed that red blood cells could be produced in the laboratory using stem cell technology, but the maturation of red blood cells was relatively inefficient and this would be difficult to apply for clinical translation. The strategy of my thesis was to enhance the production and maturation of red blood cells by genetic editing technology. I manipulated the expression of two transcription factors, Krüppel-like factor 1 (KLF1) and B-cell lymphoma/leukaemia 11a (BCL11A) during the production of red blood cells and demonstrated that this type of strategy could indeed enhance the maturation of stem cell-derived red blood cells.

Acknowledgements

I would like to express my sincere gratitude to my supervisor Prof. Lesley Forrester for your support of my PhD study. Your guidance and valuable advice helped me in all the time of research. Thank you for your patience and encouragement throughout my PhD project, as well as for your assistance while publishing our works in STEM CELLS and writing this thesis.

I would also like to thank my committee members Prof. Kamil Kranc and Dr Andrew Smith for their insightful comments and critiques. Thank Dr Richard Axton for helping me with molecular biology works. Thank Dr Melany Jackson for constructive suggestions in the lab. Thank Dr Antonella Fidanza for the support in flow cytometry, data analysis and statistics. Thank Ms Helen Taylor for the help in tissue culture rooms. My thanks also extend to Sharmin, Martha and Jose for the stimulating discussions and for all the fun we have had in the last four years. I am very lucky to be surrounded by kind friends and inspiring colleagues, the memory in the SCRM building is the most precious in my life.

I also want to thank the Edinburgh Global Research Scholarship, the Scottish Funding Council Studentship and Taiwanese Studying Abroad Scholarship for providing tuition fees and the living stipend during my PhD.

Last but not the least, I am very grateful to my dad, my mum and my bro for their fully support when I was working and studying in the UK. Special thanks to my wife and son, Chao-Hui and Huai-Shan, for being with me all the way.

Table of contents

List of figures

List of abbreviations

AGM	Aorta-Gonad-Mesonephros
AHSP	Alpha haemoglobin stabilising protein
ANOVA	Analysis of variance
BasoE	Basophilic erythroblast
BCL11A	B-cell lymphoma/leukaemia 11a
bFGF	Basic fibroblast growth factor
BFU-E	Bursting-forming unit erythroid
BMP4	Bone morphogenetic protein 4
bp	Base pair
CFU-E	Colony-forming unit erythroid
CRISPR	Clustered Regularly Interspaced Palindromic Repeats
DIG	Digoxigenin
DMSO	Dimethyl sulfoxide
DNA	Deoxyribonucleic acid
EB	Embryoid body
ECL	Enhanced chemiluminescence
EDTA	Ethylenediaminetetraacetic acid
EMP	Erythro-myeloid progenitor
Emp	Erythroblast macrophage protein
EryP-CFC	Primitive erythroid colony-forming cell
ESC	Embryonic stem cell
FITC	Fluorescein isothiocyanate
GFP	Green fluorescent protein
HBB	Haemoglobin beta / β-haemoglobin
HBE1	Haemoglobin epsilon 1 / ε1-haemoglobin
HBG1	Haemoglobin gamma 1 / γ1-haemoglobin
HCl	Hydrochloric acid
hiPSC	Human induced pluripotent stem cell
HPC	Haematopoietic progenitor

HSC	Haematopoietic stem cell
IF	Immunofluorescence
IL-1β	Interleukin-1β
IL-3	Interleukin-3
IL-6	Interleukin-6
IL-11	Interleukin-11
iPSC	Induced pluripotent stem cell
KLF1	Krüppel-like factor 1
LB	Luria-Bertani medium
MEP	Megakaryocyte-erythroid progenitor
miRNA	MicroRNA
NaCl	Sodium chloride
NaOH	Sodium hydroxide
OrthoE	Orthochromatic erythroblast
PBS	Phosphate buffered saline
PBST	Phosphate buffered saline Tween
PCR	Polymerase chain reaction
PolyE	Polychromatophilic erythroblast
ProE	Proerythroblast
qRT-PCR	Quantitative reverse transcription PCR
RBC	Red blood cell
RNA	Ribonucleic acid
SCF	Stem cell factor
SDS	Sodium dodecyl sulphate
SEM	Standard error of the mean
SSC	Saline sodium citrate
TF	Transcription factor
UCB	Umbilical cord blood
UV	Ultraviolet
VEGF	Vascular endothelial growth factor
ZFN	Zinc finger nuclease

Chapter 1
Introduction

1.1 Blood storage and transfusion

Blood transfusion is a common procedure of receiving blood components (including whole blood, red blood cells, plasma and platelets) intravenously and it is used routinely in surgery, emergency and haematological disorders, such as haemoglobinopathies and anaemias. Red blood cells (RBCs) are essential to transport oxygen and carbon dioxide in the body and RBC is the most widely transfused blood component. A voluntary donation is the main resource for RBC transfusion and in the UK, 7000 units of RBCs are needed daily for life giving transfusions (http://www.nhsbt.nhs.uk/news-and-media/news-articles/news_2013_05_31.asp). Globally, approximately 85 million units of a RBC are transfused annually [1]. Although the average life span of RBCs is about 120 days in the circulation, RBCs can be stored only up to 42 days using anticoagulant solutions [2]. However, about 0.3% of RBCs stored in the presence of standard additive solutions are haemolysed after 5 weeks of storage. Therefore, the quality, safety and efficiency of RBCs gradually decrease with storage time, for example, reducing the capacity to carry oxygen and promoting the release of potentially toxic intermediates, such as free haemoglobin that can act as a source of reactive oxygen species [2]. To keep blood safe, the World Health Organization (WHO) has developed national blood programs in various aspects of transfusion medicine, and one of Global Collaboration on Blood Safety is performing testing for transfusion-transmissible diseases (including human immunodeficiency virus, hepatitis B, hepatitis C and syphilis). These infectious agents can survive in blood and infect the person receiving the blood transfusion [3]. *In vitro* production of RBCs might overcome a scarcity of transfusable RBCs for clinical application and this source could also tackle the issues of blood storage free of infectious viruses.

1.2 Erythropoiesis *in vivo*

Erythropoiesis is the process of red blood cell (RBC) production. Due to the difficulties of studying erythropoiesis during human embryonic development, many of the molecular processes involved in mammalian erythropoiesis have been discovered using the mouse model and this will be described here. Many fundamental insights have been provided by mouse studies, including colony-forming assays and functional

transplantation for haematopoietic stem cells (HSCs). According to a recent model of haematopoietic ontogeny, haematopoiesis consists of HSC-independent haematopoiesis and HSC-dependent haematopoiesis [4]. The former provides sufficient circulating bloods to sustain the survival of the mouse embryo in the absence of HSCs. HSC-independent haematopoiesis consists of two distinct waves: the primitive haematopoiesis, which gives rise to primitive erythroid progenitors, macrophages and megakaryocytes; and definitive haematopoiesis, which produces erythro-myeloid progenitors (EMPs) as well as B and T lymphoid cells [5]. HSC-independent haematopoiesis also provides long-lived tissue-resident macrophage populations [6], [7] and provides key signals to support the blood system before HSC emergence. HSCs that emerge in the aorta-gonad-mesonephros (AGM) region generate all blood lineages in the adult body and are clearly defined by their capacity to reconstitute the entire haematopoietic system in the long term *in vivo* following transplantation [5].

1.2.1 Primitive erythropoiesis

The first blood cells are derived from "blood islands" emerging within the yolk sac and a unique erythroid progenitor was defined as primitive erythroid colony-forming cell (EryP-CFC) [8]. This transient wave of EryP-CFC emerges in the yolk sac at E7.25 in the mouse embryo but are no longer detectable by E9.0 [8]. Primitive erythropoiesis in mammals has many similarities with definitive erythropoiesis, including a loss of proliferative capacity, a decrease in cell size, accumulation of haemoglobin, and nuclear condensation. Both of them share the same processes of lineage-committed progenitors from proerythroblasts (ProE), basophilic erythroblasts (BasoE), polychromatophilic erythroblasts (PolyE), and orthochromatic erythroblasts (OrthoE). Primitive erythroid cells are also capable of maturing into reticulocytes and circulating RBCs [9].

Primitive erythrocytes are characterised by the expression of embryonic globin (εy, βH1 and ζ in the mouse; ε, γ and ζ in human). Embryonic globin genes are regulated within the beta and the alpha globin clusters. From the beta globin cluster, the embryonic εy- and βH1-globin genes are expressed in the mouse [10], [11], and the ε- and γ-globin genes are expressed in human [12]. From the alpha globin cluster in both

mouse and human, primitive cells also express the embryonic ζ-globin genes [10]–[12].

Although many primitive erythroid cells are nucleated, enucleation *per se* does not distinguish primitive and definitive erythrocytes, because chromatin condensation and enucleation can be observed in primitive yolk sac derived erythropoiesis [13]. To identify the enucleation in primitive erythroid cells using antibodies specific for embryonic globin, primitive erythroblasts did enucleate during the gestation period from E12.5-E16.5 [9]. Enucleated primitive erythrocytes have been identified in the circulation of mice for several days after birth [9], [14].

Primitive erythropoiesis is strictly regulated by transcriptional regulators, such as GATA1, FOG, LMO2 (also called RBTN2), LDB1 and SCL (also called TAL1). The defects in primitive erythroblasts result from targeted disruption of *Gata1* [15], *Fog* [16], *Lmo2* [17], *Ldb1* [18], and *Scl* [19]. A recent study has indicated that *Ldb1* and *Lmo2* encode nuclear adaptor proteins that form complexes with GATA1, GATA2, TAL1 and KLF1 in numerous haematopoietic cell types including stem/progenitor, erythroid, and megakaryocyte-erythroid progenitor (MEP) [20]. Additionally, although RUNX1 is not essential for the formation of primitive erythrocytes, primitive erythrocytes from *Runx1* $^{-/-}$ mice display abnormal morphology and reduced expression of an erythroid marker TER119. This suggests RUNX1 also plays important roles in the maturation of primitive erythroblasts [21]. Another important transcriptional regulator of erythropoiesis is the erythroid-specific Krüppel-like factor 1 (KLF1/EKLF), although KLF1 is not required for yolk sac erythropoiesis [22], [23]. KLF1 plays an important role in the maturation of primitive erythroblasts, in part by expressing erythroid marker TER119 [24], [25] and regulating cytoskeleton and maintaining the membrane stability [26], [27]. Several studies show that KLF1 also regulates embryonic globin gene expression in primitive erythrocytes [22], [25], [28], [29].

1.2.2 Definitive erythropoiesis

Definitive EMPs are found in the E8.5 / E9 yolk sac and placenta of the mouse and they migrate to the foetal liver on E11.5 to produce the first definitive erythrocytes. These erythroid progenitors can be characterised by smaller size, higher mean glycophorin A (GPA; TER119 in mouse and CD235a in human) staining and bigger faint nucleus than primitive erythroblasts [30], [31]. They form bursting-forming unit erythroid (BFU-E) in methylcellulose medium *in vitro*. Maturation of definitive erythroid precursors from ProE to OrthoE is similar to primitive erythropoiesis and characterised by limited expansion, decrease in cell size, accumulation of haemoglobins and condensation of nuclei and subsequent enucleation [9], [32].

Furthermore, definitive erythrocytes express foetal globin (consisting of α- and γ-globin ($\alpha_2\gamma_2$) in human) but there is no transient form of foetal globin in the mouse. Foetal globin genes are also regulated by the beta and the alpha globin clusters. Foetal Gγ and Aγ-globin genes are expressed from the beta globin cluster and α-globin gene is expressed from the alpha globin cluster in human definitive erythroid cells [12].

Definitive erythropoiesis is also regulated by transcriptional regulators, GATA1, LMO2, FOG, LDB1 and SCL [4]. Another crucial transcription factor in definitive erythropoiesis is KLF1. A study has reported that foetal liver-derived null KLF1 erythroid cells have an abnormal morphology and most of the cells retain their nucleus [23], [33], [34], this suggests KLF1 contributes to membrane normalities and RBC maturation in definitive red blood cells. Of note, a comparative analysis of global gene expression in primitive, foetal definitive, and adult definitive erythroid cells has reported that *Sox6* and *Myb* are highly expressed in adult definitive erythroid cells [35]. SOX6 is an important enhancer of definitive erythropoiesis to stimulate cell survival, proliferation, and terminal maturation [36]. SOX6 also mediates the suppression of embryonic globin gene expression [37], [38]. Another key role of MYB in definitive erythropoiesis is reported in a $Myb^{-/-}$ murine study, their results showed embryonic erythropoiesis in yolk sac was not impaired by the *Myb* alteration, but definitive erythropoiesis in the foetal liver was diminished in *Myb* mutants [39]. Additionally, BCL11A (B-cell lymphoma/leukaemia 11a) is not involved in definitive erythroid cell maturation, but BCL11A suppresses embryonic globin gene expression [31] and foetal

globin gene expression [37]. Therefore, some studies regard SOX6, MYB and BCL11A as markers for definitive erythropoiesis [12], [30], [32].

Interestingly, hypoxia signalling might be involved in the emergence of definitive EMPs. An embryonic developmental study has reported that BFU-E colonies were not detected under normoxia condition, but definitive erythroid colonies were observed in the low-oxygen culture conditions (5 %). This suggests that low oxygen conditions facilitate the detection of BFU-E in early mouse embryos [40].

1.2.3 HSC-dependent erythropoiesis

The first HSCs are found in the AGM region at E10.5 and migrate into the foetal liver gradually. Around the time of birth (about E19), the site of erythropoiesis switches to the bone marrow and the spleen [41]. Repopulating HSCs emerge during midgestation through a process termed endothelial-to-haematopoietic transition, and their repopulating ability is associated with clusters of round haematopoietic cells budding from endothelium [42]. Of note, the emergence of HSCs from endothelium is dependent on the transcription factor, *Runx1* (previously known as AML1). No functional HSCs can be found in *Runx1*-deficient embryos, including AGM and foetal liver at E10, E11 and E12 [43]. Another study has indicated that RUNX1 functions to develop and maintain hematogenic precursor cells in the embryonic AGM [44]. These data suggest that RUNX1 is required for functional HSCs in the AGM region. GFI1 and GFI1B are also involved in the haematopoietic commitment with these two transcription factors (TFs) controlling the loss of endothelial identity from the hemogenic endothelium [45], and thus possibly involved in the emergence of HSCs. Interestingly, BCL11A is also involved in the maintenance of HSCs. A Single-cell RNA-seq result showed that *Bcl11a*$^{-/-}$ HSCs had upregulated cyclin genes and down-regulated G2/M markers, also, a higher number of proliferative cells was observed in *Bcl11a*$^{-/-}$ HSCs compared with wild type HSCs in BrdU assay. Their data suggest that *Bcl11a*$^{-/-}$ HSCs have abnormal proliferative phenotypes [46]. *Bcl11a* deficiency results in cell-cycle delay in HSCs [47]. These two studies indicate loss of *Bcl11a* in HSCs is defective in self-renewal.

In a conventional haematopoietic hierarchy toward erythroid differentiation, HSCs can commit to common myeloid progenitors (CMPs) and subsequently megakaryocyte-erythroid progenitors (MEPs). These progenitors then give rise to the colony-forming unit erythroid (CFU-E), which generates nucleated erythroid precursors, including ProE, BasoE, PolyE and OrthoE. This maturation process occurs in postnatal bone marrow by interacting with the central macrophage within the erythroblastic islands [48]. Reticulocytes are then released to bloodstream and become circulating RBCs (Figure 1.1). During erythroid differentiation, these cells loose the stem cell marker Kit (CD117) with the time of erythroid differentiation (Figure 1.1). Subsequently, transferrin receptor protein 1 (TFRC1 in mouse and CD71 in human) is expressed in erythroblasts, GPA is expressed in erythroblasts, reticulocytes and erythrocytes [41].

Mature RBCs derived from HSCs express adult globin (consisting of α- and β-globin ($\alpha_2\beta_2$) in human) [41]. Adult globin genes are also regulated by the beta and the alpha globin clusters. From the beta globin cluster, the β1- and β2-globin genes are expressed in the mouse [10], [11], and δ- and β-globin genes are expressed in human [12]. From the alpha globin cluster in mouse and human, adult erythrocytes express the α-globin gene [10]–[12]. Nevertheless, the mechanism of globin switching to adult globin is not fully understood. To date, several TFs have been reported to be involved in the regulation of adult globin expression, including SOX6 and BCL11A. The transcriptional regulator SOX6 acts as a repressor by directly binding to the εy promoter and silences embryonic globin gene expression [38]. BCL11A is able to bind γ promoter and results in down-regulation of γ-globin [49]. Some reports also indicate BCL11A requires co-factors to regulate globin expression. Strong binding with GATA-1 is associated with foetal globin gene suppression [50]. A study of a murine erythroleukaemic cell line containing an intact human β-globin locus has indicated that double knockdowns of *Bcl11a* and *Dnmt1* (DNA methyltransferase 1) results in an induction of γ-globin expression [51]. These two studies demonstrate that BCL11A cooperates with GATA1 and DNMT1 to achieve repression of foetal globin genes.

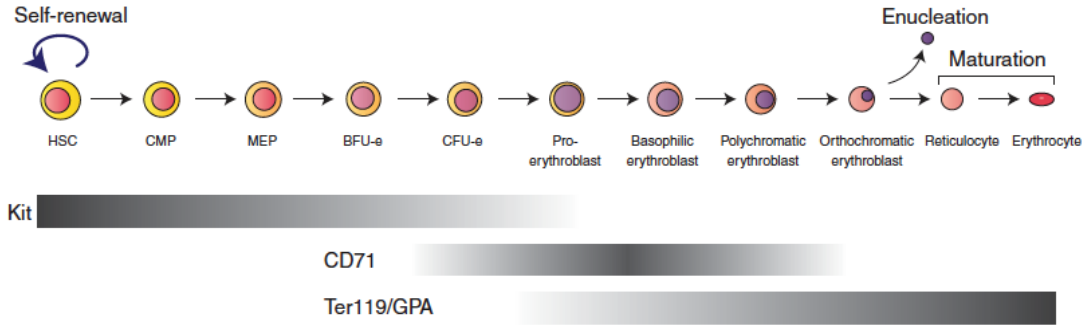

Figure 1.1 Erythroid differentiation in the mouse

The figure indicates the most commonly used surface markers to identify the different stages of erythropoiesis. Gray, low expression; black, high expression. HSC, haematopoietic stem cell; CMP, common myeloid progenitor; MEP, megakaryocyte-erythroid progenitor; BFU-e, burst-forming-unit-erythroid; CFU-e, colony-forming-unit-erythroid. Adapted from *Cold Spring Harb Perspect Med* 2013 [41].

1.2.4 Enucleation of red blood cells

In mammals, the end result of RBC maturation is enucleation, which results in the formation of reticulocytes and pyrenocytes. Reticulocytes contain cytoplasm, haemoglobin and proteins forming a unique cytoskeletal network, including F-actin, myosin, spectrin, dematin and so on [52], on the other hand, pyrenocytes (extruded nuclei) contains the condensed nucleus with thin rim of cytoplasm [53]. This quick process of enucleation is completed with actin and other cytoskeletal proteins, the time-lapse live-cell imaging showed that the erythroblast rapidly extrudes its nucleus apposed to the plasma membrane through a bleb-like structure [54]. Enucleation of erythroblasts is a complex process that involves multiple changes in morphology and structure. To date, recent studies have revealed that enucleation involves (1) histone deacetylation, (2) cytokinesis (actin polymerization) / cell cycle, (3) cell-matrix interactions, (4) specific microRNAs and (5) vesicle trafficking.

(1) Histone deacetylation

The first phenomenon in enucleation is chromatin condensation, deacetylated histones stabilise chromatin and are critical for heterochromatin formation during enucleation. A study has reported the level of several acetylated histones decreases during erythroid differentiation from mouse foetal liver erythroblasts, including H3K9Ac, H4K5Ac, H4K12Ac, and H4K8Ac [55]. Similarly, inhibition of histone deacetylase 2 (HDAC2) activity blocks chromatin condensation and enucleation in mouse foetal erythroblasts [56]. However, it has not been reported whether the deacetylated histones are localised in specific genes to regulate the process.

(2) Cytokinesis (actin polymerization) / cell cycle

Some studies have revealed that several membrane and cytoskeleton proteins are involved in the process of cytokinesis during enucleation. Filamentous actin (F-actin) was found concentrated in enucleating erythroblasts, and F-actin inhibitor leads to a complete block of enucleation.[57]. A study of yolk sac-derived erythroblasts has showed that actin and myosin accumulate at the cell cortex area surrounding the extruding nucleus during enucleation [58]. Another study of mouse bone marrow

derived erythroblasts has revealed that inhibition of Rac GTPases changes the distribution of F-actin and myosin, and then decreases enucleation efficiency [59]. Furthermore, phosphoinositide 3-kinase (PI3K) inhibition in mouse erythroblasts results in impaired cell polarisation and a severe delay in enucleation [60], it suggests the establishment of cell polarisation in enucleation is required and regulated by the microtubule-dependent PI3K. Additionally, two cell cycle inhibitors, p18 and p27, are critical for enucleation during late stages of differentiation, thereby indicating a relationship between cell cycle exit and nuclear expulsion [34].

(3) Cell-matrix interactions

The microenvironment in foetal liver and bone marrow supports erythropoiesis, and the erythroblastic island (composed of erythroblasts and central macrophage cells) plays an important role in the enucleation [48]. Previous evidence suggested that erythroblasts co-cultured with macrophages proliferate more than cultured alone by 3 fold [61], suggesting macrophages act as nursing cells to provide signals of proliferation and differentiation for surrounding erythroblasts, and possibly including enucleation signals. Among many cell surface proteins relating to erythroblast-macrophage interaction, erythroblast macrophage protein (Emp) expressed on both macrophages and erythroblasts is important for erythroblast enucleation. Evidence from a $Emp^{-/-}$ mouse study has indicated that Emp is required for erythroblast enucleation and macrophage maturation [62]. Their data show no erythroblastic islands are observed in the foetal liver, and numerous nucleated and immature erythrocytes are retained in the peripheral blood of $Emp^{-/-}$ foetuses [62]. Another important protein involved in the macrophage-erythroblast interaction is retinoblastoma (RB), RB deficiency in the mouse causes failure of enucleation in erythroblasts [63]. However, wild-type macrophages can bind Rb-deficient erythroblasts and lead them to enucleation [63]. An early study in murine erythroleukaemia cells (MELs) has indicated that the enucleation rate is increased when culturing cells on fibronectin-coated dishes [64]. Nevertheless, it is not fully understood how these above interactions affect enucleation.

(4) Specific microRNAs

A review describes several specific miRNAs are crucial in erythroid lineage determination, proliferation, maturation and enucleation [65]. A study of erythroid progenitors from mouse has revealed that miR-191 is normally down-regulated during erythropoiesis and that overexpression of miR-191 blocks enucleation [66]. This study has identified potential targets of miR-191, *Riok3* and *Mxi1*, and demonstrated that knocking down the expression of either *Riok3* or *Mxi1* blocks chromatin condensation and enucleation [66]. Furthermore, knockdown of miR-30a in human ES-derived erythroblasts increases the enucleation rate and enhances the expression *RIOK3*. This suggests miRNAs might negatively regulate enucleation in erythroid development [67].

(5) Vesicle trafficking

The formation of multiple vesicles is observed in the region between the extruding nucleus and incipient reticulocyte [57], [68]. A study of mouse foetal liver derived erythroblasts has indicated that endocytic vesicle trafficking plays an important role in enucleation [68]. Their results showed that inhibitors of clathrin-dependent vesicle trafficking block enucleation, and a small molecule inducing vacuole formation enhances the percentage of enucleated cells [68].

1.3 Erythropoiesis *in vitro*

An increasing number of scientists have been in search of protocols for "*in vitro* erythropoiesis", and a number of novel sources of RBCs are being explored including their production from adult HSCs, adult haematopoietic progenitors (HPCs), pluripotent stem cells (PSCs), immortalised erythroid progenitor cells and transdifferentiation. All of these strategies have the potential to provide clinical needs in transfusion medicine in the future. The PSC source could essentially provide a limitless supply and could be a route to producing cells of specific blood groups.

1.3.1 $CD34^+$ HPC-derived erythroid lineage cells

$CD34^+$ HPCs from umbilical cord blood (UCB) have been considered to produce RBCs for transfusion medicine. The first *in vitro* production of RBCs was performed by Douay's group [69]. The group applied cytokines to $CD34^+$ cells isolated from UCB to induce erythroid differentiation and co-culture with murine stromal cells to mature RBCs. By mimicking the marrow microenvironment, they obtained functional RBCs with an enucleation rate of 95 % [69]. To optimise the differentiation protocol for expansion, Fujimi et al co-cultured $CD34^+$ cells with human stromal cells to expand its population and induce erythroid differentiation with the application of cytokines. For the RBC maturation, erythroid lineage cells were then co-cultured with macrophages. Their result showed that $1.76x10^{13}$ RBCs with 99.4 % of enucleation (~8.8 transfusable units) were generated from 1.0 unit of UCB [70]. To overcome the drawback of co-culture system posing limits in clinical application, Miharada et al generated RBCs with applications of cytokines, but without co-culture. However, the production of RBCs is low and the enucleation rate is 77.5 % lower than co-culture system [71].

Peripheral blood (PB)-derived $CD34^+$ cells also have a potential for the *in vitro* production of RBCs. A study has revealed that PB-derived $CD34^+$ cells are able to expand and differentiate to RBCs without co-culture, but the enucleation rate is relatively low at only 45 % [72]. To improve the enucleation efficiency of PB $CD34^+$-derived RBCs, Griffith et al described an *in vitro* culture system producing functional mature RBC with enucleation ranged from 55 % to 95 % [73]. However, it is noteworthy that the quantity of RBCs that can be expanded from PB $CD34^+$ cells is lower than that from the UCB $CD34^+$ cells.

1.3.2 PSCs-derived erythroid lineage cells

Human blastocyst-derived pluripotent stem cell (PSCs) lines were first generated by James Thomson and these embryonic stem cells (ESCs) were able to develop into all cell types *in vitro* [74]. PSC-based technologies hold the potential for a number of medical applications and to cure many diseases, such as cardiovascular disease, Parkinson's disease, diabetes and leukaemias. However, ESCs are also controversial

due to ethical issues relating to their derivation, thereby representing a major obstacle to their clinical applications. In 2007, Shinya Yamanaka's group successfully reprogrammed human dermal fibroblasts into 'induced Pluripotent Stem Cells' (iPSCs) by transduction of four genes *Oct4*, *Sox2*, *Klf4* and *cMyc* [75]. Over the past one decade, iPSCs have been extensively studied and have become an alternative source of PSCs with which to potentially treat a variety of diseases. Due to the fact that iPSCs can be derived from patients or individuals with rare blood groups, iPSCs provide a good cell resource to study the molecular mechanisms associated with erythropoiesis and blood diseases. Therefore, iPSCs offer a valuable tool for the safety assessment, *ex vivo* disease models, cellular therapies, biomaterial production and drug screening.

To generate RBC from PSCs, the protocol varies in technical details and can be divided into two main categories. This first one is co-culture PSCs with stromal cells in an attempt to recreate the haematopoietic microenvironment, this co-culture system induces haematopoietic differentiation *in vitro*. The most commonly used is OP9 murine bone marrow cell line, and the erythroid differentiation is followed by selective expansion of erythroid cells with erythropoiesis supporting cytokines [76]. However, adult globin expression in PSC-derived RBC is lower than the embryonic and foetal globins, also, the rate of enucleation is low ranged from 2 % to 10 % [76]. To eliminate the xenogenic contamination for clinical application, human mesenchymal cells have been used in co-culture system and they are able to support erythroid maturation [69]. Co-culturing ESC-derived erythrocytes with FH-B-hTERT (a human foetal liver hepatocyte cell line) increases enucleation rate and those erythrocytes express more foetal globins than embryonic globins [77]. Another study has demonstrated that the conditioned media from primary human foetal liver and foetal bone marrow enables ESC-derived erythrocytes to increase the appearance of BFU-E and these ESC-derived erythrocytes express foetal and adult globins [78].

Another way to produce RBCs from PSCs is embryoid body (EB) formation followed by an array of cytokine induction. An advantage of using EB formation is that the differentiation protocol can be optimised as in a serum free and defined factor condition [79], although heterogeneity of haematopoietic cells may result from limit

contacts with cytokines and growth factors [80]. A previous study has indicated that haematopoietic cells production by EB formation supplemented with various growth factors, and different signalling pathways during different stages are required in the culture [81]. Activin / Nodal and Wnt signalling are required for the induction of the primitive streak [81], and BMP signalling is an inducer in mesoderm formation [82]. The specification of $Flk1^{+}$ mesoderm to the haematopoietic lineages requires VEGF and Wnt, but not BMP or Activin / Nodal signalling [81]. Different from BMP / Activin / Wnt signalling pathways, basic fibroblast growth factor (bFGF) regulates haematopoietic development in the proliferation instead of inducing its formation [83]. Vascular endothelial growth factor (VEGF) is not required for the formation of haematopoietic precursors, but the addition of VEGF increases the frequency of these precursors [84]. This suggests VEGF is essential for proliferation of haematopoietic precursors. Additionally, the presence of VEGF in the culture maintains the expression of haematopoietic transcription factors, including *Scl*, *Fli1* and *Lmo2* [84]. ESCs and iPSCs have been utilised to generate RBCs by the formation of EBs with an array of cytokine induction, however, the RBCs produced from ESCs or iPSCs express embryonic and foetal globins but not adult globin [85]. Lapillonne et al also noted that the low enucleation rate was observed in the result, which is 52 - 66 % in ESC-derived RBCs and 4 -10 % in iPSC-derived RBCs [85].

To overcome the low enucleation rate, recent evidence suggested that a combined strategy of EB formation and co-culture system increases the enucleation efficiency in ESC-derived RBCs [86]. Their results showed co-culturing nucleated erythroid cells with OP9 cells increased the enucleation rate from 10 % to 30 % [86]. However, these ESC-derived RBCs mainly express embryonic and foetal globins in the co-culture system [86].

To address the issue of globin expression, a study has revealed that infusion of nucleated erythroid precursors derived from iPSCs into mice enables the switching from foetal to adult globin [87]. This suggests that the process of globin switching from foetal to adult globin occurs under the influence of an adult haematopoietic microenvironment *in vivo*.

1.3.3 Immortalised Cell lines for RBC production

Generation of immortalised cell lines could also provide a limitless resource for RBC production. A recent study has revealed that human UCB-derived erythroid progenitor (HUDEP) cell lines and human iPSC-derived erythroid progenitor (HiDEP) cell lines are successfully generated, and both can be maintained in long-term culture and differentiate into mature RBCs [88]. However, the efficiency of enucleated RBC generation varies with the HUDEP cell lines and HiDEP cell lines, also, the expression of adult globin is highly expressed in HUDEP-derived RBCs but non-expression of adult globin in HiDEP-derived RBCs [88]. Hirose et al generated immortalised erythrocyte progenitor cells (imERYPCs) by transduction of *c-MYC* and *BCL11A* into HPCs-derived from PSCs, imERYPCs express high expression of *BCL11A* and present a lower fraction of apoptotic cells [89]. RBC differentiated from imERYPCs express both foetal and adult globins *in vitro*, and nearly all of the imERYPC-derived RBCs are enucleated when infusing imERYPCs into mice [89].

1.3.4 Transdifferentiation

There have been significant advances in the development of protocols for the production of RBCs from PSCs over the last few years (see Section 1.3.2), but the optimised protocol is not efficient to produce mature RBC for blood transfusion. This suggests that the culture conditions have not created the precise *in vivo* environment resulting in limited erythropoiesis. However, it is possible to use TFs to "programme" cells into specific lineages. A recent study has been reported that committed murine blood cells are able to be reprogrammed to induced haematopoietic stem cells (iHSCs) by defined TFs, RUNX1T1, HLF, LMO2, PRDM5, PBX1, and ZFP37 [90]. This result raises the prospect that blood cell reprogramming may be a strategy for the derivation of transplantable stem cells for clinical application.

A previous study has revealed that fibroblasts can be converted into endothelial-like precursor cells that subsequently generate haematopoietic stem and progenitor cell (HSPC)-like cells by inducing with a simple combination of TFs (GATA2, GFI1B, cFOS, and ETV6 [91]. These HSPC-like cells co-express haematopoietic markers, endothelial progenitor markers and hemogenic endothelium markers, and global

analysis also revealed activation of genes encoding HSC transcriptional regulators, including *Scl*, *Fli1*, *Hhex*, *Smad6*, *Lyl1*, *Lmo2*, *Runx1*, *Sox17*, *Msi2*, and *Gfi1*. This suggests the definitive haematopoietic nature of cells specified by the four TFs [91].

A similar study has indicated murine embryonic fibroblasts (MEFs) and murine adult fibroblasts (MAFs) are reprogrammed to haematopoietic progenitors by the ectopic expression of the transcription factors (ERG, GATA2, LMO2, RUNX1c, and SCL), which process is going through an intermediate hemogenic endothelial stage [92]. These reprogrammed haematopoietic progenitors are expanded on stromal cells and able to generate erythroid, megakaryocytic, myeloid, and lymphoid lineages [92].

A recent study has revealed that the minimal set of TFs (GATA1, TAL1, LMO2, and c-MYC) converts murine and human fibroblasts into induced erythroid progenitors / precursors (iEPs) [93]. Addition of KLF1 to the TF cocktail increased the appearance of "definitive" single cells expressing adult globin but did not change the expression of primitive to definitive specific genes. This indicates iEP clones possess a mixture of primitive and definitive erythropoiesis, KLF1 acts as globin switching factors by increasing adult globin couples with reduced embryonic globin [93]. However, very few "enucleated" iEP-derived erythrocytes were observed in the culture, this suggests an inefficient maturation in this strategy.

1.3.5 Limitations of RBC generation *in vitro*

Over the last few years, protocols for the production of erythroid cells from $CD34^+$ HPCs have been developed and optimised, and RBCs derived from HPCs expressing a higher ratio of adult globin / foetal globin and have a higher enucleation rate (comparing to PSC-derived RBCs) [70]. However, the expansion of HPCs in *vitro* is limited, the best yield is 75 transfusable units generated from 1 unit of UCB [94], [95].

Although ESCs and iPSCs provide a limitless cell source for RBC production, and comparing with ESCs, the iPSC source could be a route to producing cells of specific blood groups. However, the issue of inefficient production still needs to be tackled. The production efficiency of approximately 200,000 erythroid cells per one iPSC has been achieved by co-culturing with OP9 cells first and then MS-5 cells [76]. Only 200

- 3,500 erythroid cells can be generated from one iPSC via EB formation [85]. Furthermore, the enucleation efficiency is 10 % - 30 % without stromal cells and represents varied proportion between 30 % - 65% with stromal cells [86]. Most of the studies also found that the RBCs from PSCs express high levels of embryonic and foetal globins, but the expression level of adult globin is very low [96].

RBC production from immortalised Cell lines or transdifferentiation faces the same issue of inefficient erythroid maturation. Kurita et al display different efficiencies for producing enucleated RBCs from HiDEP and HUDEP cell lines [88], however, their previous study showed the efficiency of enucleated RBC production by mouse ESC-derived erythroid progenitor (MEDEP) cell line improved *in vivo* after transplantation [97]. Capellera-Garcia et al directly convert fibroblasts into RBCs by GATA1, TAL1, LMO2, and c-MYC, but they also observe very few enucleated RBCs [93]. Kongtana Trakarnsanga et al generated a human immortalised adult erythroid line (Bristol Erythroid Line Adult; BEL-A) from early adult erythroblasts, BEL-A cells were able to differentiate into mature and functional RBCs. These RBCs expressed adult β-globin, but the enucleation rate is approximately 30 % [98].

Although enucleation can somehow occur *in vivo* condition [89], [97], the advantage is that no risk of tumorigenicity occurs when transfusing enucleated RBCs, also, enucleated RBCs can be selected by size (by filtration). Another problem associated with the *in vitro* production of RBCs is the high cost due to the use of expensive cytokines and the lengthy differentiation protocol that is required for the high cell number needed for blood transfusion.

1.4 Krüppel-like factor 1 (KLF1)

1.4.1 The discovery and structure of KLF1

Krüppel-like factor 1 (*Klf1*, shows the greatest similarity to the Drosophila melanogaster gap gene *Krüppel*) was firstly identified from a comparison analysis between a mouse erythroleukaemia cell line and a mouse monocyte-macrophage cell line, their results suggested KLF1 binds to the β-globin promoter and is intimately involved in maintaining the erythroid cell phenotype [99]. A subsequent study has

showed that the expression of *Klf1* is restricted to the primitive erythroid cells in the yolk sac and definitive erythroid cells in the foetal liver [100].

The KLF1 protein contains 2 domains: a N-terminal proline-rich transactivation domain and a C-terminal DNA-binding domain – three C_2H_2 zinc fingers, which recognise and bind the sequence 5' CCM CRC CCN (where M represents A or C, R represents A or G and N represents A or T or C) [101]. This motif is found in the regulatory regions of many erythroid genes, including β-globin promoter [99], alpha haemoglobin stabilising protein (AHSP) promoter [102], dematin (band 4.9, a RBC cytoskeleton protein) promoter [27], aminolevulinic acid synthase 2 (ALAS2; a heme-synthesis enzyme) promoter [103], KLF3 promoter [104], p18 (a cell cycle inhibitor) promoter [105], E2F2 (a S-phase regulator) enhancer [106] and E2F2 promoter [107].

1.4.2 KLF1 in erythropoiesis

Erythroid differentiation is regulated by a complex network of TFs that are involved in the development and maturation of blood lineages. One of the most crucial TFs for erythropoiesis is KLF1 (also named Erythroid Krüppel-like factor; EKLF), which is highly restricted to the erythroid ontogeny [100]. Numerous studies have shown *Klf1*-deficient embryos die of anaemia during foetal liver erythropoiesis [23], [33], [108], this suggests KLF1 is not required for yolk sac erythropoiesis. However, KLF1-null primitive erythroid cells from yolk sac fail to express TER119 and appear to have an abnormal morphology [24]–[27], which indicates KLF1 is important in the primitive erythroid development.

Definitive erythrocytes from KLF1-null foetal liver have a defect on the expression of TER119 [24], [27], [34], [107] and foetal liver-derived null KLF1 erythroid cells have an abnormal morphology, and most of the cells retain their nucleus [23], [33], [34]. These studies suggest loss of KLF1 negatively impacts on the development of definitive erythropoiesis. Perkins et al demonstrated the KLF1-null definitive erythrocytes features of β-globin deficiency (similar to β-thalassaemia in humans), this suggests that KLF1 facilitates completion of the switch from foetal-to-adult [23].

A study has revealed that CD41 (a megakaryocyte/platelet marker) is highly expressed in KLF1-deficient primitive erythrocytes, and an increase of *Fli-1* (a critical TF in megakaryopoiesis) transcripts is observed in KLF1-deficient primitive erythrocytes [24]. Another gain-of-function study has demonstrated that KLF1 induction negatively affects the formation of $CD41^+$ megakaryocytes, on the other hand, it increases the proportion of $TER119^+$ erythroid lineage cells [109]. This indicates KLF1 plays a dual role in haematopoiesis by promoting erythropoiesis and repressing the megakaryocytic program at the same time.

1.4.3 KLF1 in erythroid maturation

An analysis of global gene expression has reported that *Klf1* is a core erythroid gene expressed in primitive, foetal liver definitive, and adult BM definitive erythroid cells [35]. KLF1 deficient studies in mouse [26] and in human [110] indicate KLF1 regulates many genes associated with erythropoiesis. A study of KLF1 ChIP-seq in mouse foetal liver erythroid cells has showed its targets are involved in terminal erythroid differentiation [101]. These studies suggest KLF1 plays a pivotal role in erythroid maturation through (1) cytoskeleton and transmembrane protein (blood group antigens), (2) cell cycle / anti-apoptosis / survival and (3) haemoglobin production.

(1) Cytoskeleton and transmembrane protein (blood group antigens)

Dematin (*Epb4.9*) is an important cytoskeletal protein required for membrane integrity and stability in erythrocytes [111]. Erythrocytes from $Klf1^{-/-}$ embryos were described as “wrinkled”, “ruffled” and “fragile”, this phenotype was explained by the loss of dematin expression [26], [27], [111]. The array data suggested that dematin is highly dependent on KLF1 in the foetal liver [27]. These studies might partly explain dematin maintains the shape and robust morphology of erythroid cells, because loss of other transmembrane proteins or cytoskeleton are likely to contribute to membrane defect.

A human study has reported that some cytoskeletal genes are lowly expressed in KLF1-null erythroid cells, including *ANK1* (Ankyrin 1), *SLC4A1* (Band 3), *SPTB* (β-Spectrin) and *SPTA1* (α-Spectrin) [110]. Erythrocytes from $Klf1^{-/-}$ embryos were

described as “misshapen”, and this phenotype results from loss of *ANK1*, *SLC4A1* and *SPTB* [112]. These studies suggest loss of cytoskeleton contributes to the fragility of erythrocytes.

Transferrin receptor (TFRC1; CD71) contributes to haemoglobinization in erythroblasts by uptaking transferrin-bound iron, and it appears to be a KLF1-dependent gene in foetal liver erythrocytes [27].

A study of KLF1 null neonates has indicated KLF1 targets encode many blood group antigens, such as *ERMAP* (Scianna Ag), *DARC* (Duffy Ag), *KELL* (Kell Ag) and *ICAM4* (Landsteiner-Wiener Ag) [110]. *ICAM4* is down-regulated in *Klf1*$^{-/-}$ mouse foetal liver [27] and in *KLF1*$^{-/-}$ patients [110], it is essential for the interaction of erythroblastic islands, hence, it is likely to be important for RBC maturation *in vivo* [113]. Mutations in human *KLF1* have also been associated with diseases, including the In(Lu) rare blood group (amino acid 328 Arginine was replaced by Leucine). The phenotype of In(Lu) erythroblasts expresses lower *GPA*, *EPOR* (erythropoietin receptor), *AHSP* (Alpha haemoglobin stabilising protein), *HBE1* (ε1-haemoglobin) and *HBB* (β-haemoglobin), which suggests that the phenotype is less capable of promoting erythroid maturation [114].

(2) Cell cycle / anti-apoptosis / survival

E2F2 is a critical regulator of cell proliferation by regulating S-phase entry and DNA synthesis, which is decreased in *Klf1*$^{-/-}$ foetal liver cells [107]. The loss of KLF1 leads to aberrant entry into S-phase in both primitive and definitive erythrocytes [106]. These studies suggest E2F2 regulated by KLF1 is required for cell cycle progression during terminal erythroid differentiation.

KLF1 promotes a cessation in proliferation via directly activating $p18^{INK4c}$ and $p21^{WAF1/CIP1}$, they function as cyclin-dependent kinase inhibitors and act to delay progression through G1 into S-phase [105], [115]. A recent study has reported that low level expression of p18 and p27 in the late-stage *Klf1*$^{-/-}$ foetal liver cells continue to proliferate but not enucleate, however, these two KLF1 target cell cycle inhibitors rescue abnormal proliferation and enucleation defects [34].

KLF1 is also involved in the regulation of apoptosis and survival. A study of KLF1 ChIP-seq in mouse foetal liver erythroid cells has showed that KLF1 regulates genes *Bcl2l1* (*Bcl-X*) [101], which has an anti-apoptotic function in primitive and definitive erythrocytes [116], [117] and *Pim1* [101], which is known as a survival component of erythroblasts [118].

KLF1 activates both positive and negative regulators of the cell cycle, anti-apoptosis and survival to influence the erythropoiesis and these studies suggest that KLF1 has a role in the regulation linked to proliferation arrest required for terminal differentiation.

(3) Haemoglobin production

KLF1 is able to bind β-globin promoter [99] and is required for adult β-globin gene transcription [119]. Also, KLF1 indirectly upregulates adult β-globin expression via BCL11A which silences expression of foetal globin [120], [121]. However, some *Klf1*$^{-/-}$ mouse studies have shown that loss of KLF1 diminishes the expression of εy- and βH1-globin genes, this suggests KLF1 is required for embryonic globin gene expression in primitive erythrocytes [22], [25], [28], [29].

Alpha haemoglobin stabilising protein (AHSP) is directly activated by KLF1 [102]. AHSP is an erythroid-specific protein and acts as a protector by binding cytotoxic free α-globin. Interaction with AHSP prevents reactive oxygen species producing from free α-globin aggregate and damaging the membrane [102].

KLF1 appears to regulate the heme synthesis by ABCG2 (ATP-binding cassette sub-family G member 2) and ALAS2 (aminolevulinic acid synthase 2). KLF1 regulates the *Abcg2* gene which encodes a heme transporter protein involved in the final step in the assembly of the haemoglobin molecules [101]. ALAS2 is a heme-synthesis enzyme, it is reduced in KLF1-null red cells [26], [27]. A gene knockout of *Alas2* leads to severe anaemia with the accumulation of iron and an arrest erythroid differentiation [122].

1.5 B-cell lymphoma/leukaemia 11a (BCL11A)

1.5.1 The structure and function of BCL11A

BCL11A (also called *Evi9*) has four alternative pre-mRNA splicing transcripts predicted to yield protein isoforms designated as eXtra-Long (XL; 5.9 kb / 125 kD), Long (L; 3.8 kb / 100 kD), Short (S; 2.4 kb / 35kD) and eXtra-Short (XS; 1.5 kb / 25 kD). Exon 1 and 2 are common to all isoforms and composed of the invariant C_2HC zinc finger at the N-terminus, whereas XL, L and S each utilise at least a portion of exon 4, which leads to a variable number of C_2H_2 zinc fingers at the C-terminal region [123].

BCL11A is expressed in haematopoietic progenitors [124] and is essential for normal B and T cell development [125]. It is involved in lymphoid malignancies through translocation or amplification [126]. Recent studies have been reported that BCL11A plays a key role in the suppression of foetal globin production [120], [121], thereby completing globin switching to adult globin.

1.5.2 BCL11A in haematopoiesis

BCL11A (also called *Evi9* in mouse) is firstly defined as a B cell proto-oncogene [127]. A subsequent study reported that B cell development in *Bcl11a*$^{-/-}$ mutant mice is blocked at the earliest progenitor B-cell stage [125]. Mice transplanted with *Bcl11a*-deficient cells died from T cell leukaemia, and this indicates *Bcl11a* function as a T cell tumour suppressor gene [125]. These data suggest BCL11A is essential for normal lymphopoiesis.

Interestingly, a recent study has reported that BCL11A is also involved in the regulation of HSC self-renewal and quiescence [46]. Single-cell RNA-seq results showed that *Bcl11a* deletion in HSCs alters cell cycle progression, suggesting that BCL11A deficiency leads to an increased proliferation in the HSCs. Moreover, *Bcl11a*$^{-/-}$ HSCs have a lower capacity to generate haematopoietic progenitors, this suggests BCL11A-deficient HSCs have defects in long-term self-renewal potential. Analysis of lineage gene expression suggested that *Bcl11a*$^{-/-}$ HSCs are myeloerythroid-restricted [46]. A similar study has showed that the loss of BCL11A

increases the frequency and number of phenotypic HSCs, but it results in several changes, including a decrease in B and T lymphoid development, myeloid lineage skewing, poorer HSC repopulation ability, impaired HSC self-renewal capacity and cell-cycle alterations. This suggests BCL11A is required for normal HSC function [47].

1.5.3 BCL11A in erythropoiesis

Although BCL11A was originally investigated in the lymphocyte development [125], its role in erythropoiesis has also been assessed [128]. Sankaran et al compared BCL11A variants in $CD71^+$ / $CD235^+$ erythroblasts between adult bone marrow, foetal liver, and circulating primitive cells, and found that foetal liver and primitive erythroblasts expressed the shorter BCL11A variant and high level of γ-globin. In contrast, adult bone marrow erythroblasts expressed the full-length XL / L isoforms (Figure 1.2), indicating that a low level of foetal globin is associated with increased full-length BCL11A expression [128]. Immunoprecipitation experiments demonstrated that BCL11A associates with GATA-1 and FOG-1 in erythroid cells, suggesting that the formation of this complex might be required to regulate gene expression [128]. Knockdown of *BCL11A* by siRNA and shRNA in human $CD34^+$-derived erythrocytes leads to robust foetal globin expression, suggesting that BCL11A regulates foetal γ-globin expression [128]. A subsequent study in K562 cells showed that BCL11A is able to bind GGCCGG motif in nucleotide −56 to −51 on the *HBG* proximal promoter and results in down-regulation of γ-globin [49]. *Bcl11a*$^{-/-}$ mice were generated to evaluate the function of BCL11A in erythropoiesis. Loss of BCL11A has no influences on the expression of CD71 and TER119 suggesting that BCL11A does not affect the development of erythroid lineages [31].

BCL11A can be activated by KLF1 directly binding to its promoter and regulates the globin expression switching from foetal to adult globin [120], [121]. BCL11A is only expressed in adult erythrocytes (Figure 1.2), where it suppresses the expression of embryonic globin genes [31] and foetal globin gene expression [37]. Because primitive erythrocytes lack BCL11A expression (Figure 1.2), several studies regard BCL11A as a marker for definitive erythropoiesis [12], [30], [32].

Some reports indicate BCL11A need to form a complex to regulate globin expression, including GATA1 and MYB. Strong GATA-1 binding was found in *Bcl11a* intron 2 as being highly associated with foetal globin gene suppression [50], and this suggests BCL11A and GATA-1 are co-regulators of globin expression. A study of a murine erythroleukemic cell line containing an intact human β-globin locus has indicated that double knockdowns of *Myb* and *Dnmt1* (DNA methyltransferase 1) enhances ε-globin expression, double knockdowns of *Bcl11a* and *Dnmt1* results in an induction of γ-globin expression [51]. This demonstrates that MYB and BCL11A cooperate with DNMT1 to achieve repression of embryonic and foetal globin genes.

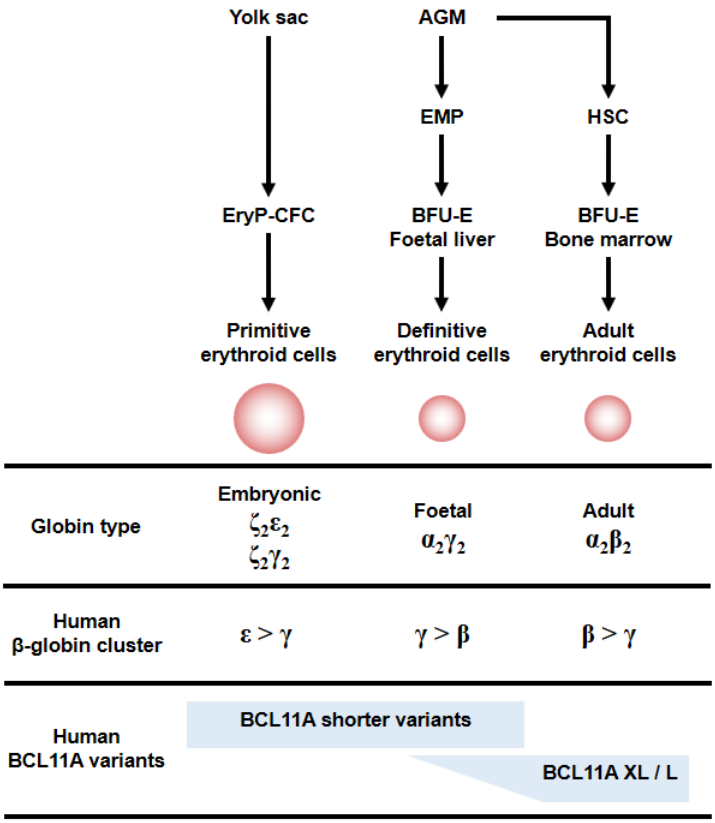

Figure 1.2 Developmental stage-specific BCL11A

The figure indicates BCL11A variants appear in the different stage of erythropoiesis. Full length forms (XL / L) of BCL11A are expressed in adult bone marrow erythroblasts, and a lower level in foetal liver erythroblasts, but absent in primitive erythroblasts. BCL11A shorter variants are expressed in primitive and foetal liver erythroblasts, both of which express γ-globin. EryP-CFC, primitive erythroid colony-forming cell; AGM, aorta-gonad-mesonephros; MEP, megakaryocyte-erythroid progenitor; HSC, haematopoietic stem cell; BFU-E, burst-forming-unit-erythroid. This figure was modified from *Nature*. 2009 [31].

1.6 Thesis aims

1.6.1. Hypothesis

Enhancing the activity of the erythroid transcription factors, KLF1 and BCL11A in human pluripotent stem cells will promote the *in vitro* differentiation and maturation of red blood cells.

1.6.2. Experiment strategy

1) Test a defined differentiation protocol for hiPSCs towards erythroid cells

A PSC differentiation protocol established by our collaborators at the University of Glasgow was tested in our lab. The phenotype of erythroid cells will be assessed by microscopy, flow cytometry, *in vitro* colony forming assays. Erythroid gene expression was monitored throughout the differentiation time course by quantitative RT-PCR.

2) Generate a tamoxifen-inducible KLF1 system in hiPSCs and validate KLF1 activation during erythroid differentiation

Inducible KLF1-ER^{T2} system was set up in the *AAVS1* locus of iPSCs, and this iKLF1 cell line was then differentiated in the presence and absence of tamoxifen. The effects on the production of mature RBCs were be evaluated by microscopy, flow cytometry, quantitative RT-PCR and HPLC.

3) Generate both tamoxifen-inducible BCL11A and tamoxifen-inducible KLF1 system in hiPSCs and validate the activation of both TFs during erythroid differentiation

Both inducible BCL11A-ER^{T2} and KLF1-ER^{T2} system was set up in the *AAVS1* locus of iPSCs, and the iBK cell line was then differentiated in the presence and absence of tamoxifen. The effects on proliferation and maturation of RBCs were be evaluated by microscopy, flow cytometry, quantitative RT-PCR and HPLC.

Chapter 2
Materials and Methods

2.1 Cell culture techniques

2.1.1 Production of iPSCs

Human iPSC lines were generated by Roslin Cells (http://roslincells.com). Briefly, fibroblasts were obtained from the skin of a O Rhesus negative individual (R Biomedical Ltd, Edinburgh, UK under REC 1/AL/0020 ethical approval) and reprogrammed to iPSCs using an episomal strategy with four transcription factors, OCT4, KLF4 SOX2 and cMYC [75]. The human iPSC line, SFCi55, was characterised by flow cytometry analyses for pluripotent markers (TRA-1-60, SSEA-1, OCT3/4 and SSEA-4) and a differentiation marker (SSEA-1) (a published work in Appendix). Karyotype analysis revealed a normal female chromosome complement and banding pattern and that was then confirmed by single nucleotide polymorphism analysis (data not shown). Hematopoietic differentiation of SFCi55 was compared with other human iPSC lines (a published work in Appendix) and used in this study.

2.1.2 Maintenance of iPSCs

2.1.2.1 Culturing of iPSCs

SFCi55 cells (a human iPSC line derived from an individual with the O Rhesus negative blood group) were maintained in STEMPRO® SFM containing 20 ng/ml human basic FGF (PHG0261, Invitrogen) on CTS™ CELLstart™ Substrate (A10142-01, Invitrogen). STEMPRO® SFM was comprised of 500 ml of DMEM/F-12 with Glutamax (10565-018, Invitrogen) supplemented with 40 ml of 25 % BSA (A10008-01, Invitrogen), 10 ml of STEMPRO® supplement (10006-01, Invitrogen), 1 ml of 50 mM 2-Mercaptoethanol (31550-010, Thermo Fisher Scientific). To coat CTS™ CELLstart™ Substrate on plates, the original stock of CTS™ CELLstart™ was diluted with DPBS containing Ca^{2+} and Mg^{2+} at 1:50.

iPSCs were passaged when cells reached 70-80 % confluency. Culture medium was exchanged with fresh STEMPRO® SFM and plates were pre-coated with CTS™ CELLstart™ 1 hour prior to passage. Cell colonies were then cut into small square pieces with STEMPRO® EZPassage™ (23181010, Invitrogen,). Suspended colonies

were transferred to new wells with fresh STEMPRO® SFM at 1:4 to 1:6. Fresh STEMPRO® SFM was replaced each day.

2.1.2.2 Cryopreservation of iPSCs

Cells from a 80 % confluent well (6-well plate) were harvested with STEMPRO® EZPassage™ and centrifuged at 200 xg for 5 minutes. Cell colonies were gently resuspended in 1 ml of cold CryoStor® cell cryopreservation media (C2874, Sigma-Aldrich) and divided into two pre-labelled cryovials. Two cryovials were placed in the cold Mr. Frosty and kept in -80 °C freezer overnight. For long-term storage, cryovials were transferred to -150 °C freezer.

2.1.2.3 Thawing of iPSCs

A cryovial of iPSCs was thawed rapidly at 37 °C in a water bath, and cell colonies were resuspended in 4 ml of pre-warmed STEMPRO® SFM. Cells were pelleted by centrifugation at 200 xg for 5 minutes and resuspended in fresh 1 ml STEMPRO® SFM supplemented with 10 μM ROCK inhibitor (Y-27632, MERCK). The cell solution was transferred to one CTS™ CELLstart™-coated well in a 6-well plate.

2.1.3 Differentiation of iPSCs

Haematopoietic differentiation was carried out in a step-wise, serum- and feeder-free protocol, as described [79], [129] (Figure 2.1).

Day 0

Briefly, one confluent well of iPSCs was cut with STEMPRO® EZPassage™ and transferred to two wells of a 6-well plate with cell repellent surface (657970, Greiner Bio-One) and then cultured in 3 ml (per well in a 6-well plate) of Stemline® II Hematopoietic Stem Cell Expansion Medium (S0192, Sigma-Aldrich) in the presence of 10 ng/ml BMP4 (314-BP-010, R&D), 10 ng/ml VEGF (293-VE010, R&D), 10 ng/ml Wnt3a (5036-WN010, R&D) and 5 ng/ml Activin A (338-AC010, R&D), and 2 μM GSK-3β inhibitor VIII (A014418, Merck Millipore). Embryoid bodies (EBs) formed spontaneously.

Day 2

The following cytokines were topped up in 0.5 ml (per well in a 6-well plate) of Stemline® II Hematopoietic Stem Cell Expansion Medium with 20 ng/ml BMP4, 30 ng/ml VEGF, 10 ng/ml Wnt3a, 5 ng/ml Activin A, 10 ng/ml FGFa (PHG0014, Thermo Fisher Scientific), 20 ng/ml SCF (PHC2111, Thermo Fisher Scientific), 2 μM GSK-3β inhibitor VIII and 0.4 ng/ml β-estradiol (E2257, Sigma-Aldrich).

Day 3 to day 9

EBs were dissociated to single cells with 0.5 ml (per well in a 6-well plate) of StemPro® Accutase® Cell Dissociation Reagent (A1110501, Thermo Fisher Scientific) for 3 minutes at 37 °C. After centrifugation at 200 xg for 5 minutes, the cells were seeded at $2x10^5$ cells per well in 3 ml of Stemline® II Hematopoietic Stem Cell Expansion Medium in the presence of 20 ng/ml BMP4, 30 ng/ml VEGF, 10 ng/ml FGFa, 30 ng/ml SCF, 10 ng/ml IGF2 (292-G2, R&D), 10 ng/ml TPO (288-TPN-25, R&D), 5 μg/ml heparin (H3149, Sigma-Aldrich), 50μM IBMX (I5879, Sigma-Aldrich) and 0.4 ng/ml β-estradiol. Fresh cytokines were topped up in 0.5 ml medium per well at days 5, 7 and 9.

Day 10 to day 17

Differentiating cells were harvested by centrifuging at 200 xg for 5 minutes and $3x10^5$ cells were seeded in 3 ml (per well in a 6-well plate) of Stemline® II Hematopoietic Stem Cell Expansion Medium in the presence of 1 μM hydrocortisone, 50 ng/ml SCF, 16.7 ng/ml Flt3L (300-19, Peprotech), 6.7 ng/ml BMP4, 6.7 ng/ml IL-3 (213-13, Peprotech), 6.7 ng/ml IL-11 (200-11, PeproTech), 3 U/ml EPO (287-TC-500, R&D) and 50μM IBMX. Fresh cytokines were topped up in 0.5 ml medium (per well in a 6-well plate) at days 12, 14 and 16.

Day 18 to day 24

From this stage, differentiating cells were cultured in IBIT medium instead of Stemline® II Hematopoietic Stem Cell Expansion Medium. The IBIT medium was made up by 240 ml of Iscove Basal Medium (FG-0465, Merck Millipore)

supplemented by 1% BSA (G10008-01, Thermo Fisher Scientific), 10 μg/ml insulin (I9278; Sigma-Aldrich), 0.2 μg/ml transferrin (T0665, Sigma-Aldrich), and 500 μl of 2-Mercaptoethanol (31550-010, Thermo Fisher Scientific). Cells at day 17 were centrifuged at 200 xg for 5 minutes and seeded in 3 ml (per well in a 6-well plate) of IBIT medium in the presence of 1 μM hydrocortisone, 20 ng/ml SCF, 20 ng/ml IGF1 (100-11, Peprotech), 6.7 ng/ml IL-3, 6.7 ng/ml IL-11 and 3 U/ml EPO. Fresh cytokines were topped up in 0.5 ml medium (per well in a 6-well plate) at days 20, 22 and 24.

Day 25

Differentiating cells were harvested by centrifuging at 200 xg for 5 minutes and seeded in 3 ml (per well in a 6-well plate) of IBIT medium in the of 3 U/ml EPO, 6.7 ng/ml IL-1β (201-LB-005, R&D), 6.7 ng/ml IL-6 (206-1L-010, R&D), 5 % AB plasma (H4522, Sigma-Aldrich) and 2 ng/ml Sodium Selenite (S5261, Sigma-Aldrich).

Day 27

Fresh IBIT medium with 5% AB plasma and 2 ng/ml Sodium Selenite were topped up in 0.5 ml medium (per well in a 6-well plate) at days 29 and day 31.

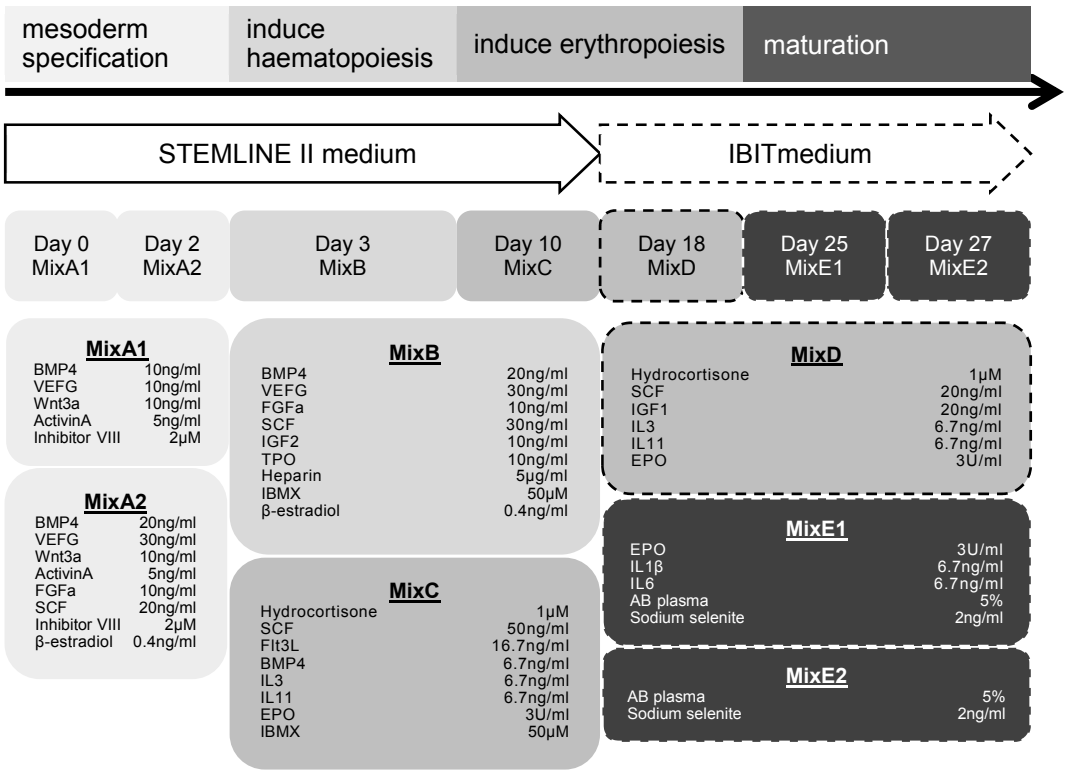

Figure 2.1 Defined erythroid differentiation protocol from PSCs

A scheme describes the erythroid differentiation from iPSCs. At day 0, one well of PSCs was harvested by EZPassage and transferred to low adherent 6-well plates. Differentiating cells were cultured in Stemline II medium with cytokines till day 17, and changed to IBIT medium with cytokines from day 18. This scheme was modified from *Stem Cells Transl Med*. 2016 [79].

2.1.4 CFU assay for iPSCs-derived cells

iPSC-derived cells at day 10 of differentiation were collected for CFU assay using MethoCult™ H4435 Enriched (04435, STEMCELL) that favour haematopoietic colony formation. Two low attachment 35 mm dishes were set up in parallel at densities of $5x10^3$ cells and $1x10^4$ cells in 1.2 ml of MethoCult™. Two dishes were incubated in a 37 °C incubator, and colonies were scored after 12 to 15 days.

2.1.5 Maintenance of COS7 cells

COS7 cells were maintained in GMEM medium (11710035, Thermo Fisher Scientific) supplemented with 10 % foetal calf serum (Lonza), 2 mM sodium pyruvate (11360070, Thermo Fisher Scientific), 1 % non-essential amino acids (11140050, Thermo Fisher Scientific), and 0.1 mM 2-Mercaptoethanol (31550-010, Thermo Fisher Scientific). COS7 cells were passaged when cells reached 80 % confluency in a T25 flask. Cells were dissociated with 0.25 % trypsin solution and harvested by centrifuging at 200 xg for 5 minutes. Cell pellets were resuspended in fresh culture medium and seeded back to a T25 flask at 1:4 ratio.

To freeze COS7 cells, cells from a T25 flask were dissociated with 0.25 % trypsin solution and harvested by centrifuging at 200 xg for 5 minutes. Cell pellets were resuspended in 1 ml of culture medium supplemented with 10 % Dimethyl Sulfoxide (DMSO) (Sigma-Aldrich). The cell solution was divided into two pre-labelled cryovials and then placed in the cold Mr. Frosty in -80 °C freezer overnight. For long-term storage, cryovials were transferred to -150°C freezer.

To thaw COS7 cells, a cryovial of COS7 cells was thawed rapidly at 37 °C in a water bath, and cell suspensions were transferred in 4 ml of pre-warmed culture medium. After centrifuging at 200 xg for 5 minutes, cell pellets were resuspended in fresh 10 ml of culture medium and transferred to a T25 flask.

2.1.6 Maintenance of K562 cells

K562 cells were maintained in DMEM medium (61965-026, Life technologies) supplemented with 10 % foetal calf serum (Lonza), 2 mM sodium pyruvate (11360070, Thermo Fisher Scientific), 1 % non-essential amino acids (11140050, Thermo Fisher

Scientific), and 0.1 mM 2-Mercaptoethanol (31550-010, Thermo Fisher Scientific). K562 cells were passaged when cells reached 80 % confluency in a T25 flask, and $5x10^5$ cells were seeded back to a new T25 flask.

To freeze K562 cells, cells from a T25 flask were harvested by centrifuging at 200 xg for 5 minutes and resuspended in 1 ml of culture medium supplemented with 10 % Dimethyl Sulfoxide (DMSO) (Sigma-Aldrich). The cell solution was divided into two pre-labelled cryovials and then placed in the cold Mr. Frosty in -80 °C freezer overnight. For long-term storage, cryovials were transferred to -150°C freezer.

To thaw K562 cells, a cryovial of K562 cells was thawed rapidly at 37 °C in a water bath, and cell suspensions were transferred in 4 ml of pre-warmed culture medium. After centrifuging at 200 xg for 5 minutes, cell pellets were resuspended in fresh 10 ml of culture medium and transferred to a T25 flask.

2.1.7 Transfection of cells

2.1.7.1 Xfect transfection of COS7 cells

One day prior to the transfection, $2x10^5$ COS7 cells were plated in a 6-well plate. On the day of transfection, 5 μg plasmid was added into 100 μl of Xfect Reaction Buffer (631317, Clontech). 1.5 μl of Xfect Polymer was added into plasmid solution and vortexed. The plasmid-polymer solution was then incubated at room temperature for 10 minutes. Old medium was replaced by 1 ml of fresh culture medium. The plasmid-polymer mix was dropped to the well and incubated overnight at 37 °C. Old medium was then replaced by fresh culture medium.

2.1.7.2 Xfect transfection of K562 cells

One day prior to the transfection, $5x10^5$ K562 cells were seeded in a 6-well plate. On the day of transfection, 5 μg plasmid was added into 100 μl of Xfect Reaction Buffer. 1.5 μl of Xfect Polymer was added into plasmid solution and vortexed. The plasmid-polymer solution was then incubated at room temperature for 10 minutes. Old medium was replaced by 1 ml of fresh culture medium. The plasmid-polymer mix was dropped

to the well and incubated overnight at 37 °C. Old medium was then replaced by fresh culture medium.

To generate stable cell lines with a transgene, K562 cells were selected by culturing with 2 μg/ml puromycin two days post transfection. Untransfected K562 cells died in the puromycin selection in few days, whereas transfected cultures contained viable cells.

2.1.7.3 Electroporation of iPSCs

Human iPSCs were electroporated using Gene Pulser Electroporation Systems (165-4447, BIO-RAD). 1 hour prior to electroporation, old medium was replaced by fresh STEMPRO® SFM supplemented with 10 μM ROCK inhibitor. hiPSC were then dissociated to single cells with accutase and resuspended in DPBS without Ca^{2+} and Mg^{2+}. $1x10^7$ cells were prepared in 700 μl of DPBS and transferred into a cuvette for electroporation. 50 μg of plasmid DNA (40 μg of pZDonor-AAVS1-puro plasmid, 5 μg of p622L and 5 μg of p622R) was added to the cuvette and mixed gently. The Gene Pulser Electroporation Systems was set up at 320 mV, 250 μF for electroporation. After the electroporation, cells were resuspended in fresh STEMPRO® SFM and then divided into ten CTS™ CELLstart™-coated 10 cm^2 petri dishes with 10 ml of STEMPRO® SFM plus 10 μM ROCK inhibitor. Two days post transfection, electroporated cells were cultured in STEMPRO® SFM supplemented with 0.3 μg/ml puromycin. After one week of puromycin selection, the concentration of puromycin was increased to 0.5 μg/ml. Single colonies emerged 14 days post transfection and then were transferred to a 24-well plate for expansion.

2.1.8 Viral transduction

Differentiating cells were harvested by centrifuging at 200 xg for 5 minutes and $3x10^5$ cells were seeded in 250 μl (per well in a 12-well plate). Viral particles and polybrene (H9268, Sigma-Aldrich; final concentration is 6 μg/ml) were diluted in 250 μl of Stemline® II Hematopoietic Stem Cell Expansion Medium and added to the well in a dropwise manner. The mixture was incubated at 37°C for one hour. Viral particles were removed by centrifuging at 200 xg for 5 minutes and transduced cells were reseeded in 3 ml of complete differentiation medium and placed in a 37 °C incubator.

A control GFP-lentivirus was used to establish a transduction protocol for iPSC-derived cells at day 10. The amount of viral particles was added to test multiplicity of infection (MOI), including 0, 1, 5, 10, 25, 50, 100 and 200 viral particles per cell. GFP fluorescence was evaluated by flow cytometry one day after virus transduction, and the maximum GFP expression was observed at a MOI of 100 (Supplementary Figure S3).

2.1.9 Immunofluorescence (IF) staining

Transfected COS7 cells and control COS7 cells were fixed in 4 % formaldehyde / PBS at room temperature for 15 minutes and permeabilized in 0.5 % Triton-X 100 / PBS. Fixed cells were incubated for one hour with PBS containing rabbit anti-human KLF1 (sc14034, Santa Cruz; in 1:100) or rabbit anti-HA tag (631207, Clontech; in 1:100) or mouse anti-BCL11A (ab19489, Abcam; in 1:50) antibodies. After washing by PBS three times, cells were successively incubated for one hour with PBS containing goat anti–rabbit IgG-FITC (F0382-1ML, Sigma-Aldrich; in 1:1000) or goat anti–mouse IgG-FITC (F0257-1ML, Sigma-Aldrich; in 1:1000) antibodies and DAPI (4',6-Diamidino-2-phenylindole, Sigma-Aldrich). After washing by PBS three times, stained cells were analysed using a Zeiss Observer microscope and processed with AxioVision and ImageJ software.

2.1.10 Cytospin and rapid Romanowsky staining

$5x10^4$ erythroid cells were prepared in 0.2 ml PBS and then loaded in cytospin slide chamber. After centrifuging at 500 rpm for 10 minutes, the cytospin slide was air-dried at room temperature. The Rapid Romanowsky Stain Pack (HS705, TCS biosciences) was used to fix and stain the cells. The air-dried slides were first dipped in Fixative Solution for 30 seconds, and immediately transferred to Solution B for 30 seconds, and then stained in Solution C for 30 seconds. The slides were rinsed in water and air-dried.

2.2 Molecular biology techniques

2.2.1 Construction of plasmids

2.2.1.1 Construction of pZDonor-AAVS1-Puromycin-CAG-HA-KLF1-ER^{T2}-PA and pZDonor-AAVS1-Puromycin-CAG-HA-Mut KLF1-ER^{T2}-PA

The CAG promoter was excised from pCAGASIP vector using EcoRV restriction enzyme digestion and subcloned into the EcoRV site of pZDonor-AAVS1 puromycin vector, and it was cloned in the reverse orientation to the *AAVS1* locus (constructed by Dr Richard Axton). After I obtained the pZDonor-AAVS1-CAG, the poly A sequence was amplified from the PL452 plasmid by polymerase chain reaction (PCR) and subcloned into the AgeI site of the pZDonor-AAVS1-CAG (Figure 2.2A). Next, the fusion gene *HA-KLF1-ER^{T2}* was amplified by PCR from the pCAG-KLF1-ER^{T2} (constructed by Rui Ma), and subcloned into the EcoRI site of pZDonor-AAVS1-CAG-PolyA vector (Figure 2.2A). The same strategy was used to introduce the *HA-Mut-KLF1-ER^{T2}* into pZDonor-AAVS1-CAG-PolyA vector, separately. Both constructs, pZDonor-AAVS1-Puromycin-CAG-HA-KLF1-ER^{T2}-PA and pZDonor-AAVS1-Puromycin-CAG-HA-Mut KLF1-ER^{T2}-PA, were verified by AgeI digestion, and the orientation of insertion was distinguished by different sized fragments. In the correct orientation (ie same direction of CAG promoter), 321 bp and 1546 bp fragments were released from AgeI digestion whereas 321 bp and 542 bp fragments were released when construct was in the reverse orientation (Figure 2.2B and C). Constructs were sequenced to confirm their identity and aligned to databases (BLAST in NCBI). Vectors were generated that carried either the wild type form or a mutant form of KLF1. In the wild type (WT-KLF1), amino acid 328 is Arginine (encoded by CGC), whereas in the mutant form (Mut-KLF1), amino acid 328 is Leucine (encoded by CTG) (Figure 2.2D). This mutation obliterates the DNA binding capacity of KLF1 and results in a lower expression of *HBE1* and *HBB* in the erythroblasts of In(Lu) rare blood group [114]. We therefore took advantage of this mutant and used it as a negative control in our experiments.

PCR primers and sequencing primers used in this project were listed in Appendix (Supplementary Table S1).

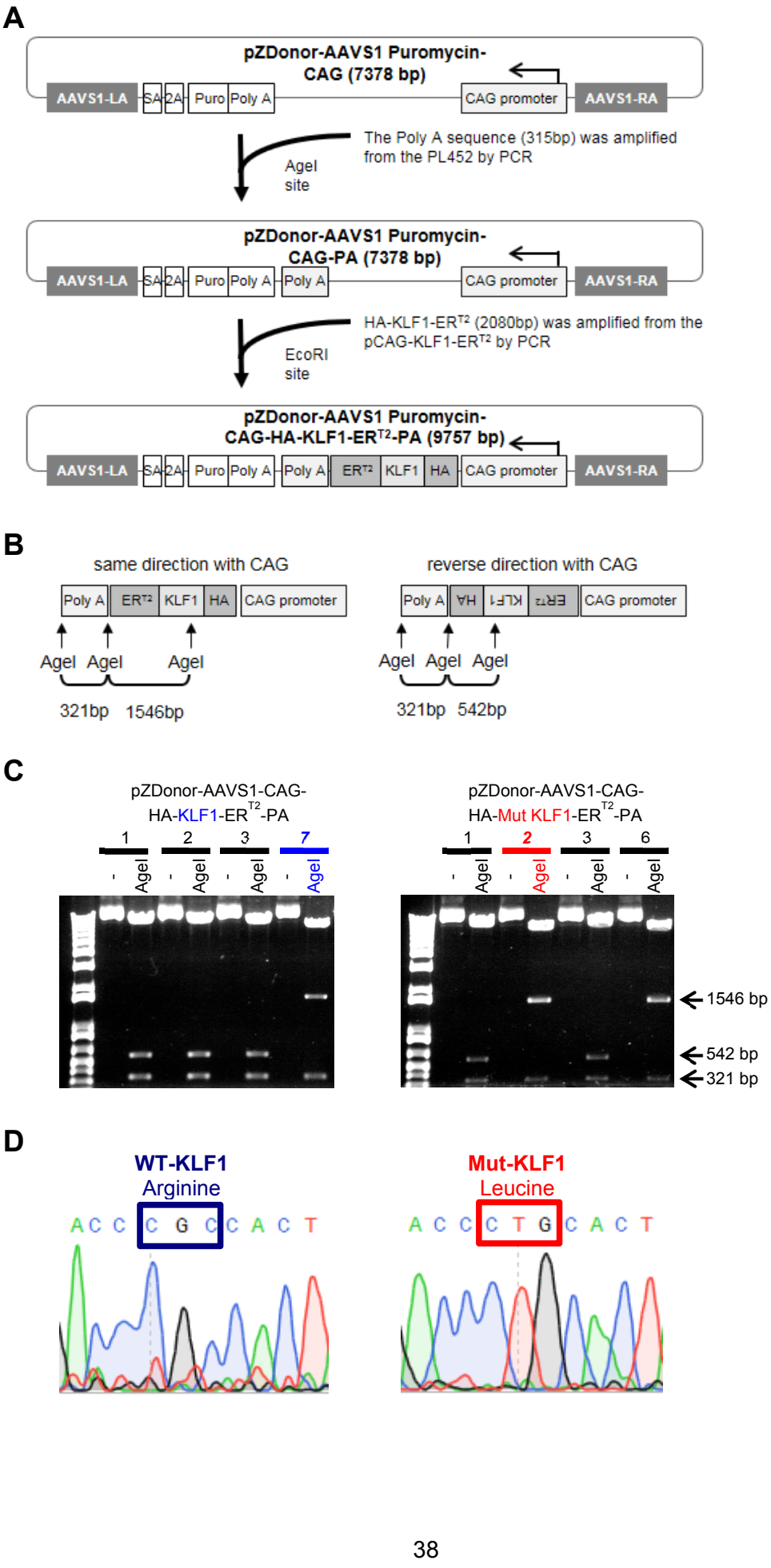
A
pZDonor-AAVS1 Puromycin-CAG (7378 bp)
AAVS1-LA
SA
2A
Puro
Poly A
CAG promoter
AAVS1-RA
AgeI site
The Poly A sequence (315bp) was amplified from the PL452 by PCR
pZDonor-AAVS1 Puromycin-CAG-PA (7378 bp)
EcoRI site
HA-KLF1-ERT2 (2080bp) was amplified from the pCAG-KLF1-ERT2 by PCR
pZDonor-AAVS1 Puromycin-CAG-HA-KLF1-ERT2-PA (9757 bp)
ERT2
KLF1
HA
B
same direction with CAG
reverse direction with CAG
AgeI
321bp
1546bp
542bp
C
pZDonor-AAVS1-CAG-HA-KLF1-ERT2-PA
pZDonor-AAVS1-CAG-HA-Mut KLF1-ERT2-PA
1546 bp
542 bp
321 bp
D
WT-KLF1
Arginine
Mut-KLF1
Leucine

Figure 2.2 Construction of pZDonor-AAVS1-Puromycin-CAG-HA-KLF1-ER^{T2}-PA and pZDonor-AAVS1-Puromycin-CAG-HA-Mut KLF1-ER^{T2}-PA

A. A schematic diagram indicates how the pZDonor-AAVS1-CAG-HA-KLF1-ER^{T2}-PA vector was constructed. AAVS1-LA, AAVS1 left homology arm; SA, splice acceptor; 2A, self-cleaving peptide sequence; Puro, puromycin resistance gene; Poly A, polyadenylation sequence; HA, HA tag sequence; AAVS1-RA, AAVS1 right homology arm. **B.** Diagram showing the orientation of gene construct in the pZDonor-AAVS1-CAG-PolyA vectors. **C.** The result of AgeI digestion indicates the correct insertion in different constructs. **D.** The sequencing results of pZDonor-AAVS1-Puromycin-CAG-HA-KLF1-ER^{T2}-PA construct 7 and pZDonor-AAVS1-Puromycin-CAG-HA-Mut KLF1-ER^{T2}-PA construct 2.

2.2.1.2 Construction of pZDonor-AAVS1-Puromycin-CAG-BCL11A-ER^{T2}-PA

Due to the GC-rich sequences and repetitive sequences in BCL11A gene, it proved difficult to clone the cDNA of K562 cells by PCR. However, we were able to amplify BCL11A from lentivirus vector pXLG3-BCL11A XL by PCR, and the ER^{T2} fragment was replicated from pCAG KLF1-ER^{T2} [130]. Subsequently, the *BCL11A-ER^{T2}* transgene was created by recombinant PCR and transferred into a shuttle vector, pGEM T EASY. The *BCL11A-ER^{T2}* cassette was then subcloned into the EcoRI site of the pZDonor-AAVS1-Puromycin-CAG-PA vector (Figure 2.3A). The pZDonor-AAVS1-CAG-BCL11A-ER^{T2}-PA construct was verified by AgeI and HindIII digestion, with the correctly orientiated version releasing 321 bp and 786 bp fragments (Figure 2.3B). Constructs were also validated by PCR using specific primers targeted to the Poly A sequence and ER^{T2} regions (data not shown). In the final confirmation, the pZDonor-AAVS1-CAG-BCL11A-ER^{T2}-PA construct 1 was sequenced (BLAST in NCBI) (data not shown).

PCR primers and sequencing primers used in this project were listed in Appendix (Supplementary Table S1).

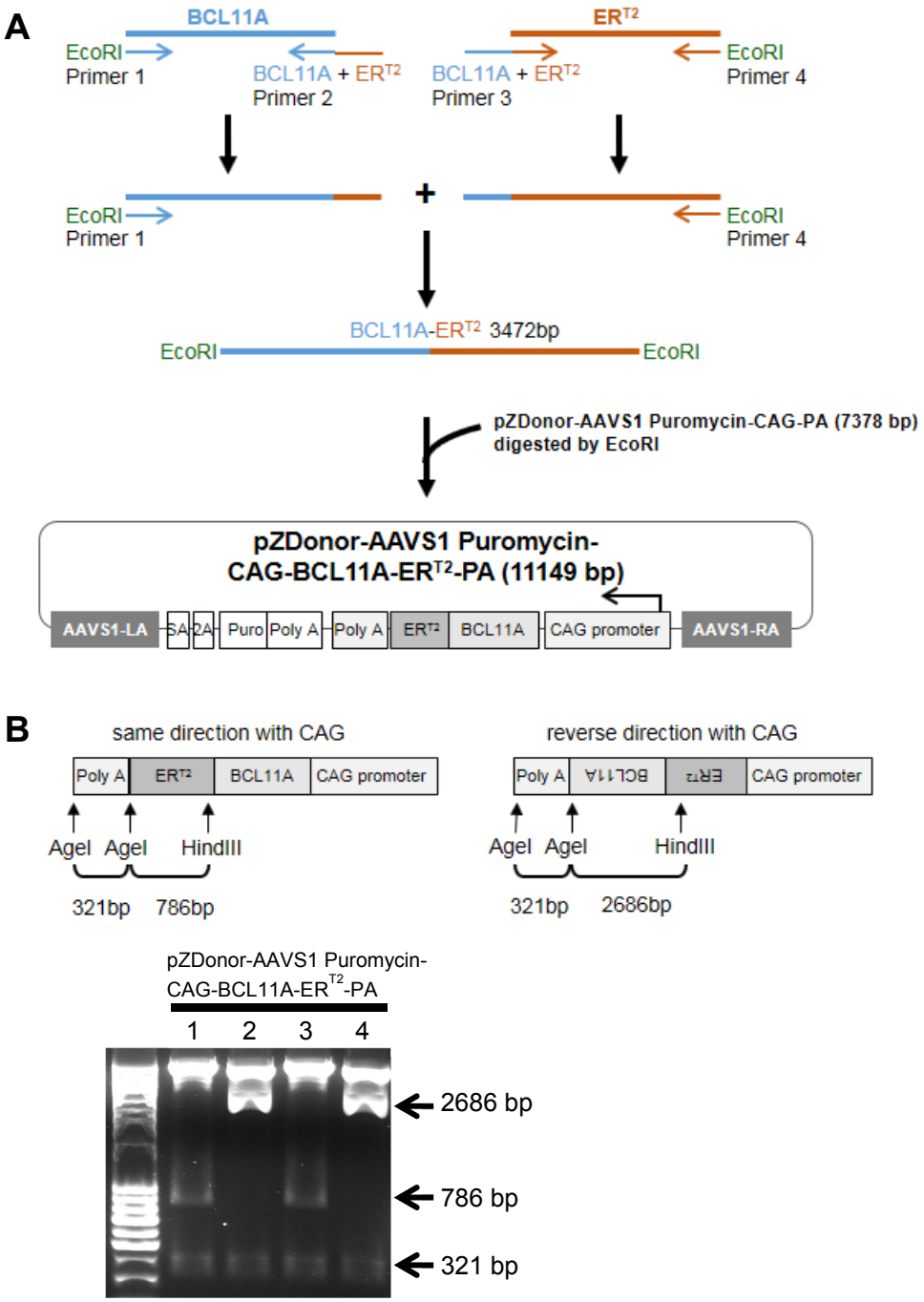

Figure 2.3 Construction of pZDonor-AAVS1-Puromycin-CAG-BCL11A-ER^{T2}-PA

A. A schematic diagram indicating how the pZDonor-AAVS1-CAG-BCL11A-ER^{T2}-PolyA was constructed. **B.** Diagram showing the orientation of gene construct in the pZDonor-AAVS1-CAG-PA vectors. AgeI / HindIII double digestion for constructs generates 786 bp and 321 bp in correctly orientated vector and 2686 bp and 321 bp when orientiated in reverse.

2.2.2 Transformation of competent cells

2 µl from a 10 µ ligation reaction or 50 ng of plasmid DNA was mixed with 50 µl of One Shot TOP10 Chemically Competent E. coli (C404003, Invitrogen) and placed on ice for 30 minutes. The mixture was heat shocked for 30 seconds at 42 °C in a water bath followed by incubation on ice for 2 minutes. After mixing with 250µl room temperature Super Optimal broth with Catabolite repression (S.O.C.) medium (Invitrogen), the 1.5 ml tube containing the mixture was placed in a shaking incubator at 37 °C for 1 hour. Plates were prepared with LB agar with ampicillin (50 µg/ml) or kanamycin (50 µg/ml) for selection. 250 µl of the mixture was spread on the plate and incubated at 37 °C overnight.

2.2.3 Plasmid purification

Plasmid preparation was performed by the QIAprep Spin Miniprep Kit (27106, QIAGEN) or QIAGEN Plasmid Midi Kit (12143, QIAGEN). One single colony was picked and expanded in 5ml (Miniprep) or 100ml (Midiprep) LB with antibiotics at 37 °C in a shaking incubator overnight. E.coli. containing plasmids were harvested by centrifugation and plasmid DNA was extracted according to the QIAGEN instructions. DNA samples were stored at -20 °C.

2.2.4 RNA extraction

RNA preparation was performed by RNeasy Mini Kit (74106, QIAGEN) following the manufacturer's instructions. To remove DNA from samples, the RNase-free DNAse Set (79254, QIAGEN) was used on-column during RNA extraction. RNA samples were stored at -80 °C.

2.2.5 Complementary DNA (cDNA) synthesis

1 µg of RNA was reverse transcribed by the High-Capacity cDNA Reverse Transcription Kit (4368814, Thermo Fisher Scientific) following the manufacturer's instructions. The 20 µl reaction was carried out at 25 °C for 5 minutes, 37 °C for 2 hours, and a final incubation of 85 °C for 5 minutes. cDNA samples were stored at -20 °C.

2.2.6 Quantitative RT-PCR analysis

Quantitative RT-PCR (qRT-PCR) reactions were performed on the ABI 7500 Fast Real-Time PCR System (Applied Biosystems) and analysis was done on the SDS software Version 1.4 (Applied Biosystems). The TaqMan® Fast Universal PCR Master Mix (2x) (4352042, Applied Biosystems) was used with primers which were designed on the Universal Probe Library (UPL) System Assay Design Center (available on the Roche website). All primers and probes used are listed in Appendix (Supplementary Table S2). Each primer set was tested for efficiency beforehand, and all reactions were performed in triplicate. The program was set at 95 °C for 3 seconds (Enzyme activation), 95 °C for 20 seconds x40 cycles (Denaturation) and 60 °C for 30 seconds (Annealing, Extension). To normalize cDNA quantity, GAPDH was used as reference gene. The ΔΔCt calculation was used for analysing qRT-PCR results.

2.2.7 Genomic DNA extraction

MasterPure™ Complete DNA and RNA Purification Kit (MC85200, Epicentre) was used for extracting genomic DNA from iPSCs. Briefly, iPSCs from 2 wells (6-well plate) were harvested by accutase and pelleted by centrifugation in a 1.5 ml tube. Cell pellet was resuspended in 300 µl of Tissue and Cell Lysis Solution supplemented with 1 µl of Proteinase K. 1.5 ml tubes were incubated at 65 °C for 15 minutes. 1 µl of RNAse A was then added in the tube and incubated at 37 °C for 30 minutes. 1.5 ml tubes were incubated on ice for 5 minutes. After adding 175 µl of MPC Protein Precipitation Solution and vortexing, 1.5 ml tubes were centrifuged at 10,000 rpm, 4 °C for 10 minutes. The supernatant was transferred to a new 1.5 ml tube with 500 µl of isopropanol, the sample was mixed by inverting the tube 25 times. Genomic DNA samples was precipitated by centrifuging at 10,000 rpm, 4 °C for 10 minutes. After removing isopropanol, genomic DNA pellet was washed by 70 % ethanol two times and then resolved in 50 µl nuclease-free water.

2.2.8 Southern blot

The Digoxygenin-labelled probes (DIG-labelled probes) were synthesized beforehand using the PCR DIG Probe Synthesis Kit (11 636 090 910, Roche) according to manufacturer's instructions. The internal probe and the 3' external probes were

designed to target the regions in the AAVS1-left arm of pZDonor AAVS1 puromycin vector and endogenous *AAVS1*, respectively (Supplementary Figure S1A and C). PCR primers used in this project were listed in Appendix (Supplementary Table S1).

11 µg of genomic DNA was digested by SphI in a 30 µl reaction volume at 37 °C overnight. 1 µg of the digested DNA was run on a 0.8 % agarose gel with 1x GelRed Nucleic Acid Stain (41003, Biotium) to visualise DNA, on the other hand, 10 µg of the digested DNA was run on another 0.8 % agarose gel without GelRed for performing the southern blot. The gel electrophoresis was run at 20V in cold room overnight. After digested DNA separating, the gel was placed in the Depurination Solution (25 ml of HCl in 1,000 ml water) on shaker for 15 minutes and rinsed with autoclaved water. The gel was successively placed in Denaturation Solution (88 g NaCl and 20 g NaOH in 1,000 ml water) for 30 minutes and Neutralizing Solution (176 g NaCl, 6.7 g Tris-base and 70.2 g Tris-HCl in 1,000 ml water) for 20 minutes two times. To transfer DNA from gel to a Hybond-N+ Membrane (RPN2020B, GE Healthcare Amersham), the "Sandwich" construct was set up for capillary transfer using 20x SSC (176 g NaCl and 88 g Trisodium citrate in 1,000 ml water, pH 7) at room temperature overnight. The membrane was UV-crosslinked and pre-hybridized with DIG Easy Hyb Buffer (11585614910, Roche) for 30 minutes at 43 °C. 1 µl of DIG-labelled probe was diluted in 5 µl of DNA dilution buffer (11585614910, Roche) and 44 µl of water. The probe mix was denatured at 95 °C for 7 minutes and immediately placed on ice for 5 minutes. Denatured probes were then added to 15 ml of DIG Easy Hyb Buffer (11585614910, Roche) and applied to the membrane at 43 °C overnight. The membrane was washed by Low Stringency Wash Buffer (2x SSC and 0.1 % SDS in 1,000 ml water) for 5 minutes two times and then washed by High Stringency Wash Buffer (0.5x SSC and 0.1 % SDS in 1,000 ml water) at 65 °C for 15 minutes. The membrane was rinsed in Washing Solution (11585762001, Roche) for 5 minutes and subsequently incubated in Blocking Solution (11585762001, Roche) for 30 minutes. Antibody Solution (11585762001, Roche) was applied to the membrane and incubated for 30 minutes. Membrane was then washed by Washing Solution for 15 minutes two times. Detection Buffer (11585762001, Roche) was added on the membrane for 2.5 minutes. Membrane was applied with 1 ml of CSPD Solution (11585614910, Roche) and incubated at room temperature for 5 minutes. Membrane

was then exposed to X-ray film for detection. To re-probe the membrane, the membrane was stripped in Stripping Buffer (0.1 % SDS in 0.2 M NaOH) for 30 minutes at 64 °C, washed by 2x SSC for 15 minutes two times, and then hybridized.

2.3 Protein analysis

2.3.1 Protein extraction

To extract total protein, cells were lysed in 100 µl of RIPA buffer (89900, Thermo Fisher Scientific) and centrifuged at 10,000 rpm, 4 °C for 10 minutes. The supernatant was transferred to a new 1.5 ml tube and stored at -80 °C.

For nuclear fractionation, the cell pellet was resuspended in 0.2 ml of Swelling Buffer (5 mM PIPES, pH 8.0; 85 mM KCl; 0.5 % NP40; protease inhibitor cocktail) for 20 minutes on ice. After centrifuging at 1,500 rpm, 4 °C for 5 minutes, the cytoplasmic supernatant was removed. The nuclear pellet was resuspended in 0.3 ml of lysis buffer (20 mM Hepes, ph 7.6; 1.5 mM $MgCl_2$; 350mM KCl; 0.2 mM EDTA; 20 % Gycerol; 0.25 % NP40; 0.5 mM DTT; protease inhibitor cocktail; Benzonase) and gently shaken at 4 °C for 1 hour. The nuclear fraction was collected after centrifuging at 13,000 rpm, 4 °C for 30 minutes and stored at -80 °C.

2.3.2 Western blot

Proper amount of protein lysates were electrophoresed on a 4–20 % Ready Gel® Tris-HCl Gel (1611105, BIO-RAD) in 1x Running Buffer (2.5 mM Tris-base, 19 mM Glycine, 0.01% SDS, pH 8.3) at 100 V for about 2 hours. To transfer protein by the Bio-Rad Trans-Blot SD Semi Dry Transfer Cell (1703940, BIO-RAD), the gel and a nitrocellulose membrane (10402580, Whatman™) were placed between Extra Thick Blot Filter Papers (1703966, BIO-RAD) soaked in Transfer Buffer (25 mM Tris-base, 190 mM Glycine, 0.1 % SDS, 20 % Methanol, pH 8.3), the programme was set at 15V for 1 hour. Next, the membrane was blocked with 5 % semi-skimmed milk in PBST (0.1 % Tween 20 in PBS) at room temperature for 1 hour. The membrane was then incubated with PBST containing rabbit anti-HA tag (631207, Clontech; in 1:1000) or rabbit anti-human KLF1 (sc14034, Santa Cruz; in 1:200) or mouse anti-BCL11A (ab19489, Abcam; in 1:1000) or goat anti-GAPDH (AF5718, R&D; in 1:2000) or

rabbit anti-LaminB1 (ab16048, abcam; 1:2000) antibodies in cold room overnight. After washing by PBST three times, the membrane was incubated with the appropriate horseradish peroxidase–conjugated IgG (rabbit IgG-HRP, HAF008, R&D, 1:1000; goat IgG-HRP, sc-2020, SantaCruz, 1:3000; mouse IgG-HRP, A90-116P, BETHYL, 1:2000) at room temperature for 1 hour. After washing by PBST three times, the membrane was applied with the WesternSure™ ECL Substrate (LI-COR) and exposed to X-ray film or C-DiGit® Blot Scanner (LI-COR).

2.3.3 Flow cytometry

2 x 10^5 differentiating cells were harvested in PBS containing 1% BSA (PBS/BSA) and centrifuged at 200 xg for 5 minutes. Cell pellets were resuspended and mixed with the appropriate volume of antibodies, CD34-PE (12-0349-41, eBioscience), CD43-APC (17-0439-42, eBioscience), CD235a-FITC (11-9987-80, eBioscience) and CD71-APC (17-0719-42, eBioscience), to a final volume of 100 µl PBS/BSA incubated on ice for 30 minutes. After washing by PBS/BSA, cell pellets were resuspended in 200 µl PBS/BSA with 7-AAD Viability Staining Solution (00-6993-50, eBioscience) and then analysed on a LSR Fortessa (BectonDickinson) using FACS Diva. Data was analysed on the FlowJo cell analysis software.

For enucleation assay, the proportion of enucleated cells present in the culture was assessed using CD235a-FITC, CD71-APC antibodies, LIVE/DEAD™ Fixable Near-IR Stain (L10119, Life Technologies) and Hoechst dye (NucBlue, Life Technologies). Live $CD235a^+$ cells were first gated, then anti-CD71 and Hoechst were used to define erythroblasts ($CD71^+$/$Hoechst^+$), nucleated RBCs ($CD71^-$/$Hoechst^+$) and enucleated RBCs ($CD71^-$/$Hoechst^-$) (Supplementary Figure S2).

2.3.4 High-performance liquid chromatography (HPLC)

A published protocol for HPLC analysis was modified to analyse globin chains [85]. Briefly, 1 x 10^6 differentiating cells were harvested and washed 3 times in PBS. Cell lysates were prepared in 50 µl water by three rapid freeze-thaw cycles and centrifuged at 13,000 xg at 4 °C for 10 minutes. Globin chain separation was performed by injecting 10 µl of the supernatant onto a C4 column (1.0 x 250 mm, Phenomenex, UK) with a 42- 56% linear gradient between mixtures of 0.1% TFA in water (Buffer A) and

0.1% TFA in acetonitrile (Buffer B) at a flow rate of 0.05 ml/minute for 55 minutes on a HPLC Ultimate 3000 system (Dionex, UK). Samples in columns were analysed at 50°C and the UV detector was set at 220 nm. Elution times of peaks generated were compared to control samples for identifying β-, Gγ-, α-, Aγ-, ε- and ζ-globins (Figure 4.4A). The area of each peak was calculated and represented as a percentage of the total globin.

2.4 Statistical analysis

The statistical analysis was performed using GraphPad Prism 6 software. All data are expressed as Mean ± Standard Error of the Mean (SEM). P values less than 0.05 were considered statistically significant and a star (*) was labelled in the figure. The following statistical analyses were used:

- To compare two factors across multiple parametric groups – Two-way ANOVA followed by Tukey's multiple comparison test, such as cell proliferation and globin expression by HPLC
- To compare one factor across multiple parametric groups – One-way ANOVA followed by Holm-Sidak's multiple comparison test, such as flow cytometry data
- To compare gene expression data were analyzed using ratio paired t test

Chapter 3
Generation of a tamoxifen-inducible KLF1 system in hiPSCs

3.1 Introduction

Dr Joanne Mountford's laboratory at the University of Glasgow developed a defined protocol for the production of HPCs and erythroid cells from PSCs [79]. We established and tested this protocol in the Forrester lab. There are four main differentiation stages in this defined protocol, including mesoderm specification, haematopoiesis, erythropoiesis and maturation (see Chapter 2 Figure 2.1). The haematopoietic capacity of day 10 differentiating cells has been described in our previous study, this suggests multi-lineage HPCs are present within the population of cells at day 10 of the differentiation process [131].

A human ESC line that expressed a tamoxifen inducible KLF1 fusion protein (KLF1-ER^{T2}) was generated in Forrester's laboratory [130]. Experiments using this cell line demonstrated that activation of KLF1 at day 10 of the differentiation protocol (when HPCs have formed) increased the percentage of erythroid cells. In this case, the *KLF1-ER^{T2}* transgene had been randomly inserted into the genome but this strategy is not ideal because random integration can be subjected to silencing and experiments using randomly integrated transgenes are difficult to reproduce. In this study, I inserted the *KLF1-ER^{T2}* transgene into the *AAVS1* locus which has been reported as a safer position in human genome [132]. This strategy should result in a more consistent and reproducible expression.

3.2 Aim

1. To evaluate the production of haematopoietic cell lineages at different time points during the defined differentiation protocol
2. To generate iPSC lines expressing an inducible form of KLF1

3.3 Approaches

1. To identify the cell population and gene expression in different stages of erythroid differentiation, differentiating cells at defined time points were harvested and the production of different haematopoietic cell populations were monitored using flow cytometry and gene expression of key haematopoietic genes was determined by qRT-PCR.
2. To obtain consistent and reproducible expression of the KLF1-ER^{T2} fusion protein, the transgene was planned to insert into the *AAVS1* locus. The pZDonor-AAVS1-CAG-HA-KLF1-ER^{T2}-PA vector was constructed and introduced into the iPSCs genome by homologous recombination. The transgene *KLF1-ER^{T2}* had been confirmed the correct integration in the genome by PCR assay and Southern blot. The KLF1-ER^{T2} fusion protein was expressed in targeted clones which were verified by Western blot.

3.4 Result

3.4.1 A defined protocol for the production of erythroid cells from hiPSCs

3.4.1.1 Cell population during erythroid differentiation

The SFCi55 iPSC line that was derived from an individual with an O-RhesusD negative blood group was assessed in the defined differentiation protocol (see Chapter 2 Figure 2.1). Differentiating cells were harvested in time course and characterised by flow cytometry. The result demonstrated that most cells at day 3 expressed CD34, indicating that most cells at this point are associated with the haematopoietic and endothelial lineages (Figure 3.1A). $CD34^+$ / $CD43^+$ cells were detected between day 7 and day 10, however, this population may appear before day 7. The maximum proportion of these double positive cells were detected at day 10 (Figure 3.1A).

$CD43^+$ haematopoietic lineage cells were observed massively from day 7, and most of these cells also co-expressed the erythroid marker CD235a (Glycophorin A) from day 7 to 10 (Figure 3.1B). We then analysed the appearance of $CD235a^+$ cells during the time course (Figure 3.1C), which reached a peak at day 10 at 75 % then dropped and then increased gradually again from 40 % at day 17 to 50 % at day 24. These results also indicate that there are heterogeneous cell populations derived from this defined differentiation protocol.

The haematopoietic capacity of day 10 differentiating cells was also confirmed in methylcellulose medium with recombinant cytokines (MethoCult), and they were able to form colony-forming unit-macrophages (CFU-M), colony-forming unit-granulocyte/macrophage (CFU-GM), colony-forming unit-mixed (CFU-Mix) and burst-forming unit-erythroid (BFU-E) (Figure 3.1D). The data suggest the cell population at day 10 of the differentiation protocol contained multi-lineage haematopoietic progenitor cells (HPCs).

The data suggest that there are heterogeneous cell populations derived from this defined differentiation protocol, and the cell population at day 10 of the differentiation protocol contained the maximum number of multi-lineage HPCs.

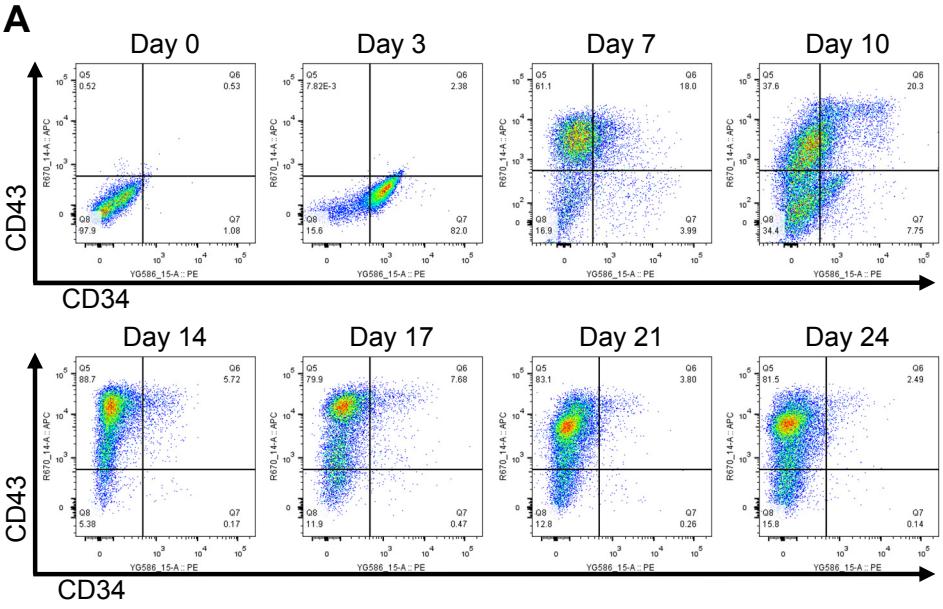
A
Day 0
Day 3
Day 7
Day 10
Day 14
Day 17
Day 21
Day 24
CD43
CD34

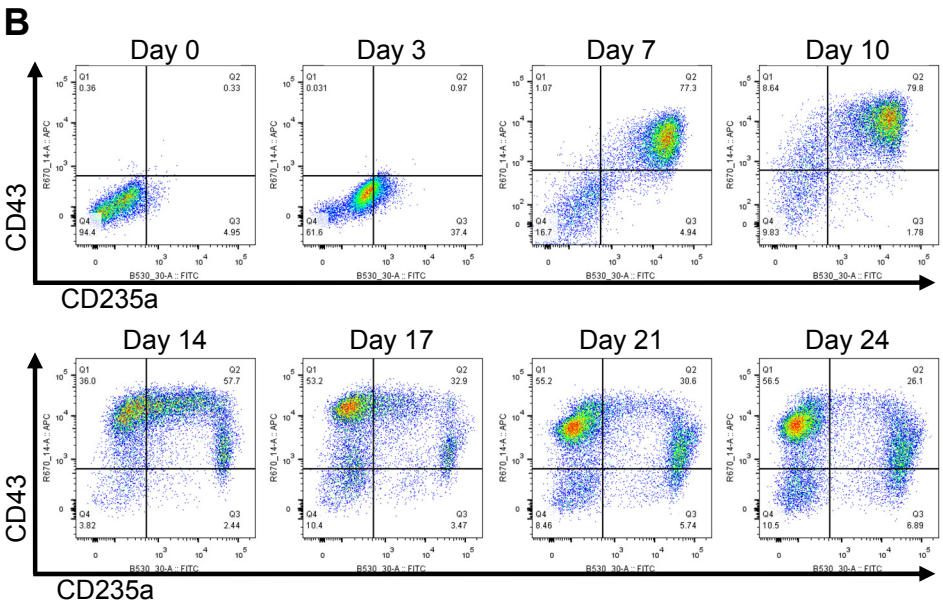
B
Day 0
Day 3
Day 7
Day 10
Day 14
Day 17
Day 21
Day 24
CD43
CD235a

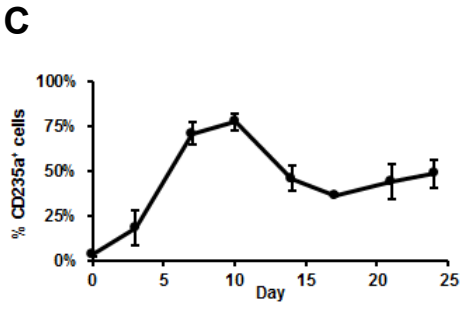
C
% CD235a+ cells
100%
75%
50%
25%
0%
0
5
10
15
20
25
Day

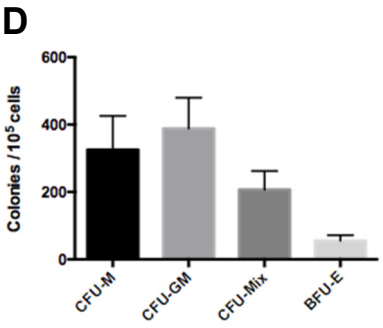
D
Colonies / 10^5 cells
600
400
200
0
CFU-M
CFU-GM
CFU-Mix
BFU-E

Figure 3.1 Identification of cell populations during erythroid differentiation

A, B. $CD34^+$ / $CD43^+$ (A) and $CD235a^+$ / $CD43^+$ cell population (B) were monitored during the time course of differentiation. Day 0, 3, 7, 10, 14, 17, 21 and 24 differentiating cells were analysed by flow cytometry using anti-CD34, anti-CD43 and anti-CD235a antibodies. **C.** The mean percentage of $CD235a^+$ cells from three independent experiments presented at different time points during the differentiation process. Error bars represent standard error of the mean (SEM). **D.** The haematopoietic potential of day 10 differentiating cell was evaluated in colonies forming assay. A CFU-GM colony contains granulocytes and macrophages. A CFU-Mix colony contains granulocytes, macrophages, erythrocytes and megakaryocytes. A CFU-M colony contains only macrophages. A BFU-E colony contains erythrocytes with high proliferation capacity. Data represent 3 independent experiments. Error bars represent standard error of the mean (SEM).

3.4.1.2 Gene expression during erythroid differentiation

RNA isolated from iPSC-derived cells at different time course were analysed by qRT-PCR (Figure 3.2). The key erythroid genes, *KLF1*, was upregulated from day 7 to 24 during erythroid differentiation, however, *KLF1* failed to activate *BCL11A* in this differentiation protocol. This was apparently in contrast to previous reports in other cell lines that showed KLF1 could directly target the promoter of BCL11A and regulate expression [120], [121]. cMYB was reported as a marker of the definitive erythrocyte lineage [39], but the expression of *cMYB* in the differentiation protocol was relatively low reaching a peak at day 10, suggesting that there might be a small population of cell of the definitive wave at this point. GATA1 plays a crucial role in the development of megakaryocytic and erythroid lineages [133], the expression reached a peak at day 17. SOX6 stimulates erythroid cell survival, proliferation, and terminal maturation during definitive murine erythropoiesis [36], the expression of *SOX6* was observed a small peak at day 5, then increased significantly from day 17 to 24. GFI1 and GFI1B are involved in the haematopoietic commitment when these two TFs control the loss of endothelial identity from the hemogenic endothelium [45]. We observed that GFI1 reached peaks at day 5 and day 17, and GFI1B hit the highest expression at day 17.

The data indicate that this defined protocol promotes the expression of TFs associated with haematopoiesis and erythropoiesis during the differentiation.

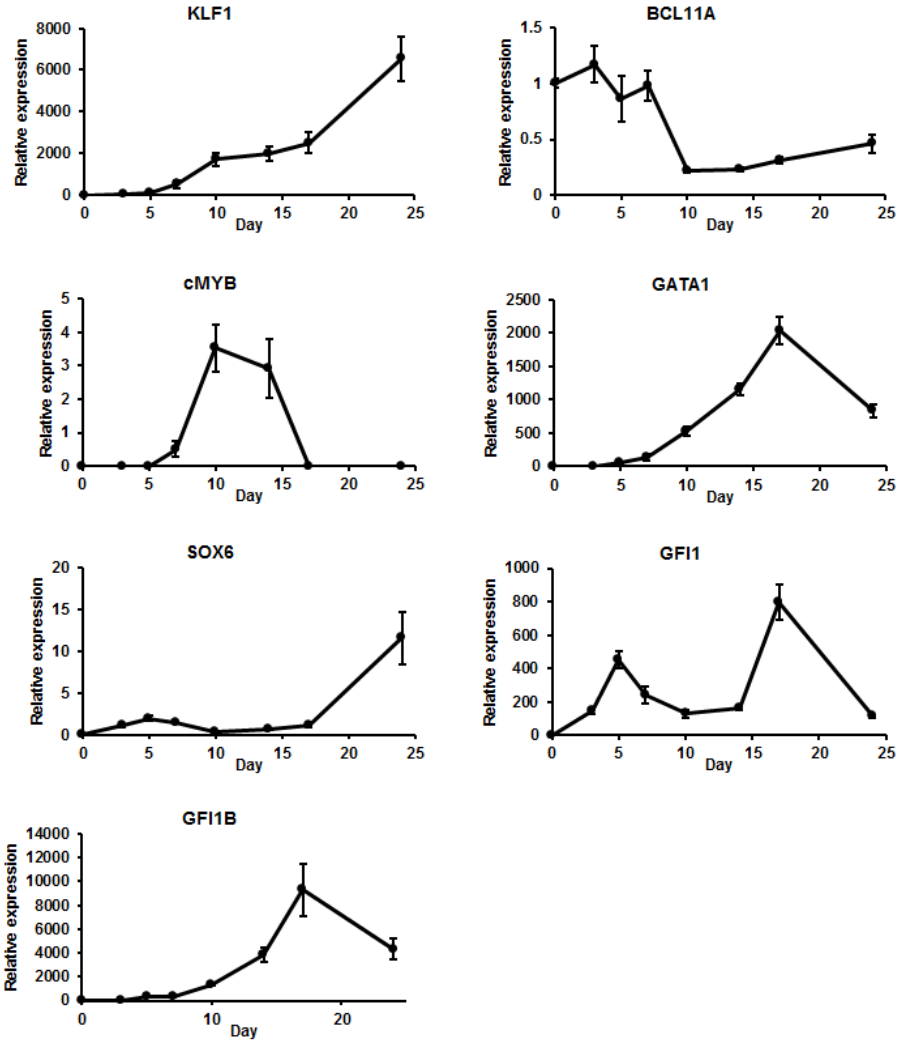

Figure 3.2 Gene expression during erythroid differentiation

Erythroid related genes were evaluated by qRT-PCR in time course. cDNA samples were prepared from day 0, 3, 7, 10, 14, 17, 21 and 24 differentiating cells, and the expression of *KLF1*, *BCL11A*, *cMYB*, *GATA1*, *SOX6*, *GFI1* and *GFI1B* were investigated by specific primers in real time PCR machine. Data represent 3 independent experiments. Error bars represent standard error of the mean (SEM).

3.4.1.3 The phenotype of iPSC-derived cells

It has been reported that hPSC-derived erythroid cells are more fragile than the erythroid cells generated from adult $CD34^+$ progenitors [79]. We therefore assessed the phenotype of the iPSC-derived cells from the defined protocol by cytospin and rapid Romanowsky staining (Figure 3.3A). A lot of debris and many cells with damaged membranes were observed on the slide (shown as blue arrows), this showed the membrane stability was poor at the late stage of erythroid differentiation. We also noted that it was difficult to find enucleated cells (shown as a red arrow), and this supported previous findings that the efficiency of enucleation was low in this defined differentiation protocol.

RNA isolated from iPSC-derived cells at different time course were also analysed by qRT-PCR (Figure 3.3B). The expressions of *HBE1* (ε1-haemoglobin) and *HBB* (β-haemoglobin) were upregulated from day 10 and day 24, respectively, however, the expression level of *HBB* was relatively lower than *HBE1*. This suggested iPSC-derived cells contained more primitive erythroid cells than definitive erythroid cells.

Taken together these data indicate there are several limitations of current differentiation protocol for hPSCs, including poor membrane stability, lower enucleation rate and enriched primitive erythroid cells.

We assessed the expression of KLF1 by Western blot and demonstrated that day 10 differentiating cell expressed a lower level of expression of KLF1 compared to $CD34^+$-derived cells (Figure 3.3C). We hypothesised that this could be one of the reasons why RBCs generated from PSCs are the lack of membrane stability and maturity *in vitro*. In this chapter, an inducible KLF1-ER^{T2} system was constructed in iPSCs, and KLF1-activated cells were evaluated in the same erythroid differentiation protocol.

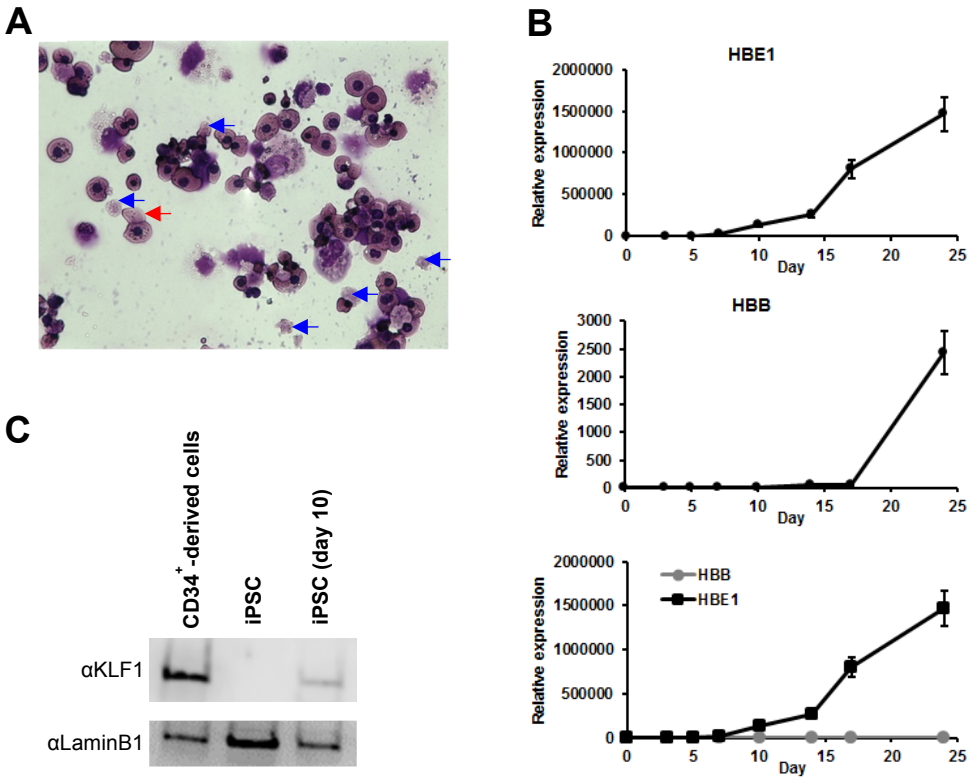

Figure 3.3 The phenotype of iPSC-derived cells from the defined differentiation protocol

A. Cytospins of differentiating cells at day 31 showed the phenotype of iPSC-derived cells (x40). The membrane-damaged cells were indicated by blue arrows, and an enucleated cell was indicated by a red arrow. **B.** Globin genes were evaluated by qRT-PCR in time course. cDNA samples were prepared from day 0, 3, 7, 10, 14, 17, 21 and 24 differentiating cells, and the expression of *HBE1* and *HBB* were investigated by specific primers in real time PCR machine. Data represent 3 independent experiments. Error bars represent standard error of the mean (SEM). **C.** Western blot analyses of nuclear cell lysates from adult $CD34^{+}$-derived cells, control undifferentiated iPSCs and iPSC-derived cells at day 10. Endogenous KLF1 was detected with the anti-KLF1 antibody (αKLF1), and the anti-Lamin B1 (αLaminB1) antibody was used to detect nuclear proteins as a loading control.

3.4.2 Generation of a tamoxifen-inducible KLF1 system in hiPSC

We hypothesised that the lower level expression of KLF1 could result in the morphological fragility and poor maturity of erythrocytes generated from PSCs *in vitro*. Rui Ma showed that activation of KLF1 at day 10 of the differentiation protocol increased the proportion of erythrocytes, but she did not study the effect on RBC maturation in detail [130]. Variability between experiments made it difficult to draw conclusions on the effect of KLF1 on RBC maturation, because one possible reason for variability is that randomly integrated *KLF1-ER^{T}* transgenes might be silenced and unstable. To obtain the stable expression of tamoxifen-inducible KLF1 in iPSCs, we chose to insert our gene construct into *AAVS1* locus rather than random integration [132]. The pZDonor-AAVS1-puromycin vector was used as the back bone vector and the CAG promoter was used to drive expression of the transgene, because it is a strong synthetic promoter frequently used to drive high levels of gene expression in mammalian cells, including ESCs [134].

3.4.2.1 Tamoxifen inducible KLF1 in COS7 cells

Construction of pZDonor-AAVS1-Puromycin-CAG-HA-KLF1-ER^{T2}-PA and pZDonor-AAVS1-Puromycin-CAG-HA-Mut KLF1-ER^{T2}-PA was described in Chapter 2 (see Chapter 2 Section 2.2.1.1). In order to confirm that the constructs are capable of producing the appropriate fusion protein in mammalian cells, the plasmids (pCAG GFP, pZDonor-AAVS1-CAG-HA-KLF1-ER^{T2}-PA and pZDonor-AAVS1-CAG-HA-Mut-KLF1-ER^{T2}-PA) were transfected into COS7 cells (a fibroblast cell line derived from monkey kidney tissue) by Xfect reagent, respectively. The efficiency of transfection was greater than 90 % as measured in pCAG-GFP-transfected cell one day post transfection (Figure 3.4A). Three days post transfection, cell lysates were analysed by Western blot using anti-HA tag, anti-KLF1 and anti-GAPDH antibodies. The predicted sized fusion proteins were detected as 74 KDa consisting of the HA tag (1KDa), KLF1 (38KDa) and ER^{T2} (35Kda) (Figure 3.4B), and some other smaller bands might be degradation products.

To confirm that the ER^{T2} fusion proteins could translocate to the nucleus upon tamoxifen induction, transfected cells treated with or without tamoxifen for one day

were evaluated by Immunofluorescence (IF) staining with the anti-HA antibody. HA-KLF1-ER^{T2} and HA-Mut-KLF1-ER^{T2} were detected in the cytoplasm in the absence of tamoxifen and these fusion proteins were detected in the nuclei (DAPI-positive) when 200 nM of tamoxifen was added (Figure 3.4C). Comparable results were observed using anti-KLF1 antibody in IF staining (Figure 3.4D). It was interesting to note that some HA-Mut-KLF1-ER^{T2} was observed in the cytoplasm in the presence of tamoxifen. This is possible because Mut-KLF1 cannot bind to DNA and thus might not be retained in the nucleus. This result suggests that KLF1, but not Mut-KLF1 functions normally in the cells.

To summarise, COS7 cells are able to express fusion proteins HA-KLF1-ER^{T2} and HA-Mut-KLF1-ER^{T2} at a detectable level using anti-HA tag and anti-KLF1 antibodies. Also, IF staining data suggest that HA-KLF1-ER^{T2} and HA-Mut-KLF1-ER^{T2} fusion proteins can translocate into the nuclei upon tamoxifen induction.

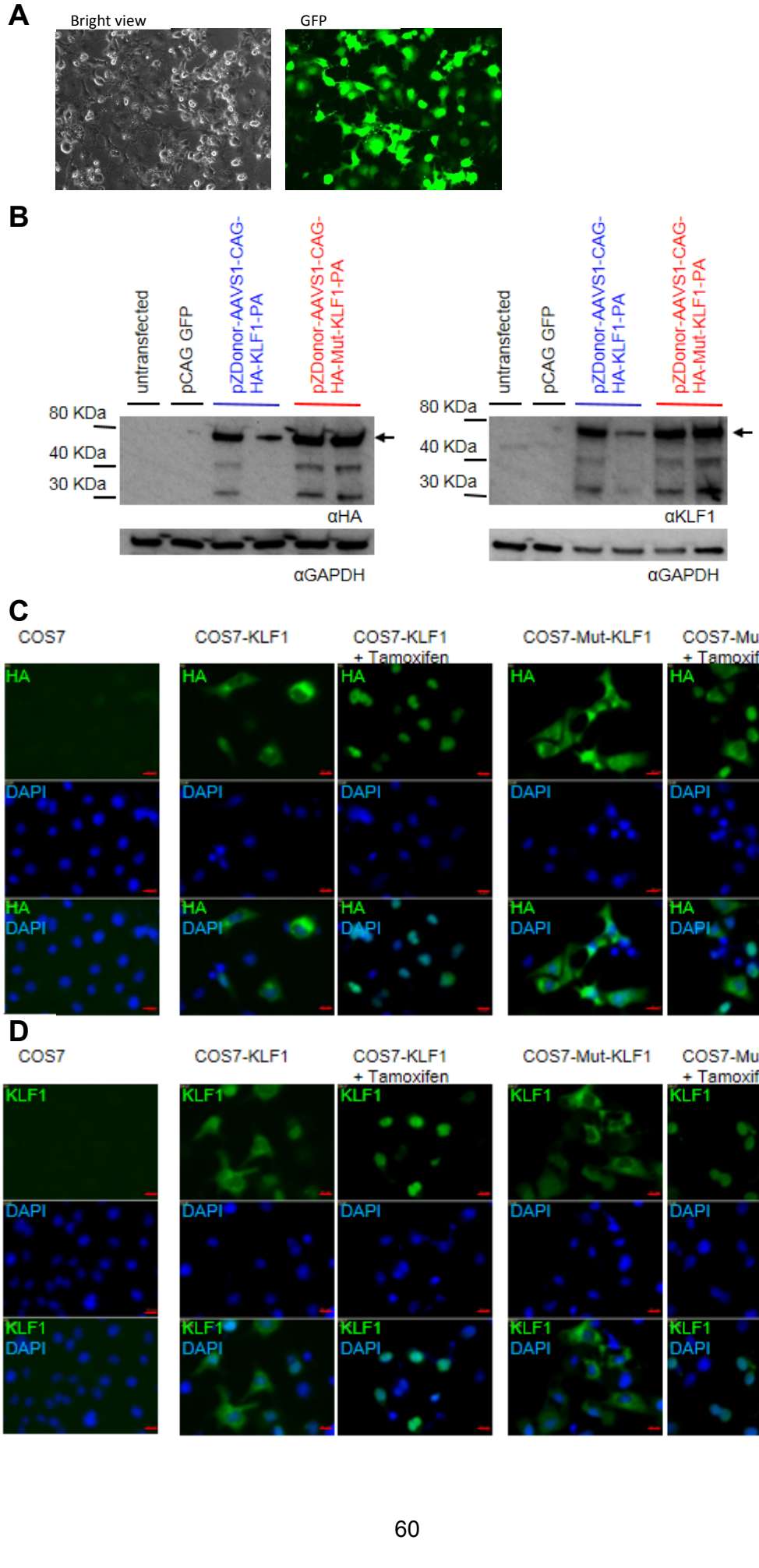
A
Bright view
GFP
B
untransfected
pCAG GFP
pZDonor-AAVS1-CAG-HA-KLF1-PA
pZDonor-AAVS1-CAG-HA-Mut-KLF1-PA
80 KDa
40 KDa
30 KDa
αHA
αGAPDH
αKLF1
C
COS7
COS7-KLF1
COS7-KLF1 + Tamoxifen
COS7-Mut-KLF1
COS7-Mut-KLF1 + Tamoxifen
HA
DAPI
D
KLF1

Figure 3.4 The nuclear translocation of tamoxifen inducible KLF1 in COS7 cells

A. Transfection efficiency in COS7 cells demonstrated by transfection with a pCAG GFP vector and observed one day post transfection. Bright field (left) and green channel (right) (x20). **B.** Fusion protein was detected by Western blot. The COS7 cells were transfected with constructs (pCAG GFP, pZDonor-AAVS1-CAG-HA-KLF1-ER^{T2}-PA and pZDonor-AAVS1-CAG-HA-Mut-KLF1-ER^{T2}-PA) and were harvested Three days post transfection. Western blot analysis was conducted to detect fusion proteins HA-KLF1-ER^{T2} and HA-Mut-KLF1-ER^{T2} using anti-HA tag (αHA), anti-KLF1 (αKLF1) and anti-GAPDH (αGAPDH) antibodies. The predicted protein size is approximately 74KDa (arrow). **C.** Nuclear localisation of fusion protein was observed by IF staining. COS7 cells were transfected with constructs (pZDonor-AAVS1-CAG-HA-KLF1-ER^{T2}-PA and pZDonor-AAVS1-CAG-HA-Mut-KLF1-ER^{T2}-PA) and subcellular localisation was evaluated by using an anti-HA tag antibody and DAPI nuclei dye. **D.** Subcellular localisation was also evaluated by using an anti-KLF1 antibody and DAPI nuclei dye. Scale bar = 10 μm.

3.4.2.2 Tamoxifen inducible KLF1 in K562 cells

To further validate these constructs, we tested them in K562 (a human chronic myelogenous leukaemia cell line) to assess whether they are able to activate any of the known KLF1 target genes. K562 cells were transfected with pCAG GFP by Xfect reagent, but the transfection efficiency of this cell line was relatively low (Figure 3.5A), so we decided to generate stable cell lines. 2 μg/ml puromycin was used to select K562 cells after transfecting with pZDonor-AAVS1-CAG-HA-KLF1-ER^{T2}-PA or pZDonor-AAVS1-CAG-HA-Mut-KLF1-ER^{T2}-PA. After two weeks of selection, untransfected K562 cells died in the puromycin selection, whereas transfected cultures contained viable cells. To confirm the function of KLF1 in selected K562 cells, the cells with inducible KLF1 or inducible Mut-KLF1 were cultured in the presence and absence of tamoxifen for three days. The expression of KLF1 targets, *AHSP* (Alpha haemoglobin stabilising protein) and *HBB* (β-haemoglobin) were analysed by qRT-PCR. Activation of KLF1, but not Mut-KLF1 upregulated *AHSP* and *HBB* expression by two and seven folds, respectively. (Figure 3.5B).

Taken together, the data demonstrate that the pZDonor-AAVS1-CAG-HA-KLF1-ER^{T2}-PA is capable of producing functional HA tagged KLF1-ER^{T2} that can activate target genes in K562 cells. We noted that the level of target gene induction observed was not as high as that seen by Rui Ma which could indicate that the HA tag affects the activity of KLF1.

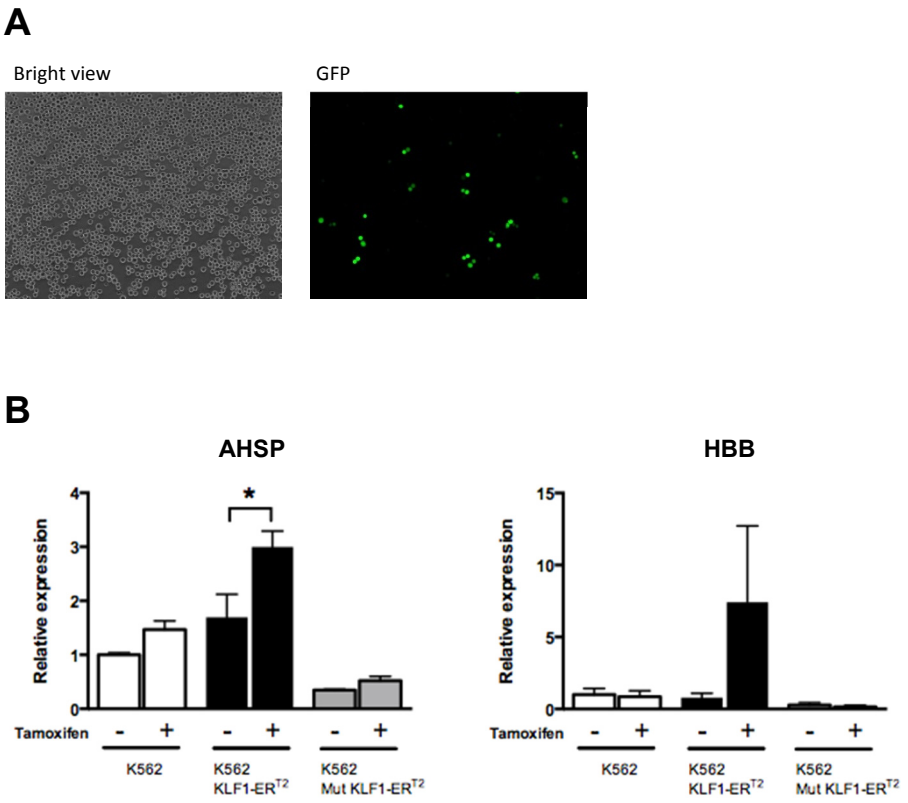

Figure 3.5 The activation of target genes by tamoxifen inducible KLF1 in K562 cells

A. Transfection efficiency in K562 cells. To assess the efficiency of transfection, K562 cells were transfected by pCAG GFP and observed one day post transfection. Bright field (left) and green channel (right) (x20). **B.** Quantitative RT-PCR analyses of RNA isolated from untransfected control cells (K562), K562 cells transfected with pZDonor-AAVS1-CAG-HA-KLF1-ER^{T2}-PA (K562 KLF1-ER^{T2}) and K562 cells transfected with or pZDonor-AAVS1-CAG-HA-Mut-KLF1-ER^{T2}-PA (K562 Mut KLF1-ER^{T2}) in the absence (-) and presence (+) of tamoxifen for 3 days using primers to *AHSP* and *HBB*. Data represent the mean of 3 independent experiments and error bars show standard error of the mean (SEM**)**. A student T test was used to assess the effect of KLF1 activation in K562 cells (*, $p<0.05$).

3.4.2.3 Tamoxifen inducible KLF1 targeted in the *AAVS1* of hiPSCs

Human iPSCs were transfected with pZDonor-AAVS1-CAG-HA-KLF1-ER^{T2}-PA, p622L and p622R (plasmids which express zinc finger nucleases - ZFNs) by electroporation, and cells were selected in puromycin for 2 weeks. 29 colonies were selected and expanded in 6 well plates. We designed internal and external primers to detect targeting events in the *AAVS1* locus of genomic DNA by PCR analysis. These primers are able to generate specific PCR products when the KLF1 construct was targeted into the expected site in the genome (Figure 3.6A). On the other hand, there would be a non-targeted PCR product if there is no integration in *AAVS1* locus (Figure 3.6B). 13 clones had an integration into both *AAVS1* alleles (ie homozygous targeted), for example, iKLF1.1 and iKLF1.2 cell lines with targeted PCR products. 14 selected clones had an integration into one of the *AAVS1* alleles (ie heterozygous targeted) as demonstrated by the fact that both targeted and non-targeted PCR products were detected, for example, iKLF1.19 and iKLF1.25 cell lines. In 2 selected cell lines, iKLF1.4 and iKLF1.27, no targeting events were detected and twice as much non-targeted PCR products were observed. In this experiment, the targeting efficiency was 93%.

The targeting results were also confirmed by Southern blot (Supplementary Figure S1). We designed the internal probe targeting the regions in the AAVS1-left arm of pZDonor AAVS1 puromycin vector. The genomic DNA was digested by SphI and detected using DIG-labelled internal probes. An expected band 6.4 Kb was observed in parental iPSCs, on the other hand, an expected band 3.9 Kb was detected in iKLF1.1 and iKLF1.2 (Supplementary Figure S1A and B). On the other hand, the external probe was designed to target the regions in the endogenous *AAVS1* locus. A band 6.4 Kb was observed in parental iPSCs, and an expected band 7.7 Kb was detected in iKLF1.2 (Supplementary Figure S1C and D). Although iKLF1.1 give rise an expected band 7.7 Kb, we also noted a band approximately 4 Kb in the result indicating that the iKLF1.1 cell line also contained a random integration (Supplementary Figure S1C and D).

The PCR data indicate that iKLF1.1 / iKLF1.2 cell lines (homozygous targeted) and iKLF1.19 / iKLF1.25 cell lines (heterozygous targeted) are correctly integrated with *KLF1-ER^{T2}* in the *AAVS1* locus, however, Southern blot data suggest the iKLF1.2 cell line is correct clone without random integration.

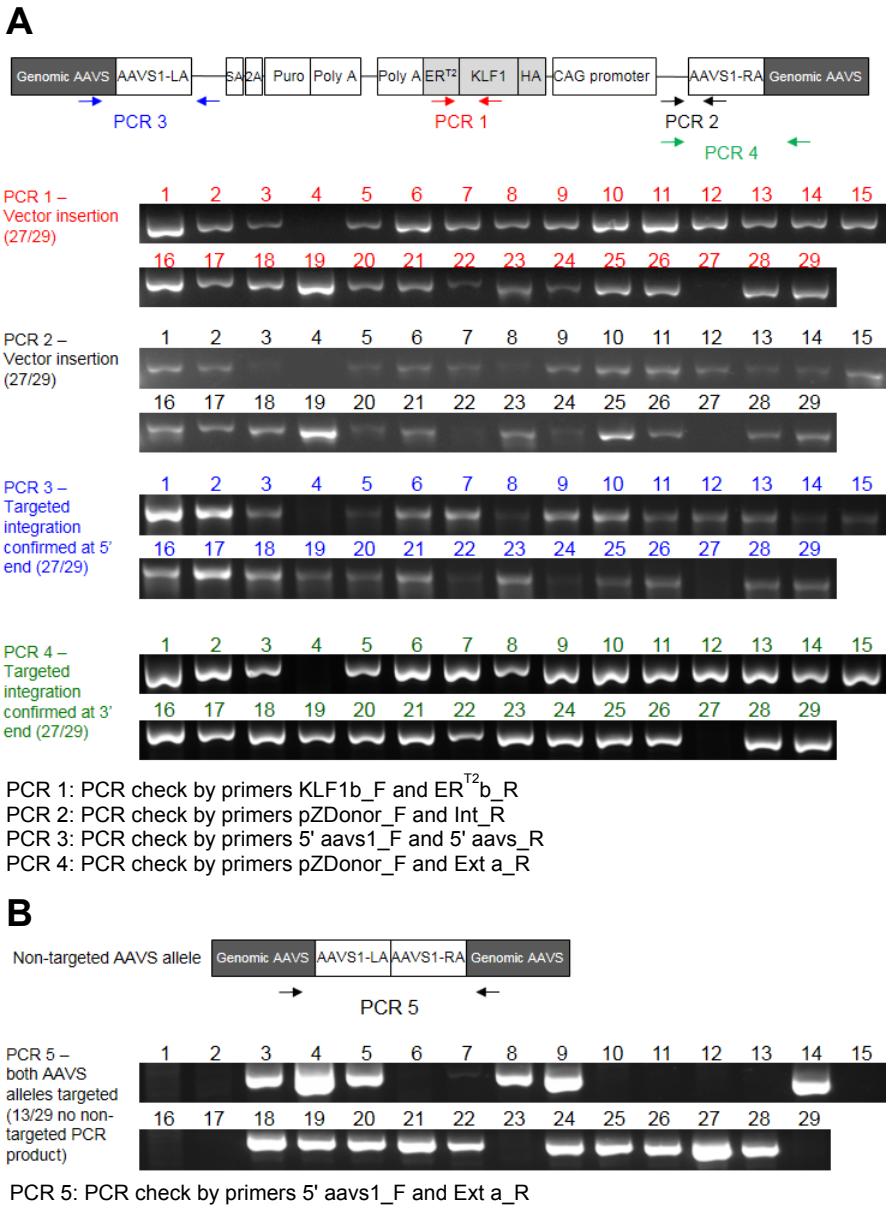

Figure 3.6 Tamoxifen inducible KLF1 targeted in the *AAVS1* locus of hiPSCs

A. Schematic of genomic structure of targeted *AAVS1* alleles showing the locations of diagnostic internal and external PCR assays. PCR product 1 and 2 were generated by internal primers, and PCR product 3 and 4 were generated by external primers. **B.** The non-targeted *AAVS1* allele was able to be detected by external primers. (AAVS1-LA, AAVS1 left homology arm; SA, splice acceptor; 2A, a self-cleaving peptide sequence; Puro, puromycin resistance gene; Poly A, polyadenylation sequence; AAVS1-RA, AAVS1 right homology arm.)

3.4.2.4 Comparison of iKLF1 cell lines

Cell lysates of iKLF1.1, iKLF1.2, iKLF1.19 and iKLF1.25 cell lines were collected for Western blot to analyse whether the fusion protein HA-KLF1-ER^{T2} was expressed in cells. The result showed that iKLF1.1 / iKLF1.2 / iKLF1.25 expressed the expected proteins (approximately 74KDa) (Figure 3.7A).

Erythroid differentiation of these 4 cell lines was initially assessed in the presence and absence of tamoxifen from day 10, and the proportion of CD235a^{+}/CD71^{+} erythroblasts were assessed by flow cytometry at day 15 (Figure 3.7B). Upon activation of KLF1 in iKLF1.1 / iKLF1.2 and iKLF1.25, the percentage of erythroid lineage cells increased and this increase was not observed in control iPSCs that did not harbour the *KLF1-ER^{T2}* transgene. In the case of the iKLF1.19 cell line, although the KLF1 construct was targeted to *AAVS1* locus (as assessed by PCR analysis of genomic DNA), these cells did not express detectable levels of the HA-KLF1-ER^{T2} fusion protein (Figure 3.7A) and the percentage of erythroid lineage cells did not increase when tamoxifen was added (Figure 3.7B). However, due to time constrains and the expense of cytokines in the differentiation medium, this experiment was performed only once and would have to be repeated before we can conclusively state that that this cell line is non-responsive to tamoxifen due to the low level of expression of the fusion protein.

We compared the levels of expression of the fusion protein and the effects of KLF1 activation on the production of erythroblasts in the three different iKLF1 cell lines (Figure 3.7A, B). The iKLF1.2 cell line was chosen for all our subsequent experiments because it demonstrated a stable fusion protein expression and the highest proportion of erythroblast production upon activation (Figure 3.7B).

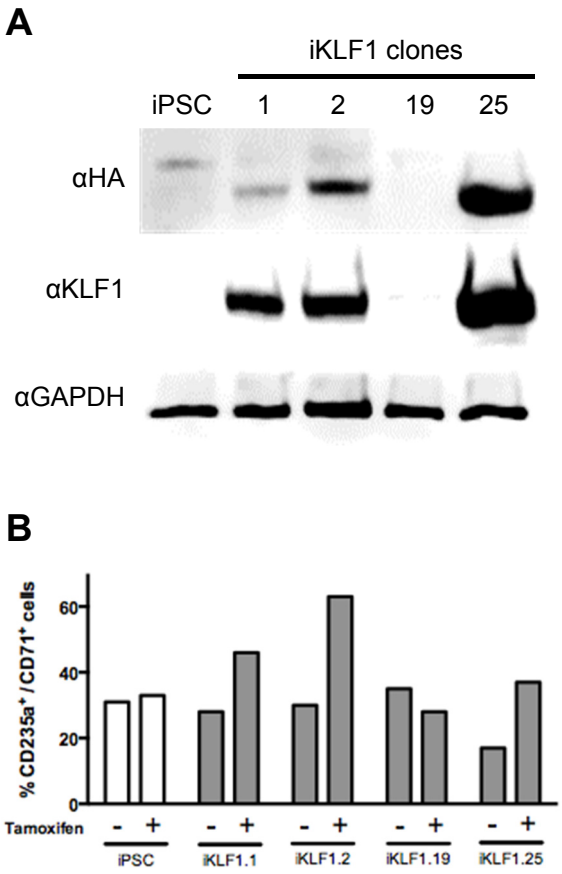

Figure 3.7 KLF1-ER^{T2} fusion protein is expressed in iKLF1 cell lines and KLF1 activation increases the erythroid lineage

A. Western blot analyses of cell lysates from control iPSCs, two homozygous targeted cell lines (iKLF1.1 and iKLF1.2) and two heterozygous targeted cell lines (iKLF1.19 and iKLF1.25) using anti-HA (αHA), anti-KLF1 (αKLF1) and anti-GAPDH (αGAPDH) antibodies. The predicted protein size is approximately 74KDa (1KDa of HA tag plus 38KDa of KLF1 plus 35KDa of ER^{T2}). **B.** Comparison of erythroid differentiation capacity among parental iPSCs and four iKLF1 cell lines. Control iPSCs, iKLF1.1, iKLF1.2, iKLF1.19 and iKLF1.25 were differentiated in the defined protocol in the presence (+) and absence (-) of tamoxifen from day 10 to day 15. Differentiating cells at day 15 were analysed by flow cytometry using antibodies against CD235a and CD71 to mark erythroblasts.

3.4.2.5 The expression of KLF1 and KLF1-ER^{T2} in iKLF1.2 cell line

We compared the expression of *KLF1* in adult CD34^{+}-derived cells, undifferentiated iPSC, iPSC-derived cells, undifferentiated iKLF1.2 and iKLF1.2-derived cells by qRT-PCR (Figure 3.8A). The result showed there was no *KLF1* transcript in undifferentiated iPSCs, and lower expression of *KLF1* in iPSC-derived cells while comparing with adult CD34^{+}-derived cells. Of note, the level expression of *KLF1* in iKLF1.2-derived cells was comparable to the level of expression in adult CD34^{+}-derived cells. Meanwhile, we confirmed that *ER^{T2}* transcript was only expressed in undifferentiated iKLF1.2 and iKLF1.2-derived cells (Figure 3.8B).

We also confirmed the endogenous KLF1 proteins and KLF1-ER^{T2} fusion proteins in nuclear extracts isolated from adult CD34^{+}-derived cells, undifferentiated iPSC, iPSC-derived cells, undifferentiated iKLF1.2 and iKLF1.2-derived cells following treatment with or without tamoxifen (Figure 3.8C). The expression of endogenous KLF1 proteins in iPSC-derived cells and iKLF1.2-derived cells were lower than in adult CD34^{+}-derived cells which were consistent with the level of *KLF1* transcript. Most importantly, an addition of tamoxifen resulted in the translocation of KLF1-ER^{T2} protein into the nucleus, and KLF1-ER^{T2} protein in iKLF1.2-derived cells in the presence of tamoxifen is comparable to the endogenous KLF1 protein in adult CD34^{+}-derived cells. Although we noted a low level of KLF1-ER^{T2} fusion protein in the crude nuclear extracts in undifferentiated iKLF1.2 and iKLF1.2-derived cells in the absence of tamoxifen, we were uncertain whether this is due to cytoplasmic contamination (GAPDH antibodies was used as a cytoplasmic loading control) or leakiness of the ER^{T2} system.

The data suggest that the physiological level of KLF1-ER^{T2} protein is expressed in iKLF1.2-derived cells in the presence of tamoxifen, therefore, iKLF1.2 was chosen to further evaluate erythropoiesis.

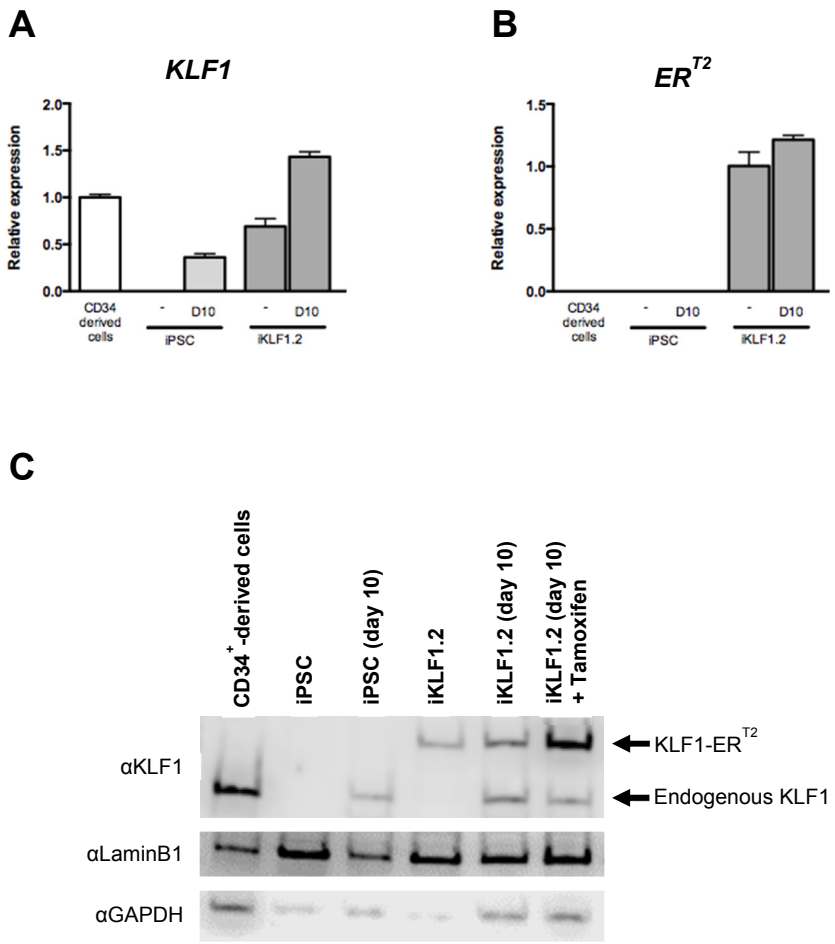

Figure 3.8 iKLF1.2-derived cells express physiological level of KLF1-ER^{T2}

A, B. Quantitative RT-PCR analyses of cells (adult CD34^{+}-derived cells that had been differentiated for 6 days into erythroid progenitors, control undifferentiated iPSCs and iPSC-derived cells at day 10, undifferentiated iKLF1.2 and iKLF1.2-derived cells at day 10) were carried out with primers to *KLF1* (A) that amplifies both endogenous *KLF1* and exogenous *KLF1-ER^{T2}*, and primers to *ER^{T2}* (B) that amplify only the exogenous transgene *KLF1-ER^{T2}*. **C.** Western blot analyses of nuclear cell lysates from above cell samples and iKLF1.2 differentiating cells with tamoxifen for 3 hours (+Tamoxifen). Endogenous KLF1 and the expected larger sized KLF1-ER^{T2} fusion protein were detected with the anti-KLF1 antibody (αKLF1). The anti-Lamin B1 (αLaminB1) and anti-GAPDH (αGAPDH) antibodies were used as a nuclear loading control and a cytoplasmic loading control, respectively.

3.5 Conclusion

1) The defined differentiation protocol was capable of generating multipotent HPCs and erythroid cells from iPSCs, and erythroid genes were detectable during the differentiation. We also noted that poor membrane stability, lower enucleation rate and enriched primitive erythroid cells were observed in the defined differentiation protocol, and these limitations might result from lower level expression of KLF1 in the iPSC-derived cells comparing to $CD34^{+}$-derived cells.
2) A tamoxifen inducible *KLF1-ER^{T2}* transgene was constructed in the pZDonor-AAVS1 puromycin vector. Nuclear translocation and functional activation of the fusion protein was confirmed in COS7 cells and K562 cells. iKLF1 iPSC lines were then generated by targeting the *KLF1-ER^{T2}* transgene to the *AAVS1* locus. The cell line iKLF1.2 was confirmed as a correct targeted cell line that expressed a physiological level of the KLF1-ER^{T2} fusion protein.

3.6 Discussion

3.6.1 Limitations of defined erythroid differentiation protocol

We evaluated the defined differentiation protocol developed by Olivier et al [79], and the haematopoietic capacity of day 10 differentiating cells has been confirmed in this chapter and in our previous study [131], this suggests multi-lineage HPCs are present within the population of cells at day 10 of the differentiation process. Our results also indicated that the iPSC could be differentiated into erythroid lineage cells, however, this differentiation protocol generated heterogeneous haematopoietic cells.

Erythroid cells generated from hPSCs have a poor membrane stability [79], [86], [96] lower enucleation rate [67], [76], [86] and express embryonic and foetal rather than adult globin [76], [85], [96], [135]. Similarly, our results showed many cells with damaged membranes and debris were observed during erythroid differentiation, this indicates a fragile morphology at the later stage of erythroid differentiation. Meanwhile, we observed a poor enucleation efficiency and high level expression of embryonic globin. Our result also showed that less KLF1 proteins were detected in iPSC-derived erythrocytes than in adult $CD34^+$-derived erythrocytes which we hypothesized could be one of the reasons for the phenotype observed.

3.6.2 Primitive? Definitive? Two waves?

We assessed the expression of genes associated with definitive erythropoiesis during the differentiation, including *cMYB* [39] and *SOX6* [36]. The result showed that a stable increase of *SOX6* and the transient expression of *cMYB* during the differentiation, which hints that definitive erythropoiesis occurs in this defined differentiation protocol. Globin genes, *HBB* and *HBE1,* were expressed in iPSC-derived erythrocytes, this also indicates both primitive and definitive erythropoiesis occur in the defined differentiation protocol. However, the transcripts of *HBB* was significantly lower than *HBE1*, likely due to the fact that this defined differentiation protocol favours the production of primitive erythroid cells. Alternatively, the lower expression of KLF1 was detected in iPSC-derived cell while comparing with $CD34^+$-derived cells, and the level expression of KLF1 might be too low to trigger BCL11A activation, thereby not completing globin switching to adult globin [120], [121].

GFI1B has been reported to be highly expressed in megakaryocyte-erythroid progenitors (MEPs) and controls erythroid differentiation [136]–[138]. We noted that the expression of *GFI1* peaked at day 5 and day 17, which indicated there were erythroid progenitors appearing at these two time points. Additionally, the percentage of $CD235a^+$ cell population was evaluated by flow cytometry during erythroid differentiation. The result showed that there were two upward trends from day 3 to 10 and from day 17 to 24, which also indicates there might be two separate waves of erythropoiesis. Collectively, qRT-PCR and flow cytometry results support the idea that there are two waves of erythropoiesis in our differentiation protocol, and the first window from day 3 to day 10 potentially being primitive erythropoiesis, and the second window from day 17 to 24 being the definitive EMP like erythropoiesis.

3.6.3 The KLF1-ER^{T2} system in hiPSC (iKLF1 cell lines)

Trakarnsanga et al reported that the expression of *KLF1* and *BCL11A* is required above a threshold level to induce adult globin expression [139]. We further evaluated the expression of endogenous *KLF1* and transgene *KLF1-ER^{T2}* in the iKLF1.2 cell line. Western blot showed the expression level of KLF1-ER^{T2} in differentiating iKLF1.2 is comparable to the expression level of endogenous KLF1 in the adult $CD34^+$-derived cells, and this indicated that physiological levels of KLF1 are achieved using this strategy.

Additionally, we noted that a low level of KLF1-ER^{T2} fusion protein in the crude nuclear extracts in undifferentiated iKLF1.2 and iKLF1.2-derived cells in the absence of tamoxifen, this might be due to cytoplasmic contamination. Although we had a cytoplasmic loading control (GAPDH) to show the possibility of cytoplasmic contamination, some studies have indicated GAPDH might appear in nucleus because of being associated with apoptosis, oxidative stress [140] and some cases, such as histone biosynthesis, the maintenance of DNA integrity and receptor mediated cell signalling [141]. Furthermore, a recent study has revealed the leakiness of ER^{T2} system in bone marrow cells [142]. We were uncertain whether leakiness of the ER^{T2} system occurs in the iKLF1.2 cell line. However, it would be difficult to quantify how much amount of ER^{T2} fusion proteins leaks into nuclei without tamoxifen induction.

Chapter 4
Evaluation of KLF1 activation during erythroid differentiation

4.1 Introduction

Due to the fact that human PSCs-derived erythroid cells have a poor membrane stability [79], [86], [96] lower enucleation rate [67], [76], [86] and express embryonic and foetal rather than adult globin [76], [85], [96], [135]. To ameliorate these issues, we considered optimising the erythroid differentiation by enhancing a key erythroid gene. We noticed that less KLF1 proteins were detected in iPSC-derived erythrocytes than in adult $CD34^+$-derived erythrocytes, this might lead to above limitations (see Chapter 3 Section 3.6.1). KLF1 is essential in definitive erythropoiesis, since *Klf1*-deficient embryos die of anaemia during foetal liver erythropoiesis [23], [33], [108]. KLF1 plays an important role in the maturation of RBC, in part of regulating cytoskeleton and maintaining the membrane stability [26], [27]. KLF1 also regulates erythroblasts in different aspects, such as enhancing erythroid differentiation coupled with reduced proliferation [143], [144], and regulating globin genes directly [22], [25], [28], [29], and indirectly [120], [121]. We hypothesised that KLF1 activation during erythroid differentiation promotes the production of mature erythrocytes.

4.2 Aim

To evaluate the effects of activating KLF1 on the production of erythroid cells from iPSCs

4.3 Approaches

1. To evaluate the effect of KLF1 activation in progenitor cells, erythroid cells were derived from iKLF1.2 cell line in the presence and absence of tamoxifen from day 10. The production and maturation of erythroid cells was assessed by microscopy, flow cytometry, qRT-PCR and HPLC.
2. To assess the effect of KLF1 activation in the late stage of erythroid cells, cells were derived from iKLF1.2 cell line in the presence and absence of tamoxifen from day 18. The production and maturation of erythroid cells was assessed by microscopy, flow cytometry, qRT-PCR and HPLC.

4.4 Result

All the data in this chapter was generated using one iPSCs clone (iKLF1.2) and we acknowledged that this might be a drawback when interpreting our data. Different iKLF1 lines could be subjected to variations of cell proliferation, differentiation efficiency and their response to tamoxifen treatment etc. We have controlled for the most likely artefactual effects of tamoxifen addition by using the control, parental iPSC cells that do not contain the *KLF1-ER^{T2}* transgene but a full analyses of additional iKLF1 clones would support for our conclusions.

4.4.1 Evaluation of activated-KLF1 during the differentiation from day 10

The cell population at day 10 of the differentiation protocol contained the maximum number of $CD34^+$ / $CD43^+$ cells, and the capacity of blood differentiation from this multi-lineage haematopoietic progenitor cells (HPCs) has been confirmed (see Chapter 3 Section 3.4.1.1). In order to evaluate the effect of KLF1 in HPCs, we activated KLF1 using tamoxifen from day 10 of the differentiation protocol.

4.4.1.1 Assessment of phenotype

In a comparison of the cultures between parental iPSC and iKLF1.2, there are no obvious differences during the maintenance of their stemness and during the period of mesoderm specification and haematopoietic induction (Figure 4.1A). After activating KLF1 from day 10, there were no obvious differences at day 17 (Figure 4.1A), but by day 24 KLF1-activated cells appeared redder, indicating enhanced erythropoiesis (Figure 4.1A).

When harvesting differentiating cells for flow cytometry at day 15, we noted that the cell pellet from KLF1-activated cells had a more intense red colour compared to parental iPSC-derived cells and non-tamoxifen-treated iKLF1.2-derived cells (Figure 4.1B). Flow cytometry analysis demonstrated that the percentage of cells expressing both CD235a and CD71 increased obviously at days 15 and 24 upon activation of KLF1 from day 10 (Figure 4.1C and D). At day 31, the flow cytometry result showed that erythroid lineage cells became more mature, because most $CD235a^+$ cells lost erythroblasts marker, CD71 (Figure 4.1E).

Taken together, activation of KLF1 from day 10 has an effect on the red appearance of the cell pellet and more percentage of erythroblasts, the data suggest KLF1 enhances erythroid differentiation.

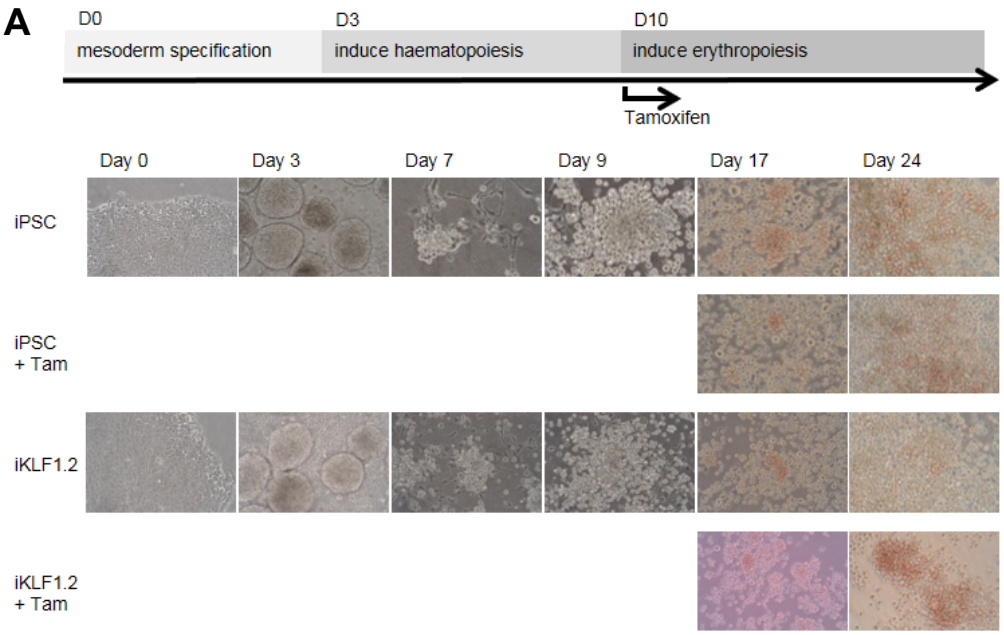
A
D0
D3
D10
mesoderm specification
induce haematopoiesis
induce erythropoiesis
Tamoxifen
Day 0
Day 3
Day 7
Day 9
Day 17
Day 24
iPSC
iPSC
+ Tam
iKLF1.2
iKLF1.2
+ Tam

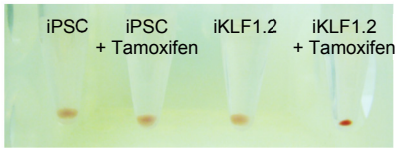
B
iPSC
iPSC
+ Tamoxifen
iKLF1.2
iKLF1.2
+ Tamoxifen

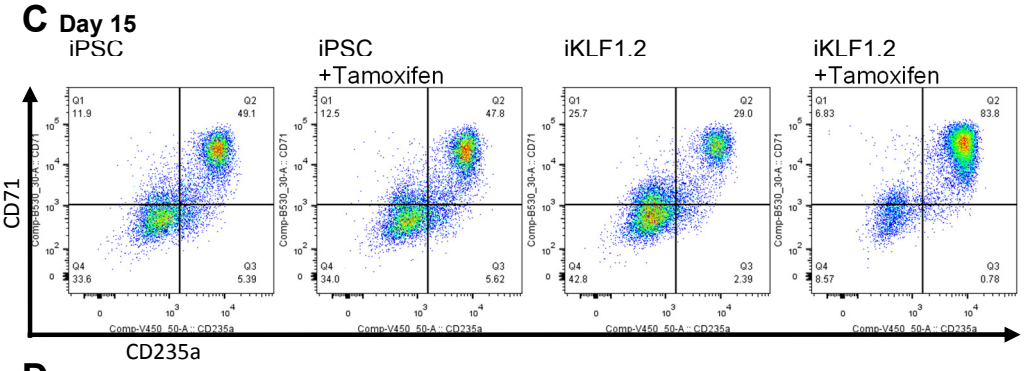
C Day 15
iPSC
iPSC
+Tamoxifen
iKLF1.2
iKLF1.2
+Tamoxifen
CD71
CD235a

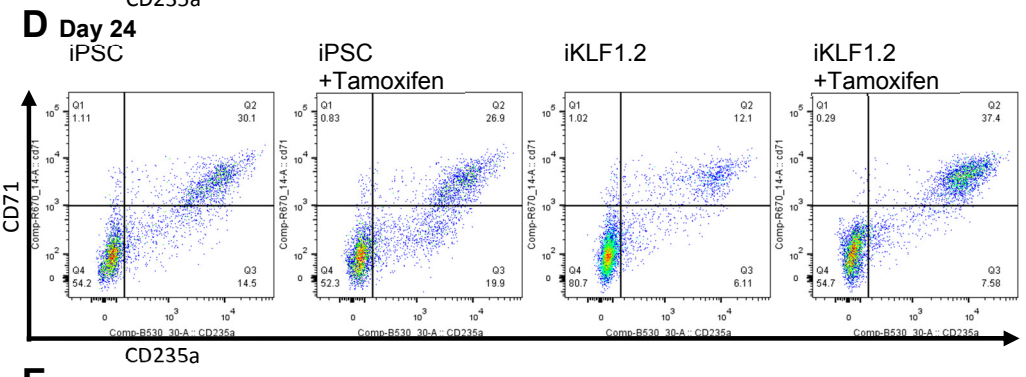
D Day 24
iPSC
iPSC
+Tamoxifen
iKLF1.2
iKLF1.2
+Tamoxifen
CD71
CD235a

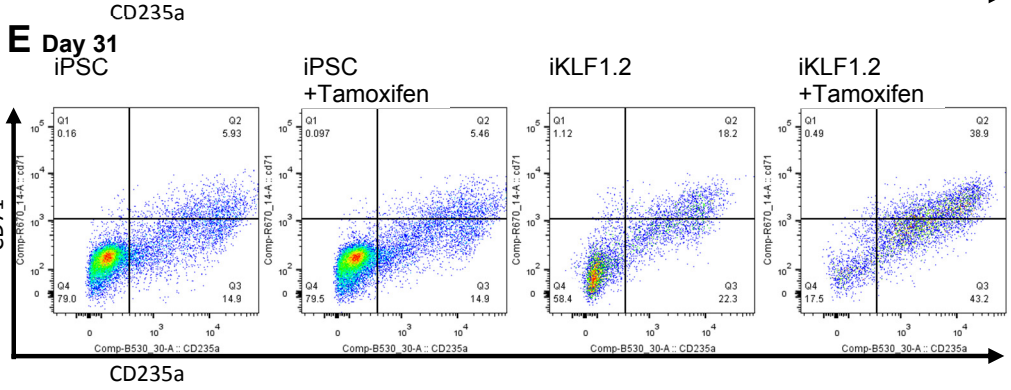
E Day 31
iPSC
iPSC
+Tamoxifen
iKLF1.2
iKLF1.2
+Tamoxifen
CD71
CD235a

Figure 4.1 Activation of KLF1 enhances erythroid differentiation

A. Diagram showing the activation of KLF1 by adding tamoxifen from day 10 during erythroid differentiation. Appearance of cultures of parental iPSCs and iKLF1.2-derived cells in the absence and presence (+Tam) of tamoxifen were observed in time course. **B.** Cell pellets of day 15 differentiating cells in the absence or presence of tamoxifen. **C-E.** Erythroid marker CD235a and erythroblast marker CD71 were assessed using flow cytometry at day 15 (C), day 24 (D) and day 31 (E).

4.4.1.2 Assessment of cell proliferation and viability

Activation of KLF1 enhanced the red appearance of cell pellet, and we also noted that tamoxifen-treated cultures generated a smaller cell pellet. To measure cell proliferation, $3x10^5$ differentiating cells were seeded at day 10 of differentiation then further differentiated in the presence or absence of tamoxifen, we confirmed quantitatively by cell counting implying that KLF1 had a detrimental effect on cell proliferation (Figure 4.2A). To address whether the poor cell proliferation is caused by cell death, flow cytometry analysed cells using LIVE/DEAD™ Fixable Near-IR Stain for viability, however, there was no significant difference in cell viability at days 15, 24 and 31 upon activating KLF1 from day 10 (Figure 4.2B), therefore, the reduced cell number does not result from cell death.

To investigate the role of KLF1 in proliferation, the expression of KLF1 target genes related to cell proliferation, apoptosis and cell cycle was analysed by qRT-PCR at day 24 (Figure 4.2C). We firstly confirmed that there were no significant effects on tamoxifen treatment when analysing iPSC-derived cells in the presence and absence of tamoxifen from day 10. The qRT-PCR results demonstrated that activation of KLF1 significantly upregulated the expression of *PIM1* (cell survival), *BCLX* (*Bcl2l1*; anti-apoptosis), *p21* and *p27* (cell cycle inhibitors), but no impacts on the expression of *E2F2* (cell proliferation) and p18 (cell cycle inhibitor).

The data suggest that activation of KLF1 reduces cell proliferation during erythroid differentiation, this might result from upregulation of *p21* and *p27* (cell cycle inhibitors). The cell proliferation arrest is not caused by cell death, the qRT-PCR result also confirmed that KLF1-activated cells represent higher expression of *PIM1* (cell survival) and *BCLX* (anti-apoptosis).

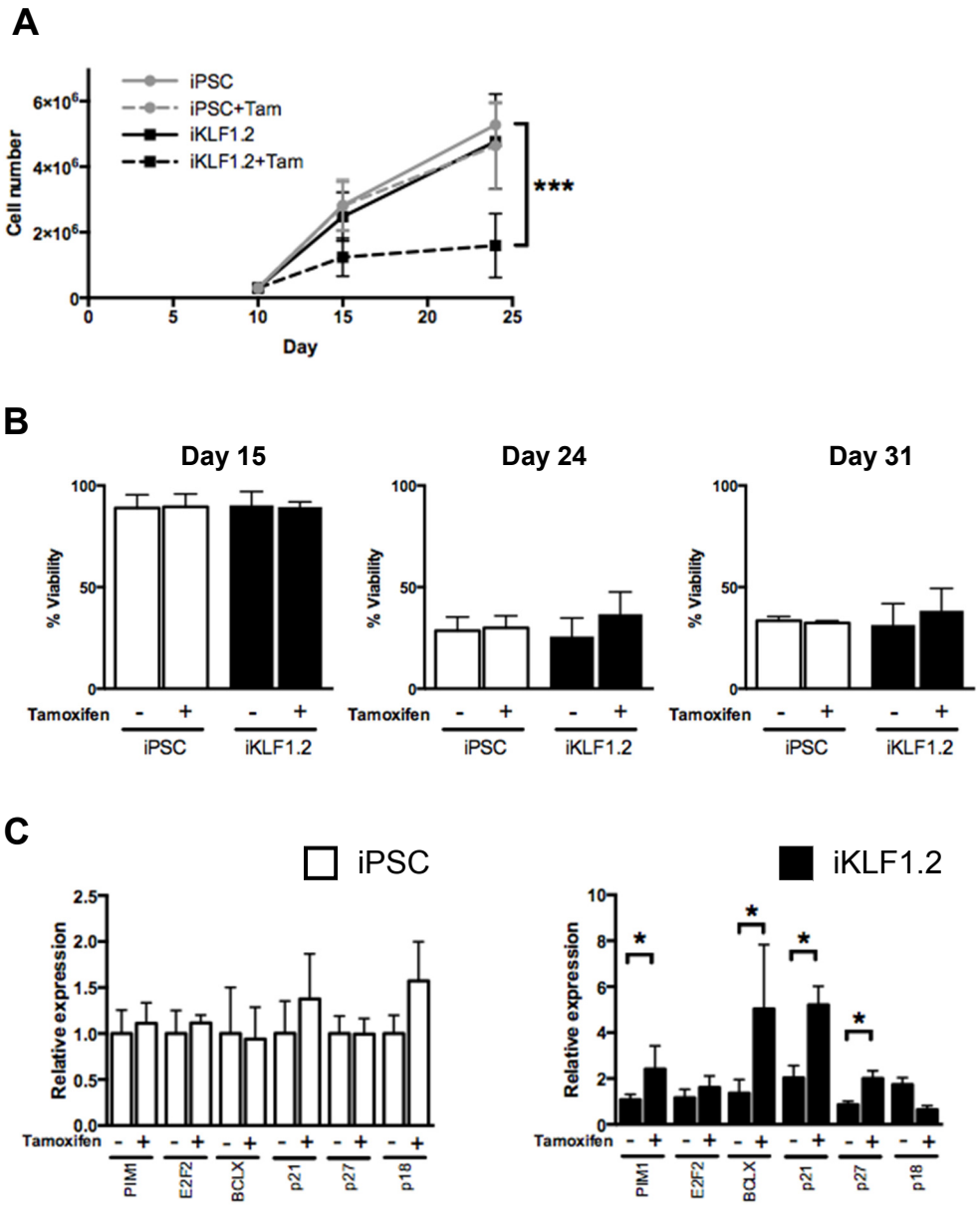
A
iPSC
iPSC+Tam
iKLF1.2
iKLF1.2+Tam
Cell number
6×10^6
4×10^6
2×10^6
0
0
5
10
15
20
25
Day
***
B
Day 15
Day 24
Day 31
% Viability
100
50
0
Tamoxifen
- + - +
iPSC
iKLF1.2
C
iPSC
iKLF1.2
Relative expression
2.5
2.0
1.5
1.0
0.5
0.0
10
8
6
4
2
0
Tamoxifen
- + - + - + - + - + - +
PIM1
E2F2
BCLX
p21
p27
p18
*

Figure 4.2 Activation of KLF1 reduces cell proliferation during erythroid differentiation

A. Cell numbers of erythroid cells derived from parental iPSCs and iKLF1.2 cell line during erythroid differentiation in the presence (+Tam) or absence of tamoxife. Data represent the mean of 3 independent experiments and error bars show standard error of the mean (SEM**).** P values were calculated using two-way ANOVA followed by multiple comparisons test (***, $p<0.0005$). **B.** Flow cytometry analysis using live/dead staining dye for viability present at days 15, 24 and 31 of the erythroid differentiation protocol in the presence (+) and absence (-) of tamoxifen from day 10. Data represent 3 independent experiments. Error bars represent standard error of the mean (SEM)**. C.** Quantitative RT-PCR analyses of RNA isolated from iPSC-derived cells and iKLF1.2-derived cells at day 24 following treatment with (+) or without (-) tamoxifen from day 10 using primers to *PIM1, E2F2, BCLX, p21, p27* and *p18.* Data represent the mean of 3 independent experiments and error bars show the standard error of the mean (SEM). A ratio paired T test was used to assess the effect of KLF1 activation (*, $p<0.05$).

4.4.1.3 Assessment of erythroid maturation

To confirm whether KLF1 activation enhances erythroid differentiation, we analysed the percentage of $CD235a^+$ / $CD71^+$ erythroblasts by flow cytometry, the data showed that the percentage of erythroblasts at day 15 significantly increased from 30 % to 60 % once activating KLF1 from day 10 (Figure 4.3A). The proportions of erythroblast population at days 24 and 31 stayed at 30 % in 4 experimental groups, this indicated KLF1 activation did not maintain the erythroblast phenotype as high percentage at the late stage of differentiation (Figure 4.3A).

When we analysed $CD235a^+$ erythroid lineage cells, the percentages in KLF1-activated group reached the highest point 70 % at days 15, 24 and 31, however, the statistical analysis only indicated the significant difference at day 15 (Figure 4.3B).

To assess the effect of KLF1 activation on erythropoiesis, RNA isolated from iPSC-derived cells and iKLF1.2-derived cells at day 15 following treatment with or without tamoxifen from day 10 was evaluated by qRT-PCR. Activation of KLF1 significantly increased the expression of *SOX6* and *AHSP* (Figure 4.3C).

The expression of genes involved in RBC maturation was also evaluated at day 24. The expression of *GYPC* (erythroid membrane protein), *ANK1* (erythroid cytoskeleton) and *SLC4A1* (erythroid cytoskeleton) and *ABCG2* (heme transport and synthesis) were significantly increased, but there were no significant increases in the expression of *SLC2A4* nor *EPB4.9* (Figure 4.3D). Interestingly, the expression of *BCL11A*, a well-known target gene of KLF1 was downregulated significantly, this might be the main reason of higher embryonic globin expression in HPLC analysis (see below).

The above data suggest KFL1 activation from day 10 accelerates the erythropoiesis and also increases the maturity of erythroid cells, but not change the proportion of erythroblast population at the late stage of erythroid differentiation.

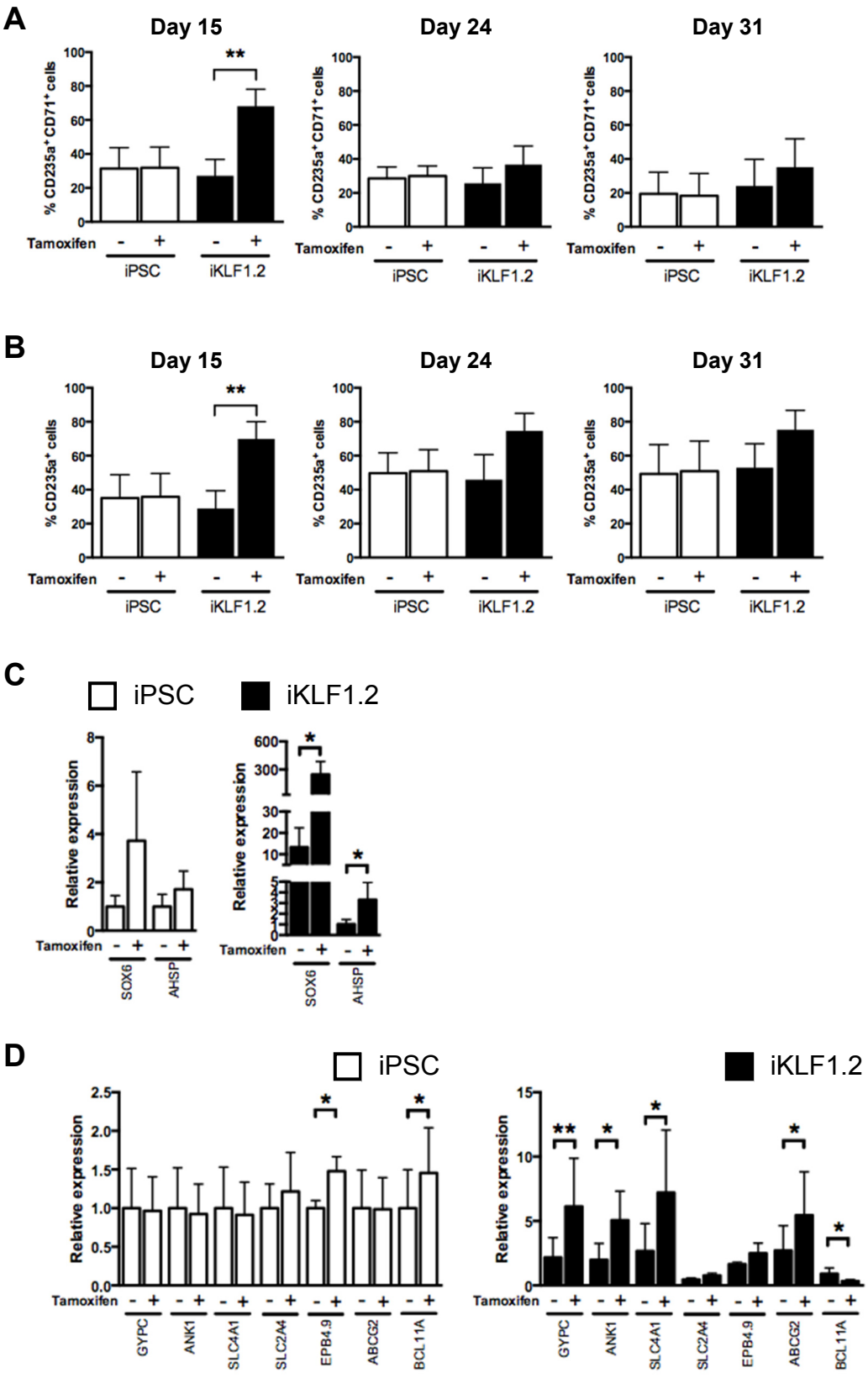
A
Day 15
Day 24
Day 31
% CD235a+CD71+ cells
Tamoxifen
iPSC
iKLF1.2
B
Day 15
Day 24
Day 31
% CD235a+ cells
C
iPSC
iKLF1.2
Relative expression
SOX6
AHSP
D
iPSC
iKLF1.2
Relative expression
GYPC
ANK1
SLC4A1
SLC2A4
EPB4.9
ABCG2
BCL11A

Figure 4.3 Activation of KLF1 accelerates the erythropoiesis and increases the maturity of erythroid cells

A, B. Quantitation of flow cytometry data for control iPSC and iKLF1.2-derived cells at days 15, 24 and 31 of the differentiation protocol in the presence (+) or absence (-) of tamoxifen from day 10. Differentiating cells were analysed by flow cytometry using antibodies against CD235a and CD71. The percentage of $CD235a^+$ / $CD71^+$ cells (A) and the proportion of the percentage of $CD235a^+$ cells (B) were represented in 3 independent experiments and error bars show standard error of the mean (SEM). P values were calculated using one-way ANOVA followed by multiple comparison test (**, $p<0.005$). **C, D.** Quantitative RT-PCR analyses of RNA isolated from control iPSC and iKLF1.2-derived cells in the presence (+) and absence (-) of tamoxifen at day 15 (C) and 24 (D). Quantitative RT-PCR analysis was conducted using primers to *SOX6, AHSP, GYPC, ANK1, SLC4A1, SLC2A4, EPB4.9, ABCG2* and *BCL11A*. Data represent the mean of 3 independent experiments and error bars show the standard error of the mean (SEM). A ratio paired T test was used to assess the effect of KLF1 activation in iKLF1.2 cells (*, $p<0.05$; **, $p<0.005$).

4.4.1.4 Assessment of globin protein profile

Cell lysates were sent to our collaborator (Jo Mountford's laboratory in the University of Glasgow) to assess the production of globin proteins by high performance liquid chromatography (HPLC) analysis (Figure 4.4). β- and α-globins were enriched in adult blood, and Gγ-, Aγ- and α-globins were mainly comprised in foetal blood. In the hPSC-derived blood sample, we were able to observe the peaks of Gγ-, Aγ-, α-, ε- and ζ-globins, but not β-globin (Figure 4.4A).

There were similar distributions of peaks in iPSC and iKLF1.2-derived erythroid cells (Figure 4.4B), and the amount of ε- and ζ-globins seemed to be higher when activating KLF1. Hence, the areas of peaks were calculated and represented as percentages for each globins (Figure 4.4C). Activation of KLF1 from day 10 to day 31 significantly increased the percentage of the embryonic ε- and ζ-globins and reduced the proportion of γ-globin. No adult β-globin was detected in either the parental iPSCs nor iKLF1.2 samples (Figure 4.4C).

These data in this context indicate that activation of KLF1 from day 10 of the differentiation protocol enhances the production of erythroid cells that express globins associated with the primitive wave of haematopoiesis.

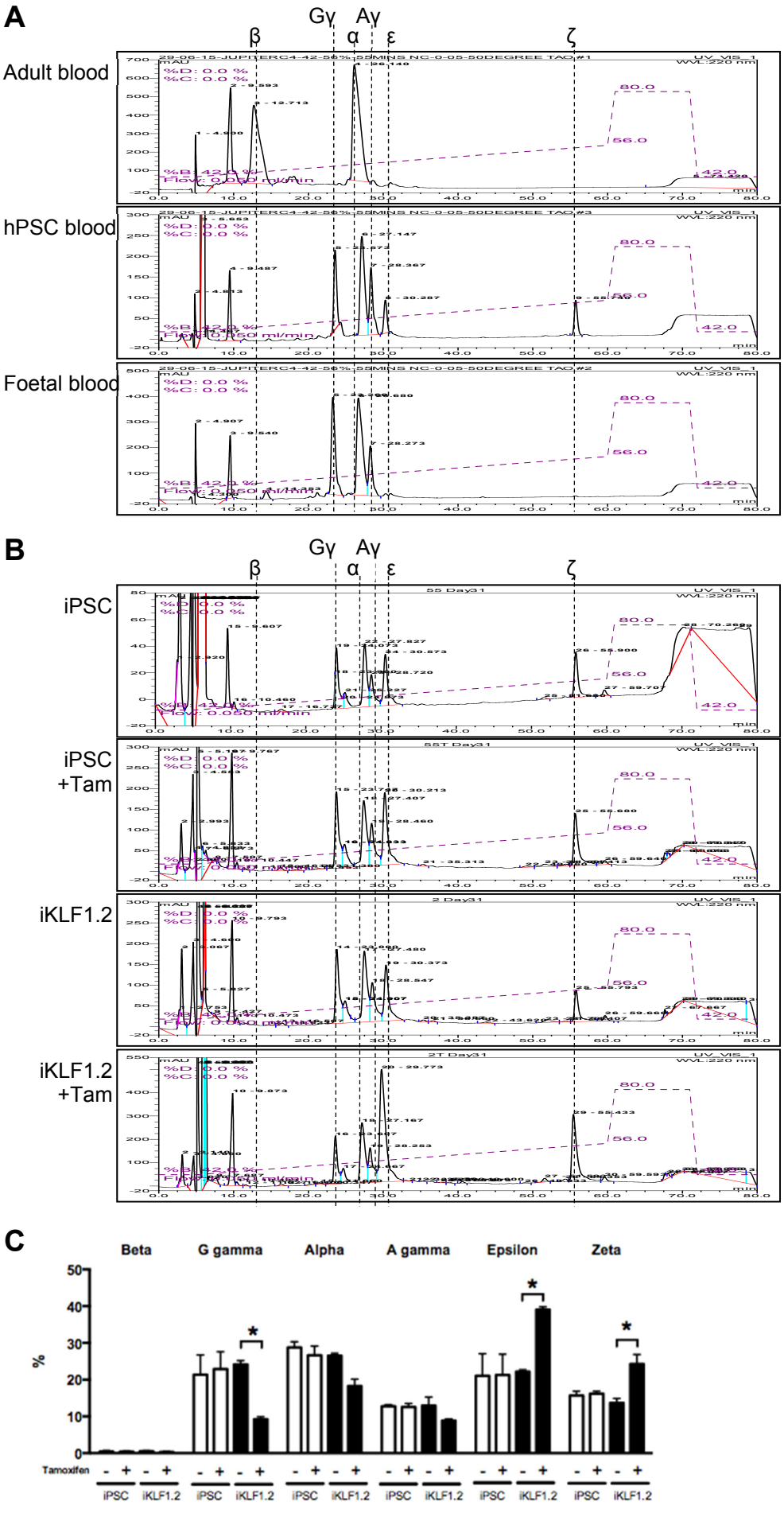
A
Gγ
Aγ
β
α
ε
ζ
Adult blood
hPSC blood
Foetal blood
B
iPSC
iPSC +Tam
iKLF1.2
iKLF1.2 +Tam
C
Beta
G gamma
Alpha
A gamma
Epsilon
Zeta
%
Tamoxifen
iPSC
iKLF1.2

Figure 4.4 Activation of KLF1 enhances embryonic globins

A. HPLC globin profiles of three control samples. Adult blood expresses β- and α-globins, hPSC-derived blood cells contain Gγ-, Aγ-, α-, ε- and ζ-globins and foetal blood contains Gγ-, Aγ- and α-globins. **B.** HPLC results showed the profile of globins in iPSC and iKLF1.2-derived erythroid cells at day 31. **C.** The amount of the different globin was calculated as the areas under the peaks and represented as a percentage of the total globin. Data represent the mean of 3 independent experiments and error bars show standard error of the mean (SEM). P values were calculated using two-way ANOVA followed by multiple comparisons test (B). (*, $p<0.05$).

4.4.1.5 Assessment of enucleation

Enucleation is an important indicator for erythroid maturation. To confirm the enucleation, iPSC-derived erythrocytes and iKLF1.2-derived erythrocytes were sorted using anti-CD235a beads in MACS beads system, and then they were cytospun on slides and conducted with rapid Romanowsky staining. KLF1-activated cells were revealed to have a more robust morphology while comparing with iPSC-derived cells and iKLF1.2-derived cells without tamoxifen treatment. Additionally, a higher frequency of enucleated erythroid cells was observed in cultures where KLF1 was activated compared to control cultures (Figure 4.5A).

To correctly quantify the proportion of enucleated erythroid cells, Dr Fidanza in Forrester's lab developed an enucleation assay in flow cytometry. Differentiating cells were harvested and stained with CD235a-FITC antibody, CD71-APC antibody, the LIVE/DEAD™ Fixable Near-IR Stain and Hoechst dye. Stained cells were analysed in flow cytometry by gating live $CD235a^+$ cells, and we expected to observe $CD235a^+$ / $CD71^+$ / $Hoechst^+$ erythroblasts, $CD235a^+$ / $CD71^-$ / $Hoechst^+$ nucleated RBCs and $CD235a^+$ / $CD71^-$ / $Hoechst^-$ enucleated RBCs (Supplementary Figure S2). A positive control was also used that consisted of human peripheral blood in which all of the RBCs were $CD235a^+$ / $CD71^-$ / $Hoechst^-$ enucleated RBCs (Supplementary Figure S2).

At day 24, the majority of cells were $CD235a^+$ / $CD71^+$ / $Hoechst^+$ erythroblasts and there was no difference in the enucleation rate between non-KLF1-activated cells and KLF1-activated cells (Figure 4.5B). Erythrocytes at day 31 of erythroid differentiation protocol lost the CD71 erythroblast marker as they became more mature (Figure 4.5C). Most importantly, the percentage of enucleated RBCs increased from approximately 2 % to 6 % when KLF1 was activated (Figure 4.5D), the result of enucleation assay in flow cytometry was consistent with cytospin result.

The data suggest the KLF1 activation leads to a more robust morphology and a higher proportion of detectable enucleated erythroid cells.

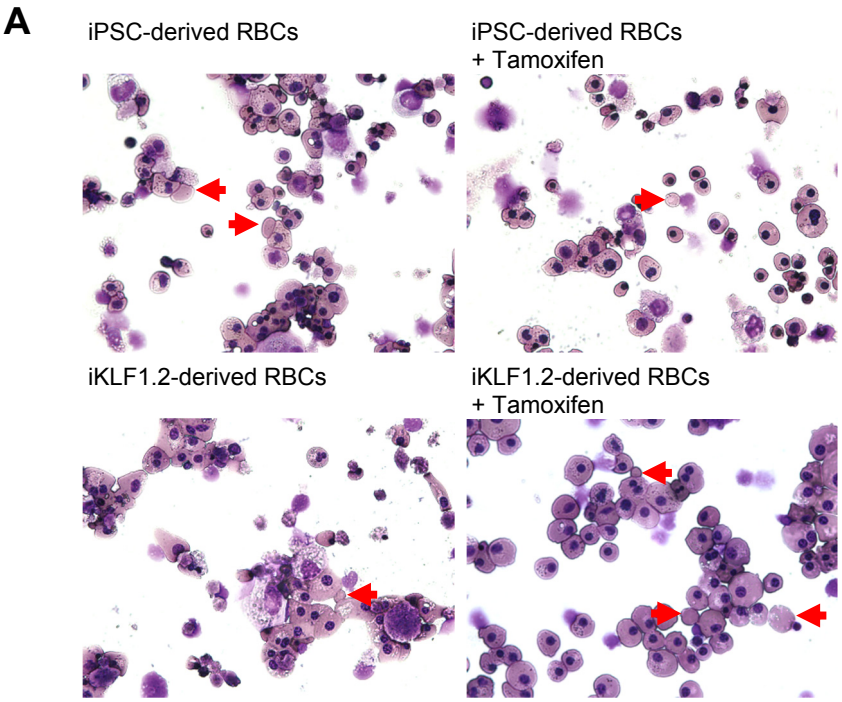
A
iPSC-derived RBCs
iPSC-derived RBCs
+ Tamoxifen
iKLF1.2-derived RBCs
iKLF1.2-derived RBCs
+ Tamoxifen

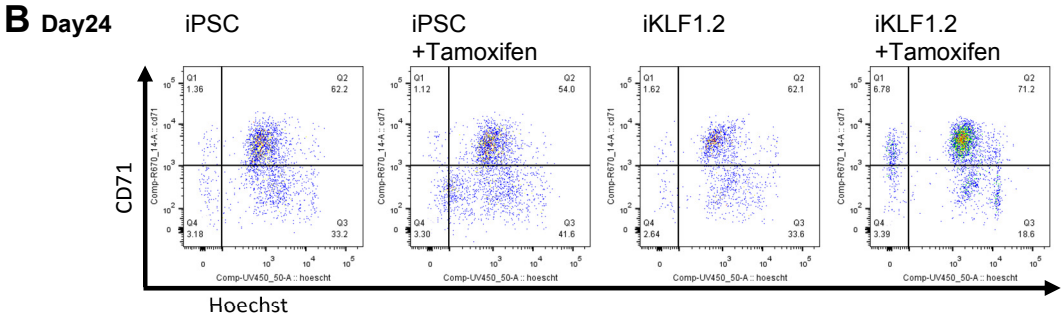
B Day24
iPSC
iPSC
+Tamoxifen
iKLF1.2
iKLF1.2
+Tamoxifen
CD71
Hoechst

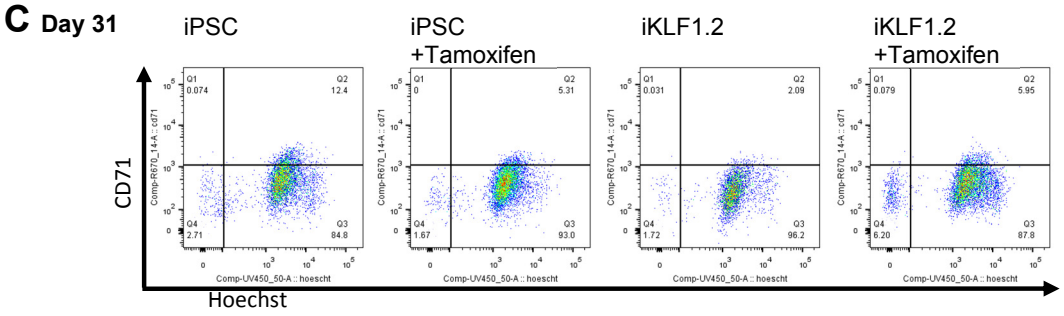
C Day 31
iPSC
iPSC
+Tamoxifen
iKLF1.2
iKLF1.2
+Tamoxifen
CD71
Hoechst

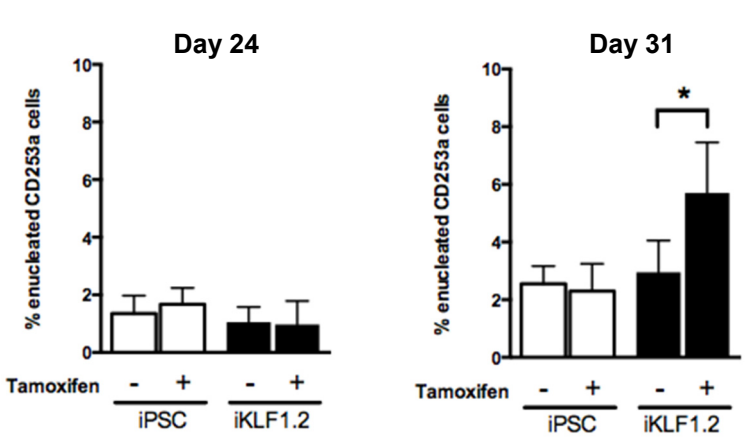
D
Day 24
Day 31
% enucleated CD253a cells
Tamoxifen
iPSC
iKLF1.2
*

Figure 4.5 Activation of KLF1 enhances the enucleation efficiency

A. Cytospins of differentiating cells at day 31. Enucleated erythroid cells were indicated by arrows (x40). **B, C.** The evaluation of enucleation rate at day 24 (B) and day 31 (C) by flow cytometry. Differentiating cells derived from control iPSCs and iKLF1.2 cell line in the presence and absence of tamoxifen were assessed by an enucleation assay. **C.** Quantification of the percentage of enucleated erythroid cells at day 24 and day 31 in three independent experiments of control iPSC and iKLF1.2-derived cells in the presence (+) and absence (-) of tamoxifen from day 10. Data represent the mean of 3 independent experiments and error bars show standard error of the mean (SEM). P values were calculated using one-way ANOVA followed by multiple comparison test (*, $p<0.05$).

4.4.2 Evaluation of activated-KLF1 during the differentiation from day 18

We have observed that activation of KLF1 from day 10 enhances the erythropoiesis, maturation and enucleation efficiency, but KLF1-activated cells expressed embryonic globins (ε and ζ). This suggests that the activation of KLF1 from day 10 in our differentiation protocol enhances primitive erythropoiesis rather than the definitive wave. This might be explained by the fact that the majority of erythroid progenitors at day 10 are with a primitive phenotype, and definitive erythroid progenitors appear at later stages of the differentiation protocol (see Chapter 3 Section 3.6.2). Therefore, we added tamoxifen to activate KLF1 from day 18 and evaluated the effect at the late stage of erythroid differentiation.

4.4.2.1 Assessment of phenotype

In order to assess the effects of KLF1 activation at the late stage of erythroid differentiation, here, we activated KLF1 adding tamoxifen from day 18 (Figure 4.6A). Erythroid cells with red colour appeared from day 21, and there was no obvious difference between the KLF1-activated group and control groups (Figure 4.6B).

Flow cytometry analysis demonstrated that there was no apparent difference in the percentage of $CD235a^+$ / $CD71^+$ cells at day 24 when KLF1 was activated from day 18 (Figure 4.6C), and erythroid lineage cells in 4 groups matured by day 31, with most $CD235^+$ cells losing CD71 (Figure 4.6D).

The data indicate that KLF1 activation at the late stage of erythroid differentiation has no effect on the appearance of red cells and phenotype.

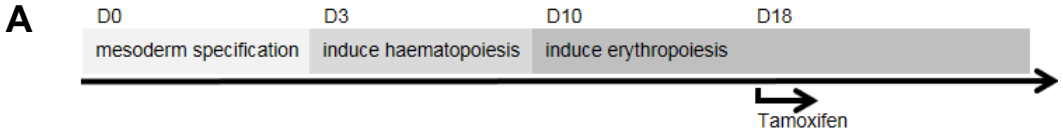
A
D0
D3
D10
D18
mesoderm specification
induce haematopoiesis
induce erythropoiesis
Tamoxifen

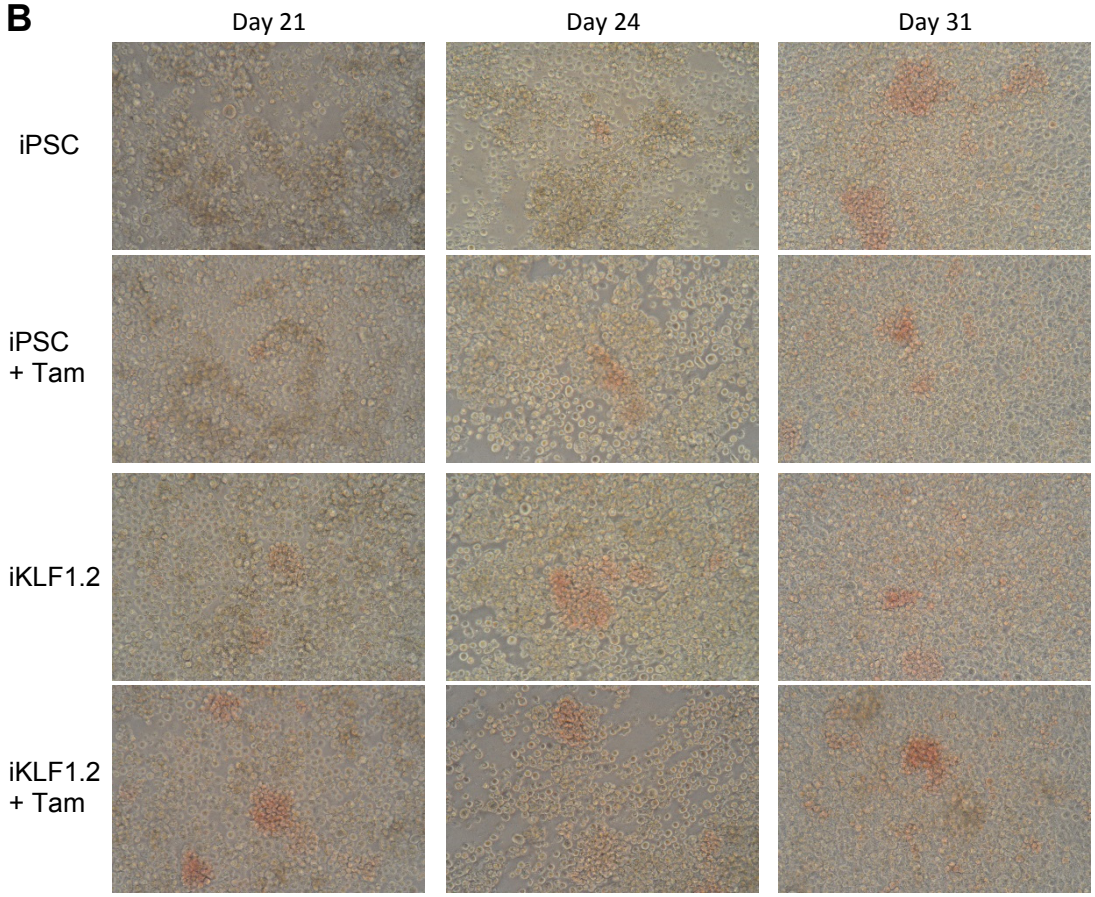
B
Day 21
Day 24
Day 31
iPSC
iPSC
+ Tam
iKLF1.2
iKLF1.2
+ Tam

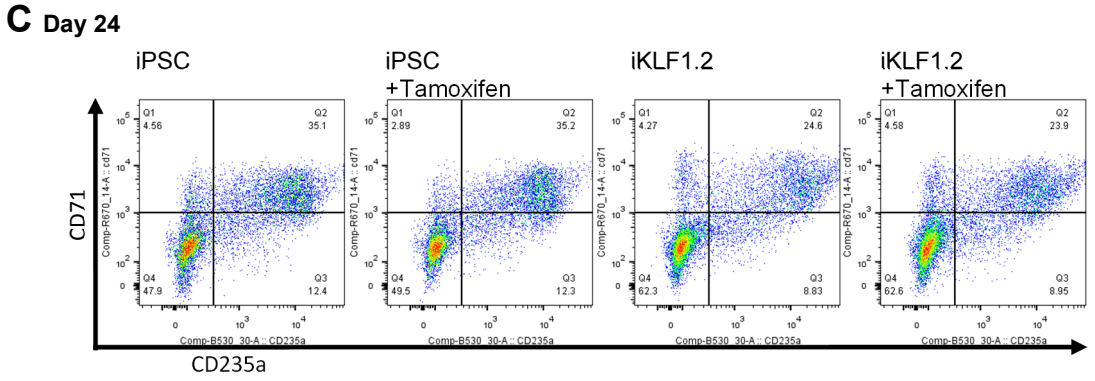
C Day 24
iPSC
iPSC
+Tamoxifen
iKLF1.2
iKLF1.2
+Tamoxifen
CD71
CD235a

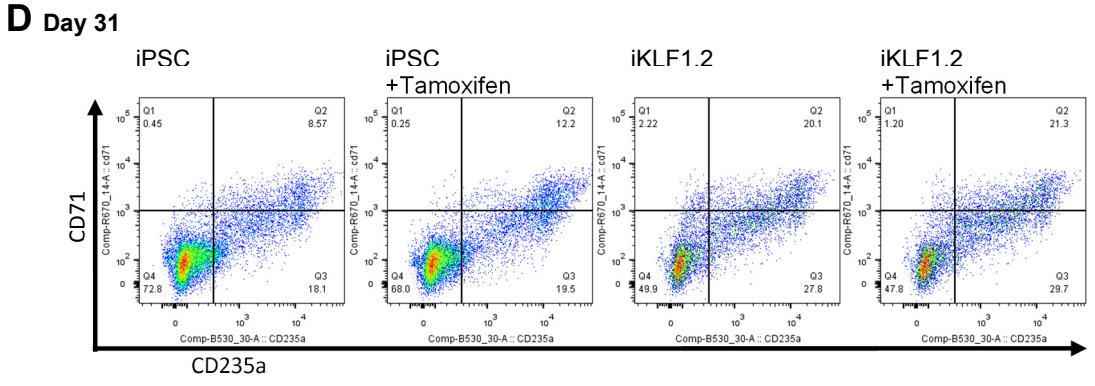
D Day 31
iPSC
iPSC
+Tamoxifen
iKLF1.2
iKLF1.2
+Tamoxifen
CD71
CD235a

Figure 4.6 Activation of KLF1 at the late stage has no effect on morphology and phenotype

A. Diagram showing the activation of KLF1 by adding tamoxifen from day 18 during erythroid differentiation. **B.** Appearance of cultures of parental iPSCs and iKLF1.2-derived cells in the absence and presence (+Tam) of tamoxifen were observed at days 21, 24 and 31. **C, D.** Erythroid marker CD235a and erythroblast marker CD71 were assessed using flow cytometry at day 24 (C) and day 31 (D).

4.4.2.2 Assessment of cell proliferation and viability

To measure the cell proliferation, $3x10^5$ differentiating cells were seeded at day 10 of differentiation then further differentiated in the presence or absence of tamoxifen from day 18. The result of counting showed that activation of KLF1 at the later stage of erythroid differentiation significantly reduced the cell number at day 31 (Figure 4.7A). We then evaluated the viability using live/dead staining in flow cytometry and demonstrated that activation of KLF1 from day 18 did not affect the cell viability (Figure 4.7B). Hence, the decrease of cell number does not result from cell death.

To assess the effect of KLF1 on proliferation arrest, the expression of KLF1 target genes associated with proliferation was analysed by qRT-PCR at day 24 (Figure 4.7C). The qRT-PCR results showed that activation of KLF1 significantly repressed the expression of *E2F2* (cell proliferation) and *p18* (cell cycle inhibitor), but no impacts on the expression of *PIM1, BCLX, p21* and *p27*.

The data suggest that activation of KLF1 at the later stage of erythroid differentiation reduces cell proliferation, down-regulation of *E2F2* might be one possible pathway leading to proliferation arrest.

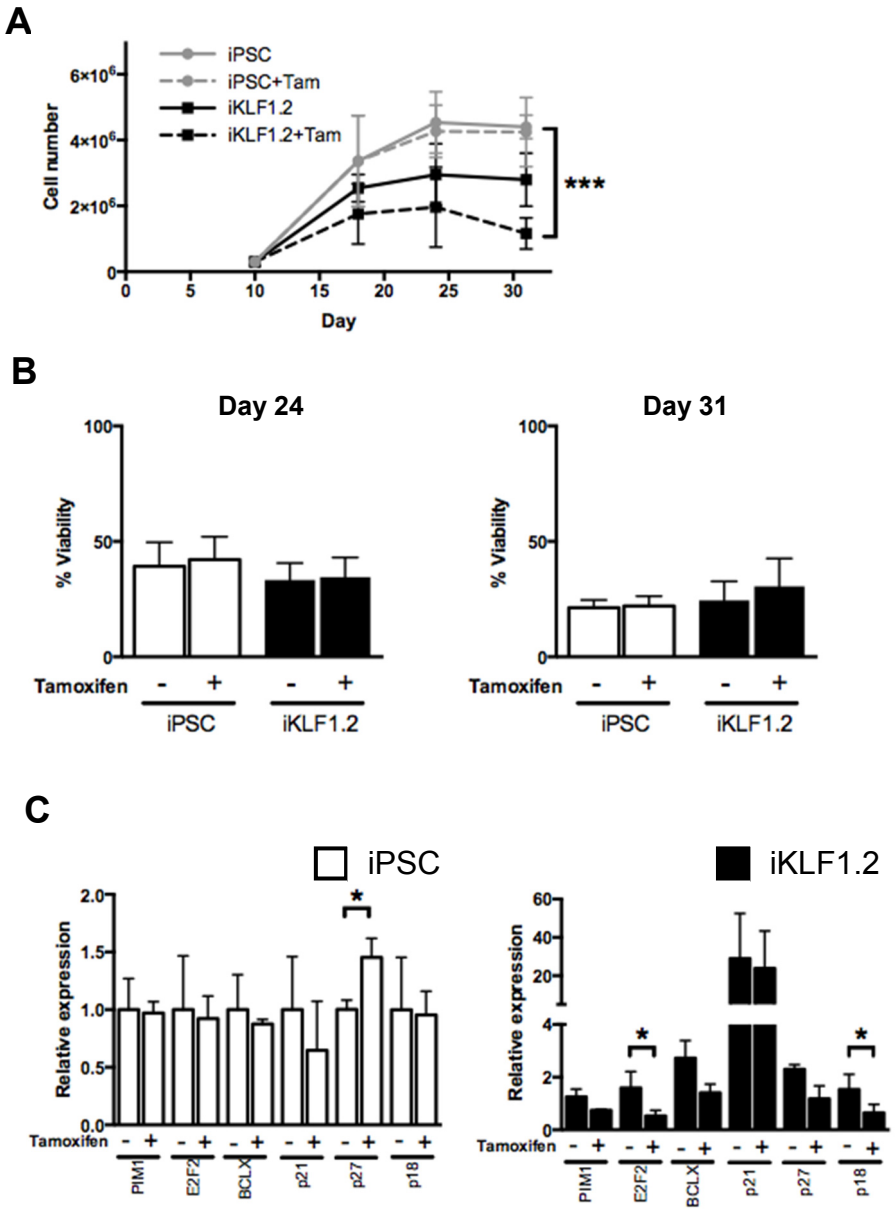
A
iPSC
iPSC+Tam
iKLF1.2
iKLF1.2+Tam
Cell number
6×10⁶
4×10⁶
2×10⁶
0
0
5
10
15
20
25
30
Day
***
B
Day 24
Day 31
% Viability
100
50
0
Tamoxifen
-
+
iPSC
iKLF1.2
C
iPSC
iKLF1.2
Relative expression
2.0
1.5
1.0
0.5
0.0
60
40
20
4
2
0
*
PIM1
E2F2
BCLX
p21
p27
p18

Figure 4.7 Activation of KLF1 at the late stage reduces cell proliferation

A. Cell numbers of erythroid cells derived from parental iPSCs and iKLF1.2 cell line during erythroid differentiation in the presence (+Tam) or absence of tamoxifen from day 18. Data represent the mean of 3 independent experiments and error bars show standard error of the mean (SEM**).** P values were calculated using two-way ANOVA followed by multiple comparisons test (***, $p<0.0005$). **B.** Flow cytometry analysis using live/dead staining dye for viability present at days 24 and 31 of the erythroid differentiation protocol in the presence (+) and absence (-) of tamoxifen from day 18. Data represent 3 independent experiments. Error bars represent standard error of the mean (SEM)**. C.** Quantitative RT-PCR analyses of RNA isolated from iPSC-derived cells and iKLF1.2-derived cells at day 24 following treatment with (+) or without (-) tamoxifen from day 18 using primers to *PIM1, E2F2, BCLX, p21, p27* and *p18.* Data represent the mean of 3 independent experiments and error bars show the standard error of the mean (SEM). A ratio paired T test was used to assess the effect of KLF1 activation (*, $p<0.05$).

4.4.2.3 Assessment of erythroid maturation

When we analysed $CD235a^+$ / $CD71^+$erythroblasts (Figure 4.8A) and $CD235a^+$ erythroid cells (Figure 4.8B) by flow cytometry, there were no significant differences while comparing the control group and KLF1-activated group at days 24 and 31.

To assess the effect of KLF1 activation on gene expression, RNA isolated from iPSC-derived cells and iKLF1.2-derived cells at day 24 following treatment with or without tamoxifen from day 18 was evaluated by qRT-PCR. There were no significant differences in the expression of most genes associated with erythroid maturation while comparing non-KLF1-activated cells and KLF1-activated cells. Interestingly, the expression of *BCL11A*, a well-known target gene of KLF1 was downregulated significantly, this might be the reason why embryonic globins were still expressed highly in HPLC analysis (see below).

The above data suggest KFL1 activation at the late stage of erythroid differentiation has no significant effect on erythroid maturation.

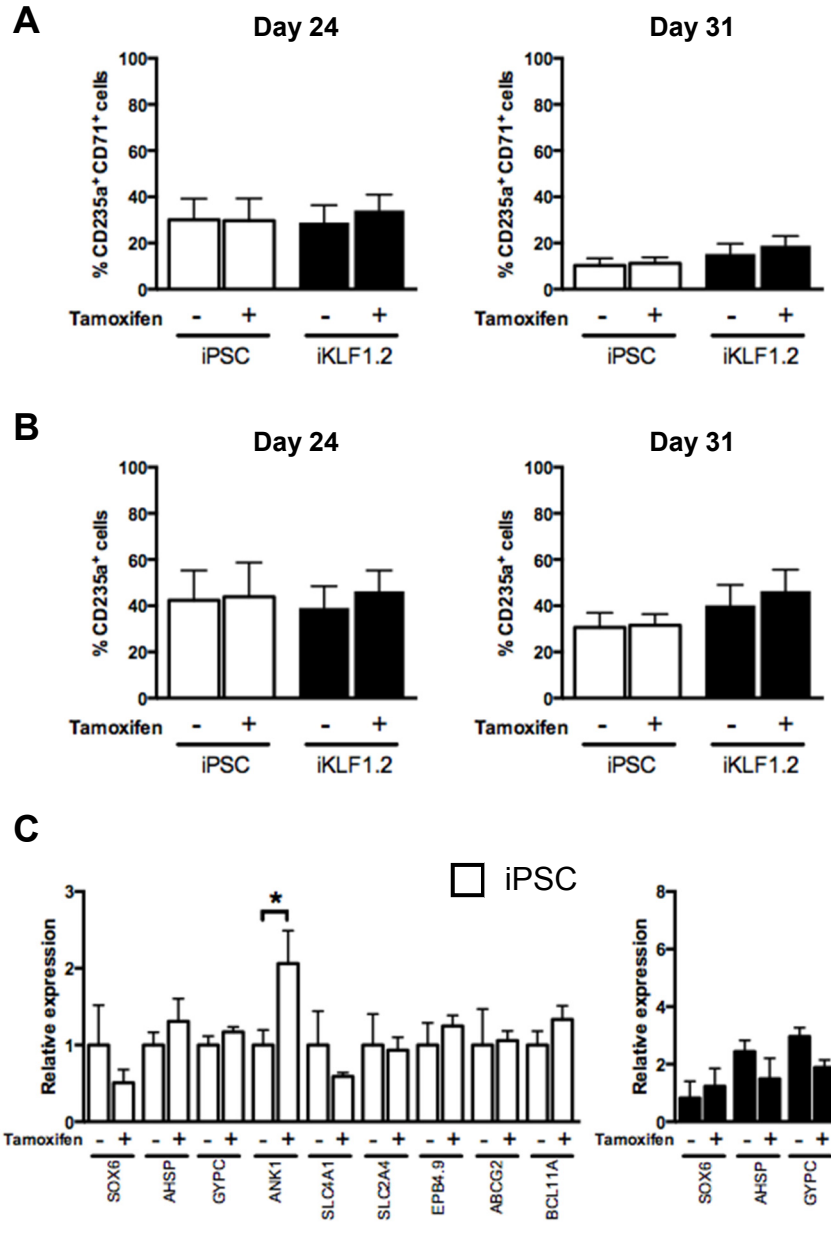
A
Day 24
Day 31
% CD235a+CD71+ cells
100
80
60
40
20
0
Tamoxifen - + - +
iPSC
iKLF1.2
B
Day 24
Day 31
% CD235a+ cells
C
iPSC
iKLF1.2
Relative expression
Tamoxifen
SOX6
AHSP
GYPC
ANK1
SLC4A1
SLC2A4
EPB4.9
ABCG2
BCL11A
*

Figure 4.8 Activation of KLF1 at the late stage has no effect on erythroid genes

A, B. Quantitation of flow cytometry data for control iPSC and iKLF1.2-derived cells at day 24 and day 31 of the differentiation protocol in the presence (+) or absence (-) of tamoxifen from day 18. Differentiating cells were analysed by flow cytometry using antibodies against CD235a and CD71. The percentage of $CD235a^+$ / $CD71^+$ cells (A) and the proportion of the percentage of $CD235a^+$ cells (B) were represented in 3 independent experiments and error bars show standard error of the mean (SEM). **C.** Quantitative RT-PCR analyses of RNA isolated from control iPSC and iKLF1.2-derived cells in the presence (+) and absence (-) of tamoxifen at day 24. Quantitative RT-PCR analysis was conducted using primers to *SOX6, AHSP, GYPC, ANK1, SLC4A1, SLC2A4, EPB4.9, ABCG2* and *BCL11A*. Data represent the mean of 3 independent experiments and error bars show the standard error of the mean (SEM). A ratio paired T test was used to assess the effect of KLF1 activation in iKLF1.2 cells (*, $p<0.05$).

4.4.2.4 Assessment of globin protein profile

The HPLC result showed that iPSC-derived erythroid cells and iKLF1.2-derived erythroid cells can express Gγ-, Aγ-, α-, ε- and ζ-globins with comparable distribution (Figure 4.9A). We calculated areas of peaks from triplicates and found that activation of KLF1 from day 18 did not result in any significant differences between the control group and KLF1-activated group (Figure 4.9B).

Therefore, activation of KLF1 at day 18 of the differentiation protocol has no impact in the late stage of erythroid cells, furthermore, this does not enhance the population of definitive erythroid cells.

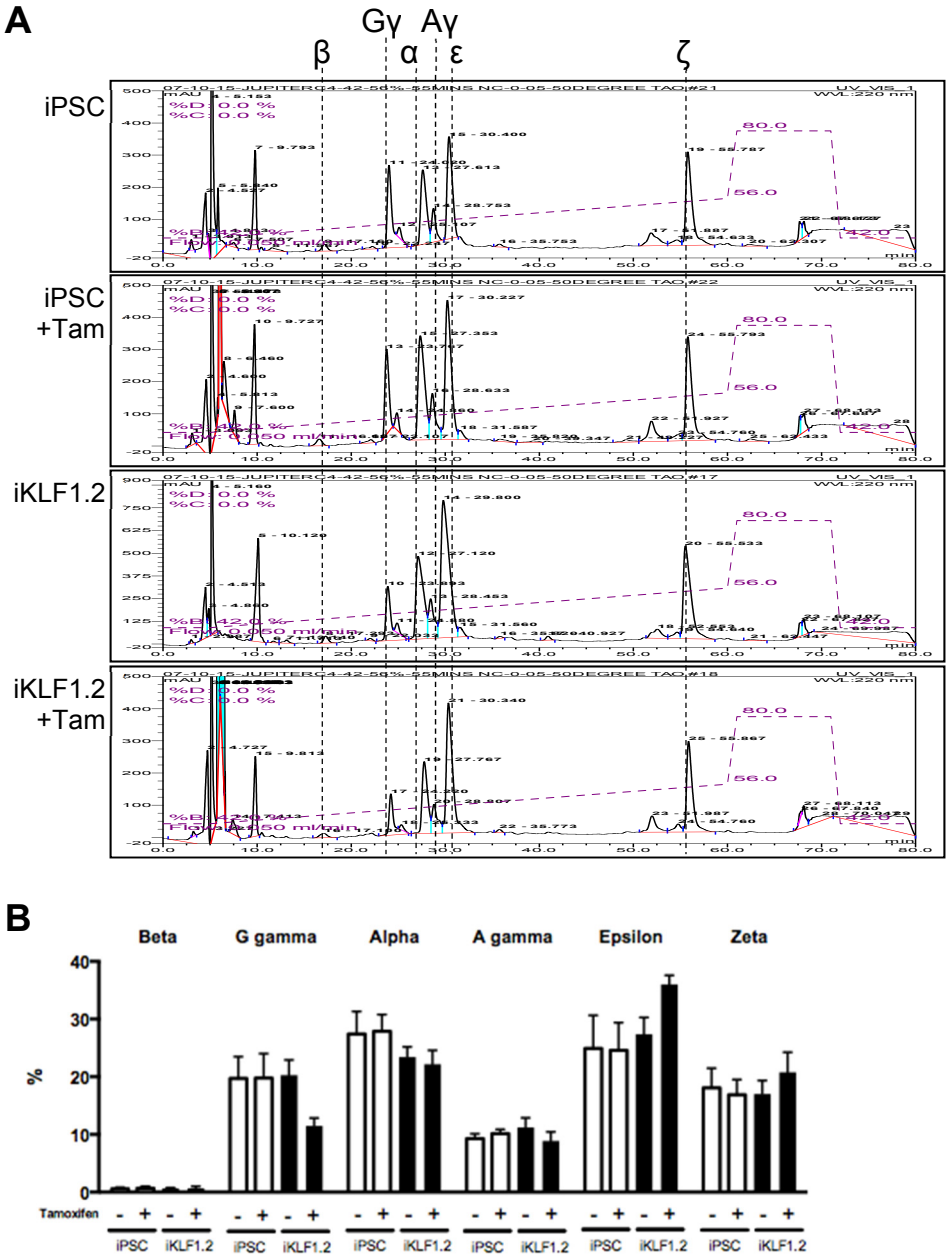

Figure 4.9 Activation of KLF1 has no effect on globin protein profile

A. HPLC results showed the profile of globins in iPSC and iKLF1.2-derived erythroid cells at day 31 following treatment with (+Tam) or without tamoxifen from day 18. **B.** The amount of the different globin was calculated as the areas under the peaks and represented as a percentage of the total globin. Data represent the mean of 3 independent experiments and error bars show standard error of the mean (SEM).

4.4.2.5 Assessment of enucleation

Differentiating cells at day 24 (Figure 4.10A) and day 31 (Figure 4.10B) were evaluated in the enucleation assay by flow cytometry, and we found the enucleation rates were as low as the previous results. Differentiating cells at day 31 were more mature than the cells at day 24, since most erythroid cells at day 31 were losing the erythroblast marker CD71.

The enucleation assay was repeated for three times, the result showed that the parental iPSC-derived erythroid cells in the presence and absence of tamoxifen from day 18 represented approximately 2 % of enucleation rate at day 24 and day 31 (Figure 4.10C). However, the enucleation efficiency of non-KLF1-activated cells and KLF1-activated cells were 6 % with no significant differences (Figure 4.10C).

Taken together, these data demonstrate that activation of KFL1 from day 18 has no impact on the efficiency of enucleation.

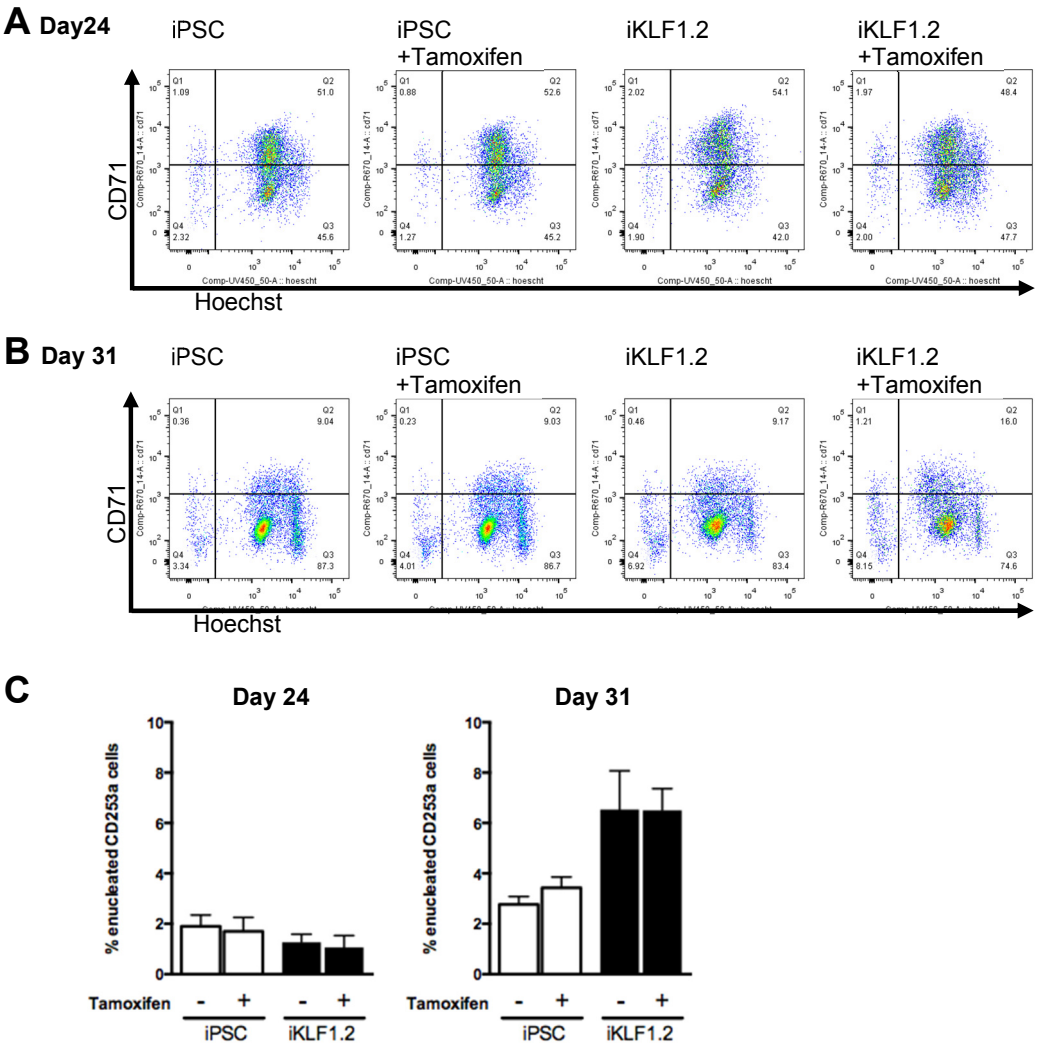

Figure 4.10 Activation of KLF1 at the late stage has no effect on the enucleation efficiency

A, B. The evaluation of enucleation rate at day 24 (A) and day 31 (B) by flow cytometry. Differentiating cells derived from control iPSCs and iKLF1.2 cell line in the presence and absence of tamoxifen from day 18 were assessed in an enucleation assay. **C.** Quantification of the percentage of enucleated erythroid cells at day 24 and day 31 in three independent experiments of control iPSC and iKLF1.2-derived cells in the presence (+) and absence (-) of tamoxifen from day 10. Data represent the mean of 3 independent experiments and error bars show standard error of the mean (SEM).

4.5 Conclusion

1) Activation of KLF1 at the HPC stage (from day 10) accelerated the erythropoiesis, enhanced erythroid maturation and enucleation efficiency at the expense of cell proliferation. However, activating KLF1 from day 10 promoted the primitive erythropoiesis and resulted in higher expression of embryonic globin.
2) There was no obvious impact on erythropoiesis upon the activation of KLF1 at the late stage of erythroid differentiation (from day 18), but KLF1 activation again reduced cell proliferation. It did not enhance the expression of adult β-globin and the enucleation efficiency.

4.6 Discussion

4.6.1 KLF1 activation results in proliferation arrest but not cause cell death

Activation of KLF1 at the HPC stage (from day 10) or the late stage of erythroid differentiation (from day 18) leads to reduced proliferation. However, there is no difference on cell viability between parental iPSC-derived cells and iKLF1.2-derived cells in the presence and absence of tamoxifen, indicating that the reduction in cell numbers is not caused by cell death and apoptosis.

Several studies have reported the role of KLF1 in proliferation, whose target genes are associated with cell proliferation, apoptosis and cell cycles, such as *PIM1, E2F2, BCLX, p21, p27* and *p18.* PIM1 is a survival component of erythroblasts and affects cell proliferation [118]. E2F2 regulated by KLF1 is required for cell cycle progression during terminal erythroid differentiation [106], [107]. BCLX has an anti-apoptotic function in primitive and definitive erythrocytes and erythroblasts [116], [117]. Three cell cycle inhibitors, p18, p21 and p27, are critical during late stages of erythropoiesis, thereby indicating a relationship between erythroid differentiation and cell cycle exit [34], [105], [115]. Our qRT-PCR result supports the point that activation of KLF1 from day 10 increased the expression of cell cycle inhibitors (*p21* and *p27*), this reveals that cell proliferation is arrested in the cell cycle during erythroid differentiation. The enhanced expression of an anti-apoptotic component (*BCLX*) and a survival component (*PIM1*) was revealed when activating KLF1 at the HPC stage (from day 10), this indicates activation of KLF1 does not lead to cell death and apoptosis.

However, the reduced cell proliferation in KLF1 activation from day 18 results from decreased expression of *E2F2*, this suggests that KLF1 regulates the proliferation arrest in HPCs and in the late stage of erythroid cells through different pathways.

4.6.2 KLF1 activation from day 10 accelerates the process of erythropoiesis

KLF1 regulates erythropoiesis by enhancing erythroid differentiation coupled with reduced proliferation [143], [144]. According to our results of a higher percentage of $CD235a^{+}$ / $CD71^{+}$ erythroblasts, higher expression of erythroid genes, more enucleated cells and a decreased cell number upon activating KLF1 from day 10, this indicates

that activation of KLF1 at the HPC stage promotes erythroid differentiation at the expense of cell proliferation. However, KLF1 activation from day 10 does not maintain the erythroblast phenotype as a high percentage at the later stage, this suggests KLF1 activation at the HPC stage accelerates the process of erythropoiesis instead of maintaining in the erythroblast stage.

4.6.3 KLF1 activation from day 10 results in erythroid cells becoming more mature and robust

Foetal liver-derived null KLF1 erythroid cells have an abnormal morphology, and most of the cells retain their nucleus [23], [33], [34], this hints that KLF1 is involved in the terminal differentiation of erythropoiesis. Our qRT-PCR result showed that KLF1 activation in HPCs upregulates the expression of *GYPC* (erythroid membrane protein) and *ABCG2* (heme transport and synthesis), this suggests KLF1-activated cells are represented as more mature phenotypes.

Furthermore, KLF1 is involved in the maturation of RBCs by regulating cytoskeleton and maintaining the membrane stability [26], [27]. The target genes include *EPB4.9* (Dematin), *ANK1* (Ankyrin 1) and *SLC4A1* (Band 3), loss of these transmembrane proteins or cytoskeleton contributes to the fragility of erythrocytes [26], [27], [111], [112]. Our qRT-PCR result indicated KLF1 activation at the HPC stage increases the expression of *ANK1* and *SLC4A1*. This supports that KLF1-activated cells have a more mature phenotype and this also explains the fact that more robust morphology in cytospin, thereby detecting a higher percentage of enucleated cells in an enucleation assay by flow cytometry.

4.6.4 KLF1 activation from day 10 promotes primitive erythropoiesis

KLF1 is required for adult β-globin gene transcription [99], [119], but loss of KLF1 diminishes the expression of εy- and βH1-globin genes [22], [25], [28], [29]. This suggests KLF1 regulates both embryonic globin and adult globin in primitive and definitive erythrocytes. HPLC analysis showed that both non-KLF1-activated cells and KLF1-activated cells express foetal globin (α-, Gγ- and Aγ-globins) and embryonic globin (ε- and ζ-globins), this indicates that a mixed population of primitive

and definitive erythroid cells are generated from the defined erythroid differentiation protocol, also, our defined differentiation protocol enriches the primitive erythropoiesis (see Chapter 3 Section 3.6.2). Therefore, that might be a reason why activation of KLF1 from day 10 enhances the production of erythroid cells that express globins associated with the primitive wave of haematopoiesis.

Of note, a well-known target gene of KLF1, *BCL11A*, silences foetal globin and indirectly upregulates adult β-globin expression [120], [121], was downregulated significantly upon activating KLF1 from day 10. This might be another reason of higher embryonic globin expression but no adult globin expression.

4.6.5 KLF1 activation from day 18 has no significant effect on erythropoiesis

We describe there might be two waves of erythropoiesis in the defined differentiation protocol (see Chapter 3 Section 3.6.2), so we activated KLF1at the later stage of erythroid differentiation and assessed whether this could promote definitive erythropoiesis. The results of KLF1 activation at the late stage of erythroid differentiation (from day 18) showed limited impact. Cell proliferation was reduced by activating KLF1 from day 18, but activation of KLF1 at the late stage of differentiation did not enhance erythropoiesis, as assessed by the proportion of erythroid lineage cells, KLF1 target gene expression, globin protein profile and enucleation efficiency. This suggests that activation of KLF1 does not affect the late stage of erythroid cells. There are several possible reasons for this finding: (1) cells at the late stage of erythropoiesis are not competent to respond to KLF1 and/or KLF1 is only required at a precise point in the process but not at day 18. A live image study has reported that nuclear import of KLF1 occurs during the ProE to BasoE transition [145], and this indicates KLF1 is required at the particular stage of erythroid development. (2) the ER^{T2} system is slightly leaky and so it is possible that there is some KLF1 activation occurring in the cells that are not treated with tamoxifen and at later stages the addition of tamoxifen might not exert any additional effect. The fact that the enucleation rate at day 31 in the iKLF1.2 cell line was higher than control cells in the absence of tamoxifen lends support to this hypothesis.

4.6.6 No adult globin is expressed in iPSC-derived cells and KLF1-activated erythroid cells

Trakarnsanga et al reported that the expression of *KLF1* and *BCL11A* is required above a threshold level to induce adult globin expression and repress embryonic and foetal globins [139]. They also showed that adult globin (β-globin) cannot be activated by only KLF1 induction [139]. This is consistent with our result that adult globin is not detected in the differentiating cells with neither activating KLF1 from day 10 nor activating KLF1 from day 18. We then hypothesised that another TFs might be required for the maturation of definitive erythrocytes. Recent studies have reported that BCL11A plays a key role in the suppression of foetal globin expression [120], [121], and it is regarded as a marker for definitive erythropoiesis [12], [30], [32]. Therefore, our next step was to evaluate the effect of both KLF1 and BCL11A during erythroid differentiation to assess whether this could result in the production of mature RBC expressing adult globin.

Chapter 5

Evaluation of lentivirus-GFP-BCL11A in control and iKLF1.2 iPSCs during erythroid differentiation

5.1 Introduction

Activation of KLF1 at the HPCs stage of iPSCs differentiation enhanced the differentiation and maturation of erythroid cells but did not increase adult globin expression indicating that additional factors are required for this process. Trakarnsanga et al also showed that an adult level of β-globin was detected in the PSC-derived cells that were transfected with KLF1 and BCL11A [139]. In another study, a low level of BCL11A-L in hPSC-derived erythroblasts is associated with impaired γ-globin silencing, and activation of BCL11A-L effectively down-regulated foetal globin and upregulated adult globin [146]. These studies led to the hypothesis that expression of BCL11A in iPSC-derived erythroid cells could enhance the expression of β-globin. To test this hypothesis, we acquired a lentivirus vector, pXLG3-BCL11A XL, from Dr Jan Frayne at the University of Bristol and transduced this into differentiating control iPSCs. To assess the effects of both KLF1 and BCL11A on erythroid differentiation and β-globin expression, iKLF1.2 were treated with tamoxifen to activate KLF1 and transduced with lentivirus-GFP-BCL11A.

5.2 Aim

1. To evaluate the effects of overexpression of BCL11A on iPSCs-derived erythroid cells
2. To assess the effects of both KLF1 and BCL11A on iPSCs-derived erythroid cells

5.3 Approaches

1. To test the lentivirus-GFP-BCL11A in iPSC-derived HPCs, the effects of BCL11A transduction on cell proliferation, RBC maturation and the expression of β-globin were assessed by cell counts, flow cytometry, qRT-PCR and HPLC.
2. To evaluate the effect of KLF1 activation and lentivirus-GFP-BCL11A transduction on the production and maturation of RBCs from iKLF1.2 cell line, differentiating cells were assessed by cell counts, flow cytometry and qRT-PCR.

5.4 Result

One iPSCs clone (iKLF1.2) was analysed in this chapter and we acknowledged that this might be a drawback when interpreting our data. Different iKLF1 lines could be subjected to variations of transduction efficiency, differentiation efficiency and their response to tamoxifen treatment etc. We have controlled for the most likely artefactual effects of tamoxifen addition by using the control, parental iPSC cells that do not contain the *KLF1-ER^{T2}* transgene but a full analyses of additional iKLF1 clones would support for our conclusions.

5.4.1 Lentivirus-GFP-BCL11A transduction in hiPSCs

5.4.1.1 Cell counts and flow cytometry analysis

A control GFP-lentivirus was used to establish a transduction protocol for iPSC-derived HPCs at day 10 (Supplementary Figure S3). GFP fluorescence was evaluated by flow cytometry one day after virus transduction, and the percentage of GFP$^+$ cells hit the highest point at a multiplicity of infection (MOI) 100 (Supplementary Figure S3).

To evaluate the effect of BCL11A on iPSC-derived cells, day 10 cells were transduced with the lentivirus-GFP-BCL11A at MOI 100. Transduction of lentivirus-GFP-BCL11A did not alter cell morphology (data not shown), nor cell number as assessed by cell counts (Figure 5.1A) and the size of the cell pellet at day 15 and 24 (Figure 5.1B). Flow cytometry analysis demonstrated that the viability was approximately 80 % at day 15 and approximately 55% at day 24 in both experimental groups (Figure 5.1C). To assess the efficiency of viral transduction, we analysed the percentage of GFP$^+$ cells. 70 % of cells expressed GFP at day 15 and 60 % at day 24 (Figure 5.1D). There was no statistical difference in the percentage of CD235a$^+$ cells between control iPSC-derived cells and BCL11A-transduced cells at days 15 and 24 (Figure 5.1E).

Taken together, our data indicate that transduction of BCL11A has no significant effect on cell proliferation and erythroid differentiation.

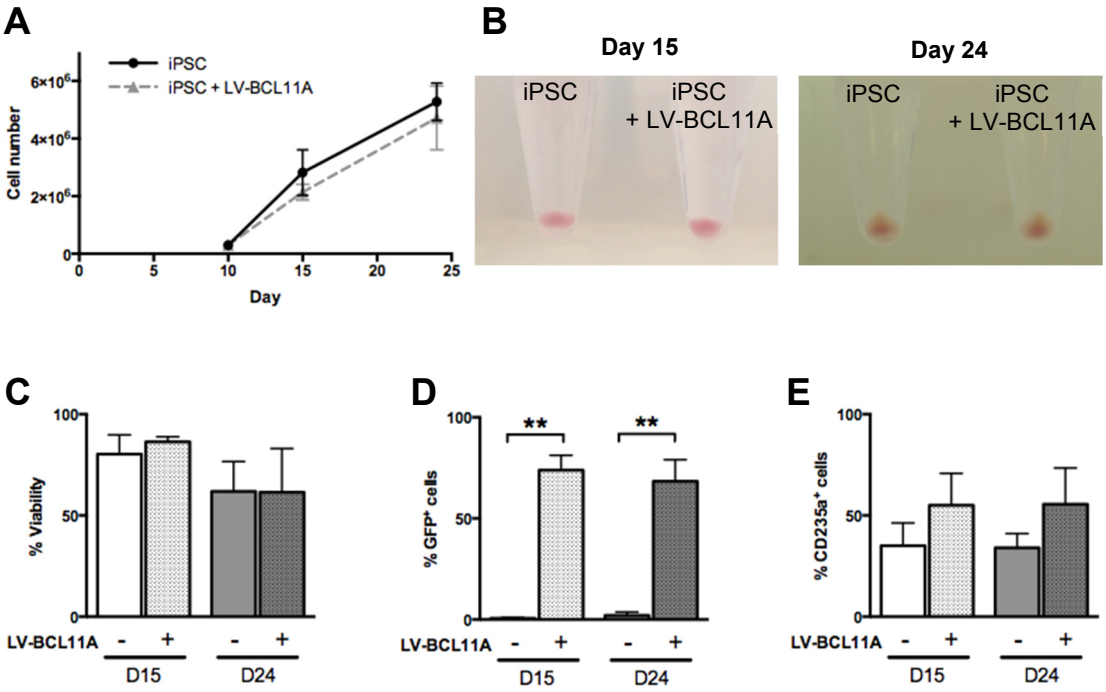

Figure 5.1 Lentivirus-GFP-BCL11A does not enhance erythroid differentiation

Day 10 iPSC-derived cells were transduced with the lentivirus-GFP-BCL11A (LV-BCL11A) at MOI 100. **A.** Total cell numbers were counted during the differentiation process. Data represent the mean of 3 independent experiments and error bars show standard error of the mean (SEM). **B.** Cell pellets of day 15 and 24 differentiating cells in the absence or presence of lentivirus-GFP-BCL11A (LV-BCL11A). **C-E.** Viability (C), transduction efficiency (D) and percentage of $CD235a^+$ cells (E) were analysed by flow cytometry at day 15 (D15) and day 24 (D24). Data represent 3 independent experiments. Error bars represent standard error of the mean (SEM). P values were calculated using one-way ANOVA and multiple comparison test (**, $p < 0.005$).

5.4.1.2 Gene expression analyses

As BCL11A is a key modulator of globin gene expression [120], [121], we sought to assess whether BCL11A transduction could increase the expression of adult globin in differentiating iPSCs. Day 10 differentiating cells were transduced with lentivirus-GFP-BCL11A then analysed by qRT-PCR at days 15 and 24. The expression of *BCL11A* and *HBB* increased significantly in BCL11A-transduced cells at day 15, but there was no effect on the expression of *KLF1*, *SOX6*, *ASHP*, *p21*, *p18* and *HBE1* (Figure 5.2A). Analyses of day 24 cells demonstrated that lentivirus-GFP-BCL11A significantly enhanced the expression of *BCL11A*, *SOX6* and *HBB* and repressed the expression of *HBE1* and *SLC2A4* apparently (Figure 5.2B).

The data suggest that BCL11A transduction promotes the expression of some definitive erythroid genes and represses the expression of embryonic globin.

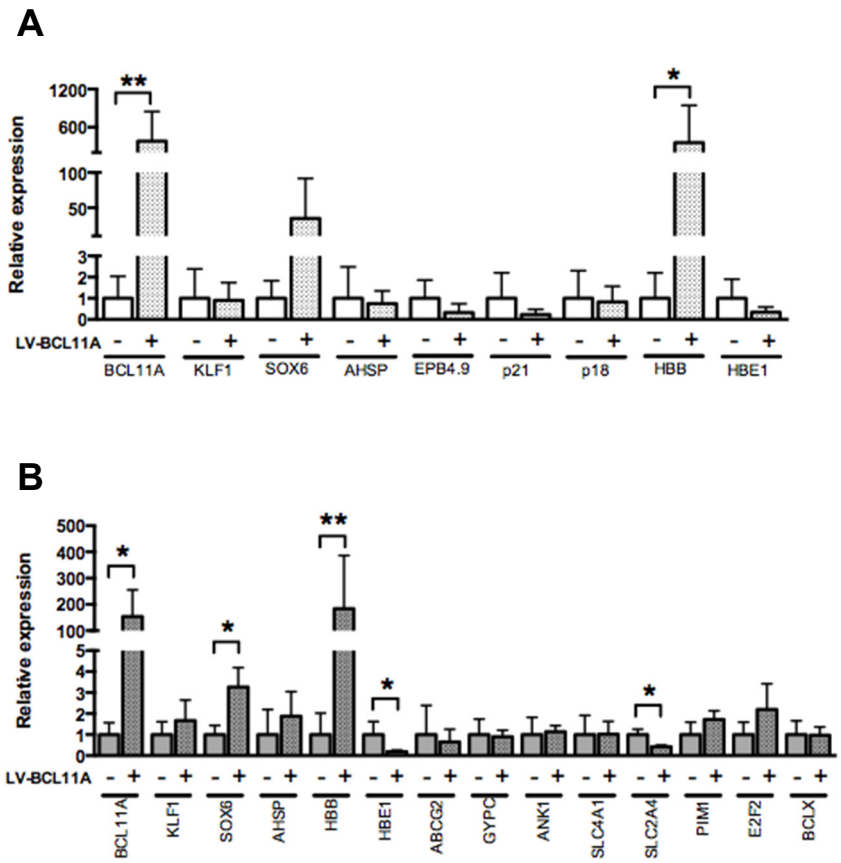

Figure 5.2 Lentivirus-GFP-BCL11A promotes the expression of some definitive erythroid genes

Gene expression was evaluated by qRT-PCR at day 15 (A) and day 24 (B). Differentiating cells were harvested from control iPSC-derived cells (-) and BCL11A-transduced cells (+), and qRT-PCR was conducted using specific primers for genes (*BCL11A, KLF1, SOX6, AHSP, EPB4.9, p21, p18, HBB, HBE1, ABCG2, GYPC, ANK1, SLC4A1, SLC2A4, PIM1, E2F2 and BCLX*). Data represent the mean of 3 independent experiments and error bars show standard error of the mean (SEM**)**. P values were calculated using a ratio paired t test (*, $p<0.05$; **, $p<0.005$).

5.4.1.3 Assessment of globin protein profile

To assess the effects of lentivirus-GFP-BCL11A transduction on the profile of globin proteins, day 24 cell lysates were harvested for HPLC analysis. The result showed that iPSC-derived erythroid cells express Gγ-, Aγ-, α-, ε- and ζ-globins (Figure 5.3A), and a small proportion of β-globin protein was observed in response to lentivirus-GFP-BCL11A transduction (Figure 5.3A). Quantification of the HPLC analyses demonstrated that transduction of BCL11A increased the proportion of β-, Gγ- and α-globins and decreased the percentages of ε- and ζ-globins (Figure 5.3B).

The data indicate that transduction of BCL11A at day 10 increases the production of α-, β-, Gγ- and Aγ-globins, thus some of BCL11A-transduced cells are definitive-like erythroid cells which expressed higher foetal and adult globins.

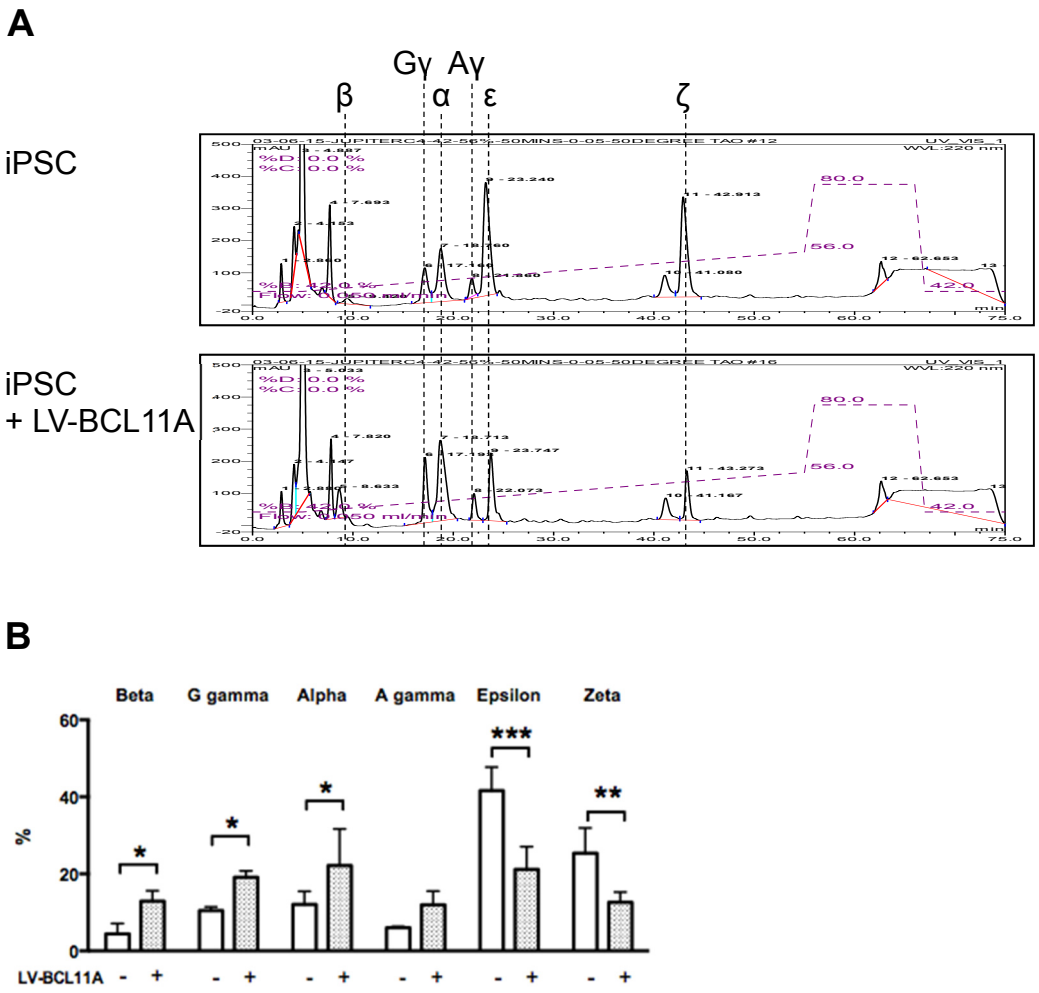

Figure 5.3 Lentivirus-GFP-BCL11A enhances the expression of adult globin

A. HPLC results showed the distribution of embryonic, foetal and adult globin proteins in control and BCL11A transduced iPSCs at day 24. **B.** Percentages of different globins were calculated by measuring the areas under the peaks. Data represent the mean of 3 independent experiments and error bars show standard error of the mean (SEM). P values were calculated using one-way ANOVA and multiple comparison test (*, $p < 0.05$; **, $p < 0.005$; ***, $p < 0.0005$).

5.4.2 Lentivirus-GFP-BCL11A transduction in iKLF1.2 cells

The above results indicated that BCL11A did not promote the production of erythroid cells from iPSCs, but did have an effect on globin switching from embryonic to foetal and adult globins. We next set out to assess whether the enhanced expression of both KLF1 and BCL11A could promote the differentiation of erythroid cells that express adult globin.

5.4.2.1 Cell counts and flow cytometry analysis

To evaluate the effects of both KLF1 and BCL11A, we transduced differentiating cells derived from the iKLF1.2 cell line with the lentivirus-GFP-BCL11A. Cell proliferation was analysed by cell counts, the result showed the lentivirus-GFP-BCL11A transduction caused a massive decrease in cell number while comparing untransduced iKLF1.2-derived cells and BCL11A-transduced iKLF1.2-derived cells (Figure 5.4A). When we activated KLF1 with tamoxifen and transduced BCL11A by lentivirus transduction system, this was detrimental to cell proliferation strictly (Figure 5.4A). The cell pellets harvested at days 15 and 24 were compared to each other, the data showed that lentivirus-GFP-BCL11A lead to a smaller size of cell pellet (Figure 5.4B).

To assess viability, cells were analysed by flow cytometry using 7-AAD viability dye. There was no apparent difference in viability between control iKLF1.2-derived cells and BCL11A-transduced iKLF1.2-derived cells at day 15 of the differentiation process with 60 – 80 % viable cells present (Figure 5.4C). Viability at day 24 dropped to approximately 40 % in BCL11A-transduced cells with tamoxifen activation from day 10 (Figure 5.4C).

The transduction efficiency in iKLF1.2-derived cells was approximately 50 – 60 % as assessed by the proportion of GFP^+ cells (Figure 5.4D). The percentage of $CD235a^+$ cells at day 15 was about 25% in the control group in the absence of KLF1 activation and BCL11A transduction, and the proportion of $CD235a^+$ cells increased to 70 % in cells that had been transduced with BCL11A and KLF1 had been activated from day 10 (Figure 5.4E).

These data demonstrate that although the presence of both BCL11A and KLF1 has an effect on the production of erythroid cells, viral transduction in this context is severely detrimental to cell proliferation.

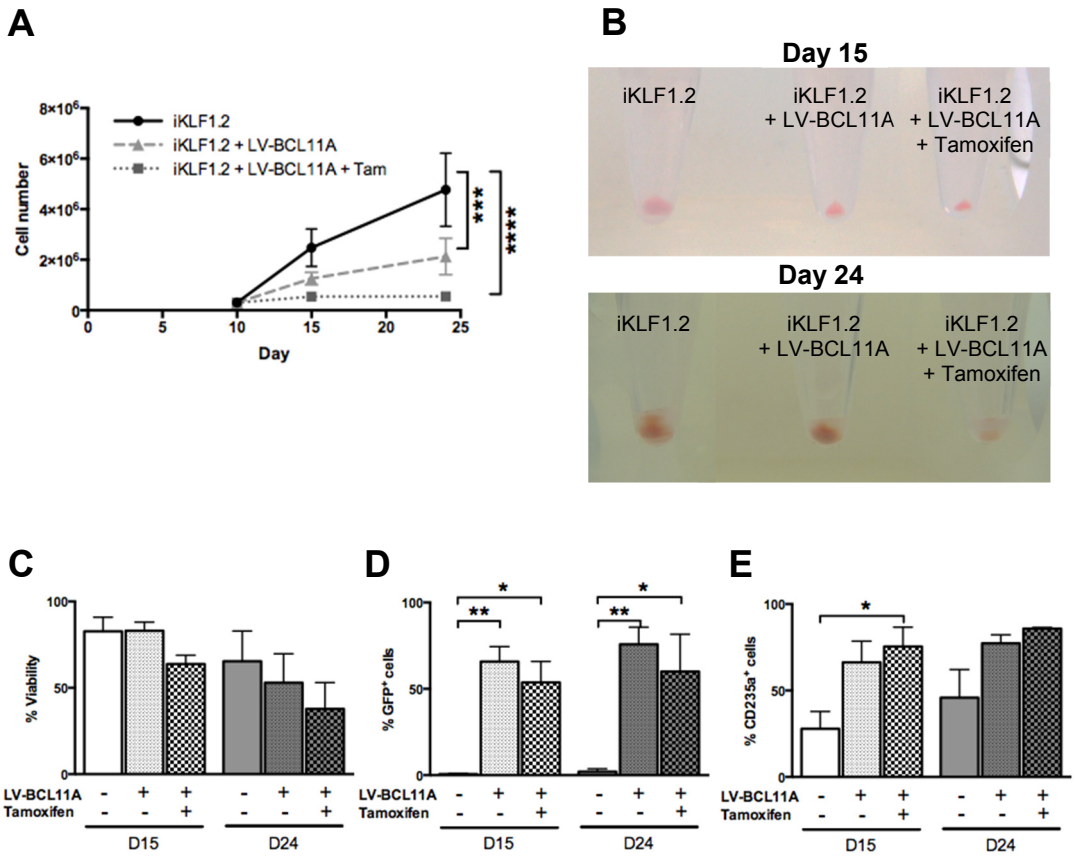

Figure 5.4 Lentivirus-GFP-BCL11A transduction in iKLF1.2-derived cells reduces cell proliferation

Day 10 iKLF1.2 differentiating cells were transduced by lentivirus-GFP-BCL11A (LV-BCL11A) and in the absence (-) or presence (+) of tamoxifen. **A.** Total cell numbers were counted during the differentiation. Data represent the mean of 3 independent experiments and error bars show standard error of the mean (SEM**)**. P values were calculated using two-way ANOVA and multiple comparison test (***, $p < 0.0005$; ****, $p < 0.00005$). **B.** Cell pellets of day 15 and 24 differentiating cells in the absence or presence of lentivirus-GFP-BCL11A (LV-BCL11A) and Tamoxifen. **C-E.** Viability (C), the transduction efficiency (D) and the percentages of $CD235a^+$ cell population (E) were analysed in flow cytometry at day 15 (D15) and day 24 (D24). Data represent 3 independent experiments. Error bars represent standard error of the mean (SEM). P values were calculated using one-way ANOVA and multiple comparison test (*, $p < 0.05$; **, $p < 0.005$).

5.4.2.2 Gene expression analysis

iKLF1.2-derived cells at day 10 were transduced by lentivirus-GFP-BCL11A and treated with or without tamoxifen, and day 15 differentiating cells were harvested for qRT-PCR to assess the gene expression. The results showed that the expression of *BCL11A*, *SOX6* and *HBB* increased significantly in BCL11A-transduced cells and BCL11A-transduced cells plus tamoxifen (Figure 5.5), however, the expression of KLF1 targets, *AHSP*, *EPB4.9*, *p21* and *p18* were not upregulated in the BCL11A-transduced cells in the presence of tamoxifen (Figure 5.5). Because viral transduction led to a significant decrease of cell proliferation, there was insufficient cell number for the qRT-PCR experiment and HPLC analysis at day 24.

These data indicate that BCL11A transduction could increase some definitive erythroid genes, however, we are not able to observe the effect of KLF1 in the BCL11A-transduced iKLF1.2-derived cells.

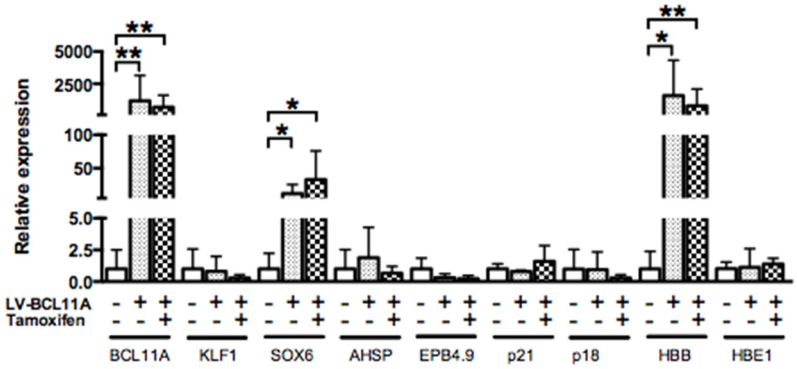

Figure 5.5 Lentivirus-GFP-BCL11A increases the expression of some definitive erythroid genes in iKLF1.2-derived cells

Day 15 differentiating cells were harvested from iKLF1.2-derived cells (LV-BCL11A: -) and BCL11A-transduced iKLF1.2-derived cells (LV-BCL11A: +) in the absence (Tamoxifen: -) and presence of tamoxifen (Tamoxifen: +) from day 10. Quantitative RT-PCR was conducted use specific primers for genes (*BCL11A, KLF1, SOX6, AHSP, EPB4.9, p21, p18, HBB and HBE1*). Data represent 3 independent experiments. Error bars represent standard error of the mean (SEM). P values were calculated using a ratio paired T test (*, $p < 0.05$; **, $p < 0.005$).

5.5 Conclusion

1) The transduction of BCL11A in iPSC-derived cells had no effect on cell proliferation and erythroid differentiation, but BCL11A transduction significantly enhanced the expression of some definitive erythroid genes and repressed the expression of embryonic globin. The HPLC assay also showed that some of BCL11A-transduced cells were definitive-like erythroid cells which expressed higher proportion of foetal and adult globins.
2) Lentivirus-GFP-BCL11A transduction in iKLF1.2-derived cells resulted in a poor cell proliferation and upregulated the expression of some definitive erythroid genes. However, it was difficult to define the effect of KLF1 activation in this viral transduction experiment.

5.6 Discussion

5.6.1 BCL11A transduction in hiPSC-derived erythroid cells increases definitive erythropoiesis but does not enhance the maturation

We first demonstrated that BCL11A-transduced iPSC-derived erythroid cells expressed a higher proportion of foetal / adult globin and a lower proportion of embryonic globin. This indicates BCL11A promotes the definitive erythropoiesis. The small proportion of embryonic globin might result from a primitive cell population which was not transduced successfully by lentivirus-GFP-BCL11A. Since the transduction efficiency at day 15 is approximately 70 %, and 30 % of non-BCL11A-transduced cells might stay at the primitive stage.

The process of globin switching from foetal globin to adult globin requires the cooperation of BCL11A, SOX6 GATA1, MYB and DNMT1, [37], [50], [51]. Our result showed that BCL11A transduction in iPSC-derived cells upregulated the expression of *SOX6* and *HBB*. The possible reason is that BCL11A transduction causes a change to the definitive phenotype, and this definitive phenotype might lead to positive feedback to recruit more co-factors toward definitive erythropoiesis.

We did not observe an increase in erythroid cell production/differentiation nor the upregulation of most erythroid-related genes when cells were transduced with BCL11A. This suggests that enhanced expression of BCL11A does not improve the production and maturation of RBCs from iPSCs. These results support the idea that BCL11A is a co-factor involved in the process of globin switching [146] but not in the production and maturation of erythroid cells [31].

5.6.2 No conclusion of the effects on BCL11A transduction in iKLF1.2-derived erythroid cells

It was not possible to make a conclusion of the effects from both KLF1 and BCL11A, because of the poor cell proliferation when BCL11A has been transduced by lentivirus-GFP-BCL11A and KLF1 has been activated by adding tamoxifen. However, we discuss a couple of points as below.

The expression of *SOX6* and *HBB* increased significantly when comparing iKLF1.2-derived erythroid cells with and without BCL11A transduction, this suggests the lentivirus-GFP-BCL11A has the same effect on iKLF1.2-derived cells and parental iPSC-derived cells (see Section 5.6.1). KLF1 has been reported to target β-globin promoter and regulate its expression [99], however, activation of KLF1 in BCL11A-transduced iKLF1.2-derived cells did not result in higher level expression of *HBB* while comparing to BCL11A-transduced iKLF1.2-derived cells. This could either the level expression of *HBB* reached a plateau or activation of KLF1 was not activated successfully by adding tamoxifen.

To compare the viability post lentiviral transfection, the viability of iPSC-derived cells was 80 % five days post transfection and 55 % fourteen days post transfection and BCL11A-transduced iKLF1.2-derived cells with 60 – 80 % viable cells and 40 – 50 % viable cells present, respectively. This suggests lentiviral transfection might cause more cell death in the iKLF1.2 cell line. However, this part of experiment did not include and empty vector control, therefore, it is not possible to assess whether the effect on reduced cell numbers resulted from lentiviral transduction or from the addition of BCL11A.

5.6.3 Leakiness of ER^{T2} system in iKLF1.2-derived erythroid cells with lentiviral transfection

The lentiviral transfection resulted in a poor cell proliferation in iKLF1.2-derived erythroid cells and our previous result showed that the anti-proliferation effect was caused by KLF1 activation (see Chapter 4 Section 4.6.1). Therefore, there is a possible reason is the leakiness of ER^{T2} system in iKLF1.2-derived erythroid cells while transducing with lentivirus-GFP-BCL11A.

In addition, BCL11A has not been reported to enhance erythropoiesis, and we did not observe the effect of enhancing erythropoiesis when transducing BCL11A in iPSC-derived cells (see Chapter 5 Section 5.6.1). However, we observed a high percentage of erythroid lineage cells in BCL11A-transduced iKLF1.2-derived cells without KLF1 activation, which level is similar to BCL11A-transduced / KLF1-activated cells (Figure 5.4E). This phenomenon supports the point that the leakiness of KLF1-ER^{T2}

occurs in this case. However, we do not have enough cell samples to demonstrate qRT-PCR assay at day 24, so that the effect of enhancing erythroid genes from leakiness of KLF1-ER^{T2} cannot be discussed.

5.6.4 The transduction of lentivirus-GFP-BCL11A

Because of random integration of lentivirus, we were uncertain of a consistent expression of BCL11A in the cells. The random integration could be subjected to silencing and experiments using randomly integrated transgenes are difficult to reproduce [147], [148], however, the mechanisms of silencing from lentivirus vectors have not been characterised.

Also, we do not know whether lentivirus-GFP-BCL11A transduction could reflect the physiological expression of BCL11A in the adult erythroid cells. All these reasons enable us to assess effects of both TFs with difficulties. To overcome these problems, we planned to generate an iPSC cell line in which both BCL11A and KLF1 are expressed in an inducible and comparable manner.

Chapter 6

Generation and evaluation of tamoxifen-inducible BCL11A / KLF1 system in hiPSCs-derived erythroid cells

6.1 Introduction

The activation of KLF1 during erythroid differentiation enhanced erythroid differentiation (see Chapter 4 Section 4.6.2 and Section 4.6.3) and transduction of the BCL11A lentiviral vector increased adult globin expression (see Chapter 5 Section 5.6.1). To assess the effects of *both* transcription factors together using comparable strategies we generated an iPSC cell line in which the *BCL11A-ER^{T2}* and *KLF1-ER^{T2}* transgenes were integrated into each of the two alleles of the *AAVS1* locus. This allowed stable and inducible expression of BCL11A and KLF1 in iPSCs during the differentiation process.

Based on our characterisation in Chapter 3, we believe that the defined differentiation protocol generates a rather heterogeneous cell population likely consisting of both primitive and definitive erythroid cells (see Chapter 3 Section 3.6.1). Analysis of the proportion of CD235a^{+} cells at defined time points revealed two upward trends; the first between days 3 to 10 and the second between days 17 to 24. We hypothesised that this represented two distinct waves of erythropoiesis (see Chapter 3 Section 3.6.2). Activation of KLF1 at the late stage of erythroid differentiation (day 18) had no significant effect on the maturation and adult globin expression (see Chapter 4 Section 4.6.5 and 4.6.6). We hypothesised that KLF1 might require a co-factor, such as BCL11A, for maturation and adult globin expression in the late stage of erythroid cells. Here, we test that hypothesis by activating BCL11A and KLF1 at the late stage of the differentiation process.

6.2 Aim

To assess the effects of activating both BCL11A and KLF1 in iPSCs-derived erythroid cells

6.3 Approaches

1. To generate consistent and reproducible expression of the BCL11A-ER^{T2} and KLF1-ER^{T2} fusion proteins in iPSCs, both transgenes were inserted into the *AAVS1* locus. To verify the iPSC targeted with both *BCL11A-ER^{T2}* and *KLF1-ER^{T2}*, the targeting events were confirmed by PCR assay and fusion proteins were verified by Western blot.
2. To assess the effects of both BCL11A and KLF1 in the late stage of iPSC-derived erythroid cells, the production and maturation of RBCs were analysed by cell counts, qRT-PCR, flow cytometry and HPLC assay.

6.4 Result

All the data in this chapter was generated using one iPSCs clone (iBK7) and we acknowledged that this might be a drawback when interpreting our data. Different iBK lines could be subjected to variations of cell proliferation, differentiation efficiency and their response to tamoxifen treatment etc. We have controlled for the most likely artefactual effects of tamoxifen addition by using the control, parental iPSC cells that do not contain both *BCL11A-ER^{T2}* and *KLF1-ER^{T2}* transgenes but a full analyses of additional iBK clones would support for our conclusions.

6.4.1 Generation of tamoxifen-inducible BCL11A and KLF1 system in hiPSC

6.4.1.1 Tamoxifen inducible BCL11A in COS7 cells

Construction of pZDonor-AAVS1-CAG-BCL11A-ER^{T2}-PA was described in Chapter 2 (Figure 2.3). To confirm that the pZDonor-AAVS1-CAG-BCL11A-ER^{T2}-PA was able to generate the correctly sized BCL11A-ER^{T2} fusion protein in mammalian cells, this vector was transfected into COS7 cells. Cell lysates from COS7 cells transfected with control GFP vector or pZDonor-AAVS1-CAG-BCL11A-ER^{T2}-PA three days post transfection were analysed by Western blotting and the predicted sized fusion protein was detected as 130 KDa consisting of BCL11A (95KDa) and ER^{T2} (35KDa) (Figure 6.1A). The smaller bands that were detected by the anti-BCL11A antibody are possibly degradation products.

To assess whether the BCL11A-ER^{T2} fusion protein could translocate to the nucleus upon addition of tamoxifen, COS7 cells were transfected with pZDonor-AAVS1-CAG-BCL11A-ER^{T2}-PA vector and treated with or without tamoxifen for one day then analysed by IF staining. The BCL11A-ER^{T2} fusion protein was detected by the anti-BCL11A antibody in the cytoplasm in the absence of tamoxifen, but after tamoxifen addition, it was detected in the nucleus (Figure 6.1B).

These data demonstrate that the BCL11A-ER^{T2} fusion protein can be expressed efficiently in COS7 cells and that it can translocate into the nuclei upon tamoxifen induction.

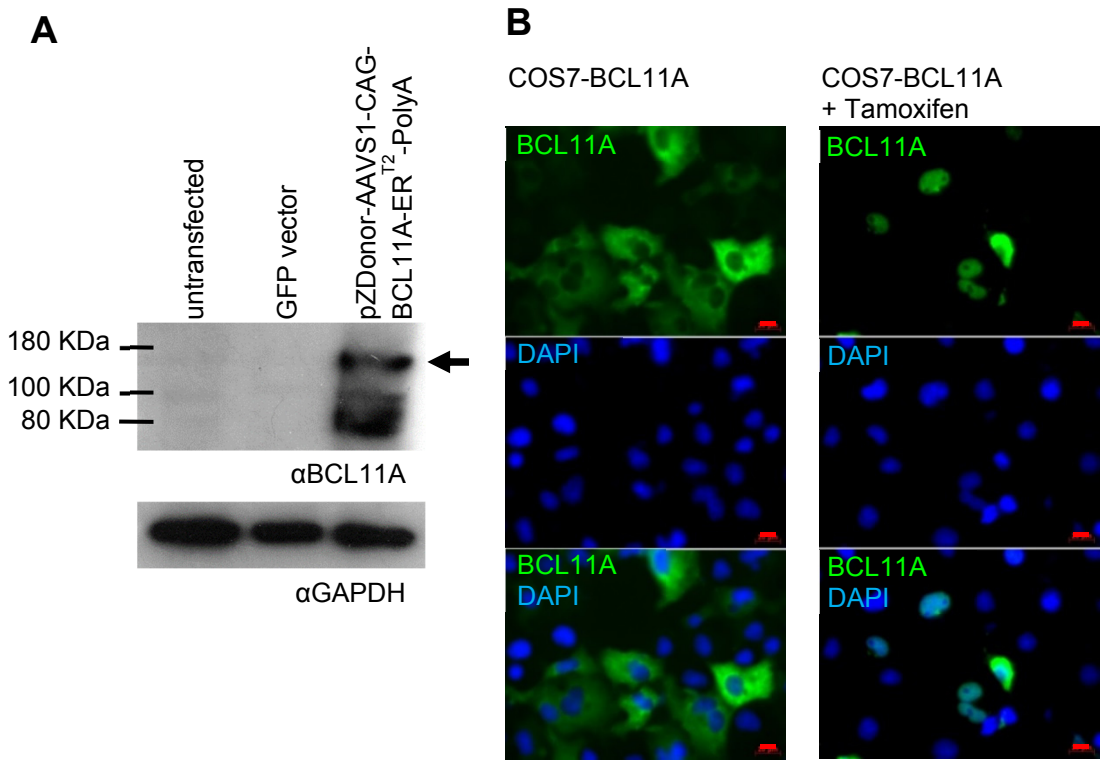

Figure 6.1 The nuclear translocation of tamoxifen inducible BCL11A in COS7 cells

A. The BCL11A-ER^{T2} fusion protein was detected by Western blot using an anti-BCL11A antibody (αBCL11A), and an anti-GAPDH antibody (αGAPDH) was used as a loading control. The predicted fusion protein size is approximately 130KDa (arrow). **B.** Subcellular localisation of the fusion protein was evaluated in transfected COS7 cells (COS7-BCL11A) in the absence and presence of tamoxifen by IF staining with an anti-BCL11A antibody and DAPI nuclei dye. Scale bar = 10 μm.

6.4.1.2 Tamoxifen inducible BCL11A in K562 cells

To further validate the pZDonor-AAVS1-CAG-BCL11A-ER^{T2}-PA construct, we tested it in K562 cells to assess whether the inducible BCL11A-ER^{T2} fusion protein could alter known BCL11A target genes, including *HBB* (β-haemoglobin), *HBE1* (ε1-haemoglobin) and *HBG1* (γ1-haemoglobin). K562 cells were transfected with pZDonor-AAVS1-CAG-BCL11A-ER^{T2}-PA and a stable cell line carrying the *BCL11A-ER^{T2}* transgene was generated by puromycin selection. RNA isolated from untransfected K562 cells and selected K562 cells with *BCL11A-ER^{T2}* following treatment with or without tamoxifen for three days was analysed by qRT-PCR. Activation of BCL11A upregulated *HBB* expression by two fold but no significant effect on the expression of *HBE1* and *HBG1* was observed (Figure 6.2).

This data indicate that the pZDonor-AAVS1-CAG-BCL11A-ER^{T2}-PA is capable of producing a functional BCL11A-ER^{T2} fusion protein that can activate the expression of *HBB* in K562 cells.

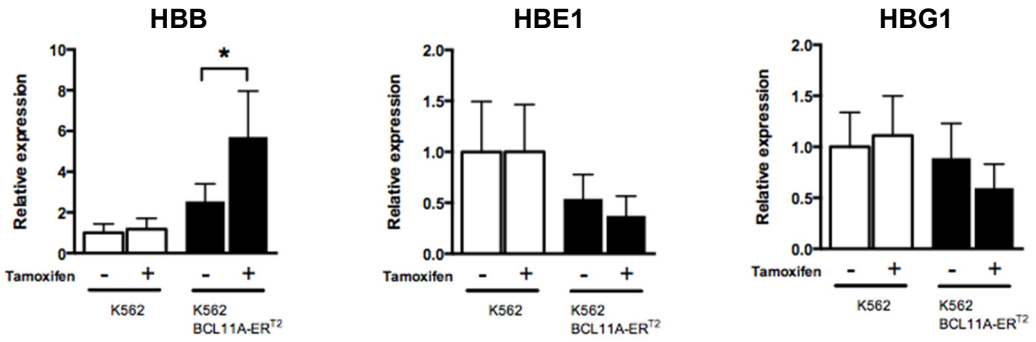

Figure 6.2 The activation of target genes by tamoxifen inducible BCL11A in K562 cells

RNA isolated from untransfected K562 cells (K562) and selected K562 cells with *BCL11A-ER^{T2}* (K562-BCL11A-ER^{T2}) following treatment with (+) or without (-) tamoxifen was analysed by qRT-PCR. The expression of genes was evaluated using primers to *HBB*, *HBE1* and *HBG1*. Data represent the mean of 3 independent experiments and error bars show the standard error of the mean (SEM). A student T test was used to assess the effect of BCL11A activation (*, $p<0.05$).

6.4.1.3 Tamoxifen inducible BCL11A and KLF1 targeted in the *AAVS1* of hiPSCs

Comparable to that described for the production of the iKLF1 cell lines, iPSCs were transfected with pZDonor-AAVS1-CAG-BCL11A-ER^{T2}-PA, pZDonor-AAVS1-CAG-HA-KLF1-ER^{T2}-PA, p622L and p622R by electroporation. After 2 weeks of puromycin selection, 12 selected colonies were expanded in 6 well plates. To analyse genomic DNA from selected cells by PCR, designed internal and external primers were able to generate specific PCR products when both *BCL11A-ER^{T2}* and *KLF1-ER^{T2}* transgenes were targeted into the expected site (Figure 6.3A). The results showed that 7 cell lines had the integration of *BCL11A-ER^{T2}* (Figure 6.3A, PCR 2 (purple)). 8 selected cell lines had the integration of *KLF1-ER^{T2}* (Figure 6.3A, PCR 3 (blue)). 9 selected cell lines had the correct integration in the *AAVS1* alleles (Figure 6.3A, PCR 4 (red) and PCR 5 (green). In this experiment, 4 selected cell lines were double targeted with both *BCL11A-ER^{T2}* and *KLF1-ER^{T2}* transgenes into each of the *AAVS1* alleles, which were iBK3, iBK6, iBK7 and iBK10 cell lines (Figure 6.3A).

For further confirmation of the double targeting event, we tested these 4 iBK cell lines by PCR analysis using the external primer recognising genomic *AAVS1* region and internal primers recognising either *BCL11A* or *KLF1* (Figure 6.3B). In this PCR assay, the correct predicted size of PCR products was generated from genomic DNA samples of these 4 selected cell lines, iBK3, iBK6, iBK7 and iBK10. The efficiency of targeting both alleles was 33% (Figure 6.3B).

We also addressed whether these 4 iBK cell lines could express both the *BCL11A-ER^{T2}* and *KLF1-ER^{T2}* transgenes. We prepared cDNAs from iBK3, iBK6, iBK7 and iBK10 cell lines and assessed the gene expression by PCR. The result showed that iBK7 and iBK10 expressed *BCL11A-ER^{T2}*, and iBK3, iBK6 and iBK7 were able to express *KLF1-ER^{T2}* (Figure 6.3C).

Cell lysates from iBK3, iBK6, iBK7 and iBK10 cell lines were collected for Western blot to analyse whether the fusion proteins BCL11A-ER^{T2} and HA-KLF1-ER^{T2} were produced. iBK7 and iBK10 cell lines expressed the expected proteins BCL11A-ER^{T2} which was approximately 130 KDa (Figure 6.3D). Consistent with PCR results, the

KLF1-ER^{T2} fusion protein (74 KDa) was detectable in iBK3, iBK6 and iBK7 cell lines (Figure 6.3D). In conclusion, the iBK7 cell line is the only clone that stably expresses both BCL11A-ER^{T2} and HA-KLF1-ER^{T2} fusion proteins.

To further validate the targeting result, genomic DNA from the iBK7 clone was analysed by Southern blot using an internal probe (Supplementary Figure S1A and B). An expected band 3.9 Kb was detected in iBK7 compared to the 6.4 Kb band in parental iPSCs. When we analysed genomic DNA using the external probe (Supplementary Figure S1C and D), an expected band 9.1 Kb was detected when the transgene *BCL11A-ER^{T2}* was correctly inserted into *AAVS1* locus. However, we did not detect the expected band 7.7 Kb band for the correct insertion of the *HA-KLF1-ER^{T2}* transgene (Supplementary Figure S1C and D). This could either result from inefficient or failed digestion, genomic rearrangement of the locus during integration or from a randomly integrated *HA-KLF1-ER^{T2}* transgene. Given the time constraints of this work, we were unable to distinguish unequivocally between these alternative explanations. As we had shown that both fusion proteins were expressed in the undifferentiated iBK7 iPSCs, we went ahead and used this iBK7 clone to evaluate the effects of both BCL11A and KLF1 on erythropoiesis but kept this point in mind in the interpretation our results.

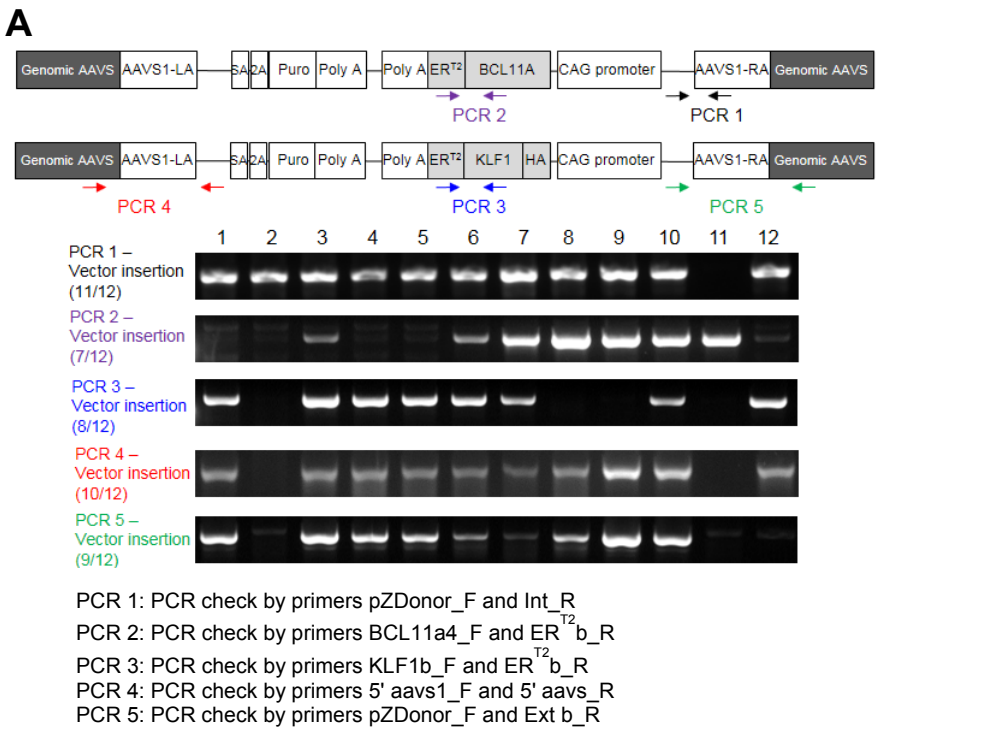

PCR 1: PCR check by primers pZDonor_F and Int_R
PCR 2: PCR check by primers BCL11a4_F and ER^{T2}b_R
PCR 3: PCR check by primers KLF1b_F and ER^{T2}b_R
PCR 4: PCR check by primers 5' aavs1_F and 5' aavs_R
PCR 5: PCR check by primers pZDonor_F and Ext b_R

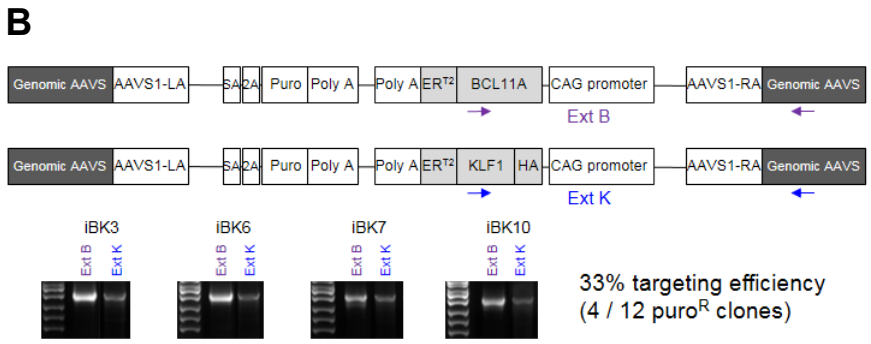

Ext B: PCR check by primers BCL11a1_R and Ext b_R
Ext K: PCR check by primers KLF1b_R and Ext b_R

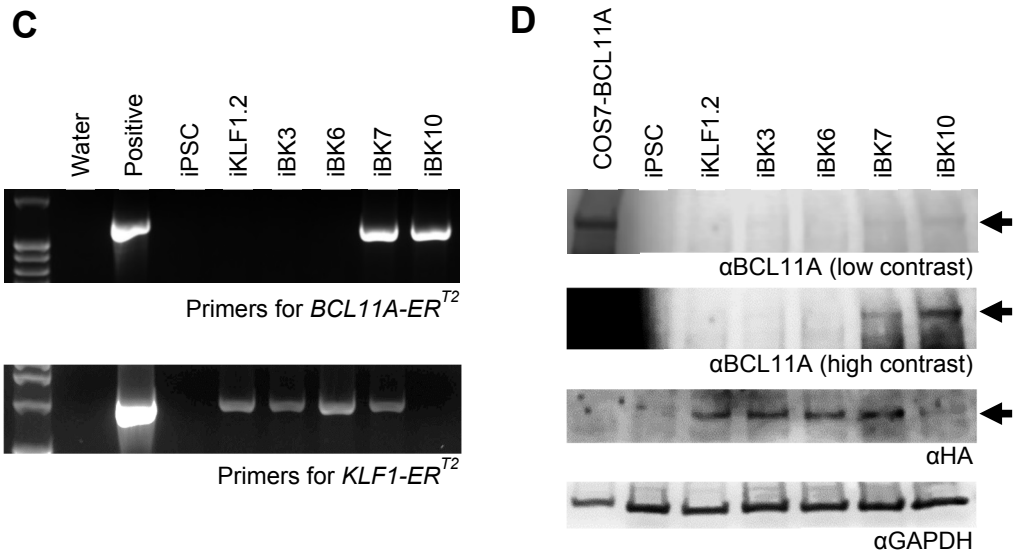

Figure 6.3 Tamoxifen inducible BCL11A and KLF1 targeted in the *AAVS1* of hiPSCs

A. The locations of diagnostic internal and external primers were shown in a schematic of *AAVS1* targeting site. PCR products 1, 2 and 3 were generated by internal primers, and PCR products 4 and 5 were generated by external primers. (AAVS1-LA, AAVS1 left homology arm; SA, splice acceptor; 2A, a self-cleaving peptide sequence; Puro, puromycin resistance gene; Poly A, polyadenylation sequence; AAVS1-RA, AAVS1 right homology arm). **B.** iBK3, iBK6, iBK7 and iBK10 cell lines were further confirmed by PCR analysis. The PCR products were labelled as Ext B in colour purple for *BCL11A-ER^{T2}* integration and Ext K in colour blue for *KLF1-ER^{T2}* integration. **C.** The expression of *BCL11A-ER^{T2}* and *KLF1-ER^{T2}* transgenes in iBK3, iBK6, iBK7 and iBK10 cell lines. The cDNA samples from 4 iBK cell lines were analysed by PCR using particular primers for *BCL11A-ER^{T2}* and *HA-KLF1-ER^{T2}*. **D.** Western blot of control cell lysates (including BCL11A-transfected-COS7 cells, parental iPSC and iKLF1.2) and cell lysates from iBK3, iBK6, iBK7 and iBK10. Fusion proteins BCL11A-ER^{T2} and HA-KLF1-ER^{T2} were detectable by using anti-BCL11A (αBCL11A) and anti-HA tag (αHA) antibodies, and anti-GAPDH (αGAPDH) antibody was used as a loading control. The predicted protein size was 130 KDa of BCL11A-ER^{T2} and 74 KDa of HA-KLF1-ER^{T2} (arrows).

6.4.2 Evaluation of activated-BCL11A and KLF1 during the differentiation from day 18

Our defined differentiation protocol likely generates both primitive and definitive erythroid cells. The appearance of CD235a$^+$ cells occurs in two periods from day 3 to 10 and from day 17 to 24, which suggests that there are two distinct waves of erythropoiesis. We observed no effect of activating KLF1 at the late stage of erythroid differentiation (day 18) and hypothesised that KLF1 might require a co-factor, such as BCL11A, to regulate maturation and globin expression at the late stage of erythroid differentiation. To test this hypothesis, the effects of activating both BCL11A and KLF1 in the late stage of iBK7-derived erythroid cells (day 18) was evaluated (Figure 6.4A).

6.4.2.1 Assessment of phenotype, cell proliferation and viability

To evaluate the phenotype, flow cytometry analyses of erythroid marker CD235a and erythroblast marker CD71 was performed on cells at day 24 and day 31 following treatment with tamoxifen from day 18 of the differentiation protocol. There was no obvious effect on the proportion of cells expressing CD235a and CD71 when both TFs were activated compared to controls (data not shown).

$3x10^5$ day 10 differentiating cells were seeded and further differentiated in the presence or absence of tamoxifen from day 18. Cell proliferation was assessed by counting cells over the next 20 days and we noted that activation of BCL11A and KLF1 at the late stage had no effect on the proliferation rate (Figure 6.4B).

Cell Viability at day 24 and 31 was assessed by flow cytometry using LIVE/DEAD™ Fixable Near-IR Stain (Figure 6.4C). Viability decreased from 40 % at day 24 to 20 % at day 31 in both iPSC-derived cells and iBK7-derived cells, but this was not affected by the activation of BCL11A and KLF1.

RNA isolated from iPSC and iBK7-derived cells at day 24 following treatment with or without tamoxifen from day 18 was evaluated by qRT-PCR (Figure 6.4D). We first confirmed that there was no significant effect of tamoxifen treatment on control iPSC-derived cells. In contrast, the expression of *PIM1, E2F2, BCLX* and *p27* was

upregulated in iBK7-derived cells upon activation of both BCL11A and KLF1, although the increases, although statistically significant, were only 0.2 fold.

Taken together, activation of BCL11A and KLF1 in the late stage of differentiating cells does not change the phenotype, proliferation rate nor viability, but the expression of some genes associated with cell proliferation and cell cycling were slightly upregulated.

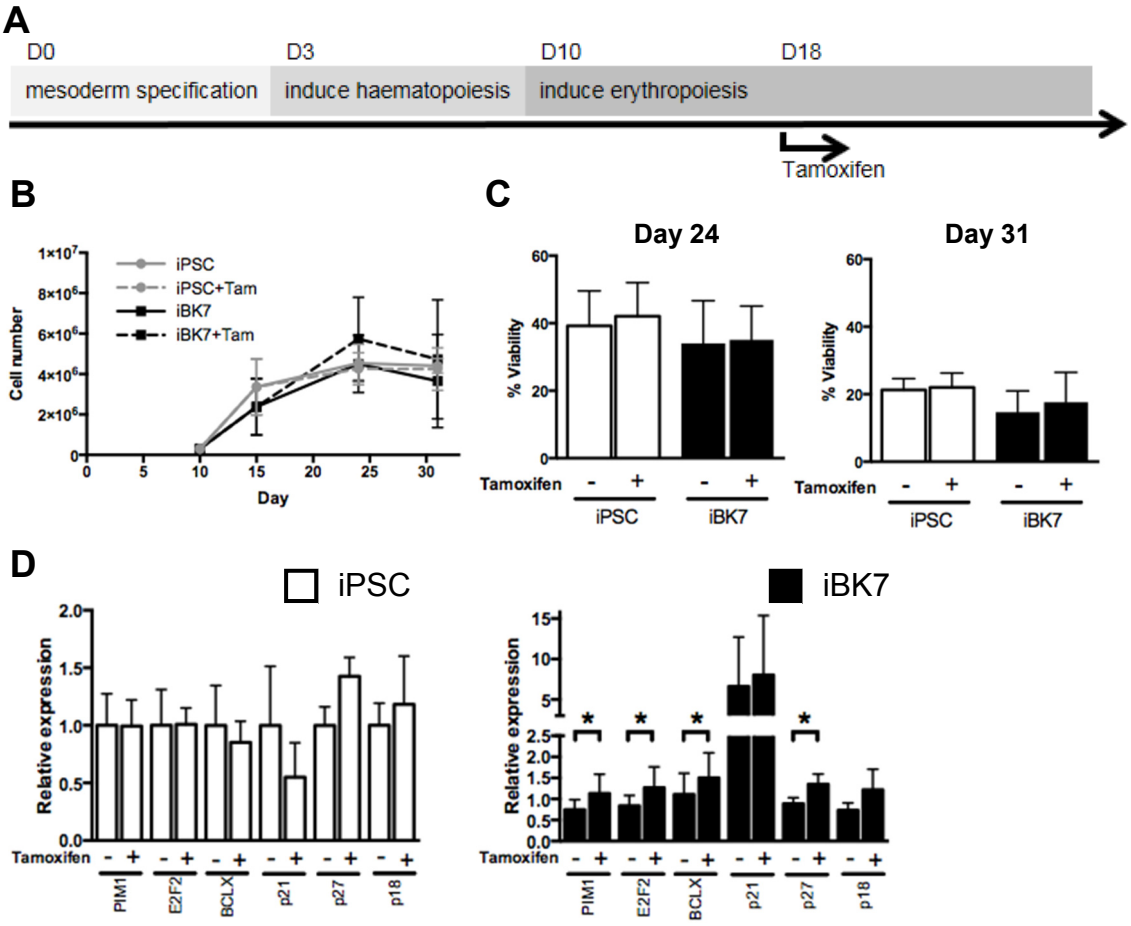

Figure 6.4 Activation of BCL11A and KLF1 at the late stage of erythroid differentiation does not change cell proliferation rate and viability

A. Diagram showing the activation of both BCL11A and KLF1 by adding tamoxifen from day 18 during erythroid differentiation. **B.** Cell number of control iPSC-derived cells (iPSC) and iBK7-derived cells (iBK7) in the presence (+) and absence (-) of tamoxifen. Data represent the mean of 3 independent experiments and error bars show standard error of the mean (SEM). **C.** The viability present at day 24 and 31 of the erythroid differentiation protocol. Data represent 3 independent experiments. Error bars represent standard error of the mean (SEM). **D.** Quantitative RT-PCR analyses at day 24 using primers to *PIM1, E2F2, BCLX, p21, p27* and *p18.* Data represent the mean of 3 independent experiments and error bars show the standard error of the mean (SEM). A ratio paired T test was used to assess the effect of both BCL11A and KLF1 activation (*, $p<0.05$).

6.4.2.2 Assessment of erythroid maturation

To assess gene expression, RNA isolated from differentiating cells at day 24 following treatment with or without tamoxifen was assessed by qRT-PCR (Figure 6.5). We firstly confirmed that tamoxifen treatment did not alter the gene expression in control iPSC-derived cells. Activation of both BCL11A and KLF1 in iBK7-derived cells from day 18 increased the expression of *GYPC, SLC4A1, EPB4.9* and *ABCG2*, genes that are associated with RBC maturity.

The data indicate that BCL11A / KLF1-activated erythroid cells express more transcripts associated with RBC maturation.

6.4.2.3 Assessment of enucleation

We assessed the enucleation efficiency in these BCL11A / KLF1-activated erythroid cells but no significant effect were observed. The rate of enucleation was approximately 3 % both in the presence and absence of activation. (data not shown)

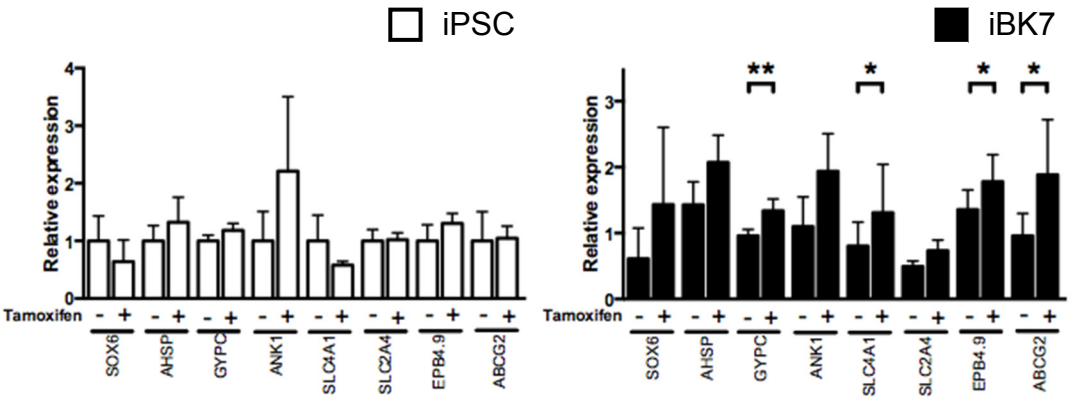

Figure 6.5 Activation of BCL11A and KLF1 at the late stage of erythroid differentiation increases some erythroid genes

Quantitative RT-PCR analyses of RNA isolated from control iPSC-derived cells and iBK7-derived cells at day 24 in the presence (+) and absence (-) of tamoxifen from day 18 using primers to *SOX6, AHSP, GYPC, ANK1, SLC4A1, SLC2A4, EPB4.9* and *ABCG2.* Data represent the mean of 3 independent experiments and error bars show the standard error of the mean (SEM). A ratio paired T test was used to assess the effect of both TFs activation in iBK7 cells (*, $p<0.05$; **, $p<0.005$).

6.4.2.4 Assessment of globin protein profile

Differentiating cells on day 31 were harvested for HPLC analysis to evaluate globin protein profile (Figure 6.6). The result showed that parental iPSC-derived cells and iBK7-derived erythroid cells contained β-, Gγ-, Aγ-, α-, ε- and ζ-globins, but β-globin protein was represented relatively low. Quantification of the HPLC analyses demonstrated that the percentage of α-globin increased significantly in tamoxifen-treated iBK7-derived erythroid cells, but no difference was observed in the proportion of other globins.

HPLC data indicate that activation of both BCL11A and KLF1 from day 18 increases the production of α-globin, thus this indicates the presence of some definitive-like erythroid cells might be enhanced by activation of both TFs at the late stage of erythroid differentiation.

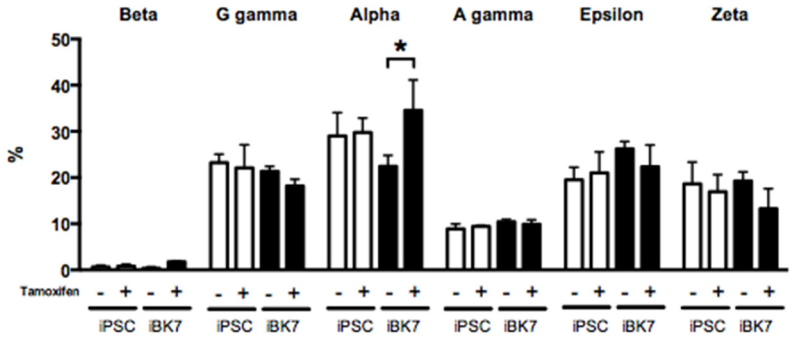

Figure 6.6 Activation of BCL11A and KLF1 from day 18 increases α-globin

The globin profiles of differentiating cells derived from control iPSC and iBK7 at day 31 of the differentiation protocol in the presence (+) or absence (-) of tamoxifen from day 18. The amount of the different globins (Beta, G gamma, Alpha, A gamma, Epsilon and Zeta) was calculated as the areas under the peaks and represented as a percentage of the total globin. Data represent the mean of 3 independent experiments and error bars show standard error of the mean (SEM). P values were calculated using two-way ANOVA followed by multiple comparisons test. (*, $p<0.05$).

6.5 Conclusion

1) We generated iPSC cell lines with inducible BCL11A and KLF1 double targeted to *AAVS1* locus. After the confirmation of PCR analysis and Western blot, iBK7 cell line was the only one clone expressing both BCL11-ER^{T2} and KLF1-ER^{T2} fusion proteins. Therefore, we decided to use iBK7 cell line to evaluate the effects of both BCL11A and KLF1 on erythropoiesis.
2) Activation of BCL11A and KLF1 from day 18 of the differentiation protocol did not change the phenotype, cell proliferation and viability, but some transcripts related to RBC maturity were slightly upregulated. Interestingly, HPLC data showed that activation of BCL11A and KLF1 at the late stage increased the production of α-globin.

6.6 Discussion

6.6.1 Human iPSC with double targeted BCL11A-ER^{T2} and KLF1-ER^{T2} in the *AAVS1* locus

Erythropoiesis is a complex procedure and involves many TFs. KLF1 plays a pivotal role in the RBC maturation [23], [26], [108], [110], [144], and BCL11A is a vital factor to complete globin switching from foetal globin to adult globin [37], [49], [50], [149]. To set up a stable and inducible expression system where we could enhance the expression of both of these TFs in differentiating iPSCs, we generated iPSC with double targeted *BCL11A-ER^{T2}* and *KLF1-ER^{T2}* in the *AAVS1* locus.

It was difficult to obtain an iPSC cell line with double targeted *BCL11A-ER^{T2}* and *KLF1-ER^{T2}* in both alleles of *AAVS1* locus correctly. Genomic DNA of iBK7 iPSCs was analysed by PCR and Southern blot, the PCR result showed that both transgenes were correctly targeted into each of the *AAVS1* alleles. However, Southern blot indicated that an unexpected band (likely 11.6 Kb) was observed in iBK7 genomic DNA samples using an internal probe and an external probe (Supplementary Figure S1), we deduced that it might be an un-digested fragment from *KLF1-ER^{T2}* targeted allele. This could result from partial digestion while digesting genomic DNA. Since we can see a more intense band in the iBK7 sample than in the iKLF1.2 sample (Supplementary Figure S1), this might indicate too much amount of DNA loading while preparing digestion reaction. If the restriction enzyme SphI works completely in the genomic DNA digestion, an expected band 7.7 Kb might be detected using an external probe. Alternatively, genomic rearrangement of the *AAVS1* locus might occur during integration, we also cannot rule out the possibility of random integration of *HA-KLF1-ER^{T2}* transgene. However, we believe that KLF1-ER^{T2} in iBK7 iPSCs was functional but not silenced by above considerations, because the same genes upregulated as the iKLF1.2 cell line (see Chapter 4 Section 4.4.1.2 and Section 4.4.1.3) were observed while activating both BCL11A and KLF1 from day 18, including *PIM1*, *BCLX*, *p27*, *GYPC*, *SLC4A1* and *ABCG2*.

The iBK7 cell line was the only one clone co-expressing BCL11A-ER^{T2} and KLF1-ER^{T2} fusion proteins, so that it was chosen to evaluate the effect of BCL11A and KLF1 during erythroid differentiation. We further compared the expression level of BCL11A and KFL1 among CD34^{+}-derived cells, iPSC-derived cells, iKLF1.2-derived cells and iBK7-derived cells by qRT-PCR (Supplementary Figure S4), the level expression of

KLF1 in undifferentiated iBK7 and iBK7-derived cells was lower than in undifferentiated iKLF1.2 and iKLF1.2-derived cells. This might be due to the fact that the iKLF1.2 cell line has two *AAVS1* alleles targeted with *KLF1-ER^{T2}* transgenes whereas the iBK7 cell line only has one allele targeted with this transgene. The lower expression of KLF1 in iBK7 iPSCs may account for slight effects of promoting erythropoiesis while activating KLF1 from day 10 in iKLF1.2 cell line (see Chapter 4 Section 4.6.2 and Section 4.6.3).

6.6.2 BCL11A appears to eliminate anti-proliferation effect of KLF1

KLF1 enhanced erythroid differentiation and this was coupled with a reduced proliferation, because it is involved in erythroid lineage commitment and helps control exit from the cell cycle [143], [144]. This proliferation arrest was observed when KLF1 was activated at the HPC stage (day 10) and at the late stage of erythroid differentiation (day 18)(see Chapter 4 Section 4.6.1). Interestingly, we did not observe a reduction in proliferation when both BCL11A and KLF1 were activated from day 18, and the expression of *PIM1* (cell survival), *E2F2* (cell proliferation) and *BCLX* (anti-apoptosis) were slightly upregulated. Thus activation of both KLF1 and BCL11A did not cause proliferation arrest in the late stage of erythroid cells. A possible explanation for this could be related to the fact that BCL11A is known to be involved in the regulation of cell cycle [46], [47], [89] and so might overcome the KLF1-associated proliferation arrest in the late stage of erythroid cells.

6.6.3 Effect of BCL11A and KLF1 on RBC maturation

Activation of both BCL11A and KLF1 at the late stage of erythroid cells (day 18) did not change the erythroid phenotype, this was consistent with our result that KLF1 activation did not alter the phenotype in the late stage of erythroid cells (see Chapter 4 Section 4.4.2.1). However, activation of both TFs from day 18 slightly increased the erythroid transcripts, including of *GYPC, SLC4A1, EPB4.9* and *ABCG2*, this was not observed in activation of KLF1 at the late stage (see Chapter 4 Section 4.4.2.3). This supports our hypothesis that KLF1 needs a co-factor to regulate gene expression associated with RBC maturation.

6.6.4 Effect of BCL11A and KLF1 on globin protein profile

The regulation of adult globin expression is complex and involves many factors, including KLF1 [22], [25], [28], [29], SOX6 [38], BCL11A [31], [37], [49], GATA-1 [50], MYB and DNMT1 [51]. Our result showed that only KLF1 activation from day 10 increases embryonic globin and decreases foetal globin (see Chapter 4 Section 4.4.1.4), but KLF1 activation from day 18 had no significant effect on globin protein profile (see Chapter 4 Section 4.4.2.4). Activation of both BCL11A and KLF1 from day 18 increased the percentage of α-globin (foetal / adult globin), indicating that BCL11A has an impact in the late stage of erythroid cells and enhances some definitive-like erythroid cells to expression foetal / adult globin.

BCL11A is down-regulated during haematopoietic cell differentiation [150], this is consistent with our result that the expression of BCL11A was decreased in the differentiating iPSC, differentiating iKLF1.2 cells and differentiating iBK7 cells (Supplementary Figure S4A). However, adult β-globin was not detected when BCL11A and KLF1 were activated in iBK7-derived cells, which could be due to the low level expression of BCL11A and KLF1 in differentiating iBK7 cells (Supplementary Figure S4A). Furthermore, BCL11A is regulated strictly during erythropoiesis and more co-factors might be required in the regulation of adult globin expression, including SOX6 [37], GATA1 [50], MYB and DNMT1 [51].

6.6.5 Comparison between iBK7 and iKLF1.2 clones

The effects of erythroid cell production and maturation in iBK7 cells and iKLF1.2 cells has been discussed above, however, it proved difficult to directly compare these two different clones. A study of cancer cell lines has reported that parental lines and some sublines derived from the limiting dilution method are characterised differently in plating efficiency, cell population doubling time and cell saturation density [151]. Hence, the iBK7 clone and the iKLF1.2 clone might have phenotypically different cell proliferations, varied differentiation efficiency, various sensitivities and responses of tamoxifen treatment etc. This might lead to a difficulty of evaluating effects due to the addition of BCL11A or due to differences between iBK7 clone and iKLF1.2 clone.

Chapter 7
Summary and Perspectives

7.1 Summary

We utilised a defined differentiation protocol for *in vitro* production of RBCs from hiPSCs. The defined differentiation protocol was capable of generating erythroid cells from iPSCs, but we noted fragile morphology, poor enucleation rate and enriched primitive erythroid cells. We considered that these deficiencies could result from a low level expression of KLF1 in the iPSC-derived cells compared to $CD34^{+}$-derived cells.

The iKLF1.2 cell line was then generated with *KLF1-ER^{T2}* targeted in the *AAVS1* locus of iPSCs. Activation of KLF1 at the HPC stage (from day 10) enhanced erythroid differentiation but we also observed an anti-proliferation effect. Erythroid genes associated with RBC maturation were upregulated upon activating KLF1, this might explain more robust erythroid cells according to the cell morphology. Those KLF1-activated erythroid cells with healthier property resulted in a higher level of enucleated cell detected in an enucleation assay. However, activating KLF1 from day 10 led to a higher level of embryonic globin, which indicated KLF1 promoted the primitive erythropoiesis.

When we activated KLF1 at the later stage of erythroid differentiation (from day 18), the effect of proliferation arrest was again observed but the enhancement of erythropoiesis was not detected with no significant effect on the proportion of erythroid cells, on erythroid gene expression, globin protein expression nor enucleation. Collectively, we deduced that KLF1 promoted erythropoiesis at the progenitor stage but had no effect on the phenotype of the cells when induced at later stages.

Adult globin was not expressed in iPSC-derived cells and KLF1-activated erythroid cells, this might result from low expression of BCL11A, which plays a key role in the suppression of foetal globin expression, thereby completing globin switching to adult globin. Our preliminary data showed that iPSC-derived erythroid cells were able to express adult globin when transduced with a BCL11A-expressing lentiviral-vector. Based on that finding, we therefore generated the iBK7 iPSC line that expressed both tamoxifen-inducible BCL11A-ER^{T2} and KLF1-ER^{T2} fusion proteins, the iBK7 cell

line was applied to our differentiation protocol and activated BCL11A and KLF1 by adding tamoxifen.

Activation of BCL11A and KLF1 from day 18 did not promote erythropoiesis as assessed by the phenotype and proportion of erythroid lineage cells, but it slightly increased the expression of some genes associated with erythroid maturation. Of note, the inclusion of BCL11A appeared to eliminate the anti-proliferation effect of KLF1 (see Chapter 6 Section 6.6.2). HPLC data showed that activation of both TFs at the late stage increased the production of α-globin (foetal / adult globin). This suggested BCL11A had an effect in the late stage of erythroid cells to promote definitive erythropoiesis.

7.2 Perspectives

7.2.1 Enrichment of definitive erythroid cells

We believe that our defined differentiation protocol likely gives rise to a rather heterogeneous cell population containing both primitive and definitive erythroid cells, making it difficult to evaluate the impact specifically on primitive and/or definitive erythroid cells. Keller's group has reported that CD235a is a marker for primitive haematopoietic progenitors at early time points in differentiating human PSC, and the cells from KDR^{+} $CD235a^{-}$ mesoderm can go through definitive haematopoiesis [152]. This suggests sorting out $CD235a^{-}$ cells at the early stage of erythroid differentiation might enrich definitive erythroid progenitors. We performed a pilot experiment where $CD235a^{+}$ and $CD235a^{-}$ cells were sorted from iBK7-derived cells at day 10, and the resultant day 31 differentiated cells from these two cell populations were assessed by HPLC. We observed that the cells from $CD235a^{+}$ sorted cells expressed lower proportion of Gγ-globin (foetal globin) and higher proportion of ε-globin (embryonic globin) (data not shown). Further experiments are in progress.

Due to the fact that perhaps our defined differentiation protocol does not generate definitive erythroid progenitors and adult-like progenitors, that might be the reason why we did not see the obvious effect of KLF1 in definitive erythropoiesis. An important TF in adult haematopoiesis, RUNX1, has been revealed that it is required for functional HSCs in the AGM region [43], [44]. Some studies regard SOX6 and MYB as markers for definitive erythropoiesis [12], [30], [32]. We may optimise the culture condition to enrich definitive erythroid progenitors and adult-like progenitors by monitoring the level expression of *RUNX1*, *SOX6* and *MYB*.

7.2.2 Inducing definitive erythropoiesis using other TFs

The activation of KLF1 from day 18 has no effect on globin expression and activation of both BCL11A and KLF1 in the late stage of erythroid cells increased the percentage of α-globin (foetal / adult globin), indicating that co-factor has an impact on the expression of foetal / adult globin (definitive erythropoiesis). *Sox6* and *Myb* are expressed in definitive erythropoiesis but not in primitive erythropoiesis [12], [30], [32], and both of them have been reported to repress embryonic globin [37], [38], [51].

Additionally, SOX6 is an important enhancer of definitive erythropoiesis to stimulate cell survival, proliferation, and terminal maturation [36]. Moreover, a recent study has been reported that committed murine blood cells are able to be reprogrammed to induced haematopoietic stem cells (iHSCs) by defined TFs, RUNX1T1, HLF, LMO2, PRDM5, PBX1, and ZFP37 [90]. Another study has indicated that the TF cocktail (GATA1, TAL1, LMO2, c-MYC, and KLF1 /or MYB) converts murine and human fibroblasts into iEPs and results in iEPs-derived cells expressing more adult globin [93]. This result raises a possible prospect of blood cell repogramming for clinical application. Therefore, it might be worthwhile inducing SOX6 and MYB during erythroid differentiation and evaluating the definitive erythroid development.

7.2.3 Identify the stage of erythroid development in the defined differentiation protocol

There are four main differentiation stages in this defined protocol, including mesoderm specification, haematopoiesis, erythropoiesis and maturation (Figure 2.1), however, we have not yet identified the stage of erythrocytes during the differentiation. So that activation of TFs from day 18 might not be the critical time point to enhance the production and maturation of RBCs. A live image study has reported that nuclear import of KLF1 occurs during the ProE to BasoE transition [145], and this suggests KLF1 target genes are activated for RBC maturation during this period. Also, the nuclear import in the specific developmental stage might be associated with adult globin expression. Therefore, the developmental stage should be determined using morphological analysis in our defined differentiation protocol, activation of KLF1 in the ProE stage might result in significant effects of promoting definitive erythropoiesis.

7.2.4 TFs work in different time points

From data acquired in this thesis, we deduce that KLF1 activation promotes erythropoiesis at the HPC stage (day 10) but not at the late stage of erythroid differentiation (day 18). Moreover, activation of BCL11A and KLF1 has an effect of increasing α-globin (foetal / adult globin) in the late stage of erythroid cells (day 18). This indicates different erythroid TFs work in particular stages, but it is impossible to activate BCL11A and KLF1 in different time point by the same tamoxifen inducible

system. Therefore, various inducible systems may be considered, for example combination of tamoxifen inducible system and doxycycline inducible system, however, it has been reported to reveal leakiness of both systems [142], [153]. Another strategy is activating endogenous gene, a recent study has revealed that CRISPR-based synergistic activation mediator (SAM) is a useful tool to investigate genetic regulation of stem cell differentiation through CRISPR-mediated activation of endogenous genes [154]. The later strategy might be a better strategy to induce endogenous gene expression without genome editing.

7.2.5 Mimic microenvironment for erythroid maturation - erythroblastic island *in vitro*

KLF1 activation from day 10 enhanced erythropoiesis and increased erythroid maturation (see Chapter 4 Section 4.6.2 and Section 4.6.3), but it is possible that effects result from activation of KLF1 in other cells that provide an extrinsic effect. Given the heterogeneity from our differentiation protocol, macrophages appeared in the differentiating culture (Figure 3.3A and Figure 4.5A). Macrophages recently have been reported to promote erythropoiesis [48]. Co-culture with macrophages decreased transit time in the G0/G1 phase of erythroblasts, thereby enhancing erythroblast proliferation [61]. $CD169^+$ / $CD163^+$ / $VCAM1^+$ macrophages in erythroblastic island are identified to promote late erythroid maturation [155]. Therefore, erythroblastic islands provide a unique microenvironment for the proliferation and maturation of RBCs. Furthermore, a recent report has revealed that KLF1 has an extrinsic role in erythroid maturation via expression of KLF1 in erythroblastic island associated macrophages [113], their data indicate that KLF1 activates the expression of *Vcam1* in macrophages and this might promote erythropoiesis through the interaction with erythrocytes [113]. Additionally, KLF1 induces the expression of *DNase2a* in macrophages, and *DNase2a* encodes a nuclease which digests pyrenocytes at the conclusion of erythroid maturation [156]. Current work in the Forrester lab is aimed at assessing the effects of KLF1 in the macrophage microenvironment during the *in vitro* differentiation of iPSC-derived erythroid cells.

References

[1] J. L. Carson, B. J. Grossman, S. Kleinman, A. T. Tinmouth, M. B. Marques, M. K. Fung, J. B. Holcomb, O. Illoh, L. J. Kaplan, L. M. Katz, S. V Rao, J. D. Roback, A. Shander, A. a R. Tobian, R. Weinstein, L. Grace, S. Mclaughlin, B. Djulbegovic, C. Transfusion, and M. Committee, "Annals of Internal Medicine Clinical Guideline Red Blood Cell Transfusion : A Clinical Practice Guideline From the AABB *," vol. 1, 2012.

[2] A. D'Alessandro, G. Liumbruno, G. Grazzini, and L. Zolla, "Red blood cell storage: the story so far.," *Blood Transfus.*, vol. 8, no. 2, pp. 82–8, Apr. 2010.

[3] C. Whitsett, S. Vaglio, and G. Grazzini, "Alternative blood products and clinical needs in transfusion medicine.," *Stem Cells Int.*, vol. 2012, p. 639561, Jan. 2012.

[4] J. Palis, "Hematopoietic stem cell-independent hematopoiesis: emergence of erythroid, megakaryocyte, and myeloid potential in the mammalian embryo," *FEBS Lett.*, pp. 1–10, 2016.

[5] M. C. Yoder, "Inducing definitive hematopoiesis in a dish," *Nat. Biotechnol.*, vol. 32, no. 6, pp. 539–541, 2014.

[6] E. Mass, I. Ballesteros, M. Farlik, F. Halbritter, P. Günther, L. Crozet, C. E. Jacome-galarza, K. Händler, J. Klughammer, Y. Kobayashi, E. Gomez-, J. L. Schultze, M. Beyer, C. Bock, and F. Geissmann, "Specification of tissue-resident macrophages during organogenesis," *Science (80-.).*, vol. 4238, no. August, p. epub, 2016.

[7] E. L. Soucie, Z. Weng, L. Geirsdottir, K. Molawi, J. Maurizio, R. Fenouil, N. Mossadegh-Keller, G. Gimenez, L. VanHille, M. Beniazza, J. Favret, C. Berruyer, P. Perrin, N. Hacohen, J.-C. Andrau, P. Ferrier, P. Dubreuil, A. Sidow, and M. H. Sieweke, "Lineage-specific enhancers activate self-renewal genes in macrophages and embryonic stem cells," *Science (80-.).*, vol. 351, no. 6274, p. aad5510, 2016.

[8] J. Palis, S. Robertson, M. Kennedy, C. Wall, and G. Keller, "Development of erythroid and myeloid progenitors in the yolk sac and embryo proper of the mouse.," *Development*, vol. 126, no. 22, pp. 5073–5084, 1999.

[9] P. D. Kingsley, J. Malik, K. A. Fantauzzo, and J. Palis, "Yolk sac-derived primitive erythroblasts enucleate during mammalian embryogenesis," *Blood*, vol. 104, no. 1, pp. 19–25, 2004.

[10] P. D. Kingsley, J. Malik, R. L. Emerson, T. P. Bushnell, K. E. McGrath, L. A. Bloedorn, M. Bulger, and J. Palis, "'Maturational' globin switching in primary primitive erythroid cells," *Blood*, vol. 107, no. 4, pp. 1665–1672, 2006.

[11] T. Trimborn, J. Gribnau, F. Grosveld, and P. Fraser, "Mechanisms of developmental control of transcription in the murine α- and β-globin loci," pp. 112–124, 1999.

[12] V. G. Sankaran and S. H. Orkin, "The switch from fetal to adult hemoglobin," *Cold Spring Harb. Perspect. Med.*, vol. 3, no. 1, p. a011643, Jan. 2013.

[13] J. Palis, J. Malik, K. E. McGrath, and P. D. Kingsley, "Primitive erythropoiesis in the mammalian embryo," *Int. J. Dev. Biol.*, vol. 54, no. 6–7, pp. 1011–1018, 2010.

[14] S. T. Fraser, J. Isern, and M. H. Baron, "Maturation and enucleation of primitive erythroblasts during mouse embryogenesis is accompanied by changes in cell-surface antigen expression," *Blood*, vol. 109, no. 1, pp. 343–352, 2007.

[15] Y. Fujiwara, C. P. Browne, K. Cunniff, S. C. Goff, and S. H. Orkin, “Arrested development of embryonic red cell precursors in mouse embryos lacking transcription factor GATA-1.,” *Proc. Natl. Acad. Sci. U. S. A.*, vol. 93, no. 22, pp. 12355–12358, 1996.
[16] A. P. Tsang, Y. Fujiwara, D. B. Horn, and S. H. Orkin, “Failure of megakaryopoiesis and arrested erythropoiesis in mice lacking the GATA-1 transcriptional cofactor FOG,” *Genes Dev.*, vol. 12, no. 8, pp. 1176–1188, 1998.
[17] A. J. Warren, W. H. Colledge, M. B. L. Carlton, M. J. Evans, A. J. H. Smith, and T. H. Rabbitts, “The Oncogenic Cysteine-rich LIM domain protein Rbtn2 is essential for erythroid development,” *Cell*, vol. 78, no. 1, pp. 45–57, 1994.
[18] M. Mukhopadhyay, A. Teufel, T. Yamashita, A. D. Agulnick, L. Chen, K. M. Downs, A. Schindler, A. Grinberg, S. P. Huang, D. Dorward, and H. Westphal, “Functional ablation of the mouse Ldb1 gene results in severe patterning defects during gastrulation,” *Development*, vol. 130, no. 3, pp. 495–505, 2003.
[19] R. a Shivdasani, E. L. Mayer, and S. H. Orkin, “Absence of blood formation in mice lacking the T-cell leukaemia oncoprotein tal-1/SCL.,” *Nature*, vol. 373, no. 6513. pp. 432–434, 1995.
[20] P. E. Love, C. Warzecha, and L. Li, “Ldb1 complexes: The new master regulators of erythroid gene transcription,” *Trends Genet.*, vol. 30, no. 1, pp. 1–9, 2014.
[21] T. Yokomizo, K. Hasegawa, H. Ishitobi, M. Osato, M. Ema, Y. Ito, M. Yamamoto, and S. Takahashi, “Runx1 is involved in primitive erythropoiesis in the mouse,” *Blood*, vol. 111, no. 8, pp. 4075–4080, 2008.
[22] C. J. Pang, W. Lemsaddek, Y. N. Alhashem, C. Bondzi, L. C. Redmond, N. Ah-Son, C. I. Dumur, K. J. Archer, J. L. Haar, J. a. Lloyd, and M. Trudel, “Kruppel-Like Factor 1 (KLF1), KLF2, and Myc Control a Regulatory Network Essential for Embryonic Erythropoiesis,” *Mol. Cell. Biol.*, vol. 32, no. 13, pp. 2628–2644, 2012.
[23] A. C. Perkins, A. H. Sharpe, and S. H. Orkin, “Lethal beta-thalassaemia in mice lacking the erythroid CACCC-transcription factor EKLF.,” *Nature*, vol. 375, pp. 318–322, 1995.
[24] J. Isern, S. T. Fraser, Z. He, H. Zhang, and M. H. Baron, “Dose-dependent regulation of primitive erythroid maturation and identity by the transcription factor Eklf,” *Blood*, vol. 116, no. 19, pp. 3972–3980, 2010.
[25] P. Basu, T. K. Lung, W. Lemsaddek, T. G. Sargent, D. C. Williams, M. Basu, L. C. Redmond, J. B. Lingrel, J. L. Haar, and J. A. Lloyd, “EKLF and KLF2 have compensatory roles in embryonic β-globin gene expression and primitive erythropoiesis,” *Blood*, vol. 110, no. 9, pp. 3417–3425, 2007.
[26] R. Drissen, M. von Lindern, A. Kolbus, S. Driegen, P. Steinlein, H. Beug, F. Grosveld, and S. Philipsen, “The erythroid phenotype of EKLF-null mice: defects in hemoglobin metabolism and membrane stability.,” *Mol. Cell. Biol.*, vol. 25, no. 12, pp. 5205–5214, 2005.
[27] D. Hodge, E. Coghill, J. Keys, T. Maguire, B. Hartmann, A. McDowall, M. Weiss, S. Grimmond, and A. Perkins, “A global role for EKLF in definitive and primitive erythropoiesis,” *Blood*, vol. 107, no. 8, pp. 3359–3370, 2006.
[28] D. S. Vinjamur, K. J. Wade, S. F. Mohamad, J. L. Haar, S. T. Sawyer, and J.

A. Lloyd, “Krüppel-like transcription factors KLF1 and KLF2 have unique and coordinate roles in regulating embryonic erythroid precursor maturation,” *Haematologica*, vol. 99, no. 10, pp. 1565–1573, 2014.

[29] Y. N. Alhashem, D. S. Vinjamur, M. Basu, U. Klingmüller, K. M. L. Gaensler, and J. A. Lloyd, “Transcription factors KLF1 and KLF2 positively regulate embryonic and fetal β-globin genes through direct promoter binding,” *J. Biol. Chem.*, vol. 286, no. 28, pp. 24819–24827, 2011.

[30] K. E. McGrath, J. M. Frame, G. J. Fromm, A. D. Koniski, P. D. Kingsley, J. Little, M. Bulger, and J. Palis, “A transient definitive erythroid lineage with unique regulation of the β-globin locus in the mammalian embryo.,” *Blood*, vol. 117, no. 17, pp. 4600–8, Apr. 2011.

[31] V. G. Sankaran, J. Xu, T. Ragoczy, G. C. Ippolito, C. R. Walkley, S. D. Maika, Y. Fujiwara, M. Ito, M. Groudine, M. a Bender, P. W. Tucker, and S. H. Orkin, “Developmental and species-divergent globin switching are driven by BCL11A,” *Nature*, vol. 460, no. 7259, pp. 1093–1097, 2009.

[32] J. Palis, “Primitive and definitive erythropoiesis in mammals,” *Front. Physiol.*, vol. 5 JAN, no. January, pp. 1–9, 2014.

[33] A. C. Perkins, K. R. Peterson, G. Stamatoyannopoulos, H. E. Witkowska, and S. H. Orkin, “Fetal expression of a human Agamma globin transgene rescues globin chain imbalance but not hemolysis in EKLF null mouse embryos.,” *Blood*, vol. 95, pp. 1827–1833, 2000.

[34] M. N. Gnanapragasam, K. E. Mcgrath, S. Catherman, L. Xue, J. Palis, and J. J. Bieker, “EKLF / KLF1-regulated cell cycle exit is essential for erythroblast enucleation,” vol. 128, no. 12, pp. 1631–1642, 2016.

[35] P. D. Kingsley, E. Greenfest-allen, J. M. Frame, T. P. Bushnell, J. Malik, K. E. Mcgrath, C. J. Stoeckert, and J. Palis, “Ontogeny of erythroid gene expression,” vol. 121, no. 6, pp. 5–14, 2015.

[36] B. Dumitriu, M. R. Patrick, J. P. Petschek, S. Cherukuri, U. Klingmuller, P. L. Fox, and V. Lefebvre, “Sox6 cell-autonomously stimulates erythroid cell survival, proliferation, and terminal maturation and is thereby an important enhancer of definitive erythropoiesis during mouse development,” *Blood*, vol. 108, no. 4, pp. 1198–1207, 2006.

[37] J. Xu, V. G. Sankaran, M. Ni, T. F. Menne, R. V. Puram, W. Kim, and S. H. Orkin, “Transcriptional silencing of γ-globin by BCL11A involves long-range interactions and cooperation with SOX6,” *Genes Dev.*, vol. 24, no. 8, pp. 783–789, 2010.

[38] Z. Yi, O. Cohen-Barak, N. Hagiwara, P. D. Kingsley, D. a Fuchs, D. T. Erickson, E. M. Epner, J. Palis, and M. H. Brilliant, “Sox6 directly silences epsilon globin expression in definitive erythropoiesis.,” *PLoS Genet.*, vol. 2, no. 2, p. e14, Mar. 2006.

[39] M. L. Mucenski, K. McLain, A. B. Kier, S. H. Swerdlow, C. M. Schreiner, T. A. Miller, D. W. Pietryga, W. J. Scott, and S. S. Potter, “A functional c-myb gene is required for normal murine fetal hepatic hematopoiesis,” *Cell*, vol. 65, pp. 677–689, 1991.

[40] L. Borges, M. Iacovino, T. Mayerhofer, N. Koyano-nakagawa, J. Baik, D. J. Garry, M. Kyba, M. Letarte, R. C. R. Perlingeiro, and W. Dc, “A critical role for endoglin in the emergence of blood during embryonic development A critical role for endoglin in the emergence of blood during embryonic

development," vol. 119, no. 23, pp. 5417–5428, 2012.
[41] E. Dzierzak and S. Philipsen, "Erythropoiesis: development and differentiation.," *Cold Spring Harb. Perspect. Med.*, vol. 3, no. 4, p. a011601, Apr. 2013.
[42] M. F. T. R. De Bruijn, X. Ma, C. Robin, K. Ottersbach, M. Sanchez, and E. Dzierzak, "to the Endothelial Cell Layer in the Midgestation Mouse Aorta," vol. 16, pp. 673–683, 2002.
[43] Z. Cai, M. de Bruijn, X. Ma, B. Dortland, T. Luteijn, R. J. Downing, and E. Dzierzak, "Haploinsufficiency of AML1 affects the temporal and spatial generation of hematopoietic stem cells in the mouse embryo.," *Immunity*, vol. 13, no. 4, pp. 423–431, 2000.
[44] Y. Mukouyama, N. Chiba, T. Hara, H. Okada, Y. Ito, R. Kanamaru, a Miyajima, M. Satake, and T. Watanabe, "The AML1 transcription factor functions to develop and maintain hematogenic precursor cells in the embryonic aorta-gonad-mesonephros region.," *Dev. Biol.*, vol. 220, no. 1, pp. 27–36, 2000.
[45] C. Lancrin, M. Mazan, M. Stefanska, R. Patel, M. Lichtinger, G. Costa, O. Vargel, N. K. Wilson, T. Möröy, C. Bonifer, B. Göttgens, V. Kouskoff, and G. Lacaud, "GFI1 and GFI1B control the loss of endothelial identity of hemogenic endothelium during hematopoietic commitment.," *Blood*, vol. 120, no. 2, pp. 314–22, Jul. 2012.
[46] J. C. H. Tsang, Y. Yu, S. Burke, F. Buettner, C. Wang, A. A. Kolodziejczyk, S. A. Teichmann, L. Lu, and P. Liu, "Single-cell transcriptomic reconstruction reveals cell cycle and multi-lineage differentiation defects in Bcl11a-deficient hematopoietic stem cells.," *Genome Biol.*, vol. 16, no. 1, p. 178, 2015.
[47] S. Luc, J. Huang, J. L. McEldoon, E. Somuncular, D. Li, C. Rhodes, S. Mamoor, S. Hou, J. Xu, and S. H. Orkin, "Bcl11a Deficiency Leads to Hematopoietic Stem Cell Defects with an Aging-like Phenotype," *Cell Rep.*, vol. 16, no. 12, pp. 3181–3194, 2016.
[48] J. A. Chasis and N. Mohandas, "Erythroblastic islands : niches for erythropoiesis," vol. 112, no. 3, pp. 470–479, 2016.
[49] Z. Chen, H. Luo, M. H. Steinberg, and D. H. K. Chui, "BCL11A represses HBG transcription in K562 cells.," *Blood Cells. Mol. Dis.*, vol. 42, no. 2, pp. 144–9, 2009.
[50] K. Jawaid, K. Wahlberg, S. L. Thein, and S. Best, "Binding patterns of BCL11A in the globin and GATA1 loci and characterization of the BCL11A fetal hemoglobin locus.," *Blood Cells. Mol. Dis.*, vol. 45, no. 2, pp. 140–6, Aug. 2010.
[51] M. Roosjen, B. McColl, B. Kao, L. J. Gearing, M. E. Blewitt, and J. Vadolas, "Transcriptional regulators Myb and BCL11A interplay with DNA methyltransferase 1 in developmental silencing of embryonic and fetal β-like globin genes," *FASEB J.*, vol. 28, no. 4, pp. 1610–1620, 2014.
[52] J. Liu, X. Guo, N. Mohandas, J. A. Chasis, and X. An, "Membrane remodeling during reticulocyte maturation," *Blood*, vol. 115, no. 10, pp. 2021–2027, 2010.
[53] K. E. McGrath, P. D. Kingsley, A. D. Koniski, R. L. Porter, T. P. Bushnell, and J. Palis, "Enucleation of primitive erythroid cells generates a transient population of 'pyrenocytes' in the mammalian fetus," *Blood*, vol. 111, no. 4,

pp. 2409–2417, 2008.
[54] A. Manuscript, “Formation of mammalian erythrocytes chromatin condensation and enucleation,” vol. 21, no. 7, pp. 409–415, 2012.
[55] S. R. Jayapal, K. L. Lee, P. Ji, P. Kaldis, B. Lim, and H. F. Lodish, “Down-regulation of Myc is essential for terminal erythroid maturation,” *J. Biol. Chem.*, vol. 285, no. 51, pp. 40252–40265, 2010.
[56] P. Ji, V. Yeh, T. Ramirez, M. Murata-Hori, and H. F. Lodish, “Histone deacetylase 2 is required for chromatin condensation and subsequent enucleation of cultured mouse fetal erythroblasts,” *Haematologica*, vol. 95, no. 12, pp. 2013–2021, 2010.
[57] S. T. Koury, M. J. Koury, and M. C. Bondurant, “Cytoskeletal distribution and function during the maturation and enucleation of mammalian erythroblasts,” *J. Cell Biol.*, vol. 109, no. 6 I, pp. 3005–3013, 1989.
[58] H. Takano-Ohmuro, M. Mukaida, and K. Morioka, “Distribution of actin, myosin, and spectrin during enucleation in erythroid cells of hamster embryo.,” *Cell Motil. Cytoskeleton*, vol. 34, no. 2, pp. 95–107, 1996.
[59] D. G. Konstantinidis, S. Pushkaran, J. F. Johnson, J. A. Cancelas, S. Manganaris, C. E. Harris, D. A. Williams, Y. Zheng, and T. A. Kalfa, “Signaling and cytoskeletal requirements in erythroblast enucleation,” *Blood*, vol. 119, no. 25, pp. 6118–6127, 2012.
[60] J. Wang, T. Ramirez, P. Ji, S. R. Jayapal, H. F. Lodish, and M. Murata-Hori, “Mammalian erythroblast enucleation requires PI3K-dependent cell polarization,” *J. Cell Sci.*, vol. 125, no. 2, pp. 340–349, 2012.
[61] M. M. Rhodes, P. Kopsombut, M. C. Bondurant, J. O. Price, and M. J. Koury, “Adherence to macrophages in erythroblastic islands enhances erythroblast proliferation and increases erythrocyte production by a different mechanism than erythropoietin,” *Blood*, vol. 111, no. 3, pp. 1700–1708, 2008.
[62] S. Soni, S. Bala, B. Gwynn, K. E. Sahr, L. L. Peters, and M. Hanspal, “Absence of erythroblast macrophage protein (Emp) leads to failure of erythroblast nuclear extrusion,” *J. Biol. Chem.*, vol. 281, no. 29, pp. 20181–20189, 2006.
[63] A. Iavarone, E. R. King, X.-M. Dai, G. Leone, E. R. Stanley, and A. Lasorella, “Retinoblastoma promotes definitive erythropoiesis by repressing Id2 in fetal liver macrophages,” *Nature*, vol. 432, no. 7020, pp. 1040–1045, 2004.
[64] V. P. Patel and H. F. Lodish, “A fibronectin matrix is required for differentiation of murein erythroleukemia cells into erythrocytes.,” *J. Cell Biol.*, vol. 105, no. 6, pp. 3105–3118, 1987.
[65] S. M. Hattangadi, P. Wong, L. Zhang, J. Flygare, H. F. Lodish, and W. Dc, “From stem cell to red cell : regulation of erythropoiesis at multiple levels by multiple proteins , RNAs , and chromatin modifications,” *Blood*, vol. 118, no. 24, pp. 6258–6268, 2011.
[66] L. Zhang, J. Flygare, P. Wong, B. Lim, and H. F. Lodish, “miR-191 regulates mouse erythroblast enucleation by down-regulating Riok3 and Mxi1,” *Genes Dev.*, vol. 25, no. 2, pp. 119–124, 2011.
[67] S. Rouzbeh, L. Kobari, M. Cambot, C. Mazurier, N. Hebert, A. M. Faussat, C. Durand, L. Douay, and H. Lapillonne, “Molecular signature of erythroblast enucleation in human embryonic stem cells,” *Stem Cells*, vol. 33, no. 8, pp. 2431–2441, 2015.

[68] G. Keerthivasan, S. Small, H. Liu, A. Wickrema, J. D. Crispino, and W. Dc, "Vesicle trafficking plays a novel role in erythroblast enucleation Vesicle trafficking plays a novel role in erythroblast enucleation," *Cancer*, vol. 116, no. 17, pp. 3331–3340, 2011.
[69] M.-C. Giarratana, L. Kobari, H. Lapillonne, D. Chalmers, L. Kiger, T. Cynober, M. C. Marden, H. Wajcman, and L. Douay, "Ex vivo generation of fully mature human red blood cells from hematopoietic stem cells.," *Nat. Biotechnol.*, vol. 23, no. 1, pp. 69–74, 2005.
[70] A. Fujimi, T. Matsunaga, M. Kobune, Y. Kawano, T. Nagaya, I. Tanaka, S. Iyama, T. Hayashi, T. Sato, K. Miyanishi, T. Sagawa, Y. Sato, R. Takimoto, T. Takayama, J. Kato, S. Gasa, H. Sakai, E. Tsuchida, K. Ikebuchi, H. Hamada, and Y. Niitsu, "Ex vivo large-scale generation of human red blood cells from cord blood CD34+ cells by co-culturing with macrophages," *Int. J. Hematol.*, vol. 87, no. 4, pp. 339–350, 2008.
[71] K. Miharada, T. Hiroyama, K. Sudo, T. Nagasawa, and Y. Nakamura, "Efficient enucleation of erythroblasts differentiated in vitro from hematopoietic stem and progenitor cells," *Nat. Biotechnol.*, vol. 24, no. 10, pp. 1255–1256, 2006.
[72] D. Boehm, W. G. Murphy, and M. Al-Rubeai, "The potential of human peripheral blood derived CD34+ cells for ex vivo red blood cell production," *J. Biotechnol.*, vol. 144, no. 2, pp. 127–134, 2009.
[73] R. E. Griffiths, S. Kupzig, N. Cogan, T. J. Mankelow, V. M. S. Betin, K. Trakarnsanga, E. J. Massey, J. D. Lane, S. F. Parsons, and D. J. Anstee, "Maturing reticulocytes internalize plasma membrane in glycophorin A-containing vesicles that fuse with autophagosomes before exocytosis," *Blood*, vol. 119, no. 26, pp. 6296–6306, 2012.
[74] J. a. Thomson, "Embryonic Stem Cell Lines Derived from Human Blastocysts," *Science (80-.).*, vol. 282, no. 5391, pp. 1145–1147, Nov. 1998.
[75] K. Takahashi, K. Tanabe, M. Ohnuki, M. Narita, T. Ichisaka, K. Tomoda, and S. Yamanaka, "Induction of pluripotent stem cells from adult human fibroblasts by defined factors.," *Cell*, vol. 131, no. 5, pp. 861–72, Nov. 2007.
[76] J. Dias, M. Gumenyuk, H. Kang, M. Vodyanik, J. Yu, J. a Thomson, and I. I. Slukvin, "Generation of red blood cells from human induced pluripotent stem cells.," *Stem Cells Dev.*, vol. 20, no. 9, pp. 1639–47, Sep. 2011.
[77] C. Qiu, E. N. Olivier, M. Velho, E. E. Bouhassira, and W. Dc, "Globin switches in yolk sac – like primitive and fetal-like definitive red blood cells produced from human embryonic stem cells," vol. 111, no. 4, pp. 2400–2408, 2011.
[78] K. Y. Lee, B. S. P. Fong, K. S. Tsang, T. K. Lau, P. C. Ng, A. C. Lam, K. Y. Y. Chan, C. C. Wang, H. F. Kung, C. K. Li, and K. Li, "Fetal stromal niches enhance human embryonic stem cell-derived hematopoietic differentiation and globin switch.," *Stem Cells Dev.*, vol. 20, no. 1, pp. 31–38, 2011.
[79] M. Sciences, S. N. Blood, T. Service, and U. Kingdom, "High-Efficiency Serum-Free Feeder-Free Erythroid Differentiation of Human Pluripotent Stem Cells Using Small Molecules," pp. 1–12, 2016.
[80] H. Sakamoto, K. Tsuji-Tamura, and M. Ogawa, "Hematopoiesis from pluripotent stem cell lines," *Int. J. Hematol.*, vol. 91, no. 3, pp. 384–391, 2010.
[81] M. C. Nostro, X. Cheng, G. M. Keller, and P. Gadue, "Wnt, Activin, and BMP

Signaling Regulate Distinct Stages in the Developmental Pathway from Embryonic Stem Cells to Blood," *Cell Stem Cell*, vol. 2, no. 1, pp. 60–71, 2008.

[82] C. Lengerke, S. Schmitt, T. V. Bowman, I. H. Jang, L. Maouche-Chretien, S. McKinney-Freeman, A. J. Davidson, M. Hammerschmidt, F. Rentzsch, J. B. A. Green, L. I. Zon, and G. Q. Daley, "BMP and Wnt Specify Hematopoietic Fate by Activation of the Cdx-Hox Pathway," *Cell Stem Cell*, vol. 2, no. 1, pp. 72–82, 2008.

[83] P. Faloon, E. Arentson, a Kazarov, C. X. Deng, C. Porcher, S. Orkin, and K. Choi, "Basic fibroblast growth factor positively regulates hematopoietic development.," *Development*, vol. 127, no. 9, pp. 1931–1941, 2000.

[84] S. Pearson, P. Sroczynska, G. Lacaud, and V. Kouskoff, "The stepwise specification of embryonic stem cells to hematopoietic fate is driven by sequential exposure to Bmp4, activin A, bFGF and VEGF.," *Development*, vol. 135, no. 8, pp. 1525–1535, 2008.

[85] H. Lapillonne, L. Kobari, C. Mazurier, P. Tropel, M.-C. Giarratana, I. Zanella-Cleon, L. Kiger, M. Wattenhofer-Donzé, H. Puccio, N. Hebert, A. Francina, G. Andreu, S. Viville, and L. Douay, "Red blood cell generation from human induced pluripotent stem cells: perspectives for transfusion medicine.," *Haematologica*, vol. 95, no. 10, pp. 1651–9, Oct. 2010.

[86] S.-J. Lu, Q. Feng, J. S. Park, L. Vida, B.-S. Lee, M. Strausbauch, P. J. Wettstein, G. R. Honig, and R. Lanza, "Biologic properties and enucleation of red blood cells from human embryonic stem cells.," *Blood*, vol. 112, no. 12, pp. 4475–84, Dec. 2008.

[87] L. Kobar, F. Yates, N. Oudrhiri, A. Francina, L. Kiger, C. Mazurier, S. Rouzbeh, W. El-Nemer, N. Hebert, M. C. Giarratana, S. François, A. Chapel, H. Lapillonne, D. Luton, A. Bennaceur-Griscelli, and L. Douay, "Human induced pluripotent stem cells can reach complete terminal maturation: In vivo and in vitro evidence in the erythropoietic differentiation model," *Haematologica*, vol. 97, no. 12, pp. 1795–1803, 2012.

[88] R. Kurita, N. Suda, K. Sudo, K. Miharada, T. Hiroyama, H. Miyoshi, K. Tani, and Y. Nakamura, "Establishment of Immortalized Human Erythroid Progenitor Cell Lines Able to Produce Enucleated Red Blood Cells," *PLoS One*, vol. 8, no. 3, 2013.

[89] S. I. Hirose, N. Takayama, S. Nakamura, K. Nagasawa, K. Ochi, S. Hirata, S. Yamazaki, T. Yamaguchi, M. Otsu, S. Sano, N. Takahashi, A. Sawaguchi, M. Ito, T. Kato, H. Nakauchi, and K. Eto, "Immortalization of erythroblasts by c-MYC and BCL-XL enables large-scale erythrocyte production from human pluripotent stem cells," *Stem Cell Reports*, vol. 1, no. 6, pp. 499–508, 2013.

[90] J. Riddell, R. Gazit, B. S. Garrison, G. Guo, A. Saadatpour, P. K. Mandal, W. Ebina, P. Volchkov, G.-C. Yuan, S. H. Orkin, and D. J. Rossi, "Reprogramming Committed Murine Blood Cells to Induced Hematopoietic Stem Cells with Defined Factors," *Cell*, vol. 157, pp. 549–564, 2014.

[91] C. F. Pereira, B. Chang, J. Qiu, X. Niu, D. Papatsenko, C. E. Hendry, N. R. Clark, A. Nomura-Kitabayashi, J. C. Kovacic, A. Ma'Ayan, C. Schaniel, I. R. Lemischka, and K. Moore, "Induction of a hemogenic program in mouse fibroblasts," *Cell Stem Cell*, vol. 13, no. 2, pp. 205–218, 2013.

[92] K. Batta, M. Florkowska, V. Kouskoff, and G. Lacaud, "Direct

Reprogramming of Murine Fibroblasts to Hematopoietic Progenitor Cells," *Cell Rep.*, vol. 9, no. 5, pp. 1871–1885, 2014.
[93] S. Capellera-Garcia, J. Pulecio, K. Dhulipala, K. Siva, V. Rayon-Estrada, S. Singbrant, M. N. E. Sommarin, C. R. Walkley, S. Soneji, G. Karlsson, Á. Raya, V. G. Sankaran, and J. Flygare, "Defining the Minimal Factors Required for Erythropoiesis through Direct Lineage Conversion," *Cell Rep.*, vol. 15, no. 11, pp. 2550–2562, 2016.
[94] G. F. Rousseau, M.-C. Giarratana, and L. Douay, "Large-scale production of red blood cells from stem cells: what are the technical challenges ahead?," *Biotechnol. J.*, vol. 9, no. 1, pp. 28–38, 2014.
[95] M. Giarratana, H. Rouard, A. Dumont, L. Kiger, I. Safeukui, P. Y. Le Pennec, S. Francois, G. Trugnan, T. Peyrard, T. Marie, S. Jolly, N. Hebert, C. Mazurier, N. Mario, L. Harmand, H. Lapillonne, J. Y. Devaux, and L. Douay, "Proof of principle for transfusion of in vitro generated red blood cells," *Blood*, vol. 118, no. 19, pp. 5071–5079, 2011.
[96] K.-H. Chang, H. Bonig, and T. Papayannopoulou, "Generation and characterization of erythroid cells from human embryonic stem cells and induced pluripotent stem cells: an overview.," *Stem Cells Int.*, vol. 2011, p. 791604, Jan. 2011.
[97] T. Hiroyama, K. Miharada, K. Sudo, I. Danjo, N. Aoki, and Y. Nakamura, "Establishment of mouse embryonic stem cell-derived erythroid progenitor cell lines able to produce functional red blood cells," *PLoS One*, vol. 3, no. 2, 2008.
[98] K. Trakarnsanga, R. E. Griffiths, M. C. Wilson, A. Blair, T. J. Satchwell, M. Meinders, N. Cogan, S. Kupzig, R. Kurita, Y. Nakamura, A. M. Toye, D. J. Anstee, and J. Frayne, "An immortalized adult human erythroid line facilitates sustainable and scalable generation of functional red cells," *Nat. Commun.*, vol. 8, no. May 2016, p. 14750, 2017.
[99] I. J. Miller and J. J. Bieker, "A novel, erythroid cell-specific murine transcription factor that binds to the CACCC element and is related to the Krüppel family of nuclear proteins.," *Mol. Cell. Biol.*, vol. 13, no. 5, pp. 2776–86, 1993.
[100] C. M. Southwood, K. M. Downs, and J. J. Bieker, "Erythroid Kruppel-like factor exhibits an early and sequentially localized pattern of expression during mammalian erythroid ontogeny," *Dev. Dyn.*, vol. 206, no. 3, pp. 248–259, 1996.
[101] M. R. Tallack, T. Whitington, W. S. Yuen, M. T. Kassouf, J. R. Hughes, S. Taylor, Y. Cheng, D. C. King, L. C. Dore, E. N. Wainwright, J. R. Keys, B. B. Gardiner, E. Nourbakhsh, N. Cloonan, S. M. Grimmond, T. L. Bailey, and A. C. Perkins, "A global role for KLF1 in erythropoiesis revealed by ChIP-seq in primary erythroid cells," *Genome Res.*, vol. 53, pp. 1052–1063, 2010.
[102] J. R. Keys, M. R. Tallack, D. J. Hodge, S. O. Cridland, R. David, and A. C. Perkins, "Genomic organisation and regulation of murine alpha haemoglobin stabilising protein by erythroid Kruppel-like factor," *Br. J. Haematol.*, vol. 136, no. 1, pp. 150–157, 2007.
[103] M. F. Kramer, P. Gunaratne, and G. C. Ferreira, "Transcriptional regulation of the murine erythroid-specific 5-aminolevulinate synthase gene," *Gene*, vol. 247, no. 1–2, pp. 153–166, 2000.

[104] A. P. W. Funnell, C. A. Maloney, L. J. Thompson, J. Keys, M. Tallack, A. C. Perkins, and M. Crossley, "Erythroid Kruppel-like factor directly activates the basic Kruppel-like factor gene in erythroid cells," *Mol. Cell. Biol.*, vol. 27, no. 7, pp. 2777–2790, 2007.
[105] M. R. Tallack, J. R. Keys, and A. C. Perkins, "Erythroid Kruppel-like Factor Regulates the G1 Cyclin Dependent Kinase Inhibitor p18INK4c," *J. Mol. Biol.*, vol. 369, pp. 313–321, 2007.
[106] M. R. Tallack, J. R. Keys, P. O. Humbert, and A. C. Perkins, "EKLF/KLF1 controls cell cycle entry via direct regulation of E2f2," *J. Biol. Chem.*, vol. 284, no. 31, pp. 20966–20974, 2009.
[107] A. M. Pilon, M. O. Arcasoy, H. K. Dressman, S. E. Vayda, Y. D. Maksimova, J. I. Sangerman, P. G. Gallagher, and D. M. Bodine, "Failure of terminal erythroid differentiation in EKLF-deficient mice is associated with cell cycle perturbation and reduced expression of E2F2.," *Mol. Cell. Biol.*, vol. 28, no. 24, pp. 7394–7401, 2008.
[108] B. Nuez, D. Michalovich, A. Bygrave, R. Ploemacher, and F. Grosveld, "Defective haematopoiesis in fetal liver resulting from inactivation of the EKLF gene.," *Nature*, vol. 375, pp. 316–318, 1995.
[109] P. Frontelo, D. Manwani, M. Galdass, H. Karsunky, F. Lohmann, P. G. Gallagher, and J. J. Bieker, "Novel role for EKLF in megakaryocyte lineage commitment," *Blood*, vol. 110, no. 12, pp. 3871–3880, 2007.
[110] R. E. D. Cells, G. W. Magor, M. R. Tallack, K. R. Gillinder, C. C. Bell, N. Mccallum, B. Williams, and A. C. Perkins, "KLF1-null neonates display hydrops fetalis and a deranged erythroid transcriptome," vol. 125, no. 15, pp. 2405–2418, 2015.
[111] R. Khanna, S. H. Chang, S. Andrabi, M. Azam, A. Kim, A. Rivera, C. Brugnara, P. S. Low, S.-C. Liu, and A. H. Chishti, "Headpiece domain of dematin is required for the stability of the erythrocyte membrane.," *Proc. Natl. Acad. Sci. U. S. A.*, vol. 99, no. 10, pp. 6637–42, 2002.
[112] D. G. Nilson, D. E. Sabatino, D. M. Bodine, and P. G. Gallagher, "Major erythrocyte membrane protein genes in EKLF-deficient mice," *Exp. Hematol.*, vol. 34, no. 6, pp. 705–712, 2006.
[113] L. Xue, M. Galdass, M. N. Gnanapragasam, D. Manwani, and J. J. Bieker, "Extrinsic and intrinsic control by EKLF (KLF1) within a specialized erythroid niche.," *Development*, vol. 141, no. 11, pp. 2245–54, 2014.
[114] B. K. Singleton, N. M. Burton, C. Green, R. L. Brady, and D. J. Anstee, "Mutations in EKLF/KLF1 form the molecular basis of the rare blood group In(Lu) phenotype.," *Blood*, vol. 112, no. 5, pp. 2081–8, Sep. 2008.
[115] M. Siatecka, F. Lohmann, S. Bao, and J. J. Bieker, "EKLF directly activates the p21WAF1/CIP1 gene by proximal promoter and novel intronic regulatory regions during erythroid differentiation.," *Mol. Cell. Biol.*, vol. 30, no. 11, pp. 2811–2822, 2010.
[116] N. Motoyama, T. Kimura, T. Takahashi, T. Watanabe, and T. Nakano, "Bcl-X Prevents Apoptotic Cell Death of Both Primitive and Definitive Erythrocytes At the End of Maturation.," *J. Exp. Med.*, vol. 189, no. 11, pp. 1691–8, 1999.
[117] M. M. Rhodes, P. Kopsombut, M. C. Bondurant, J. O. Price, and M. J. Koury, "Bcl-xL prevents apoptosis of late-stage erythroblasts but does not mediate the antiapoptotic effect of erythropoietin," *Blood*, vol. 106, no. 5, pp. 1857–1863,

2005.
[118] P. Sathyanarayana, A. Dev, J. Fang, E. Houde, O. Bogacheva, O. Bogachev, M. Menon, S. Browne, A. Pradeep, C. Emerson, and D. M. Wojchowski, "EPO receptor circuits for primary erythroblast survival," *Blood*, vol. 111, no. 11, pp. 5390–5399, 2008.
[119] R. Drissen, R. Drissen, R. Palstra, R. Palstra, N. Gillemans, N. Gillemans, E. Splinter, E. Splinter, F. Grosveld, F. Grosveld, S. Philipsen, S. Philipsen, W. De Laat, and W. De Laat, "The active spatial organization of the beta-globin locus requires the transcription factor EKLF," *Genes Dev.*, pp. 2485–2490, 2004.
[120] D. Zhou, K. Liu, C.-W. Sun, K. M. Pawlik, and T. M. Townes, "KLF1 regulates BCL11A expression and gamma- to beta-globin gene switching.," *Nat. Genet.*, vol. 42, no. 9, pp. 742–4, Sep. 2010.
[121] J. Borg, P. Papadopoulos, M. Georgitsi, L. Gutiérrez, G. Grech, P. Fanis, M. Phylactides, A. J. M. H. Verkerk, P. J. van der Spek, C. a Scerri, W. Cassar, R. Galdies, W. van Ijcken, Z. Ozgür, N. Gillemans, J. Hou, M. Bugeja, F. G. Grosveld, M. von Lindern, A. E. Felice, G. P. Patrinos, and S. Philipsen, "Haploinsufficiency for the erythroid transcription factor KLF1 causes hereditary persistence of fetal hemoglobin.," *Nat. Genet.*, vol. 42, no. 9, pp. 801–5, Sep. 2010.
[122] O. Nakajima, S. Takahashi, H. Harigae, K. Furuyama, N. Hayashi, S. Sassa, and M. Yamamoto, "Heme deficiency in erythroid lineage causes differentiation arrest and cytoplasmic iron overload," *EMBO J.*, vol. 18, no. 22, pp. 6282–6289, 1999.
[123] H. Liu, G. C. Ippolito, J. K. Wall, T. Niu, L. Probst, B.-S. Lee, K. Pulford, A. H. Banham, L. Stockwin, A. L. Shaffer, L. M. Staudt, C. Das, M. J. S. Dyer, and P. W. Tucker, "Functional studies of BCL11A: characterization of the conserved BCL11A-XL splice variant and its interaction with BCL6 in nuclear paraspeckles of germinal center B cells.," *Mol. Cancer*, vol. 5, p. 18, 2006.
[124] Y. Saiki, Y. Yamazaki, M. Yoshida, O. Katoh, and T. Nakamura, "Human EVI9, a homologue of the mouse myeloid leukemia gene, is expressed in the hematopoietic progenitors and down-regulated during myeloid differentiation of HL60 cells.," *Genomics*, vol. 70, pp. 387–391, 2000.
[125] P. Liu, J. R. Keller, M. Ortiz, L. Tessarollo, R. A. Rachel, T. Nakamura, N. A. Jenkins, and N. G. Copeland, "Bcl11a is essential for normal lymphoid development.," *Nat. Immunol.*, vol. 4, no. 6, pp. 525–32, 2003.
[126] E. Satterwhite, T. Sonoki, T. G. Willis, L. Harder, R. Nowak, E. L. Arriola, H. Liu, H. P. Price, S. Gesk, D. Steinemann, B. Schlegelberger, D. G. Oscier, R. Siebert, P. W. Tucker, and M. J. S. Dyer, "The BCL11 gene family : involvement of BCL11A in lymphoid malignancies The BCL11 gene family : involvement of BCL11A in lymphoid malignancies," *Cytogenetics*, vol. 98, no. 12, pp. 3413–3420, 2011.
[127] T. Nakamura, Y. Yamazaki, Y. Saiki, M. Moriyama, D. a Largaespada, N. a Jenkins, and N. G. Copeland, "Evi9 encodes a novel zinc finger protein that physically interacts with BCL6, a known human B-cell proto-oncogene product.," *Mol. Cell. Biol.*, vol. 20, no. 9, pp. 3178–86, 2000.
[128] V. G. Sankaran, T. F. Menne, J. Xu, T. E. Akie, G. Lettre, B. Van Handel, H.

K. A. Mikkola, J. N. Hirschhorn, A. B. Cantor, and S. H. Orkin, “Human fetal hemoglobin expression is regulated by the developmental stage-specific repressor BCL11A,” vol. 189, no. 2001, 2005.
[129] M. Jackson, R. Ma, A. H. Taylor, R. A. Axton, J. Easterbrook, M. Kydonaki, E. Olivier, L. Marenah, E. G. Stanley, A. G. Elefanty, J. C. Mountford, and L. M. Forrester, “Enforced Expression of HOXB4 in Human Embryonic Stem Cells Enhances the Production of Hematopoietic Progenitors but Has No Effect on the Maturation of Red Blood Cells,” *Stem Cells Transl. Med.*, pp. 1–10, 2016.
[130] R. Ma, “Optimizing the Production of Erythroid Cells from Human Embryonic Stem Cells,” *PhD Thesis*, 2014.
[131] M. Jackson, R. A. Axton, A. H. Taylor, J. A. Wilson, S. A. M. Gordon-Keylock, K. D. Kokkaliaris, J. M. Brickman, H. Schulz, O. Hummel, N. Hubner, and L. M. Forrester, “HOXB4 can enhance the differentiation of embryonic stem cells by modulating the hematopoietic niche,” *Stem Cells*, vol. 30, pp. 150–160, 2012.
[132] M. Sadelain, E. P. Papapetrou, and F. D. Bushman, “Safe harbours for the integration of new DNA in the human genome.,” *Nat. Rev. Cancer*, vol. 12, no. 1, pp. 51–8, Jan. 2012.
[133] K. Ohneda and M. Yamamoto, “Roles of hematopoietic transcription factors GATA-1 and GATA-2 in the development of red blood cell lineage,” *Acta Haematol.*, vol. 108, pp. 237–245, 2002.
[134] A. N. Alexopoulou, J. R. Couchman, and J. R. Whiteford, “The CMV early enhancer/chicken beta actin (CAG) promoter can be used to drive transgene expression during the differentiation of murine embryonic stem cells into vascular progenitors.,” *BMC Cell Biol.*, vol. 9, p. 2, Jan. 2008.
[135] C. T. Yang, A. French, P. A. Goh, A. Pagnamenta, S. Mettananda, J. Taylor, S. Knight, A. Nathwani, D. J. Roberts, S. M. Watt, and L. Carpenter, “Human induced pluripotent stem cell derived erythroblasts can undergo definitive erythropoiesis and co-express gamma and beta globins,” *Br. J. Haematol.*, vol. 166, no. 3, pp. 435–448, 2014.
[136] L. Vassen, H. Beauchemin, W. Lemsaddek, J. Krongold, and M. Trudel, “Growth Factor Independence 1b (Gfi1b) Is Important for the Maturation of Erythroid Cells and the Regulation of Embryonic Globin Expression,” vol. 9, no. 5, 2014.
[137] V. Randrianarison-Huetz, B. Laurent, V. Bardet, G. C. Blobe, F. Huetz, and D. Duménil, “Gfi-1B controls human erythroid and megakaryocytic differentiation by regulating TGF-beta signaling at the bipotent erythro-megakaryocytic progenitor stage.,” *Blood*, vol. 115, no. 14, pp. 2784–95, Apr. 2010.
[138] S. Saleque, S. Cameron, and S. H. Orkin, “The zinc-finger proto-oncogene Gfi-1b is essential for development of the erythroid and megakaryocytic lineages,” pp. 301–306, 2002.
[139] K. Trakarnsanga, M. C. Wilson, W. Lau, B. K. Singleton, S. F. Parsons, P. Sakuntanaga, R. Kurita, Y. Nakamura, D. J. Anstee, and J. Frayne, “Induction of adult levels of β-globin in human erythroid cells that intrinsically express embryonic or fetal globin by transduction with KLF1 and BCL11A-XL,” *Haematologica*, vol. 99, no. 11, pp. 1677–1685, 2014.

[140] Z. Dastoor and J. L. Dreyer, “Potential role of nuclear translocation of glyceraldehyde-3-phosphate dehydrogenase in apoptosis and oxidative stress.,” *J. Cell Sci.*, vol. 114, pp. 1643–1653, 2001.
[141] M. A. Sirover, “Subcellular dynamics of multifunctional protein regulation: Mechanisms of GAPDH intracellular translocation,” *J. Cell. Biochem.*, vol. 113, no. 7, pp. 2193–2200, 2012.
[142] T. Seime, M. Kolind, K. Mikulec, M. A. Summers, L. Cantrill, D. G. Little, and A. Schindeler, “Inducible cell labeling and lineage tracking during fracture repair,” *Dev. Growth Differ.*, vol. 57, no. 1, pp. 10–23, 2015.
[143] E. Coghill, S. Eccleston, V. Fox, L. Cerruti, C. Brown, J. Cunningham, S. Jane, and A. Perkins, “Erythroid Kruppel-like factor (EKLF) coordinates erythroid cell proliferation and hemoglobinization in cell lines derived from EKLF null mice,” *Blood*, vol. 97, no. 6, pp. 1861–1868, 2001.
[144] M. Siatecka and J. J. Bieker, “The multifunctional role of EKLF/KLF1 during erythropoiesis.,” *Blood*, vol. 118, no. 8, pp. 2044–54, Aug. 2011.
[145] Y. C. Shyu, T. L. Lee, X. Chen, P. H. Hsu, S. C. Wen, Y. W. Liaw, C. H. Lu, P. Y. Hsu, M. J. Lu, J. Hwang, M. D. Tsai, M. J. Hwang, J. R. Chen, and C. K. James Shen, “Tight regulation of a timed nuclear import wave of EKLF by PKCθ and FOE during Pro-E to Baso-E transition,” *Dev. Cell*, vol. 28, no. 4, pp. 409–422, 2014.
[146] K. Ochi, N. Takayama, S. Hirose, T. Nakahata, H. Nakauchi, and K. Eto, “Multicolor staining of globin subtypes reveals impaired globin switching during erythropoiesis in human pluripotent stem cells.,” *Stem Cells Transl. Med.*, vol. 3, no. 7, pp. 792–800, 2014.
[147] D. J. Ellis, “Silencing and Variegation of Gammaretrovirus and Lentivirus Vectors,” *Http://Dx.Doi.Org/10.1089/Hum.2005.16.1241*, vol. 1246, no. November, pp. 1241–1246, 2005.
[148] Y. Ma, A. Ramezani, R. Lewis, R. G. Hawley, and J. A. Thomson, “High-level sustained transgene expression in human embryonic stem cells using lentiviral vectors,” *Stem Cells*, vol. 21, no. 1066–5099, pp. 111–117, 2003.
[149] J. Xu, D. E. Bauer, M. a Kerenyi, T. D. Vo, S. Hou, Y.-J. Hsu, H. Yao, J. J. Trowbridge, G. Mandel, and S. H. Orkin, “Corepressor-dependent silencing of fetal hemoglobin expression by BCL11A.,” *Proc. Natl. Acad. Sci. U. S. A.*, vol. 110, no. 16, pp. 6518–23, Apr. 2013.
[150] Y. Yu, J. Wang, W. Khaled, S. Burke, P. Li, X. Chen, W. Yang, N. a Jenkins, N. G. Copeland, S. Zhang, and P. Liu, “Bcl11a is essential for lymphoid development and negatively regulates p53.,” *J. Exp. Med.*, vol. 209, no. 13, pp. 2467–83, 2012.
[151] J. H. Ware, Z. Zhou, J. Guan, A. R. Kennedy, and L. Kopelovich, “Establishment of human cancer cell clones with different characteristics: a model for screening chemopreventive agents,” *Anticancer Res*, vol. 27, no. 1A, pp. 1–16, 2007.
[152] C. M. Sturgeon, A. Ditadi, G. Awong, M. Kennedy, and G. Keller, “Wnt signaling controls the specification of definitive and primitive hematopoiesis from human pluripotent stem cells.,” *Nat. Biotechnol.*, vol. 32, no. 6, pp. 554–61, 2014.
[153] D. Klopotowska, L. Strzadala, and J. Matuszyk, “Inducibility of doxycycline-regulated gene in neural and neuroendocrine cells strongly depends on the

appropriate choice of a tetracycline-responsive promoter," *Neurochem. Int.*, vol. 52, no. 1, pp. 221–229, 2008.
[154] K. Xiong, Y. Zhou, P. Hyttel, L. Bolund, K. K. Freude, and Y. Luo, "Generation of induced pluripotent stem cells (iPSCs) stably expressing CRISPR-based synergistic activation mediator (SAM)," *Stem Cell Res.*, vol. 17, no. 3, pp. 665–669, 2016.
[155] A. Chow, M. Huggins, J. Ahmed, D. Hashimoto, D. Lucas, Y. Kunisaki, S. Pinho, M. Leboeuf, C. Noizat, N. van Rooijen, M. Tanaka, Z. J. Zhao, A. Bergman, M. Merad, and P. S. Frenette, "CD169^{+} macrophages provide a niche promoting erythropoiesis under homeostasis and stress.," *Nat. Med.*, vol. 19, no. 4, pp. 429–36, 2013.
[156] S. Porcu, M. F. Manchinu, M. F. Marongiu, V. Sogos, D. Poddie, I. Asunis, L. Porcu, M. G. Marini, P. Moi, A. Cao, F. Grosveld, and M. S. Ristaldi, "Klf1 affects DNase II-alpha expression in the central macrophage of a fetal liver erythroblastic island: a non-cell-autonomous role in definitive erythropoiesis.," *Mol. Cell. Biol.*, vol. 31, no. 19, pp. 4144–54, 2011.

Appendix

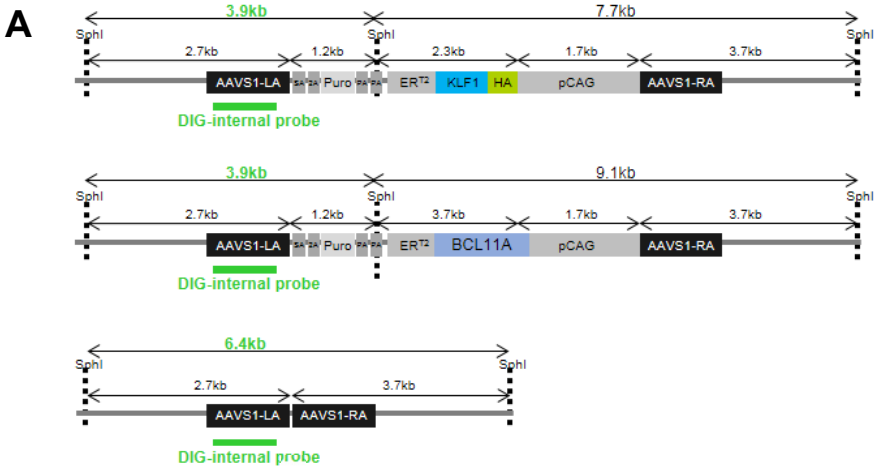
A
3.9kb
7.7kb
SphI
SphI
SphI
2.7kb
1.2kb
2.3kb
1.7kb
3.7kb
AAVS1-LA
Puro
ER^{T2}
KLF1
HA
pCAG
AAVS1-RA
DIG-internal probe
3.9kb
9.1kb
SphI
SphI
SphI
2.7kb
1.2kb
3.7kb
1.7kb
3.7kb
AAVS1-LA
Puro
ER^{T2}
BCL11A
pCAG
AAVS1-RA
DIG-internal probe
6.4kb
SphI
SphI
2.7kb
3.7kb
AAVS1-LA
AAVS1-RA
DIG-internal probe

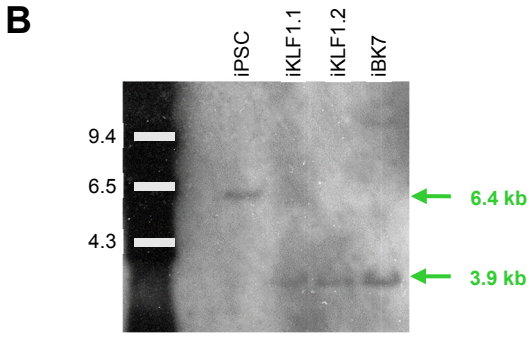
B
iPSC
iKLF1.1
iKLF1.2
iBK7
9.4
6.5
4.3
6.4 kb
3.9 kb

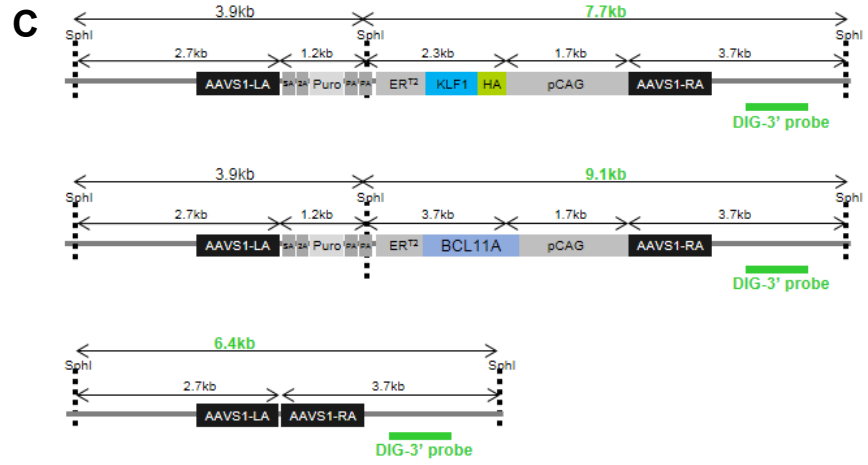
C
3.9kb
7.7kb
SphI
SphI
SphI
2.7kb
1.2kb
2.3kb
1.7kb
3.7kb
AAVS1-LA
Puro
ER^{T2}
KLF1
HA
pCAG
AAVS1-RA
DIG-3' probe
3.9kb
9.1kb
SphI
SphI
SphI
2.7kb
1.2kb
3.7kb
1.7kb
3.7kb
AAVS1-LA
Puro
ER^{T2}
BCL11A
pCAG
AAVS1-RA
DIG-3' probe
6.4kb
SphI
SphI
2.7kb
3.7kb
AAVS1-LA
AAVS1-RA
DIG-3' probe

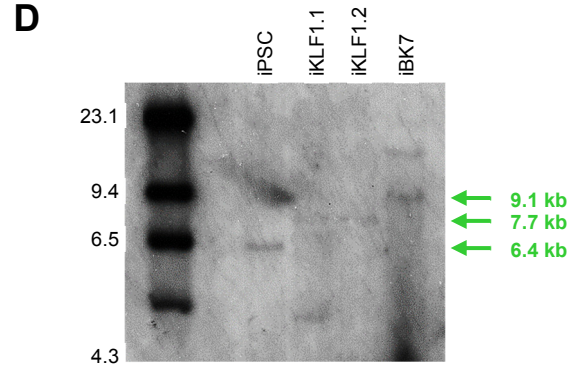
D
iPSC
iKLF1.1
iKLF1.2
iBK7
23.1
9.4
6.5
4.3
9.1 kb
7.7 kb
6.4 kb

Figure S1 Southern blot confirmed the correct targeting in the *AAVS1* locus

A. A figure indicates the positions of SphI digestion site and DIG-internal probe targeting site on the genomic AAVS locus. **B.** Southern blot analyse genomic DNA samples from iPSCs, iKLF1.1, iKLF1.2 and iBK7 cell lines. For the correct targeting of KLF1-ER^{T2} and BCL11A-ER^{T2} constructs, 3.9 Kb of DNA fragments were detected using DIG-internal probe. The non-targeted iPSC gave 6.4 Kb of DNA fragments. **C.** A figure indicates the positions of SphI digestion site and DIG-3' probe targeting site on the genomic AAVS locus. **D.** Southern blot analyse genomic DNA samples from iPSCs, iKLF1.1, iKLF1.2 and iBK7 cell liness. For the correct targeting of KLF1-ER^{T2} and BCL11A-ER^{T2} constructs, 7.7 Kb and 9.1 Kb of DNA fragments were detected using DIG-3' probe, respectively. The non-targeted iPSC gave 6.4 Kb of DNA fragments.

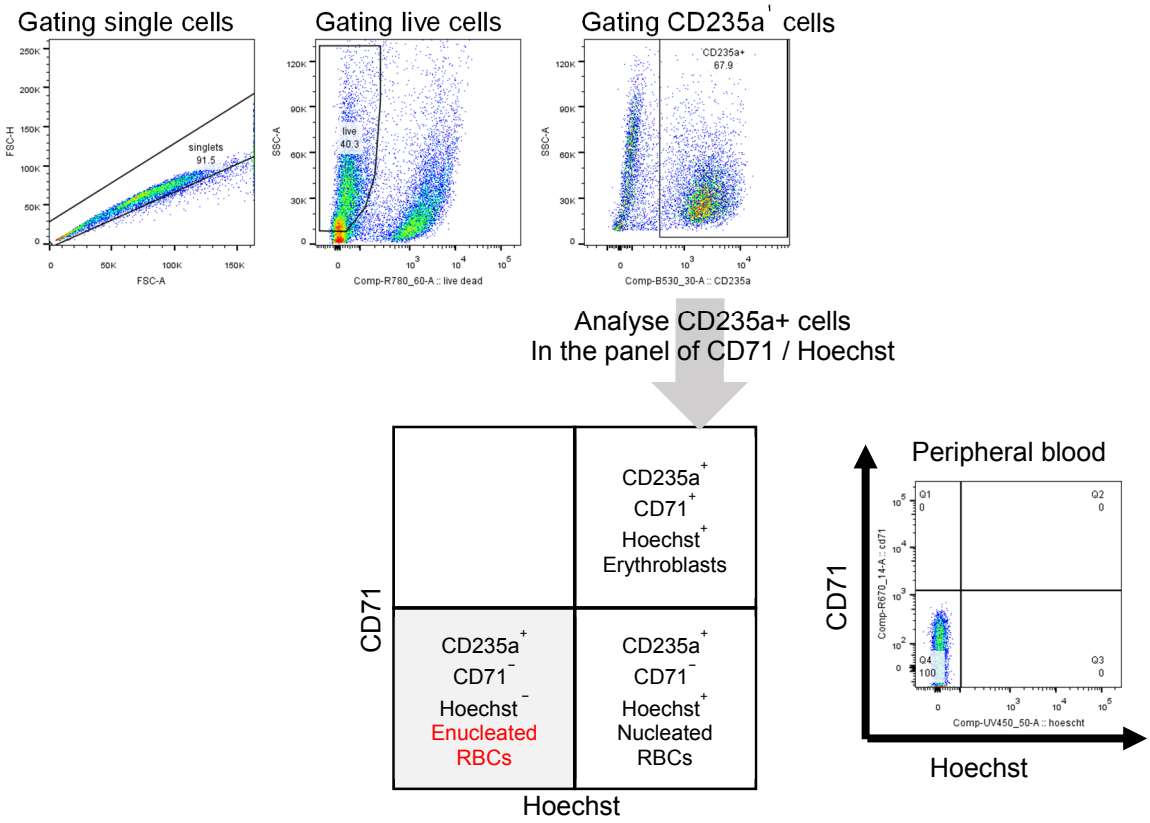

Figure S2 The gating strategy for the enucleation assay in flow cytometry

Differentiating cells were stained with anti-CD235a, anti-CD71 antibodies, Hoechst and the LIVE/DEAD™ Fixable Near-IR Stain then analysed by flow cytometry. The single cells population was gated in FSC-A and FSC-H panel, and then live cells were identified by the R780_60 filter. The gating thresholds for CD235a was set using the appropriate FMO minus CD235a antibody, and live CD235a positive cells were then assessed in the enucleation assay. Next, the gating thresholds for CD71 and Hoechst were also set using the appropriate FMOs. $CD235a^{+}$ / $CD71^{-}$ / $Hoechst^{-}$ enucleated RBCs were expected to appear in Q4 quadrant. Control human peripheral blood was a positive control which indicates the enucleated RBCs in the panel of Hoechst and CD71.

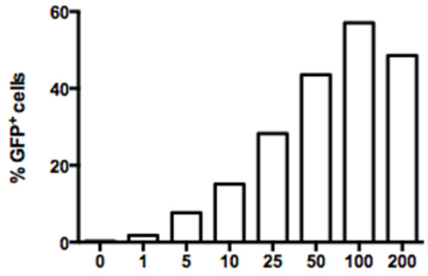

Figure S3 The transduction efficiency of control GFP-lentivirus at day 10 differentiating cells

Day 10 differentiating cells were transduced by GFP-lentivirus with MOI 0 to 200 and analysed by flow cytometry one day after viral transduction. Transfection efficiency was measure by the percentage of GFP^+ cells detected as a proportion of the live cells present.

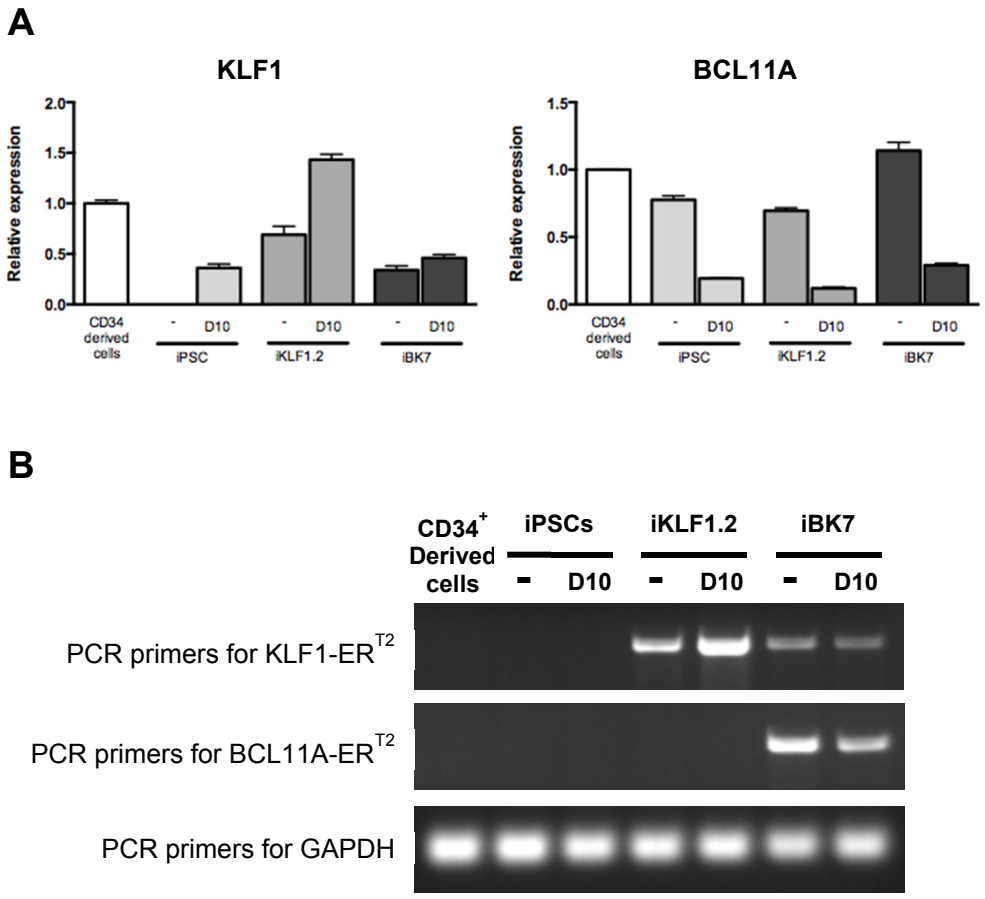

Figure S4 The expression of KLF1 and BCL11A among CD34$^+$-derived cells, iKLF1.2-derived cells and iBK7-derived cells

Cell samples were harvested from adult CD34$^+$ cells that had been differentiated for 6 days into erythroid progenitors, control undifferentiated iPSCs and day 10 differentiated iPSCs, undifferentiated iKLF1.2 and day 10 differentiated iKLF1.2, undifferentiated iBK7 and day 10 differentiated iBK7. A, B. RNAs isolated from cell samples were analysed by QRT-PCR using carried primers to KLF1 (A), BCL11A (B). **C.** cDNAs prepared from cell samples were assessed by PCR analysis using particular primers for *KLF1-ER^{T2}* and *BCL11A-ER^{T2}* transgenes. The forward primer targets to *KLF1* or *BCL11A*, and the reverse primer targets to *ER^{T2}*.

Gene	primer sequence	Purposes
EcoRI-HA-KLF1_F	GAATTCCACCATGTACCCATACGATGTTCCAGATTACGCTGCCA CAGCCGAGACCGCCTTG	introduce an EcoRI site and a HA tag at the upstream of KLF1
ER^{T2}-EcoRI_R	GAATTCCTATGAGACTGTGGCAGGGAAACCCTCTGC	introduce an EcoRI site at the downstream of ER^{T2}
KLF1a_F	ATGGCCACAGCCGAGACCGCCTTG	sequence KLF1
KLF1b_F	TGGTGGCTGGGCTTTTGGGTTCGGA	sequence KLF1
KLF1a_R	TCAAAGGTGGCGCTTCATGTGCA	sequence KLF1
KLF1b_R	TCCGAACCCAAAAGCCCAGCCACCA	sequence KLF1
ER^{T2}a_F	CCATCTGCTGGAGACATGAGAGCTG	sequence ER^{T2}
ER^{T2}b_F	CTTAATTCTGGAGTGTACACATTTC	sequence ER^{T2}
ER^{T2}a_R	CTTCATGCTGTACAGATGCTCCATG	sequence ER^{T2}
EcoRI-BCL11A_F	GAATTCCACCATGTCTCGCCGCAAGCAAGGCAAACCCCAGCAC TTAAGCAAACGGGAGTTCTCG	introduce an EcoRI site at the upstream of BCL11A
BCL11A-ER^{T2}_R	CTCATGTCTCCAGCAGATGGTTCAGTTTTTATATCATTATTC	generate BCL11A-ER^{T2} fusion cassette
BCL11A-ER^{T2}_F	GAATAATGATATAAAAACTGAACCATCTGCTGGAGACATGAG	generate BCL11A-ER^{T2} fusion cassette
BCL11a1_F	GTGGAGGTTGGCATCCAGGTCAC	sequence BCL11A
BCL11a2_F	CTGCGGTTGAATCCAATGGCTATG	sequence BCL11A
BCL11a3_F	GAGCTGACGGAGAGCGAGAGGGTG	sequence BCL11A
BCL11a4_F	GGAGCTGGACGGAGGGATCTCG	sequence BCL11A
BCL11a1_R	GTGTTCGCTTTCTAAGTAGATTC	sequence BCL11A
pZDonor_F	CCGTCGACGCTCTCTAGAGCTAG	PCR check targeting in genomic DNA
Int_R	TCTCCTGGGCTTGCCAAGGACTCAAAC	PCR check targeting in genomic DNA
5' aavs1_F	CGGAACTCTGCCCTCTAACGCTGCCG	PCR check targeting in genomic DNA
5' aavs_R	CTGCCAGATCTCTCGAGGCCCTGTGG	PCR check targeting in genomic DNA
Ext a_R	ACAGCCCCAGGTGGAGAAACTG	PCR check targeting in genomic DNA
Ext b_R	ACACCCAGACCTGACCCAAACCCAG	PCR check targeting in genomic DNA
int aavs_F	TGCTTTCTCTGACCTGCATTCTCTC	generate DIG-labelled probes for Southern Blot
int aavs_R	GCCCCACTGTGGGGTGGAGGGGACAG	generate DIG-labelled probes for Southern Blot
3' aavs_F	CCTGGACTCCTTCATCTGAGGGCGGAAG	generate DIG-labelled probes for Southern Blot
3' aavs_R	CAGCAGATACTCTGCAGGAACGAAGC	generate DIG-labelled probes for Southern Blot

Table S1 A list of PCR primers used in this project

Gene	Forward primer	Reverse primer	Probe
GAPDH	ATGACCCCTTCATTGACCTCAA	GAATTTGCCATGGGTGGAAT	TAACGTTAGTCAAGGCTG
KLF1	CGGACACACAGGATGACTTCCT	CCATGTCCTGCGCCTCTT	AGTGGTGGCGCTCC
HBE1	GGAGAAGGCTGCCGTCACTA	TTCACCTCCAGCCTCTTCCA	CTGTGGAGCAAGATGA
HBG1	TGTGACAAGCTGCATGTGGAT	CGGTCACCAGCACATTTCC	CTGAGAACTTCAAGCTC
HBB	CTGAGTGAGCTGCACTGTGACA	GTTGCCCAGGAGCCTGAA	TGCACGTGGATCCT
BCL11A	CCAAACAGGAACACATAGCAGA	GAGCTCCATGTGCAGAACG	UPL 52
cMYB	GGGATATATCATTCCTCAACATGA	TAAATGCACTTGGTCGTGCT	UPL 7
GATA1	CACTGAGCTTGCCACATCC	ATGGAGCCTCTGGGGATTA	UPL 26
SOX6	GCTTCTGGACTCAGCCCTTTA	GGCCCTTTAGCCTTTGGTTA	UPL 50
GFI1	AACGGAGCTCGGAGTTTGA	ATGGGCACATTGACTTCTCC	UPL 19
GFI1B	CCTCTTGTGCCCAGCACT	CGTGAGGGGTGGAGAAGAC	UPL 41
AHSP	CCTCAAGAGTGTGGGTGAGAC	TCCTTATTGGCCTTAAGAAGAGC	UPL 8
ER^{T2}	TCTCCCACATCAGGCACAT	TAGTGGGCGCATGTAGGC	UPL 70
PIM1	ATCAGGGGCCAGGTTTTC	GGGCCAAGCACCATCTAAT	UPL 13
E2F2	AGGGGAAGTGCATCAGAGTG	GCGAAGTGTCATACCGAGTCT	UPL 23
BCLX	AGCCTTGGATCCAGGAGAA	AGCGGTTGAAGCGTTCCT	UPL 66
p21	TCACTGTCTTGTACCCTTGTGC	GGCGTTTGGAGTGGTAGAAA	UPL 32
p27	TTTGACTTGCATGAAGAGAAGC	AGCTGTCTCTGAAAGGGACATT	UPL 60
p18	GACTATCCCTTCGGCGAGA	AAGGCTCGGCCATTCTTTAG	UPL 65
GYPC	GACGAGAAGCCCCAACAG	CAATGGTGGTAGTATGCATTGTG	UPL 16
ANK1	TTCACCCAAGTGGTGCAG	CTCATCCGTGAATTGCTCCT	UPL 32
SLC4A1	TCTTCAGGAACGTGGAGCTT	CCTCATCAAAGGTTGCCTTG	UPL 89
SLC2A4	TCACAGTGACCGTGTCTACCA	GGGCTTCCTCAGGGTGAC	UPL 65
EPB4.9	CAGGGAGTGAGACTGGAAGC	TCTGCTCCAGCACACAGG	UPL 88
ABCG2	TGGCTTAGACTCAAGCACAGC	TCGTCCCTGCTTAGACATCC	UPL 56

Table S2 A list of qRT-PCR primers and probes used in this project

Re: Greetings from Rightslink_use widget on abstract to obtain license which is proof of permission [ref:_00D30oeGz._5000c1Oq7L9:ref]

noreply@salesforce.com on behalf of customercare@copyright.com

Wed 30/08/2017 22:26

To: YANG Cheng-tao <Cheng-Tao.Yang@ed.ac.uk>;

Dear Cheng-Tao:

Thank you for your reply. My apologies that I did not realize it was an open access article and it was your article. In this instance due to the content being 'open access' there is no formal permission to provide. The screenshot below could be used and you could provide the details Wiley's gives regarding this type of material: https://authorservices.wiley.com/author-resources/Journal-Authors/licensing-open-access/open-access/index.html

Title: Activation of KLF1 Enhances the Differentiation and Maturation of Red Blood Cells from Human Pluripotent Stem Cells

Author: Cheng-Tao Yang,Rui Ma,Richard A. Axton,Melany Jackson,A. Helen Taylor,Antonella Fidanza,Lamin Marenah,Jan Frayne,Joanne C. Mountford,Lesley M. Forrester

Publication: Stem Cells

Publisher: John Wiley and Sons

Date: Jan 19, 2017

Logged in as:
Christine Zoro
Account #:
3000504764
LOGOUT

Welcome to RightsLink

This article is available under the terms of the Creative Commons Attribution License (CC BY) (which may be updated from time to time) and permits use, distribution and reproduction in any medium, provided that the Contribution is properly cited.

For an understanding of what is meant by the terms of the Creative Commons License, please refer to Wiley's Open Access Terms and Conditions.

Permission is not required for this type of reuse.

Wiley offers a professional reprint service for high quality reproduction of articles from over 1400 scientific and medical journals. Wiley's reprint service offers:

- Peer reviewed research or reviews
- Tailored collections of articles
- A professional high quality finish
- Glossy journal style color covers
- Company or brand customisation
- Language translations
- Prompt turnaround times and delivery directly to your office, warehouse or congress.

Please contact our Reprints department for a quotation. Email corporatesaleseurope@wiley.com or corporatesalesusa@wiley.com or corporatesalesDE@wiley.com .

If that does not suffice you could email the publisher John Wiley and Sons with the subject line," Not available via Rightslink_need formal permission for OA article". The email is RightsLink@wiley.com

Sincerely,
Christine
Christine M. Zoro
Customer Account Specialist
Copyright Clearance Center
222 Rosewood Drive
Danvers, MA 01923
+1.855.239.3415 Customer Service Toll Free
+.978.750.8400 Corporate HQ

STEM CELLS®

EMBRYONIC STEM CELLS/INDUCED PLURIPOTENT STEM CELLS

Activation of KLF1 Enhances the Differentiation and Maturation of Red Blood Cells from Human Pluripotent Stem Cells

CHENG-TAO YANG,[a] RUI MA,[a] RICHARD A. AXTON,[a] MELANY JACKSON,[a] A. HELEN TAYLOR,[a] ANTONELLA FIDANZA,[a] LAMIN MARENAH,[b,c] JAN FRAYNE,[d] JOANNE C. MOUNTFORD,[b,c] LESLEY M. FORRESTER[a]

Key Words. Erythroid differentiation • Induced pluripotent stem cells • Transcription factors • Gene delivery systems in vivo or in vitro

[a]Centre for Regenerative Medicine, University of Edinburgh, Edinburgh, United Kingdom; [b]Institute of Cardiovascular & Medical Sciences, University of Glasgow, Glasgow, United Kingdom; [c]Scottish National Blood Transfusion Service, Scotland, United Kingdom; [d]Department of Biochemistry, University of Bristol, United Kingdom

Correspondence: Lesley M. Forrester, BCs (Hons) PhD, MRC Centre for Regenerative Medicine, Scottish Centre for Regenerative Medicine, Edinburgh BioQuarter, 5 Little France Drive, Edinburgh EH16 4UU, United Kingdom. Telephone: +44 131 651 9553; Fax: +44 131 651 9501; e-mail: l.forrester@ed.ac.uk

C.-T.Y. and R.M. contributed equally to this article

Received October 17, 2016; accepted for publication December 8, 2016; first published online in STEM CELLS *EXPRESS* December 27, 2016.

1066-5099/2016/$30.00/0

http://dx.doi.org/10.1002/stem.2562

ABSTRACT

Blood transfusion is widely used in the clinic but the source of red blood cells (RBCs) is dependent on donors, procedures are susceptible to transfusion-transmitted infections and complications can arise from immunological incompatibility. Clinically-compatible and scalable protocols that allow the production of RBCs from human embryonic stem cells (hESCs) and induced pluripotent stem cells (iPSCs) have been described but progress to translation has been hampered by poor maturation and fragility of the resultant cells. Genetic programming using transcription factors has been used to drive lineage determination and differentiation so we used this approach to assess whether exogenous expression of the Erythroid Krüppel-like factor 1 (EKLF/KLF1) could augment the differentiation and stability of iPSC-derived RBCs. To activate KLF1 at defined time points during later stages of the differentiation process and to avoid transgene silencing that is commonly observed in differentiating pluripotent stem cells, we targeted a tamoxifen-inducible KLF1-ER^{T2} expression cassette into the *AAVS1* locus. Activation of KLF1 at day 10 of the differentiation process when hematopoietic progenitor cells were present, enhanced erythroid commitment and differentiation. Continued culture resulted the appearance of more enucleated cells when KLF1 was activated which is possibly due to their more robust morphology. Globin profiling indicated that these conditions produced embryonic-like erythroid cells. This study demonstrates the successful use of an inducible genetic programing strategy that could be applied to the production of many other cell lineages from human induced pluripotent stem cells with the integration of programming factors into the *AAVS1* locus providing a safer and more reproducible route to the clinic. STEM CELLS *2017;35:886–897*

SIGNIFICANCE STATEMENT

Production of red blood cells from human pluripotent stem cells in the laboratory could solve many of the problems associated with blood transfusion but clinical trials have been hampered by the poor maturation status and fragility of differentiated cells. Here, we demonstrate the successful use of an inducible transcription factor programing strategy that results in the enhanced differentiation and maturation of red blood cells. This strategy could be applied to the production of many other cell lineages from pluripotent stem cells with the integration of programming factors into a safer harbor locus providing a safer and more reproducible route to the clinic.

INTRODUCTION

The generation of an unlimited supply of red blood cells (RBCs) from human pluripotent stem cells (hPSCs) such as human embryonic stem cells (hESCs) or induced pluripotent stem cells (iPSCs), could alleviate many of the current problems facing the blood transfusion services such as transfusion transmitted infection, donor supply and immune compatibility. Scalable, clinically compatible protocols to produce erythroid cells from hPSCs have been developed but progress to translation has been hampered by the lack of terminal maturation of the resultant cell. In contrast to RBCs generated in vitro from adult bone marrow or mobilised peripheral blood CD34$^+$ progenitors cells, erythroid cells produced from both hESCs and iPSCs have a fragile morphology, a poor enucleation rates and express embryonic and foetal rather than adult globin [1–7].

Transcription factors are arguably the most important route to controlling cell type

identity as they drive lineage-specific genes associated with their functional properties [8]. Transcription factor programming has been used to direct hESC/iPSC differentiation into distinct cell types such as cardiomyocytes and neurons [9, 10]. Enhanced expression of transcription factors known to be involved in the development and maintenance of the hematopoietic system such as SCL/TAL1, RUNX1, HOXA9, or HOXB4 have been used to increase the production of hematopoietic stem/progenitor cells from hESCs/iPSCs [11–16] and four transcription factors (GATA1, LMO2, SCL/TAL1, and cMYC) directly converted fibroblast into primitive erythroid progenitors [17].

Erythroid Kruppel-like factor 1 (EKLF/KLF1) is a zinc finger DNA binding protein that plays a critical role in regulating the expression of genes involved in erythroid cell identity and function including those involved in heme biosynthesis, red cell membrane stability and adult globin [18, 19]. Coassociations of KLF1-regulated genes at specialized nuclear hotspots is thought to optimize the coordinated transcriptional control [20]

Detailed analyses of mouse mutants demonstrated that *Klf1* deficiency results in defects in hemoglobin metabolism and membrane stability and that KLF1-null erythroid cells in the fetal liver have an abnormal morphology with many retaining their nuclei [21–25]. Deficiencies in *KLF1* have also been associated with human disease [26, 27]. For example, a missense mutation in *KLF1* results in a dominant-negative congenital dyserythropoietic anemia [28]. Reduced activity of *KLF1* has been associated with the rare blood group In (Lu) phenotype with amino acid substitutions within zinc finger domains predicted to abolish the interactions of KLF1 with downstream targets [29–31]. Genomic sequencing has uncovered the fact that a broad range human red cell disorders are caused by variants in *KLF1* [32].

We noted that KLF1 was expressed at a lower level in erythroid cells derived from hESCs compared to adult $CD34^+$-derived cells and, given its importance in erythroid maturation, we hypothesized this low level of expression of *KLF1* might be one reason for their lack of maturity. We first assessed the effects of constitutive expression of KLF1 and noted a significant reduction in the proliferative capacity of differentiating hESCs and a high variability in expression and stability of the transgene. We, therefore, developed a strategy where we could induce activity of KLF1 at later time-points during the differentiation process after hematopoietic progenitor cells (HPCs) had formed by generating and testing a human KLF1-ER^{T2} fusion protein. To achieve a consistent and physiological level of expression and to avoid transgene silencing, we employed the "safe harbor" approach by integrating the inducible KLF1-ER^{T2} transgene into the *AAVS1* locus [33–35].

We show for the first time that the inducible activation of KLF1 at a defined time point during the differentiation of both hESC and iPSCs enhanced erythroid commitment and differentiation. Continued culture of KLF1-activated cells resulted in a more robust morphology and a higher proportion of detectable enucleated cells. Globin profiling indicated that erythroid cells produced under these conditions had an embryonic-like phenotype.

Materials and Methods

Plasmid Construction

cDNAs encoding human wild type KLF1 or mutant R328L KLF1 [31] were amplified by polymerase chain reaction (PCR) and cloned into the EcoRI-digested pCAG-IRES-puro plasmid (pCAG-SIP). Tamoxifen inducible KLF1-ER^{T2} and R328L-ER^{T2} fusion cassettes were generated by recombineering (Supporting Information Fig. S1B, S1D, S1E). CAG-HA-KLF1-ER^{T2}-PolyA was cloned into the multiple cloning site of the pZDonor-AAVS1 Puromycin vector (PZD0020, Sigma-Aldrich, Gillingham, UK, http://www.sigmaaldrich.com/).

Production of iPSCS from ORhesus Negative Individuals

Dermal fibroblasts were obtained from blood group O Rhesus negative individuals by R Biomedical Ltd, Edinburgh, UK, (http://www.rbiomedical.com) under REC 1/AL/0020 ethical approval. Fibroblasts were reprogrammed to iPSCs using an episomal strategy with the transcription factors, *OCT4, KLF2 SOX2,* and *cMYC* [8] (http://roslincells.com). Characterization of the SFCi55 cell line used in this study included flow cytometry for key pluripotency and differentiation markers (Supporting Information Fig. S2A, S2B). Chromosomal spreads revealed a normal 46XX karyotype that was then confirmed by SNP analysis (data not shown). Hematopoietic differentiation of SFCi55 compared favorably to H1 hESCs (data not shown) and other published iPSC lines (Supporting Information Fig. S2C).

Maintenance and Differentiation of hESC and iPSCs

hESC and iPSCs were maintained in STEMPRO hESC SFM (Thermo Fisher Scientific Life Sciences, Waltham, MA, http://www.thermofisher.com) containing 20 ng/ml bFGF (FGF2) (R&D Systems, Abingdon, U.K., https://www.rndsystems.com) on CTS CELLstart Substrate (Thermo Fisher Scientific Life Sciences) and passaged (1:4) when 70%-80% confluent using STEMPRO EZPassage (Thermo Fisher Scientific Life Sciences, Waltham, MA, http://www.thermofisher.com). Hematopoietic differentiation was carried out in a step-wise, serum-, and feeder-free protocol as described in detail previously [15, 36]

Transfection of hESC and iPSCs

H1 hESC or iPSCs were fed with STEMPRO hESC SFM containing 20 ng/ml bFGF, and 10 μM Rock inhibitor (Y-27632, Calbiochem, Darmstadt, Germany. http://www.merckmillipore.com) was added at least 1 hour prior to electroporation as described previously [11, 37]. Single cell suspensions were generated using Accutase (Thermo Fisher Scientific Life Sciences), washed and resuspended (10^7 cells per 0.5 ml) in Dulbecco's phosphate-buffered saline without Ca^{2+} and Mg^{2+} (DPBS) and electroporated with 30 μg of linearized vector (BioRad Hemel Hempstead, UK http://www.bio-rad.com, Gene pulser; 320V 250 μF). Cells were plated on CTS CELLstart substrate in STEMPRO hESC SFM containing 20 ng/ml bFGF and 10 μM Rock inhibitor and 0.6 μg/ml puromycin for 10 days then resistant colonies were picked, expanded, and screened by PCR and Western blotting.

K562 Cell Maintenance and Electroporation

K562 cells were seeded at 10^5/ml in DMEM medium (Thermo Fisher Scientific Life Sciences) supplemented with 10% fetal calf serum, 2 mM sodium pyruvate (Thermo Fisher Scientific Life Sciences), 1% nonessential amino acids (Thermo Fisher Scientific Life Sciences), and 0.1 mM β-mercaptoethanol

(Thermo Fisher Scientific Life Sciences) and passaged every 2-3 days. K562 cells (10^7 cells in 700 μl DPBS) were electroporated (BioRad, Gene pulser; 320 V, 500 μF), then pools of cells were selected in 2.0 μg/ml puromycin (Sigma Aldrich) 2 days later. Hemin (50 μM) (Sigma Aldrich) was added to the cultures to induce differentiation then cells were harvested and analyzed after 4 days.

COS7 Cell Maintenance and Transfection

COS7 cells were maintained in GMEM medium (Thermo Fisher Scientific Life Sciences) supplemented with 10% fetal calf serum, 2 mM sodium pyruvate (Thermo Fisher Scientific Life Sciences), 1% nonessential amino acids (Thermo Fisher Scientific Life Sciences), and 0.1 mM β-mercaptoethanol (Thermo Fisher Scientific Life Sciences) and passaged at 1:5 ratio. Cells were seeded at 5×10^4/well in a 6-well-plate and transfected with 2.5 μg of DNA plasmid using the Xfect Transfection Reagent (Clontech, Saint-Germain-en-Laye, France. http://www.clontech.com).

Quantitative Reverse-Transcriptase Polymerase Chain Reaction

RNA was extracted using RNeasy Mini Kit (QIAGEN), and reverse transcription was performed by High-Capacity cDNA Reverse Transcription Kit (Thermo Fisher Scientific Life Sciences) following the manufacturer's instructions. To normalize cDNA quantity, GAPDH was used as reference gene. PCR reactions were carried out in triplicate using Applied Biosystems 7500 Fast Real-Time PCR System and data was analyzed on SDS v1.4 software (Thermo Fisher Scientific Life Sciences).

Protein Extraction and Western Blotting

Cells were lysed in RIPA buffer (Thermo Fisher Scientific Life Sciences) for total protein extraction. For nuclear fractionation, the cell pellet was resuspended in 0.2 ml of Swelling Buffer (5 mM PIPES, pH 8.0; 85 mM KCL; 0.5% NP40; protease inhibitor cocktail) for 20 minutes on ice. After spinning at 1,500 rpm at 4°C, the cytoplasmic supernatant was removed. The nuclear pellet was resuspended in 0.3 ml of lysis buffer (20 mM Hepes, pH 7.6; 1.5 mM MgCl2; 350 mM KCl; 0.2 mM EDTA; 20% Gycerol; 0.25% NP40; 0.5 mM DTT; protease inhibitor cocktail; Benzonase) and gently shaken at 4°C for 1 hour. The nuclear fraction was collected after centrifuged at 13,000 rpm, 4°C, for 30 minutes and stored at −80°C. Proper amount of protein lysates were electrophoresed on 4%-20% Ready Gel (BioRad), transferred to nitrocellulose membranes (10402580, Whatman, Sigma Aldrich) and probed with anti-HA tag (631207; Clontech), anti-KLF1 (sc14034, Santa Cruz, CA USA www.scbt.com), anti-GAPDH (AF5718, R&D) antibodies or LaminB1 (ab16048, abcam, Cambridge, UK, http://www.abcam.com). Antibody binding was detected using the appropriate horseradish peroxidase-conjugated IgG (HAF008, R&D Systems, Abingdon, U.K., https://www.rndsystems.com; sc-2020, SantaCruz) visualized by the WesternSure ECL Substrate (LI-COR, Cambridge, UK, https://www.licor.com).

CFU-C Assay

Day 10 differentiating cells (5×10^3 or 10^4) were plated into 1.5 ml of MethoCult (04435, Stem Cell Technologies, Cambridge, UK, https://www.stemcell.com) in 35 mm low attachment dishes (Greiner, Stonehouse, UK, https://www.gbo.com), incubated at 37°C in a humid chamber then scored for hematopoietic colony formation 12-15 days later.

Flow Cytometry

10^5 differentiating cells were harvested in phosphate-buffered saline (PBS) containing 1% bovine serum albumin (BSA) (PBS/BSA) and centrifuged at 200 g for 5 minutes. Cell pellets were resuspended and mixed with the appropriate volume of antibody, CD34-PE (12-0349-41, eBioscience, eBioscience Ltd., Hatfield, UK, http://www.ebioscience.com/), CD43-APC (17-0439-42, eBioscience), CD235a-FITC (11-9987-80, eBioscience), and CD71-APC (17-0719-42, eBioscience), to a final volume of 100 μl PBS/BSA, incubated for 30 minutes then analyzed on a LSR Fortessa (BD Biosciences, Oxford, UK, http://www.bdbiosciences.com/) using FACS Diva. The proportion of enucleated cells present in the culture was assessed using CD235a-FITC, CD71-APC antibodies, LIVE/DEAD Fixable Near-IR Stain (L10119, Thermo Fisher Scientific) and Hoechst dye (NucBlue, Thermo Fisher Scientific). Live $CD235a^+$ cells were first gated, then anti-CD71 and Hoeschst were used to define erythroblasts ($CD71^+$/$Hoechst^+$), nucleated RBCs ($CD71^-$/$Hoechst^+$) and enucleated RBCs ($CD71^-$/$Hoechst^-$) (Supporting Information Fig. S7).

Immunofluorescence Staining

COS7 cells were fixed in 4% formaldehyde/PBS for 15 minutes and permeabilized in 0.5% Triton-X 100/PBS (PBST) and successively incubated for 1 hour with rabbit anti-human KLF1 (sc14034, Santa Cruz), goat anti–rabbit IgG-FITC (F0382-1ML, SIGMA-ALDRICH) antibodies, and DAPI (4',6-Diamidino-2-phenylindole; SIGMA-ALDRICH). Stained cells were analyzed using a Zeiss Observer microscope and processed with AxioVision and ImageJ software.

Morphological Analysis

5×10^4 erythroid cells were resuspended in 0.2 ml PBS, loaded in cytospin slide chamber, and centrifuged at 500 rpm for 10 minutes. Rapid Romanowksy staining of air-dried slides was performed according to manufacturer's instructions (HS705, TCS biosciences, Buckinghamshire, UK, http://www.tcsbiosciences.co.uk).

High-Performance Liquid Chromatography

High-performance liquid chromatography (HPLC) globin chain separation was performed using a protocol modified from Lapillonne et al. [38]. Briefly, cells were washed three times in PBS, lysed in 50 μl water by three rapid freeze-thaw cycles and centrifuged at 13,000 g at 4°C for 10 minutes. Globin chain separation was performed by injecting 10 μl of the supernatant onto a 1.0×250 mm C4 column (Phenomenex, Macclesfield, U.K., http://www.phenomenex.com/) with a 42%-56% linear gradient between mixtures of 0.1% TFA in water (Buffer A) and 0.1% TFA in acetonitrile (Buffer B) at flow rate of 0.05 ml/min for 55 minutes on a HPLC Ultimate 3000 system (Dionex, Thermo Fisher Scientific Life Sciences). The column temperature was fixed at 50°C during analysis and the UV detector was set at 220 nm. Elution times of peaks generated were compared to control samples (e.g., adult and foetal blood) for

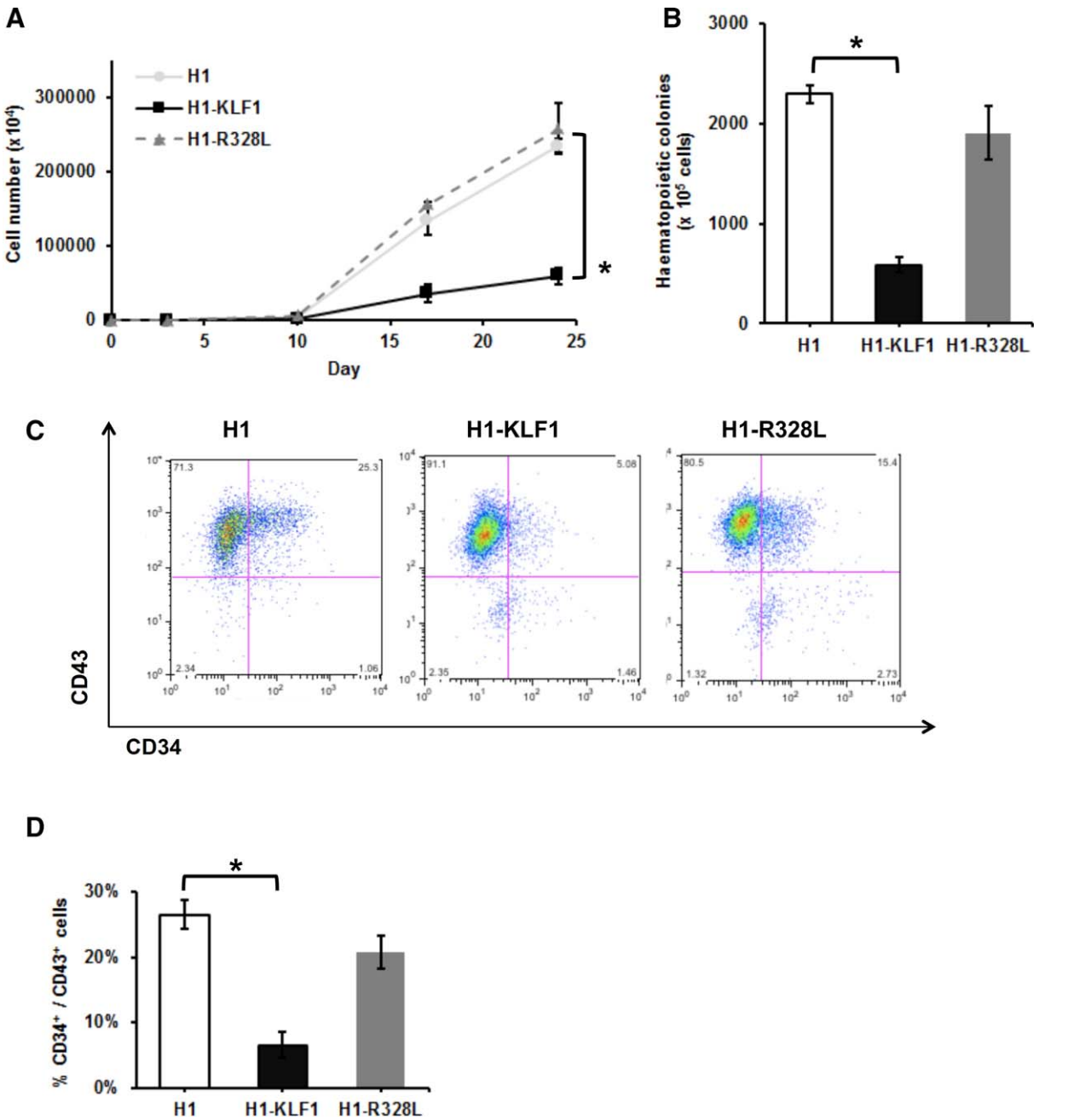

Figure 1. Constitutive KLF1 expression in human embryonic stem cells (hESCs) results in reduced proliferation and hematopoietic progenitor cell production. (**A**): Cell counts throughout the erythroid differentiation protocol of control H1 hESCs (H1) and H1 hESCs transfected with a vector containing either wild type KLF1 (H1-KLF1) or the mutant form of KLF1 (H1-R328L). **(B)**: Total number of CFU-Cs generated from differentiating H1, H1-KLF1, and H1-R328L hESCs at day 10 of the differentiation protocol. **(C)**: Flow cytometry analysis of differentiating H1, H1-EKLF, and H1-R328L hESC at day 10 of the differentiation protocol using antibodies against CD34 and CD43 to mark hematopoietic progenitor cells (HPCs). **(D)**: Quantification flow cytometry data showing the %$CD34^+/CD43^+$ HPCs at day 10 of the differentiation protocol. All data represents the mean of at least three independent experiments with error bars representing SEM. *p* values were calculated using two-way ANOVA followed by Tukey's multiple comparisons test (A) or one-way ANOVA followed by Holm-Sidak's multiple comparison test (B and D) ($*p < .05$).

identification and the area under the curve was used to calculate the proportion of each globin peak as a percentage of the total.

Statistical Analysis

The statistical analysis was performed using GraphPad Prism 6 software. For cell proliferation (Figs. 1A, 4A) and globin expression by HPLC (Fig. 6), data were analyzed using two-way ANOVA followed by Tukey's multiple comparisons test. CFU-C (Fig. 1B) and flow cytometry data (Figs. 1D, 3D, 7C) were analyzed using one-way ANOVA followed by Holm-Sidak's multiple comparison test. Gene expression data were analyzed using ratio paired *t* test.

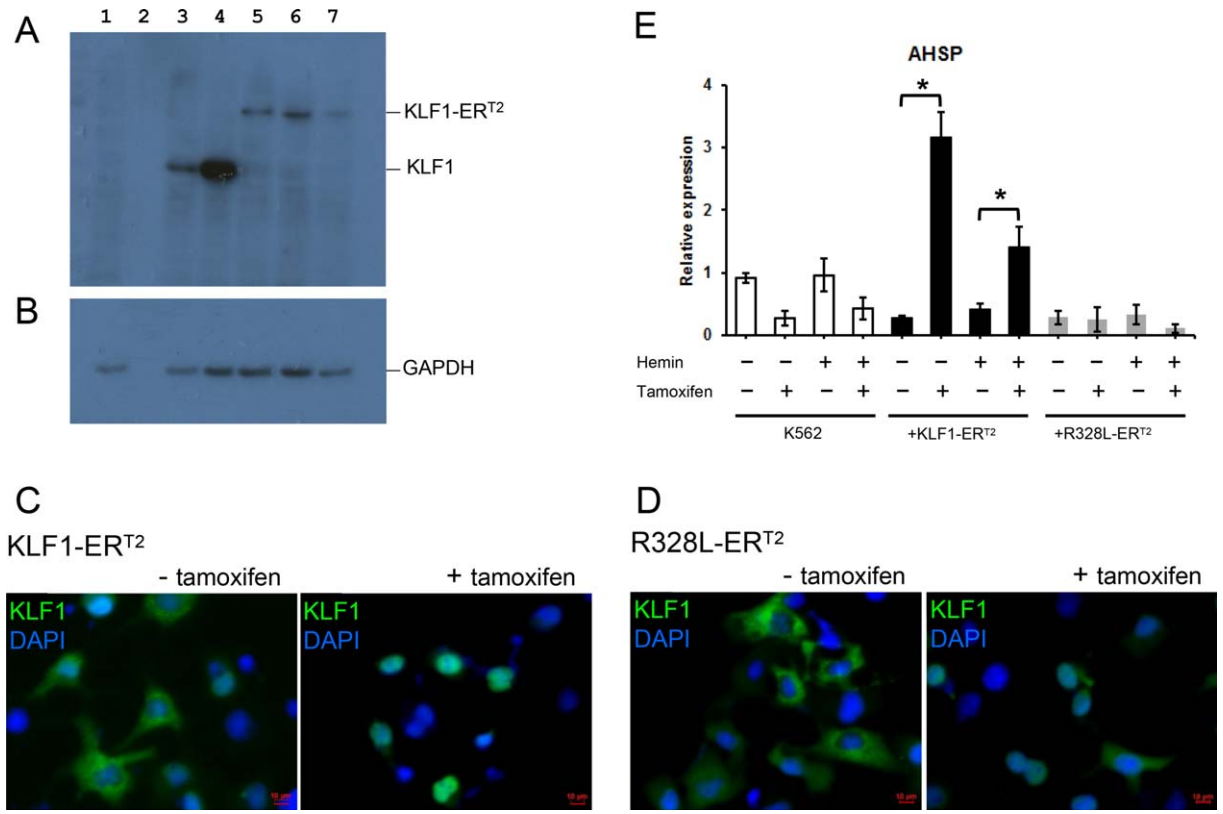

Figure 2. Functional assessment of KLF1-ER^{T2} and R328L-ER^{T2} fusion proteins. **(A, B)**: Western blot analyses of cell lysates isolated from untransfected COS7 cells (lane 1), COS7 cells transfected with pCAG-KLF1 (lane 3); pCAG-R328L (lane 4); pCAG-KLF1-ER^{T2} (lane 5); pCAG-R328L-ER^{T2} (lane 6) and the murine CAG- KLF1-ER^{T2} (lane 7) using an anti-KLF1 antibody (A) and GAPDH as a loading control (B). Lane 2 is blank. **(C, D)**: Immunofluorescence staining of COS7 cells transfected with either the CAG-KLF1-ER^{T2} (A) or CAG-R328L-ER^{T2} (B) constructs then stained with anti-KLF1 antibodies (green) and the DAPI nuclear dye (blue) in the presence and absence of tamoxifen as indicated. (Scale bar 10 μm). **(E)**: Quantitative reverse-transcriptase polymerase chain reaction analyses of RNA isolated from control and hemin and/or tamoxifen-treated K562 cells and K562 cells transfected with either CAG-KLF1-ER^{T2} or CAG-R328L-ER^{T2} vectors using primers for the KLF1 target gene, *AHSP*. Data represent three independent experiments and error bars represent SEM. *p* values were calculated using using one-way ANOVA followed Tukey's multiple comparisons test. (*$p < .05$).

Results

Constitutive Overexpression of KLF1 in Differentiating hESCs Leads to Reduced Cell Proliferation and Hematopoietic Progenitor Cell Production

KLF1 was expressed at a lower level in erythroid progenitors derived from hESC compared to those derived from adult peripheral blood CD34$^+$ progenitors (Supporting Information Fig. S1A) and we hypothesized that this could be one of the reasons for their lack of maturity. H1 hESCs were transfected with vectors carrying either wild type KLF1 or mutant (R328L) KLF1 cDNA under the control of the constitutive CAG promoter followed by an intraribosomal entry site and the puromycin resistance gene (Supporting Information Fig. S1B). The R328L mutant protein had an arginine (R) to leucine (L) substitution in the second zinc finger domain at position 328 that abolishes activity in a transactivation assay (Supporting Information Fig. S1C) [29], but does not interfere with the activity of WT KLF1. There was no significant difference in the morphology of control H1, H1-KLF1, and H1-R328L hESC lines and all cell lines were maintained as undifferentiated hESCs in comparable conditions (data not shown). The morphology of transfected hESCs during the initial days of our erythroid differentiation protocol [15, 36] was comparable to parental H1 hESCs but the proliferation rate at later stages of the differentiation protocol was significantly lower in H1-KLF1 cells (Fig. 1A). There was a significant reduction in the total number of CFU-C colonies detected in H1-KLF1 cells compared to control H1 cells and H1-R328L cells (Fig. 1B). Flow cytometry confirmed the reduction in HPCs with fewer CD34$^+$ CD43$^+$ double positive cells generated in the H1-KLF1 hESC line (Fig. 1C, 1D). Thus, constitutive expression of KLF1 resulted in a significant reduction in the proliferative capacity and an associated reduction in the production of HPCs hampering our ability to assess the specific effects of KLF1 on erythroid differentiation and maturation.

KLF1-ER^{T2} Fusion Protein Can Translocate to the Nucleus and Can Activate KLF1 Target Genes upon Induction

We established an inducible strategy where we could activate KLF at specific time points during differentiation to assess the effects of this transcription factor on later erythroid cell production and maturation. We fused the human KLF1 and the mutant KLF1 (R328L) to the mutated form of the oestrogen receptor (ER^{T2}) (Supporting Information Fig. S1D, S1E) and created the expected sized fusion protein of 74 kD (Fig. 2A, 2B). Before investing resources on assessing this strategy on

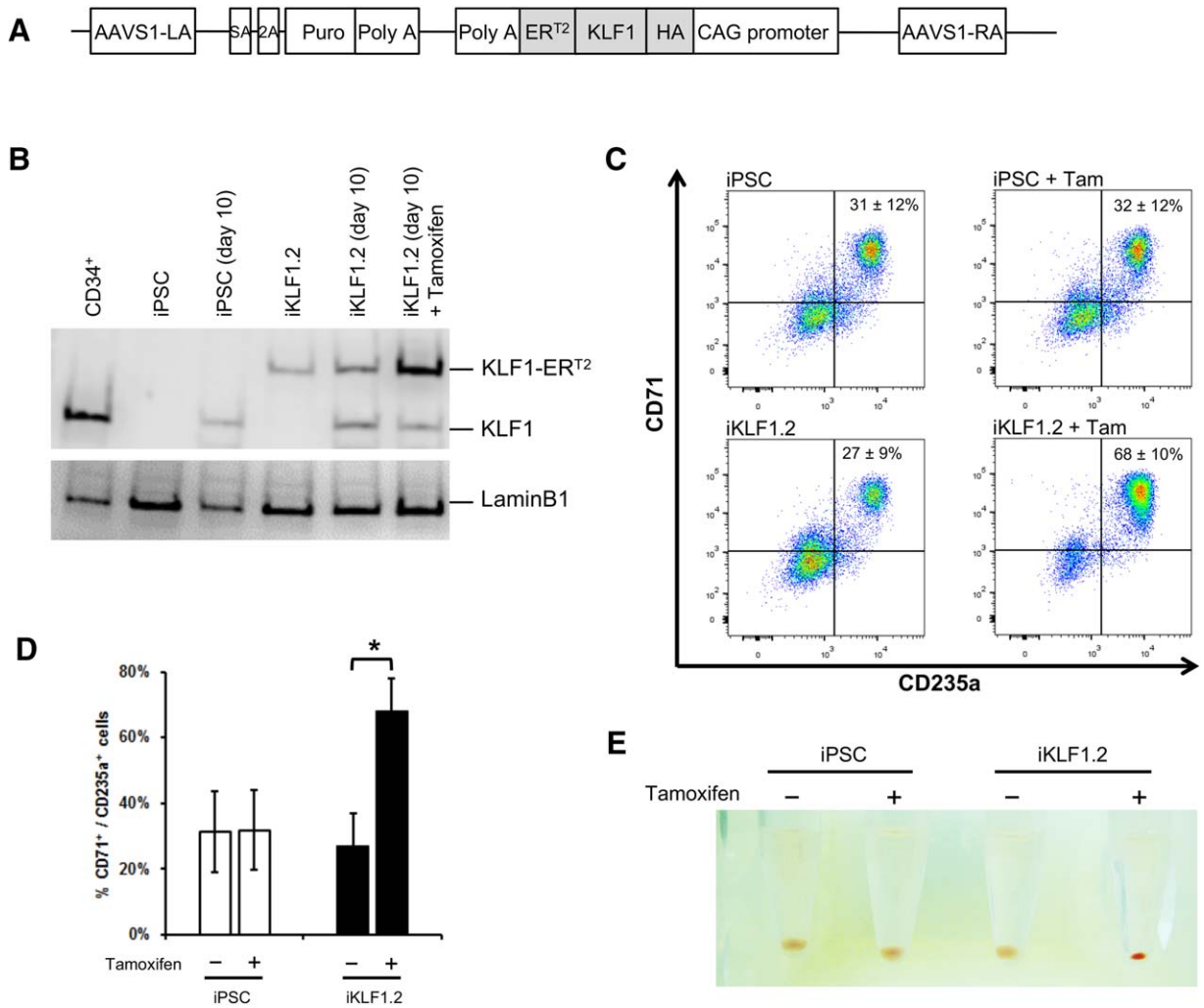

Figure 3. Activation of KLF1 at day 10 of differentiation results in enhanced erythroid differentiation of hiPSCs. **(A)**: Schematic of the pZDonor-AAVS1 Puro-CAG-HA-KLF1-ER^{T2}-PA construct. **(B)**: Western blot analyses of nuclear cell lysates from adult CD34$^+$ cells that had been differentiated for 6 days into erythroid progenitors, control undifferentiated and differentiated (day 10) induced pluripotent stem cells (iPSCs), undifferentiated iKLF1.2 iPSCs and iKLF1.2 iPSC that had been differentiated for 10 days then treated with tamoxifen for 3 hours. Endogenous KLF1 and the expected larger sized KLF1-ER^{T2} fusion protein was detected with the anti-KLF1 antibody and the anti-Lamin B1 antibody was used to detect nuclear proteins as a loading control. **(C)**: Flow cytometry analysis using antibodies against CD235a and CD71 of cells present at day 15 of the erythroid differentiation protocol in control iPSCs and iKLF1.2 iPSC cell lines in the presence (+) and absence (−) of tamoxifen from day 10. **(D)**: Quantitation of flow cytometry data representing three independent experiments. Error bars represent SEM. *p* values were calculated using one-way ANOVA followed by Holm-Sidak's multiple comparison test (*$p < .05$). **(E)**: Image showing the cell pellets from one representative experiment demonstrating a smaller but more intense red pellet in the tamoxifen-treated iKLF1.2 cell line. Abbreviation: iPSCs, induced pluripotent stem cells.

hiPSCs, we first tested the functionality of the KLF1 inducible strategy on simpler well-established cell systems. We used transiently transfected COS7 cells where high levels of transgene expression enable the subcellular location of fusion proteins to be assessed by immunofluorescence staining. This demonstrated that wild type KLF1-ER^{T2} and mutant R328L-ER^{T2} fusion proteins are sequestered in the cytoplasm and, upon tamoxifen treatment, they are released and can translocate to the nucleus (Fig. 2C, 2D).

To assess whether the KLF1-ER^{T2} fusion protein could activate the expression of KLF1 target genes within a hematopoietic context, we used the K562 human leukemia cell line that could be induced to differentiate into the erythroid cells. Pools of puromycin-resistant K562 cells were generated then RNA was isolated after culturing in the presence or absence of tamoxifen. Functionality of the KLF1-ER^{T2} fusion protein was confirmed by demonstrating that the addition of tamoxifen enhanced the expression level of a known KLF1 target gene, Alpha Hemoglobin Stabilizing Protein (*AHSP*) (Fig. 2E). No significant increase in *AHSP* expression was observed after tamoxifen treatment of cells transfected with the CAG-R328L-ER^{T2} construct confirming the lack of transcriptional activity of the mutant form that had been predicted previously from luciferase assays (Supporting Information Fig. S1C). Comparable levels of KLF1-ER^{T2} and CAG-R328L-ER^{T2} protein were produced, excluding the possibility that that the lack of activity of the mutant R328L-ER^{T2} was due to a lower level of expression (Fig. 2A).

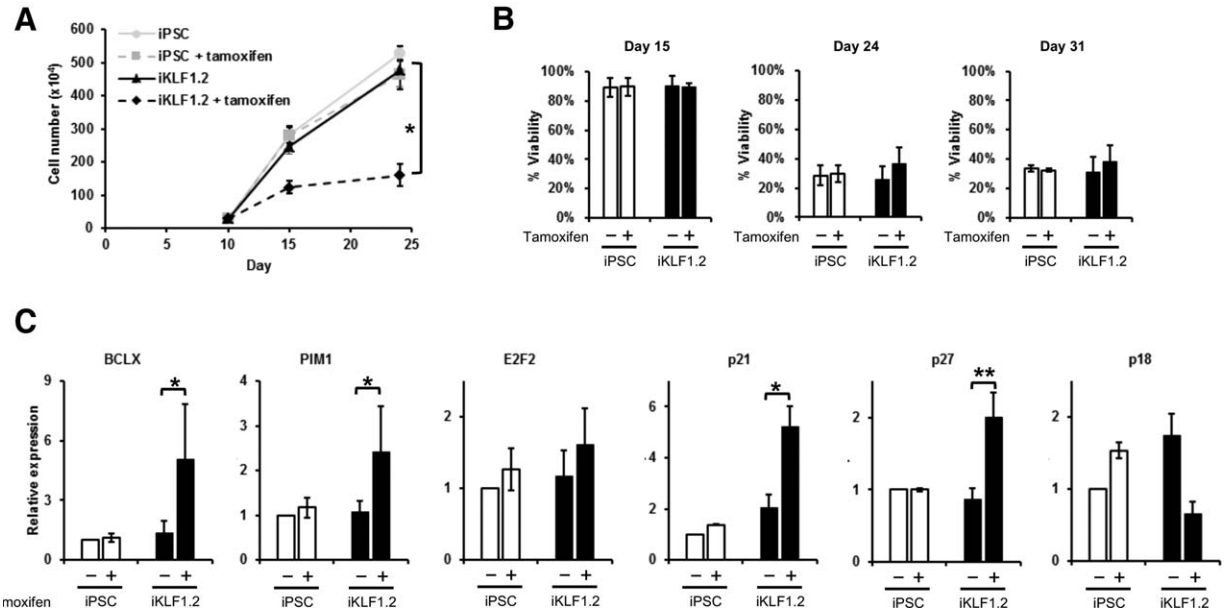

Figure 4. Activation of KLF1 enhances erythroid differentiation at the expense of cell proliferation. **(A)**: Cell numbers of control and iKLF1.2 induced pluripotent stem cells (iPSCs) during erythroid differentiation. 3×10^5 cells were seeded at day 10 of differentiation then further differentiated in the presence or absence of tamoxifen. Data represent the mean of three independent experiments and error bars represents SEM. *p* values were calculated using two-way ANOVA followed by Tukey's multiple comparisons test ($*p < .05$). **(B)**: Flow cytometry analysis using LIVE/DEAD Fixable Near-IR Stain of viable cells present at day 15, 24, and 31 of the erythroid differentiation protocol in control iPSCs and iKLF1.2 iPSC cell lines in the presence (+) and absence (−) of tamoxifen from day 10. **(C)**: Quantitative reverse-transcriptase polymerase chain reaction analyses of RNA isolated from control (iPSC) and iKLF1 iPSC (iKLF1.2) at day 24 following treatment with (+) or without (−) tamoxifen from day 10 using primers to *BCLX, PIM1* and *E2F2, p21, p27,* and *p18*. Data represent the mean of three independent experiments and error bars show the SEM. For each gene, the expression level of control iPSCs in the absence of tamoxifen was used as the calibrator and set at 1 and the expression of all other samples expressed as fold change. A ratio paired *t* test was used to assess the effect of KLF1 activation in iKLF1.2 cells ($*p < .05$ $**p < .005$). Abbreviation: iPSCs, induced pluripotent stem cells.

Activation of KLF1 Promoted Erythroid Differentiation of hESC and iPSCs

We then tested the effects of KLF1 activation on the production and maturation of erythroid cells during hESC and iPSC differentiation. Pilot experiments where pCAG-KLF1-ER^{T2} and pCAG-R382R-ER^{T2} constructs were randomly integrated into the genome of the H1 hESCs indicated that activation of KLF1 promoted the differentiation of erythroid cells as assessed by an increase in the proportion of CD235a$^+$ CD71$^+$ expressing cells and an increase in the level of CD235a expression (Supporting Information Fig. S3). However, given the known silencing issues associated with random integration of transgenes and the potential detrimental effects of insertion mutagenesis, we adopted a 'safe harbor' approach and targeted the CAG-HA-KLF1-ER^{T2} transgene to the *AAVS1* locus (Fig. 3A) [34]. We generated the AAVS1-HA-KLF1-ER^{T2} targeting vector (Fig. 3A) and electroporated this together with the AAVS1 zinc finger nuclease (ZFN) plasmids (a gift from Dr C.J. Chang, Icahn School of Medicine at Mount Sinai, New York) [33, 35] into the human iPSC line, SFCi55 (Supporting Information Fig. S2). Puromycin-resistant colonies were screened by genomic PCR (Supporting Information Fig. S4). 93% (27/29) of iPSC clones were correctly targeted with both *AAVS1* alleles targeted in 13 clones (Supporting Information Fig. S4A-4G). Western blot analyses using the $\alpha-$HA antibody detected the fusion protein in targeted iPSC clones (herein referred to as iKLF1.1 and iKLF1.2) (Supporting Information Fig. S5A). We confirmed the presence of the predicted sized KLF1-ER^{T2} fusion protein in nuclear extracts isolated from undifferentiated and differentiated (day 10) iKLF1.2 iPSCs and noted that the level of expression of KLF1 protein in day 10 differentiating iPSCs was significantly lower than in adult CD34$^+$ cells (Fig. 3B) as was the level of *KLF1* transcript (Supporting Information Fig. S5C) as previously demonstrated (Supporting Information Fig. S1). We noted the presence of a low level of KLF1-ER^{T2} fusion protein in our crude nuclear extracts in the absence of tamoxifen but it is unclear whether this is due to cytoplasmic contamination or leakiness of the ER^{T2} system (Fig. 3B). Addition of tamoxifen for 3 hours resulted in the translocation of KLF1-ER^{T2} protein into the nucleus (Fig. 3B). The level KLF1 protein expression in differentiating iKLF1.2 iPSCs is comparable to the level of expression of endogenous KLF1 in differentiating adult CD34$^+$ cells indicating that, unlike lentiviral expression strategies that result in very high, non-physiological levels of transgene expression, this strategy results in physiological levels of KLF1 (Fig. 3B, Supporting Information Fig. S5C).

The clonal iKLF1.2 iPSC line was differentiated using the erythroid differentiation protocol [36] and we assessed the production of erythroid cells at day 15 in the presence and absence of tamoxifen (from day 10). Upon activation of KLF1, the percentage of CD235a$^+$ CD71$^+$ double positive erythroid cells increased in the iKLF1.2 iPSC lines, but not in control iPSCs (Fig. 3C, 3D). This increase was also observed in the independently derived iKLF1.1 cell line (Supporting Information Fig. S5B) and was consistent with the results using randomly inserted constructs in hESCs (Supporting Information

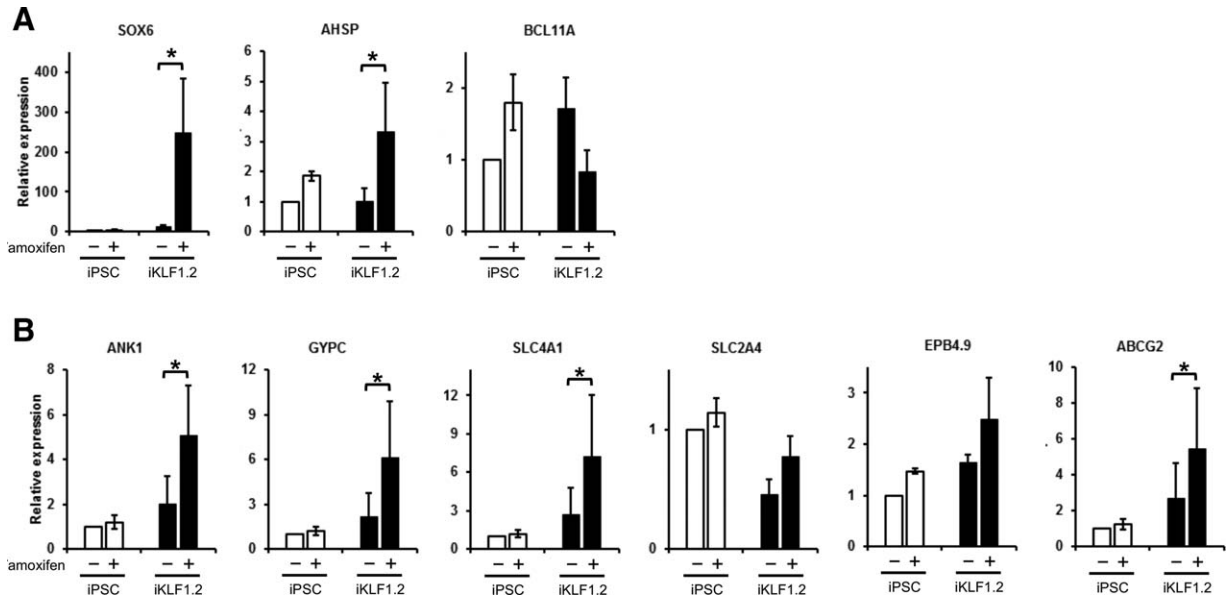

Figure 5. A subset of KLF1 target genes are upregulated upon activation of KLF1 during erythroid differentiation. Quantitative reverse-transcriptase polymerase chain reaction analyses of RNA isolated from control induced pluripotent stem cell (iPSC) and iKLF1 iPSC (iKLF1.2) at day 15 (**A**) and day 24 (**B**) following treatment with (+) or without (−) tamoxifen from day 10 using primers to *SOX6, AHSP, BCL11A, ANK1, GYPC, SLC4A1, SLC2A4, EPB4.9,* and *ABCG2*. Data represent the mean of three independent experiments and error bars show the SEM. For each gene, the expression level of control iPSCs in the absence of tamoxifen was used as the calibrator and set at 1 and the expression of all other samples expressed as fold change. A ratio paired *t* test was used to assess the effect of KLF1 activation in iKLF1.2 cells (*$p < .05$). Abbreviation: iPSCs, induced pluripotent stem cells.

Fig. S3A). These data indicate that activation of KLF1 enhanced erythroid differentiation, visually evident by the enhanced red appearance of the cell pellet (Fig. 3E). We also noted that tamoxifen treated cultures generated a smaller cell pellet and a significantly lower number of cells (Fig. 4A). There was no significant difference in cell viability at days 15, 24, and 31 when KLF1 was activated at day 10 indicating that the reduced cell number was not the result of increased apoptosis or cell death. (Fig. 4B). Furthermore, quantitative reverse-transcriptase polymerase chain reaction analyses of differentiating cells (day 24) demonstrated that activation of KLF1 resulted in a significant upregulation of the cell cycle inhibitors *P21* and *P27*, the anti-apoptotic gene, *BCLX* and *PIM1* that regulates cell proliferation and survival (Fig. 4C). Interestingly KLF1 activation did not result in the upregulation of *P18* which has been shown to mediate the effects of KLF1 effect on cell cycle exit in the murine system [39]. Taken together, our data suggest that activation of KLF1 promotes erythroid differentiation at the expense of cell proliferation.

Activation of KLF1 Enhanced the Expression of Genes Associated with Erythropoiesis

To investigate the impact of KLF1 activation on genes associated with erythropoiesis, we conducted real-time PCR on RNA isolated from differentiating control hiPSCs and iKLF1.2 at day 15 in the presence or absence of tamoxifen from day 10 (Fig. 5A, Supporting Information Fig. S6A). Activation of KLF1 significantly increased the expression of the erythroid transcription factor-encoding gene, *SOX6* consistent with the higher proportion of erythroid cells. Consistent with our findings in K562 cells, expression of the known KLF1 target gene *AHSP* was significantly upregulated upon KLF1 activation. Interestingly the expression of *BCL11A,* a known target gene of KLF1 was not enhanced in this assay but this is possibly explained by the fact that these cells have a "primitive"-like signature (see below). The expression of KLF1 target genes associated with RBC maturation was also analyzed at a later stage in the differentiation process (day 24) (Fig. 5B, Supporting Information Fig. S6B). At this time point, expression of genes associated with cell membrane and cytoskeleton, including *ANK1*, *GYPC*, and *SLC4A1* were significantly increased upon KLF1 activation but there was no significant increase in the expression of *SLC2A4* nor *EPB4.9*. The expression of *ABCG2* that is involved in transport and heme synthesis was also upregulated by KLF1 activation. The above results suggest KLF1 activation from day 10 increased the maturity of erythroid cells and accelerated the process of erythropoiesis.

KLF1-Activated Erythroid Cells Express Embryonic Globins

HPLC analyses of protein isolated from cells at day 31 of the differentiation protocol showed that activation of KLF1 in iKLF1.2-derived erythroid cells significantly enhanced the proportion of the embryonic ϵ- and ζ-globin and reduced the proportion of γ-globin protein. No adult β-globin protein was detected in any of the samples (Fig. 6). Taken together these data suggests that, in this differentiation system, activation of KLF1 at day 10 of the differentiation protocol enhances the production and maturation of primitive erythroid cells.

KLF1 Activation Increases the Proportion of Enucleated Erythroid Cells

Given previous reports that KLF1 null mice had more nucleated RBCs [25], we hypothesized that activation of exogenous KLF1 might enhance the efficiency of maturation and/or their stability. Differentiating KLF1-ER^{T2}-expressing cells were treated with

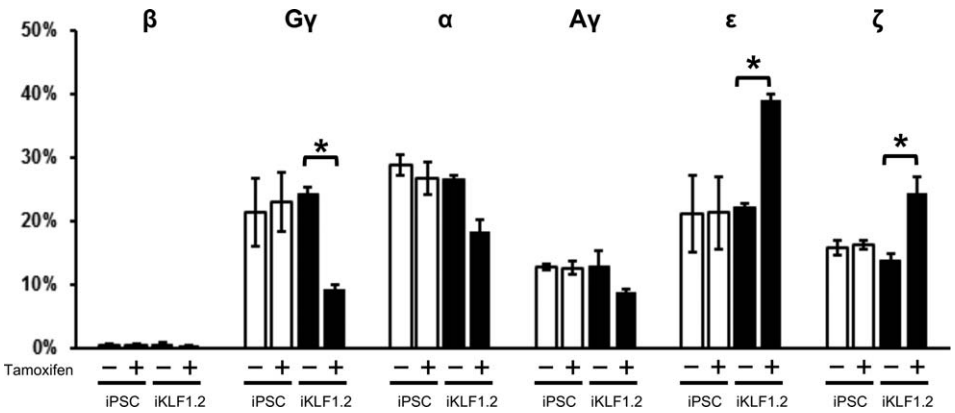

Figure 6. Activation of KLF1 enhances the production erythroid cells expressing embryonic globins. Results of HPLC analysis of globin proteins in cell lysates isolated from control induced pluripotent stem cells and iKLF1.2 cells at day 31 of the differentiation protocol in the presence (+) or absence (−) of tamoxifen from day 10. Data represent the mean of three independent experiments and error bars represents SEM. *p* values were calculated using two-way ANOVA followed by Tukey's multiple comparisons test. (*$p < .05$). Abbreviation: iPSCs, induced pluripotent stem cells.

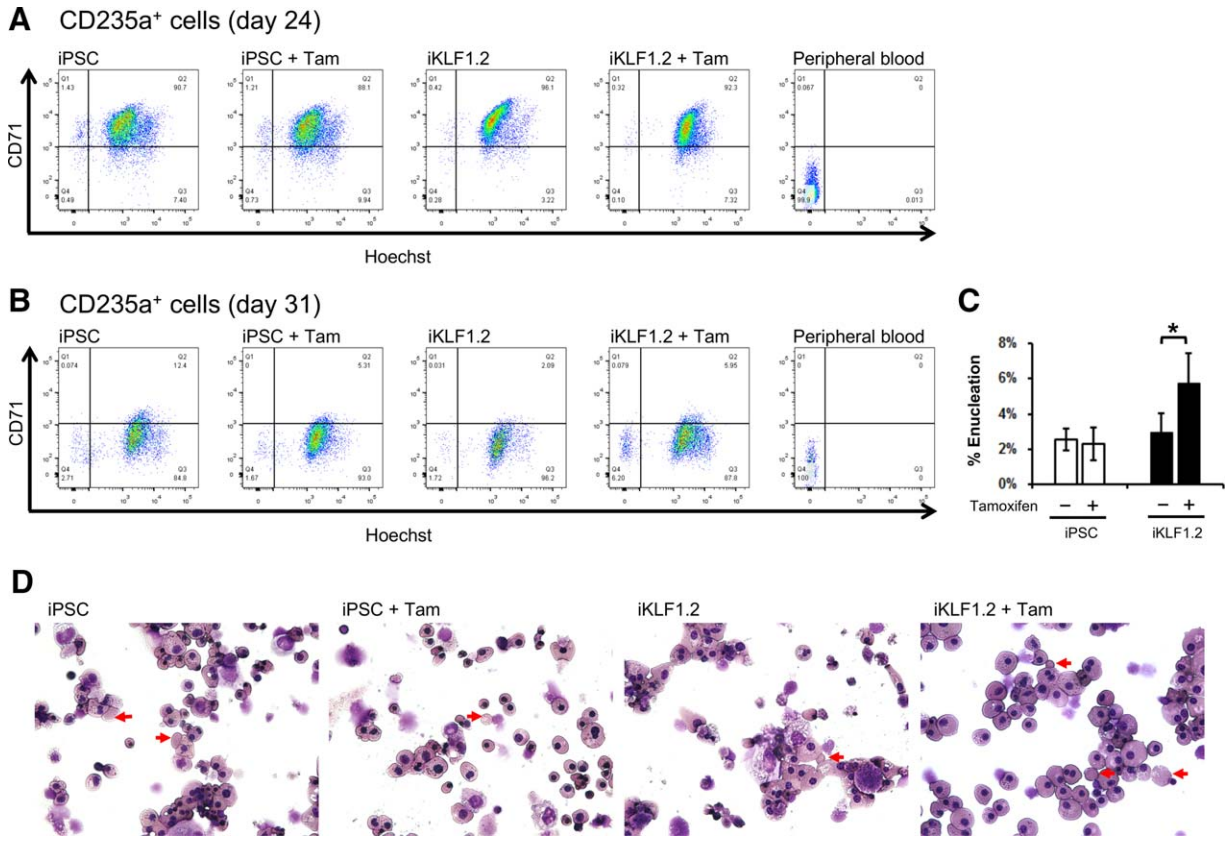

Figure 7. KLF1 activation increases the proportion of detectable enucleated cells. (**A, B**): CD71 and Hoechst staining of live, CD235a gated cells at day 24 (A) and day 31 (B) derived from control induced pluripotent stem cell (iPSC) and KLF1-ER^{T2}-expressing (iKLF1.2) cells in the presence and absence of tamoxifen. Control enucleated cells derived from adult peripheral blood is shown. (see Supporting Information Fig. S7 for gating strategy) **(C)** Quantification of the proportion of enucleated cells at day 31 of control iPSCs and iKLF1.2 cells in the presence and absence of tamoxifen. Data represent the mean of three independent experiments and error bars represents SEM. *p* values were calculated using one-way ANOVA followed by Holm-Sidak's multiple comparison test (*$p < .05$). (**D**): Cytospins of day 31 cells demonstrating the more robust phenotype of iKLF1 cells after tamoxifen treatment and the presence of some enucleated cells (arrows) (Magnification x40). Abbreviation: iPSCs, induced pluripotent stem cells.

tamoxifen then the presence of enucleate cells assessed by flow cytometry. Live CD235a$^+$ cells were gated and CD235a$^+$/CD71$^+$/Hoechst$^+$ erythroblasts, CD235a$^+$/CD71$^-$/Hoechst$^+$ nucleated RBCs and CD235a$^+$/CD71$^-$/Hoechst$^-$ enucleated RBCs were identified (Supporting Information Fig. S7). Human peripheral blood was used as a positive control for the identification of live, CD235a$^+$/CD71$^-$/Hoechst$^-$ enucleated RBCs. The majority of differentiating cells at day 24 were nucleated

$CD235a^+/CD71^+/Hoechst^+$ erythroblasts (Fig. 7A). By day 31 $CD235a^+$ cells began to lose the CD71 marker, indicating that they represented a more mature erythroid population (Fig. 7B). Activation of KLF1 in differentiating iPSCs reproducibly increased the proportion of enucleated RBCs that were detected in this assay (Fig. 7B, 7C). Morphological analyses indicated that that KLF1-activated cells had a more robust morphology which could explain the fact that more enucleated cells were detected (Fig. 7D).

Discussion

Current protocols to produce RBCs from hPSC have limitations because they generate a relatively low proportion of enucleated cells and express embryonic/foetal but not adult globin [6]. Forward programming using lineage specific transcription factors has been used to enhance the production of a number cell types from hPSCs including hematopoietic lineages [16, 17, 40]. Here we describe the first application of an inducible programming strategy to modify the production and maturation of RBCs from hPSCs. We used the transcription factor KLF1 because it was expressed at low levels in hPSC-derived erythroid cells compared adult-derived cells and it plays a pivotal role in the final steps of definitive erythropoiesis [19]. Genes that are regulated by KLF1 include many of the key genes associated with erythroid development and maturation [19, 25, 41, 42].

We established an inducible activation strategy whereby the exogenous KLF-ER^{T2} fusion protein is tethered in the cytoplasm but upon addition of tamoxifen it can translocate to the nucleus and activate the expression of target genes. The level expression of KLF1 in differentiating iKLF1.2 iPSCs is comparable to the level of expression in differentiating adult $CD34^+$ cells indicating that physiological levels of expression are achieved using this strategy.

Activation of KLF1 at day 10 after HPC formation resulted in an increase in the proportion of erythroid cells but the overall number of cells was lower than controls. The fact that we observed no effect on the viability of cells suggests that activation of KLF1 is driving HPCs to differentiate at the expense of proliferation [43]. It is well documented that erythroid terminal differentiation requires proliferation arrest and exit from the cell cycle with a balance between proliferation and maturation being fine-tuned at later stages of erythropoiesis [24, 44]. The antiproliferative effect of KLF1 during erythropoiesis is thought to be via its interactions with cell cycle related genes including *PIM1, E2F2, p27*, *p21, p18* [19, 39, 45]. We demonstrate that activation of KLF1 significantly altered the expression levels of *p27*, *p21,* and *PIM1* but not *p18* suggesting that some, but not all, of these interactions are conserved between mouse and human. Our results are consistent with a study using a similar KLF1-ER^{T2} strategy in murine ESCs where activation of KLF1 resulted in reduced proliferation coupled with enhanced differentiation [46]. Another study using a tetracycline-inducible KLF1 strategy in murine ESCs expression reported that KLF1 promoted the expression of erythroid lineage genes while repressing the onset of megakaryopoiesis [43]. We detected an increase in expression of KLF1 target genes associated with heme synthesis and transport including *ABCG2* and *AHSP*, supporting the notion that KLF1-activation enhanced the erythroid maturation and differentiation process.

Activation of exogenous KLF1 resulted in an increase in the proportion of detectable enucleated erythroid cells. It has been proposed that hPSC-derived erythroid cells may be more fragile than their counterparts generated from adult CD34 progenitors [36] and so it is possible that the effect of KLF1 is due to enhanced membrane stability rather than a direct effect on the enucleation process per se. The final stages of RBC maturation are associated with cell membrane and cytoskeleton remodelling and a number of KLF1 target genes have been associated with these processes [19, 21, 26, 47]. Furthermore, the phenotype of KLF1 deficient mice has been associated with decreased membrane stability [21]. Activation of KLF1 in our system enhanced the expression of some of these KLF1 targets including *ANK1, GYPC, SLC4A1*, and *ABCG2* which supports our hypothesis that activation of KLF1 results in the production of more robust erythroid cells.

The mechanisms of enucleation is known to involve multiple molecular and cellular pathways including histone deacetylation, actin polymerization, cytokinesis, cell-matrix interactions, specific microRNAs, and vesicle trafficking [48]. Enucleation efficiency of iPSC-derived erythroid cells was improved with stromal cell culture and when cells were derived from cultures involving prolonged three-dimensional culture [1, 5]. More recently KLF1 has been shown to have an extrinsic role in erythroid maturation via expression of KLF1 in erythroid-island associated macrophages [49, 50] so KLF1 may be playing an extrinsic role during the differentiation process. It is also possible that KLF1 activation is altering the expression of miRNAs or long noncoding RNAs that have been identified as key players in erythroid development and maturation [1, 51].

The majority of hPSC differentiation protocols generate RBCs that express embryonic ϵ-globins and/or foetal γ-globins, but little or no adult β-globin [6, 7]. We show that KLF1 enhanced the expression of embryonic ϵ- and ζ-globin proteins, but no adult β-globin was detected in any of the conditions suggesting that this strategy is enhancing the production of embryonic erythroid cells and that KLF1 alone is not sufficient to enhance the expression of adult β-globin. A low level of expression of KLF1 and BCL11A in K562 cell and cord blood derived erythroid cells was shown to be associated with fetal globlin expression and transduction of *KLF1* and *BCL11A* lentiviral vectors resulted in adult levels of β−globin in these cells [52]. Interestingly that study also demonstrated that lentiviral transduction of *BCL11A* alone was sufficient to induce the expression of β−globin in the immortalized iPSC-derived HiDEP-1 cell line because that cell lines had adult-like levels of KLF1 [52]. A recent study that added KLF1 to iEP cells showed adult-like globin [17]. The erythroid cells derived from the SFCi55 iPSC cell line used in this study have lower levels of KLF1 compared to differentiated adult $CD34^+$ cells (Fig. 3B, Supporting Information Fig. S5C) and, although *BCL11A* has been reported as a KLF1 target gene, we did not see a significant alteration in the level of expression of *BCL11A* upon KLF1 activation in our system. Activation of KLF1 target genes will rely on the presence of specific cofactors which will be cell context dependent. More recent studies highlight the complexity of interaction between KLF1 and its regulated genes and specialized transcription factories in

nuclear hotspots have been identified that are likely where coregulated genes cooperate for optimal efficiency and coordinated transcriptional control [20]. Our ongoing studies are assessing the effects of exogenous expression of both *KLF1* and *BCL11A* on the expression of the different globin proteins in differentiating iPSCs.

Flow cytometry analyses of erythroid markers throughout the differentiation protocol indicates that there are two waves of erythropoiesis in our culture system [36] and our data suggest that activation of KLF1 at day 10 is enhancing the primitive rather than the definitive wave.

This study is the first to demonstrate enhanced erythropoiesis from hPSCs using a forward programming approach by activation of a single transcription factor, KLF1 at levels that are comparable to physiological level. However, the successful production of adult-like erythroid cells in sufficient quantities from iPSCs will undoubtedly require the use of multiple transcription factors in a combinatorial forward programming approach as recently described for the production of platelets form hPSCs [40] and primitive erythroid cells from fibroblasts [17]. The key to this strategy is to define the complex cocktail of transcription factors that define the development and maintenance of adult erythroid cells and to induce their expression at defined timepoints in a reproducible manner. Integration of inducible transcription factors into the *AAVS1* locus could provide a safer and more reproducible strategy for clinical translation.

This study assessed the effects of KLF1 on the production and maturation of erythroid cells from differentiating human pluripotent stem cells. We generated a human iPSC line carrying a tamoxifen-inducible form of KLF1 in the AAVS1 locus. Activation of KLF1 alone promoted erythroid differentiation, enhanced the expression of key erythroid genes and generated a slightly higher proportion of mature enucleated cells. However, activation of KLF1 promoted the differentiation of primitive, not definitive erythroid cells as defined by an increase in embryonic globins. The enhanced erythroid differentiation is associated with a proliferation arrest and the upregulation of the cell cycle inhibitors P21 and P27 resulting in a significant reduction in the overall number of cells generated.

Acknowledgments

This work was carried out as part of the Novosang consortium (www.novosang.co.uk) with funding from Wellcome Trust and Scottish Funding Council. CTY received a Global Scholarship from University of Edinburgh College of Medicine and Veterinary Medicine). We thank Dr CJ Cheng (Icahn School of Medicine, at Mount Sinai, New York) for reagents used to target the *AAVS1* locus, Dr Belinda Singleton for human KLF1 cDNAs and Prof David Anstee for valuable discussions. R.M. is currently affiliated with Peking University Institute of Hematology, Peking University People's Hospital, Beijing100044, China.

Author Contributions

C.-T.Y.: Performed research, analysed data and wrote paper; R.M.: Performed research and analysed data; R.A.A.: Performed research; M.J.: performed research; A.H.T.: Performed research; A.F.: Performed research and analysed data; L.M.: Performed research; J.F., J.C.M.: Designed research and analysed data; L.M.F.: Designed research, analysed data and wrote paper.

Disclosure of Potential Conflicts of Interest

The authors indicate no potential conflicts of interest.

References

1 Rouzbeh S, Kobari L, Cambot M et al. Molecular signature of erythroblast enucleation in human embryonic stem cells. Stem Cells 2015;33:2431–2441.
2 Yang CT, French A, Goh PA et al. Human induced pluripotent stem cell derived erythroblasts can undergo definitive erythropoiesis and co-express gamma and beta globins. Br J Haematol 2014;166:435–448.
3 Mountford J, Olivier E, Turner M. Prospects for the manufacture of red cells for transfusion. Br J Haematol 2010;149:22–34.
4 Giarratana MC, Rouard H, Dumont A et al. Proof of principle for transfusion of in vitro-generated red blood cells. Blood 2011; 118:5071–5079.
5 Lu SJ, Feng Q, Park JS et al. Biologic properties and enucleation of red blood cells from human embryonic stem cells. Blood 2008;112:4475–4484.
6 Chang KH, Bonig H, Papayannopoulou T. Generation and characterization of erythroid cells from human embryonic stem cells and induced pluripotent stem cells: An overview. Stem Cells Int 2011;2011:791604.
7 Cerdan C, Rouleau A, Bhatia M. VEGF-A165 augments erythropoietic development from human embryonic stem cells. Blood 2004;103:2504–2512.
8 Takahashi K, Yamanaka S. Induction of pluripotent stem cells from mouse embryonic and adult fibroblast cultures by defined factors. Cell 2006;126:663–676.
9 Yang N, Ng YH, Pang ZP et al. Induced neuronal cells: How to make and define a neuron. Cell Stem Cell 2011;9:517–525.
10 Miki K, Yoshida Y, Yamanaka S. Making steady progress on direct cardiac reprogramming toward clinical application. Circ Res 2013;113:13–15.
11 Jackson M, Axton RA, Taylor AH et al. HOXB4 can enhance the differentiation of embryonic stem cells by modulating the hematopoietic niche. Stem Cells 2012;30:150–160.
12 Ramos-Mejia V, Navarro-Montero O, Ayllon V et al. HOXA9 promotes hematopoietic commitment of human embryonic stem cells. Blood 2014;124:3065–3075.
13 Ran D, Shia WJ, Lo MC et al. RUNX1a enhances hematopoietic lineage commitment from human embryonic stem cells and inducible pluripotent stem cells. Blood 2013;121: 2882–2890.
14 Real PJ, Ligero G, Ayllon V et al. SCL/TAL1 regulates hematopoietic specification from human embryonic stem cells. Mol Ther 2012;20:1443–1453.
15 Jackson M, Ma R, Taylor AH et al. Enforced expression of HOXB4 in human embryonic stem cells enhances the production of hematopoietic progenitors but has no effect on the maturation of red blood cells. Stem Cells Transl Med 2016;8:981–990.
16 Easterbrook J, Fidanza A, Forrester LM. Concise review: Programming human pluripotent stem cells into blood. Br J Haematol 2016;173:671–679.
17 Capellera-Garcia S, Pulecio J, Dhulipala K et al. Defining the minimal factors required for erythropoiesis through direct lineage conversion. Cell Rep 2016;15:2550–2562.
18 Yien YY, Bieker JJ. EKLF/KLF1, a tissue-restricted integrator of transcriptional control, chromatin remodeling, and lineage determination. Mol Cell Biol 2013;33:4–13.
19 Tallack MR, Perkins AC. KLF1 directly coordinates almost all aspects of terminal erythroid differentiation. IUBMB Life 2010; 62:886–890.
20 Schoenfelder S, Sexton T, Chakalova L et al. Preferential associations between co-regulated genes reveal a transcriptional interactome in erythroid cells. Nat Genet 2010;42:53–61.
21 Drissen R, von Lindern M, Kolbus A et al. The erythroid phenotype of EKLF-null mice: Defects in hemoglobin metabolism and membrane stability. Mol Cell Biol 2005;25: 5205–5214.
22 Nilson DG, Sabatino DE, Bodine DM et al. Major erythrocyte membrane protein

genes in EKLF-deficient mice. Exp Hematol 2006;34:705–712.
23 Hodge D, Coghill E, Keys J et al. A global role for EKLF in definitive and primitive erythropoiesis. Blood 2006;107:3359–3370.
24 Siatecka M, Sahr KE, Andersen SG et al. Severe anemia in the Nan mutant mouse caused by sequence-selective disruption of erythroid Kruppel-like factor. Proc Natl Acad Sci USA 2010;107:15151–15156.
25 Perkins AC, Peterson KR, Stamatoyannopoulos G et al. Fetal expression of a human Agamma globin transgene rescues globin chain imbalance but not hemolysis in EKLF null mouse embryos. Blood 2000;95: 1827–1833.
26 Magor GW, Tallack MR, Gillinder KR et al. KLF1-null neonates display hydrops fetalis and a deranged erythroid transcriptome. Blood 2015;125:2405–2417.
27 Huang J, Zhang X, Liu D et al. Compound heterozygosity for KLF1 mutations is associated with microcytic hypochromic anemia and increased fetal hemoglobin. Eur J Hum Genet 2015;10:1341–1348.
28 Arnaud L, Saison C, Helias V et al. A dominant mutation in the gene encoding the erythroid transcription factor KLF1 causes a congenital dyserythropoietic anemia. Am J Hum Genet 2010;87:721–727.
29 Singleton BK, Burton NM, Green C et al. Mutations in EKLF/KLF1 form the molecular basis of the rare blood group In(Lu) phenotype. Blood 2008;112:2081–2088.
30 Singleton BK, Frayne J, Anstee DJ. Blood group phenotypes resulting from mutations in erythroid transcription factors. Curr Opin Hematol 2012;19:486–493.
31 Singleton BK, Lau W, Fairweather VS et al. Mutations in the second zinc finger of human EKLF reduce promoter affinity but give rise to benign and disease phenotypes. Blood 2011;118:3137–3145.
32 Perkins A, Xu X, Higgs DR et al. "Kruppeling" erythropoiesis: An unexpected broad spectrum of human red blood cell disorders due to KLF1 variants unveiled by genomic sequencing. Blood 2016;127:1856–1862.
33 DeKelver RC, Choi VM, Moehle EA et al. Functional genomics, proteomics, and regulatory DNA analysis in isogenic settings using zinc finger nuclease-driven transgenesis into a safe harbor locus in the human genome. Genome Res 2010;20:1133–1142.
34 Sadelain M, Papapetrou EP, Bushman FD. Safe harbours for the integration of new DNA in the human genome. Nat Rev Cancer 2012;12:51–58.
35 Hockemeyer D, Soldner F, Beard C et al. Efficient targeting of expressed and silent genes in human ESCs and iPSCs using zinc-finger nucleases. Nat Biotechnol 2009;27:851–857.
36 Olivier EN, Marenah L, McCahill A et al. High-efficiency serum-free feeder-free erythroid differentiation of human pluripotent stem cells using small molecules. Stem Cells Transl Med 2016;10:1394–1405.
37 Zwaka TP, Thomson JA. Homologous recombination in human embryonic stem cells. Nat Biotechnol 2003;21:319–321.
38 Lapillonne H, Kobari L, Mazurier C et al. Red blood cell generation from human induced pluripotent stem cells: Perspectives for transfusion medicine. Haematologica 2010;95:1651–1659.
39 Gnanapragasam MN, McGrath KE, Catherman S et al. EKLF/KLF1-regulated cell cycle exit is essential for erythroblast enucleation. Blood 2016;128:1631–1641.
40 Moreau T, Evans AL, Vasquez L et al. Large-scale production of megakaryocytes from human pluripotent stem cells by chemically defined forward programming. Nat Commun 2016;7:11208.
41 Nuez B, Michalovich D, Bygrave A et al. Defective haematopoiesis in fetal liver resulting from inactivation of the EKLF gene. Nature 1995;375:316–318.
42 Siatecka M, Bieker JJ. The multifunctional role of EKLF/KLF1 during erythropoiesis. Blood 2011;118:2044–2054.
43 Frontelo P, Manwani D, Galdass M et al. Novel role for EKLF in megakaryocyte lineage commitment. Blood 2007;110:3871–3880.
44 Tallack MR, Keys JR, Perkins AC. Erythroid Kruppel-like factor regulates the G1 cyclin dependent kinase inhibitor p18INK4c. J Mol Biol 2007;369:313–321.
45 Zhao Y, Hu J, Buckingham B et al. Pim-1 kinase cooperates with serum signals supporting mesenchymal stem cell propagation. Cells Tissues Organs 2014;199:140–149.
46 Coghill E, Eccleston S, Fox V et al. Erythroid Kruppel-like factor (EKLF) coordinates erythroid cell proliferation and hemoglobinization in cell lines derived from EKLF null mice. Blood 2001;97:1861–1868.
47 Tallack MR, Whitington T, Yuen WS et al. A global role for KLF1 in erythropoiesis revealed by ChIP-seq in primary erythroid cells. Genome Res 2010;20:1052–1063.
48 Ji P, Murata-Hori M, Lodish HF. Formation of mammalian erythrocytes: Chromatin condensation and enucleation. Trends Cell Biol 2011;21:409–415.
49 Porcu S, Manchinu MF, Marongiu MF et al. Klf1 affects DNase II-alpha expression in the central macrophage of a fetal liver erythroblastic island: A non-cell-autonomous role in definitive erythropoiesis. Mol Cell Biol 2011;31:4144–4154.
50 Xue L, Galdass M, Gnanapragasam MN et al. Extrinsic and intrinsic control by EKLF (KLF1) within a specialized erythroid niche. Development 2014;141:2245–2254.
51 Alvarez-Dominguez JR, Hu W, Yuan B et al. Global discovery of erythroid long noncoding RNAs reveals novel regulators of red cell maturation. Blood 2014;123:570–581.
52 Trakarnsanga K, Wilson MC, Lau W et al. Induction of adult levels of beta-globin in human erythroid cells that intrinsically express embryonic or fetal globin by transduction with KLF1 and BCL11A-XL. Haematologica 2014;99:1677–1685.

See www.StemCellsTM.com for supporting information available online.

Yang et al. Supplementary Figures.

Supplementary Figure S1

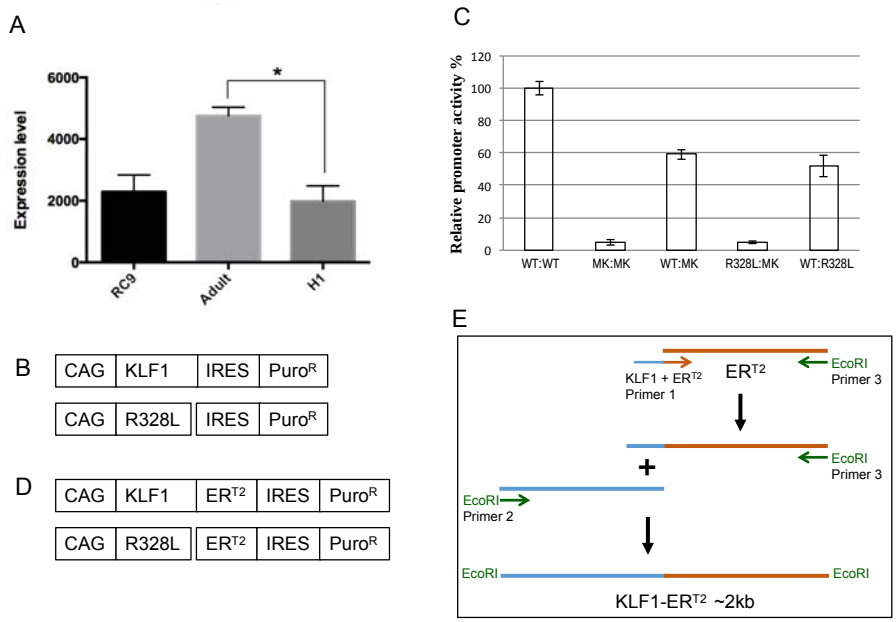

Supplementary Figure S1.

A. Relative expression of KLF1 extracted from microarray data of erythroid cells derived either from hESCs (RC9 and H1) and adult peripheral blood (adult). P values were calculated using one-way ANOVA followed by Dunn's multiple comparison test. (*, $p<0.05$). Microarray data was confirmed by qRT-PCR (data not shown).

B. Schematic of vectors used to express constitutive wild type KLF1 / mutant R328L cDNAs under the control of the CAG promoter linked to puromycin resistance gene by intra-ribosomal entry site (IRES).

C. The R328L KLF1 mutant is nonfunctional in a β-globin promoter-*f*luc assay and does not interfere with activity of wild type KLF1.

Relative promoter activity in K562 cell extracts 24 hours after transient co-transfection with β-globin promoter-*f*luc construct, pRL CMV and 5mg of either empty vector (EV) or constructs expressing wild type (WT) or R328L mutant EKLF (R328L). Relative promoter activity is expressed as the firefly luciferase activity normalised for transfection efficiency using renilla luciferase activity. Results are shown as means +/- SD (n=3).

D. Schematic of vectors used to express the inducible wild type KLF1-ER^{T2} / mutant R328L-ER^{T2} cassettes under the control of the CAG promoter linked to puromycin resistance gene by intra-ribosomal entry site (IRES).

The ER^{T2} domain was first amplified using Primers 1 and 3 then this PCR product was mixed with KLF1 cDNA and primers 2 and 3 and the KLF1-ERT2 was amplified using FailSafe PCR (Epicentre) with the premix J solution (FS99100) according to manufacturer's instructions.

Primer 1: primer with an KLF1 sequence at the 5'end of the ER^{T2} sequence.

Primer 2: primer with an EcoRI site at the 5'end of the KLF1 sequence.

Primer 3: primer with an EcoRI site at the 3'end of the ER^{T2} sequence.

Supplementary Figure S2

A

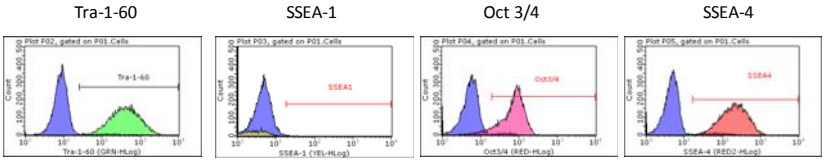

B

Sample ID	Tra-1-60+ (%)	SSEA1+ (%)	Oct3/4 + (%)	SSEA4 +(%)
SFCi55 unstained	0.04	0.01	0.01	0.02
SFCi55 stained	93.50	4.01	65.12	90.61
SFCi55 iso	6.80	1.04	4.36	6.45

C

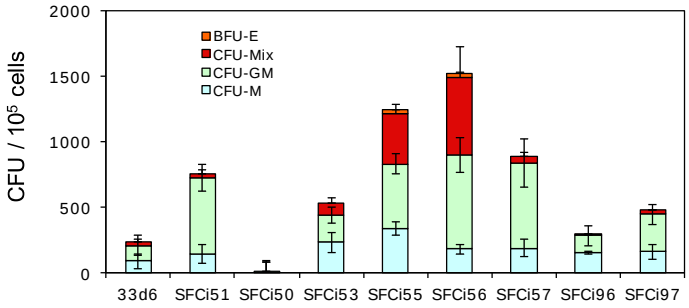

Supplementary Figure S2. Characterisation of O RhesusD negative iPSCs.

A/B. Flow cytometry analyses of SFCi55 iPSC line of pluripotency markers (TRA1-60, SSEA-4, OCT4) and differentiation marker (SSEA-1).

C. CFU-C formation indicative of the hematopoietic differentiation potential of SFCi55 iPSCs was compared to a number of other iPSC lines was assessed at day 10 of the differentiation protocol (Olivier et al 2016).

Supplementary Figure S3

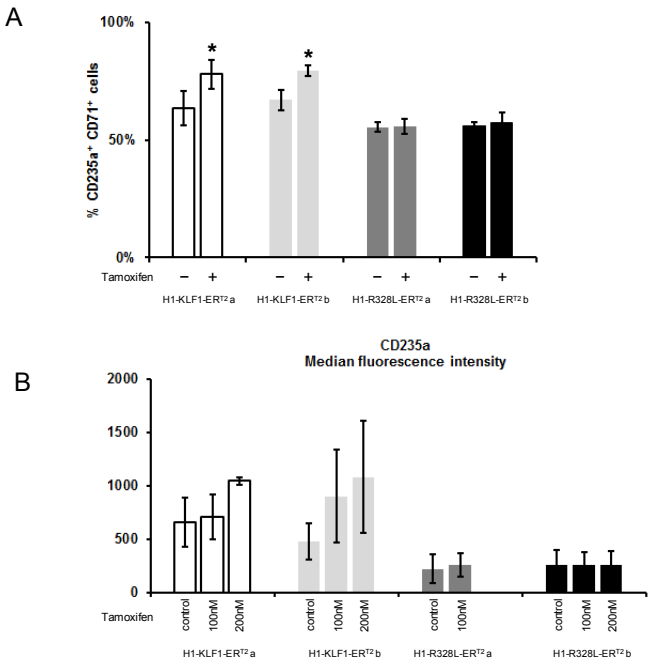

Supplementary Figure S3. Inducible KLF1-ER^{T2} system in H1-ESCs.

A**.** Percentage of CD235a and CD71 double positive cells in the presence or absence of 200nM tamoxifen at day 17.

B**.** Mean Fluorescence intensity (MFI) measurements of CD235a expression in day 17 cells following administration of 0 (control) 100 or 200nM tamoxifen from day 10 of differentiation.

All data represent the mean of 3 independent experiments with error bars showing the standard error of the mean (SEM). P values were calculated using paired t-test (*p<0.05)

Supplementary Figure S4

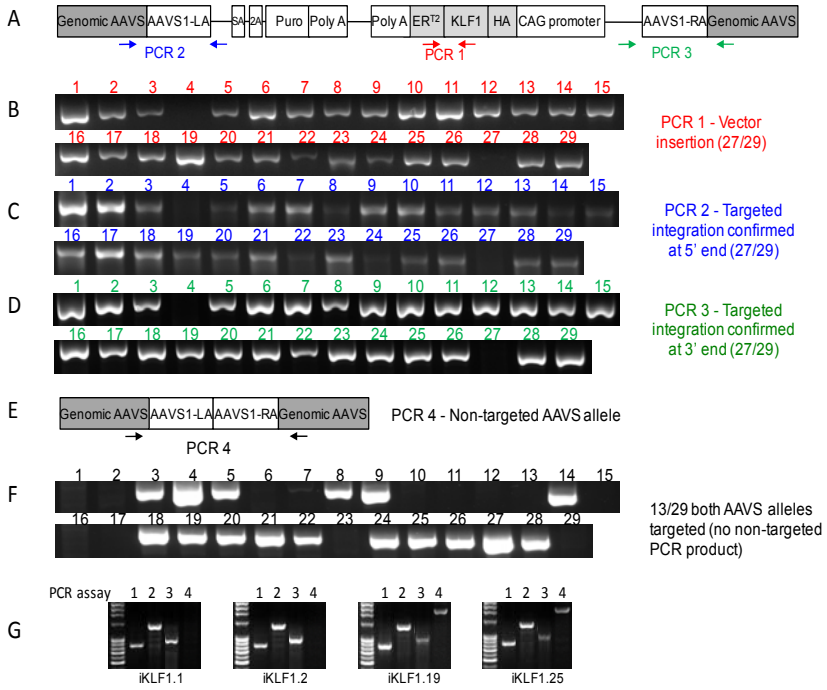

Supplementary Figure S4. AAVS targeting strategy

A. Schematic of genomic structure of targeted alleles showing the locations of diagnostic internal and external PCR assays, 1-3.

B-D. Genomic PCR analyses using internal primer pair (PCR 1) demonstrating integration of the vector (B) and diagnostic PCR confirming correct targeting at the 5' (PCR 2)(C) and 3' end (PCR 3)(D) in 27/29 clones.

E. Schematic of genomic structure of the endogenous, untargeted AAVS locus.

F. Genomic PCR analysis using primer pair, PCR 4 distinguished homozygous and heterozygous targeted events. Note that the two clones (no 4 and 27) that were not targeted (identified in C and D above) generated a more intense PCR product in this untargeted PCR assay as predicted. Thus 13/29 of the clones were targeted at both AAVS alleles (homozygous), 14/29 at one allele (heterozygous) and 2/29 were not targeted.

G. PCR genotypes of 2 homozygous (iKLF1.1 and iKLF 1.2) and 2 heterozygous (iKLF1.19 and iKLF 1.25) were confirmed using the 4 PCR assays, 1-4.

AAVS1-RA, AAVS1 right homology arm; SA, splice acceptor; 2A, a self-cleaving peptide sequence; Puro, puromycin resistance gene; PolyA, polyadenylation sequence; AAVS1-LA, AAVS1 left homology arm.

Supplementary Figure S5

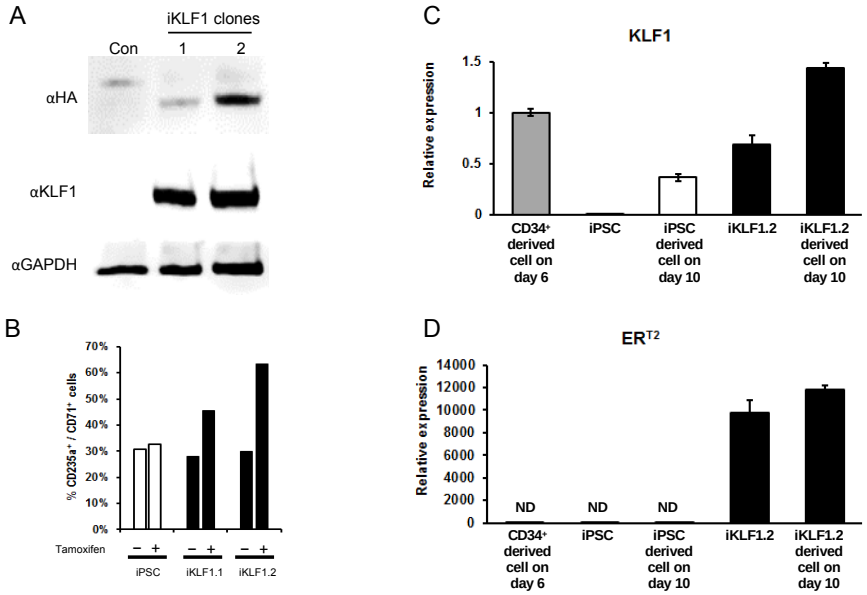

Supplementary Figure S5. KLF1 expression and production of erythroid cells from control iPSCs and iPSC lines iKLF1.1 and iKLF1.2.

A. Western blot analyses of cell lysates from control iPSCs (Con) and two puromycin-resistant iKLF1 iPSC clones (iKLF1.1 and iKLF1.2) using anti-HA (αHA), anti-KLF1 (αKLF1) and anti-GAPDH (αGAPDH) antibodies. (The band observed in Control sample with the αHA antibody is non-specific)

B. %CD235a+/CD71+ cells in day 15 differentiated control iPSCS and in two independently-derived iKLF1 cell lines (iKLF1.1 and iKLF1.2) in the presence (+) and absence (-) of tamoxifen from day 10 to day 15. This experiment was performed once on iKLF1.1 and iKLF1.2 so no error bars are shown. Three repeat experiments on iKLF1.2 are shown in Figure 3D.

C, D. Expression of KLF1 and KLF1-ER^{T2} in CD34+ cells, undifferentiated iPSCs and iKLF1.2 cells and iPSCs and iKLF1.2 cells differentiated for 10 days in the erythroid differentiation protocol when the majority of CD34^{+} cells are present. Note the lower level of endogenous KLF1 in iPSCs compared to adult CD34^{+} cells and that the expression of KLF1 in transgenic iKLF1.2 cells is significantly higher than in control iPSCs at same stage in differentiation protocol. Real time PCR analyses was carried out with primers to KLF1 (C) that amplifies both endogenous and exogenous KLF1 and primers that amplify only the KLF1-ER^{T2} exogenous transgene (D)

Supplementary Figure S6

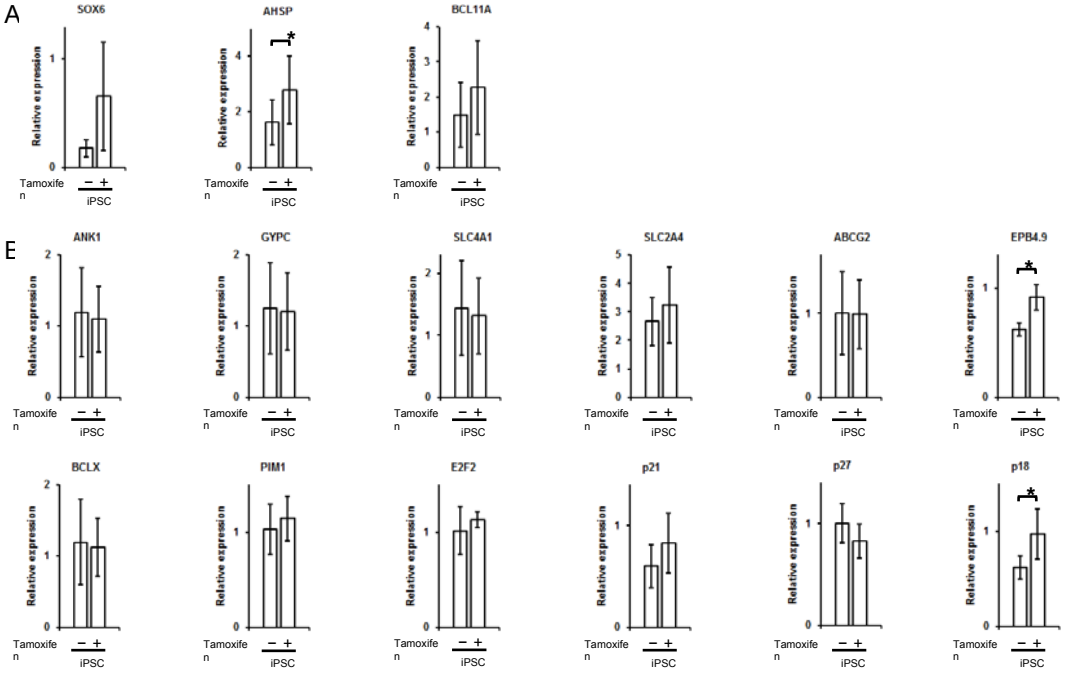

Supplementary Figure S6. Tamoxifen has no effect on the expression levels of KLF1 target genes in control iPSCs

In Figure 4, statistical analysis of the data to assess the effects of KLF1 activation in iKLF1 cells was performed by using the gene expression level of control iPSCs as the calibrator (set as 1) precluding a valid statistical analysis of these control cells. To demonstrate that tamoxifen had minimal effect of the expression level of these genes in control iPSCs we calculated the 'fold change' in these cells in the presence and absence of tamoxifen using iKLF1 (no tamoxifen) as the calibrator. A ratio paired T test was used to assess the effect of tamoxifen in iPSC derived cells (*, $p<0.05$).

Samples are as Figure 4 from day 15 (A) and Day 24 (B).

Supplementary Figure S7

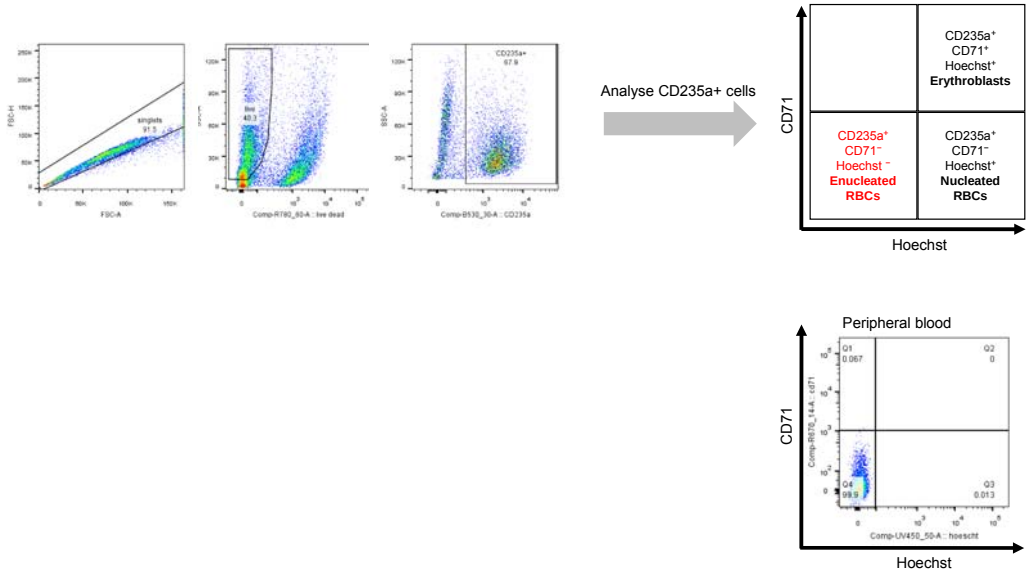

Supplementary Figure S7. Flow cytometry gating strategy for the enucleation assay

Differentiating cells were stained with anti-CD235a, -CD71 antibodies, Hoechst and the LIVE/DEAD™ Fixable Near-IR Stain then analysed by flow cytometry. Single cells were gated by FSC-A and FSC-H, and live cells were identified by the R780_60 filter. Gating thresholds were all set using the appropriate FMO and live CD235a positive cells were then assessed in the enucleation assay. Similarly, the gating thresholds for CD71 and Hoechst were set using the appropriate FMOs minus CD71 antibody and minus Hoechst. $CD235a^{+}$ / $CD71^{-}$ / $Hoechst^{-}$ enucleated RBCs were expected to appear in Q4 quadrant. Control human peripheral blood was used as a positive control for enucleated RBCs.